Two million years of environmental change:

a case study from Wonderwerk Cave, Northern Cape, South Africa

Michaela Sarah Ecker

Keble College

Research Laboratory for Archaeology and the History of Art

University of Oxford

Michaelmas Term 2015

A thesis presented to the University of Oxford in partial fulfilment of the requirements for the Degree Doctor of Philosophy.

Abstract

The arid interior of South Africa lacks long, continuous and well-dated climate and environmental proxy records that can be compared with cultural sequences and with broader global climate records. This thesis develops the first substantial terrestrial environmental sequence for the interior of southern Africa at the site of Wonderwerk Cave, spanning two million years of prehistory. Changes in vegetation and humidity over time were investigated by means of carbon and oxygen stable isotope analysis on fossil herbivore enamel and ostrich eggshell, creating two independent proxy datasets. The Holocene record was used as a baseline for comparing the Pleistocene sequence, but required chronological tightening. Therefore, nine new radiocarbon dates were obtained, and calibrated and modelled with existing dates to provide a firmer chronology.

The ostrich eggshell isotope record suggests arid but variable conditions, with distinct phases of increased humidity in the Early Pleistocene and mid-Holocene. Enamel stable isotope results show clear differences in local resource availability between the Early and Mid-Pleistocene, and then between the Pleistocene and Holocene, with an overall trend of increasing aridity. In particular, the onset of dietary specialisation in grazers at 0.8Ma is linked to expanding C_4 grasslands. Aridity was not the driver behind the increase in C_4 grasses, but changing pCO_2 levels at the Mid Pleistocene transition were identified as a possible key factor. The presence of C_3 and C_4 grasses in the Early Pleistocene, when compared to the domination of C_4 grasses today, was fostered by reduced rainfall seasonality. Regional independent developments have to be considered, as other regions in South and East Africa show C_4 dominated diets in herbivores at earlier times than at Wonderwerk Cave. In the Holocene, higher temporal resolution indicates phases of environmental change coinciding with changes in the cultural record.

Preface and Acknowledgements

Firstly, I want to thank my supervisor Julia Lee-Thorp for all her help, encouragement, supervision and support over the last few years. She first proposed this thesis topic to me, resulting from her long-term involvement in old and new projects at Wonderwerk Cave. We combined her ostrich eggshell data and radiocarbon dates from a collaboration with Peter Beaumont with some additional stable isotope measurements and a first Bayesian model of the radiocarbon dates in Lee-Thorp and Ecker 2015. Many thanks to Liora Kolska Horwitz, who enthusiastically supported the project from the start. She was crucial in introducing me to the site, organising access to samples, data and accommodation. Her expertise and ideas were also much help in working with the fauna and ostrich eggshell samples. I also thank her for reading and commenting on some chapters of the thesis, which significantly improved them. Our shared interest in ostrich eggshell as a palaeoenvironmental source led to the publication of Ecker et al. 2015, in which most of the data in Chapter 5 was included. The interest was shared with Jennifer Botha-Brink and I thank her for pictures, data and collaboration in writing the paper. Many thanks to Michael Chazan, who, as the Wonderwerk Cave Principle Investigator with Liora, agreed to trust me with this project. I am grateful for the possibility to join the 2013 excavation team and take on responsibility for the measurement system and database. Michael also provided several references over the last few years and the valuable perspective of a lithics expert and field archaeologist to the environmental research. I thank Francesco Berna for sponsoring the 2013 field season, including my expenses, and making the excavation such fun. Thanks to Megan Thibodau I was able to expand my FTIR knowledge during the excavations.

This thesis would not have been possible without the work of James Brink in identifying the Wonderwerk enamel samples. Due to his patience I learned a lot about South African fauna. I also would like to thank him for his hospitality in Florisbad and Bloemfontein. Another invaluable contact in Bloemfontein is Louis Scott, who was incredibly kind in sharing unpublished data, discussing results and even helping to fund some of the stable isotope measurements. David Morris gave permission to sample the Wonderwerk fauna, charcoal and ostrich eggshell. I also thank him for providing access to the McGregor Museum and for helping to obtain literature. Lloyd Rossouw discussed the phytolith data from Wonderwerk and provided data for our 2013 ESHE poster. Many thanks to Marion

Bamford for identifying the charcoal samples for radiocarbon dating, teaching me about the local vegetation and for several lifts to/from Johannesburg. During my first stay in Bloemfontein in 2013 Sharon Holt provided great hospitality, for which she has many thanks. I have to thank Jaco and the whole Florisbad team for their hospitality in 2013 and 2014. Everyone thanked so far is part of the current Wonderwerk team, which shows what an incredible joy it is to work with this team. I definitely profited a lot from everyone's expertise.

Many thanks to Daryl Codron for open discussions about stable isotope research and for the Codron et al. 2008 dataset. Andy Gledhill in Bradford ran all the stable isotope samples speedily and efficiently, and also explained the procedure during a visit to Bradford. In Oxford, Peter Ditchfield lent technical support. I have to thank many people from the Oxford Radiocarbon Unit for making the radiocarbon dating and modelling possible. Tom Higham and Christopher Bronk Ramsey kindly discussed the ORAU application and model possibilities with us respectively. Fiona Brock and Richard Staff processed the radiocarbon samples with me. Richard Staff was of incredible help in fighting with the Bayesian model, as was Mike Dee. He also kindly read and commented on a chapter.

Funding for living costs and fees during the DPhil were provided by a School of Archaeology bursary, a German Academic Exchange Service (DAAD) 'Jahresstipendium für Doktoranden' and a Yueng-Pen Loke scholarship through Keble College. Funding for fieldwork and sample analysis was provided by two Boise Fund Awards, a Quaternary Research Association New Research Workers Award, the School of Archaeology postgraduate research award and an ORADS Radiocarbon Award (with Julia Lee-Thorp). Some stable isotope samples were funded by a NRF award to Louis Scott. Funding for conferences was provided by the Meyerstein fund, the Keble Association and the Pan-African Archaeological Association. Curator David Morris (McGregor Museum Kimberley) granted permission for isotopic and radiocarbon analyses. The necessary South African Heritage Resources Agency (SAHRA) permits were obtained. Ostrich eggshell samples were exported from South Africa to Oxford under export permit ID: 1898, Case ID: 6245. Enamel and radiocarbon samples were exported from South Africa to Oxford under the export permits numbers 1719 and 1898, Case IDs 5233 and 6245.

A huge shout out to Amy Jeffrey, Francisca Santana Sagredo, Emma Loftus and the whole DPhil room community for friendship while sharing the same experiences as a DPhil

student. Also to Keble MCR for a great welcome to Oxford, many great events and friendships, especially with the other two “M” from my year, Mariann Nowack and Moujan Matin. I also have to thank Mariann for being the first person who explained OxCal to me. Thank you also to my friends and former colleagues in Tübingen who supported me earlier in my archaeological career, particularly Nicholas Conard and Andrew Kandel. Much love to Chris Green, who helped create the maps in this thesis and was of invaluable moral support. Finally, my largest thank you to my family who always believed in me and all their support over the years to make my dream come true.

Table of contents

List of Figures

Chapter 4

Chapter 5

Chapter 6

Chapter 7

Chapter 8

List of Tables

Chapter 5

Chapter 6

Chapter 7

Chapter 8

List of Abbreviations

Abbreviation	Full text
AMS	accelerator mass spectrometry
BP	years before present (1950)
C_3	Calvin cycle of photosynthesis
C_4	Hatch-Slack cycle of photosynthesis
CAB	Congo Air Boundary
CAM	Crassulacean acid metabolism
CV	coefficient of variation
ENSO	El Niño Southern Oscillation
ESA	Early Stone Age
IAEA	International Atomic Energy Agency
ITCZ	Intertropical Convergence Zone
ka	thousand years before present
LGM	Last Glacial Maximum
LMA	Land Mammal Age
LSA	Later Stone Age
n	number of samples
MAP	mean annual precipitation
MAR	mean annual rainfall
MARH	mean annual relative humidity
MIS	Marine Isotope Stage
MNI	minimum numbers of individuals
MPT	Mid Pleistocene Transition

MSA	Middle Stone Age
MU	Major Unit, as defined in Beaumont and Vogel (2006)
NISP	Number of identified specimen
OES	Ostrich eggshell
OIS	Oxygen Isotope Stage
OSL	Optical Stimulated Luminescence
pCO_2	partial pressure of carbon dioxide
PCR	photosynthetic carbon reduction
ppmv	part per million by volume
RuBisCO	Ribulose-1,5-bisphosphate carboxylase/oxygenase
SAHRA	South African Heritage Resources Agency
SST	sea surface temperatures
RH	relative humidity
U-Pb	Uranium-lead
VPDB	Vienna Pee Dee Belemnite
VSMOW	Vienna Standard Mean Ocean Water

Chapter 1 - Introduction

1.1 Introduction to the research topic

The role of climatic and environmental change in human evolution has been a strong focus of interest for decades. Theoretical frameworks stretch back to the savannah hypothesis (Dart 1925, 1953), later the turnover pulse hypothesis (Vrba 1985, 1993), and more recently, variations on the variability selection hypothesis (Potts 1998, 2013; Maslin and Trauth 2009) or amplifier lakes hypothesis (Trauth et al. 2010). The principal idea behind the more recent models is that hominins evolved biologically and culturally in response to a highly fluctuating climate that influenced environmental opportunities (Potts 2013). The key feature is the role of periods of environmental instability (Potts 2012), compared to periods of environmental stability (Trauth et al. 2015), for driving biological and, later, cultural evolution. These recent models are largely based, and tested on, information from East Africa. Following the earlier pioneering work of Dart and Vrba, the evidence for climate and environmental change in southern Africa[1] has remained obscure. One reason is the lack of long, well-dated climate and environmental proxy records that can be compared with cultural sequences and with broader global climate records. The available data is sparse, discontinuous and/or poorly chronologically resolved especially in South Africa's interior and hinders construction of reliable environmental sequences.

This thesis is about developing the first terrestrial environmental sequence for the interior of southern Africa and one of the first extensive ones for the whole subregion. The site of Wonderwerk Cave in the Northern Cape region of South Africa is the lens through which I focus my research on this topic. Wonderwerk Cave has currently the longest temporally

[1] When referring to southern Africa in this thesis, Lesotho, Swaziland and the southern parts of Namibia, Botswana, Zimbabwe and Mozambique are included alongside South Africa itself.

stratified sequence associated with hominin occupation in southern Africa. It provides for the first time a sequence of cultural evidence in a context in which the environmental sequence can be determined. The sediments date back almost two million years (Chazan et al. 2012) and the cultural record contains Early Stone Age (ESA), Middle Stone Age (MSA) and Later Stone Age (LSA) lithic technologies (Thackeray 1981, Beaumont and Vogel 2006, Chazan et al. 2012). It includes, therefore, the whole timespan of the development of our species, from *Homo erectus* all the way to the *Homo sapiens*. The site has been dated by cosmogenic burial dating, palaeomagnetism, optically stimulated luminescence (OSL), Uranium-series, Uranium-lead (U-Pb), radiocarbon and biochronology (Beaumont 1990, Matmon et al. 2011, Chazan et al. 2012, Pickering et al. 2015). The sequence, despite large gaps, includes phases that are rarely preserved in southern Africa's interior, for example an early MSA record. Wonderwerk Cave is located at the southern edge of the Kalahari, an area which is sensitive to past climate shifts such as increasing aridity, or the expansion of the winter rainfall belt (Cockcroft et al. 1987, Lee-Thorp and Beaumont 1995, Chase and Meadows 2007). The data produced in this study also enables comparisons with East African sites.

1.2 Research aims and approach

The overarching aim of this thesis is to explore what environmental changes occurred in the Wonderwerk sequence, and to evaluate if and how they relate to changes visible in the archaeological record. Principal objectives are sampling of tooth enamel from herbivore species and ostrich eggshell (OES) from LSA, MSA and ESA levels of Wonderwerk Cave (Excavation 1 and Excavation 2). Isotopic variability amongst species will be determined by bulk isotopic analysis ($\delta^{13}C$ and $\delta^{18}O$) of enamel and OES.

The results will be used to test the following hypotheses:

- Climate and vegetation shifts appear in phase with changes in global climate variability, e.g. with the onset of the Walker circulation 1.9-1.7 Ma (Maslin and Christensen 2007, Hopley et al. 2007a) and the Middle Pleistocene Transition ~1Ma (Trauth et al. 2005).
- The evolutionary shift in African ungulates towards greater niche separation is driven by constant exposure to C_4 grasses (Codron et al. 2008), which is evident in the rising proportions of C_4 vegetation in the landscape over time.
- Besides large scale influences, the South African interior remains largely arid through the Pleistocene and Holocene, punctuated by occasional moister episodes. The OES and enamel isotope study will show similar trends in $\delta^{18}O$ and $\delta^{13}C$.
- Higher $\delta^{18}O$ values in non-obligate drinking ungulates (Sponheimer and Lee-Thorp 1999a) correspond with higher $\delta^{18}O$ values determined from the ostrich eggshell data and proportionally more arid adapted species in the faunal material.
- Phases of high variability between moist and arid conditions correspond with phases of change and innovation (Potts 2012, 2013) in the Wonderwerk archaeological record.

In testing these hypotheses, the ultimate goal is to combine the information to create a key referential palaeoenvironmental sequence for the Pleistocene and Holocene of the region. To achieve these goals, the Holocene sequence of Wonderwerk Cave was strengthened with nine new radiocarbon samples, as well as calibration and Bayesian modelling of all available dates, filling significant gaps in the previous chronology (Chapter 4). Stable light carbon and oxygen isotope analysis was carried out on the inorganic fraction of 158 OES fragments (Chapter 5) to provide an independent proxy sequence of aridity. Furthermore, as the main objective, stable light carbon and oxygen isotopes were analysed on enamel of

438 specimens from 18 species (Chapter 6). The principles of this method are explained in the next part.

1.3 Application of stable light isotopes to animal diet and environmental context

Stable light isotope analysis is a well-established method for constructing proxy palaeoclimate and palaeoenvironmental records. This section outlines the underlying principles of this method and how stable isotopes in plants are used as proxy evidence to reconstruct past conditions. Natural abundances of the isotopes of carbon and oxygen reflect the major pathways in vegetation and hydrology. Details on the uptake in consumer tissues follow in Chapter 5 (OES) and Chapter 6 (Enamel).

The variations in the atomic mass of one element (e.g. in the formation of bonds) lead to differences in the thermodynamic properties, called isotopic effects. Those can be equilibrium effects (e.g CO_2 in air and solution during speleothem formation) or kinetic effects (non-equilibrium, e.g. H_2O during evapotranspiration, reaction of CO_2 with RuBisCO (Ribulose-1,5-bisphosphate carboxylase/oxygenase) during photosynthesis). This is expressed in the fractionation factor α: $\alpha_{A\text{-}B}=R_A/R_B$, where R is the molar ratio of any two isotopes (A and B) (Sharp 2007).

In practice the ratio of the heavier to the lighter isotope is measured in a mass spectrometer and compared to an international standard. The difference to the standard ratio is the delta (δ) value, given in per mill (‰), for example:

$$\delta^{13}C = \{[(^{13}C/^{12}C_{sample}/^{13}C/^{12}C_{standard}) - 1] \times 1000\} \quad \text{..... Equation 1}$$

International Standards for various elements are determined and provided by the International Atomic Energy Agency (IAEA). The international oxygen isotope standard is VSMOW (Vienna Standard Mean Ocean Water), whereas $\delta^{13}C$ and $\delta^{18}O$ abundances in

carbonates are measured relative to VPDB (Vienna Pee Dee Belemnite). Additionally, commercial and in-house standards are used (Sharp 2007).

1.3.1 Carbon isotopes in plants

Carbon has two naturally occurring stable isotopes (globally ^{12}C – 98.9% abundance; ^{13}C – 1.1% abundance) and one radiogenic isotope (^{14}C) (Sharp 2007). Carbon in the atmosphere is bound in CO_2. The amount of CO_2 in the atmosphere is in general lower in glacials (180-210ppm) than interglacials (280-300ppm) over the last two million years, although variation exists (Petit et al. 1999; Chapter 7). The $\delta^{13}C$ value of atmospheric CO_2 is not constant, and has changed from a pre-industrial level of about -6.5‰ to the present day level of around -8‰ as a result of fossil fuel burning, accelerated by the industrial revolution (Keeling et al. 1976, Keeling et al. 2005). Results from modern stable isotope samples need to be corrected for this difference before being compared to results from fossil samples.

The main factor controlling ^{13}C depletion in plants is the photosynthetic pathway (Farquhar et al. 1989). Three different pathways evolved, that are known as C_3, C_4 and Crassulacean acid metabolism (CAM) respectively. Typical C_3 plants are trees, shrubs, herbs and temperate grasses, which includes 80-90% of all land plant types. Their $\delta^{13}C$ values range from - 24‰ to - 36‰ (Figure 1.1; Cerling and Harris 1999). C_3 plants use the photosynthetic carbon reduction (PCR) pathway, or Calvin-Benson cycle. Mesophyll CO_2 is converted by the enzyme RuBisCO which discriminates against the heavier ^{13}C isotope, leading to fractionation. A model to describe the fractionation during C_3 photosynthesis was developed by Farquhar et al. (1989):

$$\Delta^{13}C = a + (b - a)*P_i/P_a \quad \text{.....Equation 2}$$

where a is a constant due to the fractionation occurring as a result of diffusion of CO_2, b is the net fractionation caused by carboxylation (mainly by RuBisCO), P_a is the ambient and P_i the intercellular partial pressures of CO_2 (Farquhar et al. 1989). This equation shows that stomatal conductance is the main factor modulating the expression of fractionation by the RuBisCO enzyme. As a result, C_3 plants are sensitive to environmental influences such as CO_2, aridity, heat, and light.

C_4 plants have evolved a secondary carbon fixation pathway (sometimes called the Hatch-Slack-cycle), which first uses the enzyme PEP (phosphoenolpyruvate) to convert CO_2 into a 4-carbon compound (Sage 2004) (Figure 1.2). There are three different types of C_4 photosynthetic sub pathways, named after the second decarboxylation enzymes: NADP-me, NAD-me and PCK (Hattersley 1982, 1992, Sage 2004). The product is transported from the outer mesophyll cells to bundle sheath cells. Most C_4 plants have developed this 'Kranz' anatomy of bundle sheath cells surrounded by mesophyll cells which concentrates the CO_2. The carbon is released to the RuBisCO cycle afterwards, minimising photorespiration compared to C_3 plants (Hatch 1971, Osmond 1971). The $\delta^{13}C$ of C_4 plants is less variable and close to a mean of -12.5‰ (Figure 1.1; Farquhar et al. 1989, Cerling and Harris 1999). The isotopic composition of C_4 grasses using the NADP-me sub-pathway are systematically enriched in ^{13}C by about 1±2‰ compared to those using the other sub-pathways. NADP-me C_4 plants favour mesic environments while the NAD-me and PCK C_4 grasses are found in more xeric localities (Hattersley 1982, 1992).

Lower CO_2 levels in the atmosphere, changing rainfall regimes and disturbance by herbivory and fire are all possible explanations for the occurrence and expansion of C_4 plants (van Langevelde et al. 2003, Bond et al. 2005, Osborne and Beerling 2006, Dupont et al. 2013), which occur in southern Africa from 4-5Ma onwards. By 3Ma they are a

dominant part of the ecosystem (Lee-Thorp et al. 2007, Ségalen et al. 2007), with a further expansion at 1.7Ma (Hopley et al. 2007a). The C_4 pathway is used by only approximately 20 plant families, including tropical grasses and sedges, but they account for ca. 50% of net primary productivity in the tropics today (Cerling et al. 2015).

In the third photosynthetic pathway, CAM plants are able to fix CO_2 at night, which is more water efficient as the stomata can be closed during the day preventing evapotranspiration (Farquhar et al. 1989). The enzyme PEP is used to fix the CO_2 similarly to C_4 plants, while it is then released to the RuBisCO cycle during the day. CAM plants therefore have isotopic values intermediate of C_4 and C_3 plants. Many CAM species are flexible in the amounts of photosynthesis during the night and day, making them highly adaptable to drought conditions (Mooney et al. 1977). They are mainly succulents, which are not a significant part of the vegetation in the Wonderwerk region today (Chapter 3.1.2). Additionally they tend to be unsuitable food for most herbivores. They should therefore have little influence on the carbon isotope values in this study.

Environmental factors influencing the isotopic value of the CO_2 entering the leaves can be the recycling of respired CO_2 as well as reduced light conditions in dense and closed canopies (known as canopy effect) (Tieszen 1994). More relevant in the Wonderwerk region today is the plants' reaction to water stress by stomatal closure, which results in a discrimination against ^{13}C (see Equation 2). C_3 plants are strongly influenced by these environmental factors, whereas C_4 plants are little influenced, due to their CO_2-concentrating mechanism (Farquhar et al. 1989). It allows them to use all the CO_2 captured, without exposing the plant to water loss as the stomata can remain closed. Further intrinsic $\delta^{13}C$ influences are temperature, inorganic nutrient supply, increased osmotic stress in leaves and the CO_2 partial pressure. Small scale fractionation occurs when CO_2 is

transported in the form of sugars after photosynthesis to form different plant parts (Tieszen 1994, McCarroll and Loader 2004).

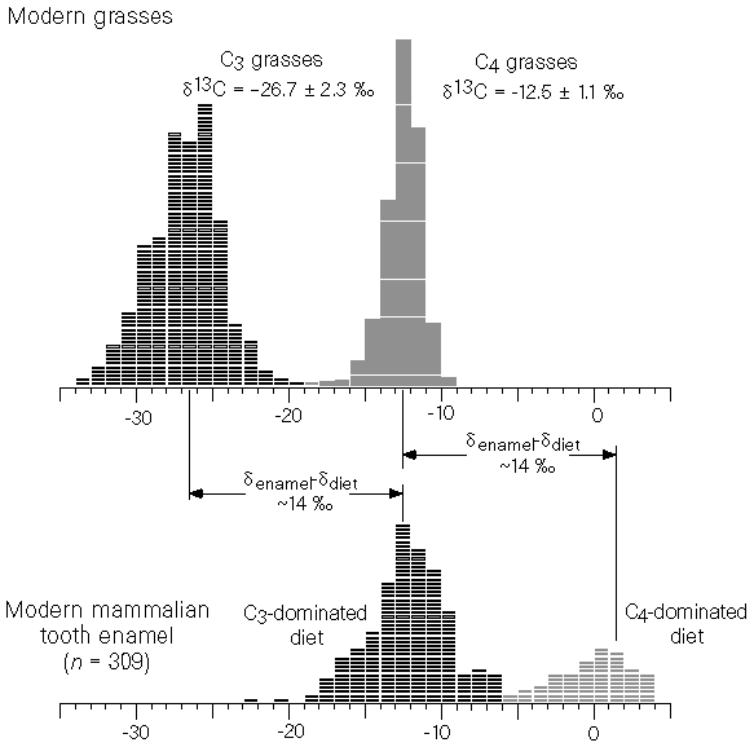

Figure 1.1: Histogram of $\delta^{13}C$ in modern C_3 and C_4 grasses and modern mammalian tooth enamel (modified after Cerling et al. 1997). The suggested δ_{enamel}-δ_{diet} spacing of 14‰ is the upper limit for large herbivores (e.g. Passey et al. 2005).

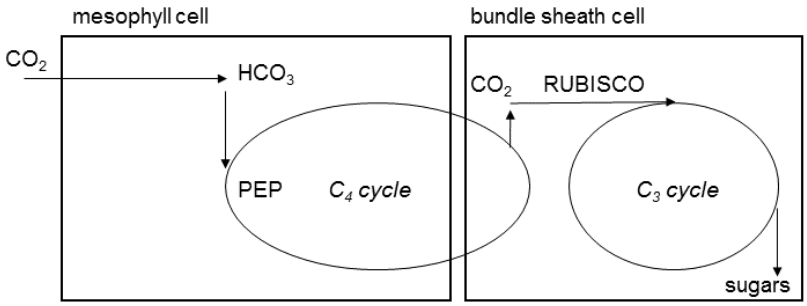

Figure 1.2: Simple schematic diagram of the C_4 photosynthetic pathway showing compartmentalization of the different enzyme systems involved, and the connection between CO_2-pumping by the C_4 cycle and CO_2-fixation by the C_3 cycle. Abbreviations: HCO3, bicarbonate; PEP, phosphoenolpyruvate carboxylase; RUBISCO, ribulose-1,5-bisphosphate carboxylase/oxygenase (modified after Osborne and Beerling 2006).

1.3.2 Oxygen isotopes in the environment

In hydrology and in plants, the $^{18}O/^{16}O$ ratio is analysed in stable light isotope studies of oxygen (Sharp 2007). The largest oxygen reservoirs are the atmosphere and the water cycle. Oxygen in the atmosphere is relatively constant over time (Kroopnick and Craig 1972). Most important for oxygen isotope analysis in organic tissues is the oxygen bound in H_2O. Meteoric water is bound to evaporation, condensation and rainfall in the water cycle, which influences the oxygen isotope abundance in surface water, underground water, springs, lakes, river systems and glaciers. ^{16}O atoms evaporate faster than the heavier ^{18}O ones (so-called Rayleigh distillation). Uprising vapour over the oceans is therefore isotopically lighter than the ocean water. With rainfall, the heavier $H_2{}^{18}O$ molecules leave the cloud more easily. This leads to ^{18}O-depleted precipitation with distance to the moisture source and increasing latitude (Araguas-Araguas et al. 2000). Seasonal variability in $\delta^{18}O$ rainfall mostly follows changes in temperature (in mid-high latitudes) (Dansgaard 1964) and/or changes in the moisture source and amount (in tropical regions) (Rozanski et al. 1993, Araguas-Araguas et al. 2000).

Plants are enriched in ^{18}O and influenced by source water, surface versus soil water, leaf evaporative environment and isotopic exchange between plant water and organic molecules (Dawson et al. 2002). Isotope fractionation does not occur during uptake of water in the root (Dawson and Ehleringer 1991), but does in the leaf due to evapotranspiration (Gonfiantini et al. 1965). The escaping vapour is ^{18}O-depleted, leaving the water in the leaf enriched in $H_2{}^{18}O$ (Yakir 1992, Kohn 1996, Helliker and Ehleringer 2000, Barbour 2007).

1.3.3 Summary and implications for this study

This study uses carbon and oxygen stable light isotopes in ostrich eggshell and herbivore tooth enamel to reconstruct the past environment at Wonderwerk Cave. Today, all grasses

in the Wonderwerk region are C_4 plants, while trees, shrubs and herbs follow the C_3 pathway. CAM plants are not a significant part of the ecosystem. It can therefore be expected that $\delta^{13}C$ values of local herbivores will show the proportions of C_3 and C_4 plant types in the animals' diet, making it possible to distinguish animals with a grazing, browsing or mixed-feeding diet. Shifts at broadly similar times over several taxa must reflect vegetation shifts.

There are no permanent water sources directly at Wonderwerk Cave today, although there is evidence of streams and pans existing nearby in the past (Goldberg et al. 2015). Data from a survey of $\delta^{18}O$ and δD in modern ground and tap water in South Africa showed that mean annual precipitation and distance to coast were the main influences on ground water (West et al. 2014). Wonderwerk Cave is far inland and in principle could be influenced by moisture from the Atlantic and the Indian Oceans. The expectation is that $\delta^{18}O$ values, especially in the ostrich eggshell, reflect rainfall seasonality.

1.4 Thesis structure

The structure of this thesis is as follows. In this Chapter, the main method used in this thesis, stable light isotopes, has been outlined and the research questions and aims for the thesis are given above. Chapter 2 provides background information relevant to the thesis, namely a review of the past and present climate and environment and of the archaeology of southern Africa. The focus is on the Northern Cape where Wonderwerk Cave is located, as well as on the savannah biome and on the summer rainfall region. Chapter 3 introduces the site of Wonderwerk Cave with a description of the site, its research history, and details of its stratigraphy and dating. It includes descriptions of the lithics, faunal remains, non-lithic artefacts and features and previous and ongoing environmental analyses. Those chapters set the background against which the study results will be evaluated.

The Holocene environmental context, and shifts in particular, need a good chronological context. Chapter 4 contains the radiocarbon dating, calibration and modelling completed for this thesis. Following a summary of the principles of radiocarbon dating and a review of previous radiocarbon dating of Wonderwerk Cave material, I outline the rationale for selection of new samples, chemical pretreatment procedures, and the results. The chapter also provides the method and outcome of calibration and modelling work using OxCal. The results close gaps in the Holocene stratigraphy of Wonderwerk and are discussed in the light of the Holocene archaeological sequence in the region. This high-resolution study of the Holocene environment is essential to evaluate the Pleistocene data.

Chapter 5 introduces ostrich eggshell (OES) as a climatic proxy. It gives background to ostrich ecology and OES composition, followed by the analysed material from Wonderwerk Cave and the detailed methods used. The results are analysed statistically and graphically, and conclusions about changes through time in the ostrich diet inferred from carbon isotope values are given. Changes in oxygen isotope values are interpreted as an index of aridity.

Chapter 6 comprises the key part of the thesis, the stable isotope analyses on herbivore enamel from Wonderwerk Cave. It includes background information on tooth formation and the use of enamel as an environmental proxy, as well as diet, habitat and physiology of the sampled species. Materials and methods of carbon and oxygen isotope analysis on samples from Wonderwerk Excavation 1 and 2 are described in detail. Results are analysed statistically and graphically, and listed by species. Dietary, vegetation and aridity changes at Wonderwerk through time are discussed. The enamel results are combined with the OES results in Chapter 7, and their correlation, as well as comparisons to other environmental proxy records from Wonderwerk are explored. From those results, conclusions are drawn

about environmental and climatic change in the Wonderwerk region over the last two million years, and compared to proxy evidence from southern Africa. Section 7.5 investigates the implications of the environmental results for the archaeological sequence at Wonderwerk. It tests the hypothesis that phases of climatic variability coincide with innovative changes in the cultural record. This is followed by a comparison of these results against other relevant stable isotope and environmental studies in the Northern Cape, South Africa's interior and East Africa in Chapter 8. The question is what contributions can be made to the knowledge of the past ecology, palaeoclimate and past environment of South Africa, and how this might differ from the much better explored East African record. Chapter 9 provides a brief summary overview of the major results, and proceeds to discuss how the research questions and hypotheses outlined in this introduction have been addressed, and suggestions for further research.

Chapter 2 - The research region and its archaeology

This chapter introduces the relevant research region where this thesis is based, in first describing the modern climate and environment of Southern Africa, with the focus on the summer rainfall region and the savannah biome. Proxy archives as well as possible drivers of environmental change are discussed. Subsequently, the available information about past climate, environment and archaeology over the last two million years in this region is summarized. Emphasis is on the Northern Cape region to provide a summary of the current state of research; the site of Wonderwerk Cave is described in detail in Chapter 3.

2.1. Modern climate and its drivers in southern Africa

Southern Africa is located in a unique position between the Atlantic and Indian Oceans. It occupies a smaller landmass than northern Africa, resulting in a more complex climate than in the northern part of the continent (Singarayer and Burrough 2015). The temperature gradients as well as the circulation are stronger and the circulation belts lie more equatorward (Tyson 1986). Compared to East Africa, South Africa is tectonically stable; the main process in landform evolution is erosion rather than deposition (Deacon and Lancaster 1988).

Today's climate in southern Africa is dry with strongly seasonal precipitation. Rainfall reaches the south-western Cape from the Atlantic Ocean mainly in the winter (June to August), whereas rain arrives from the Indian Ocean in northern and eastern southern Africa in summer (December to February). A small intermediate zone on the southern coast receives year round rainfall, while the northern intermediate zone lies in a rain shadow. The winter rainfall follows the northward migration of the westerlies, which are located south of the continent in summer (Fig. 2.1). In contrast, rains in the summer rainfall region derive

from summer monsoonal activity, which is dependent on the formation of robust convection cells over the Indian Ocean, a result of high sea surface temperatures (SST) (Tyson and Preston-Whyte 2000). Over the equator, heated air rises, creating a low pressure area called the Intertropical Convergence Zone (ITCZ). It sits on the contact between the northern and the southern hemisphere Hadley cells, producing large amounts of precipitation. The rising air moves towards the poles and is cooled by expansion causing saturation, condensation, cloud formation and rain. Hadley cells move seasonally in concert with the ITCZ, which migrates to the northern hemisphere in winter (Fig. 2.1). The ITCZ reaches its southernmost position in summer at 23°S over the south-western Indian Ocean (Tyson and Preston-Whyte 2000). The sinking air is dry and causes high pressure belts (called Anticyclones) resulting in deserts such as the Kalahari at ~30°S (Singarayer and Burrough 2015). The equivalent to the ITCZ in the west is the Congo Air Boundary (CAB; formally Zaire Air Boundary (ZAB), sometimes called the Inter-Ocean Convergence Zone (OICZ)), which also fluctuates seasonally (Nicholson 2011) (Figure 2.1).

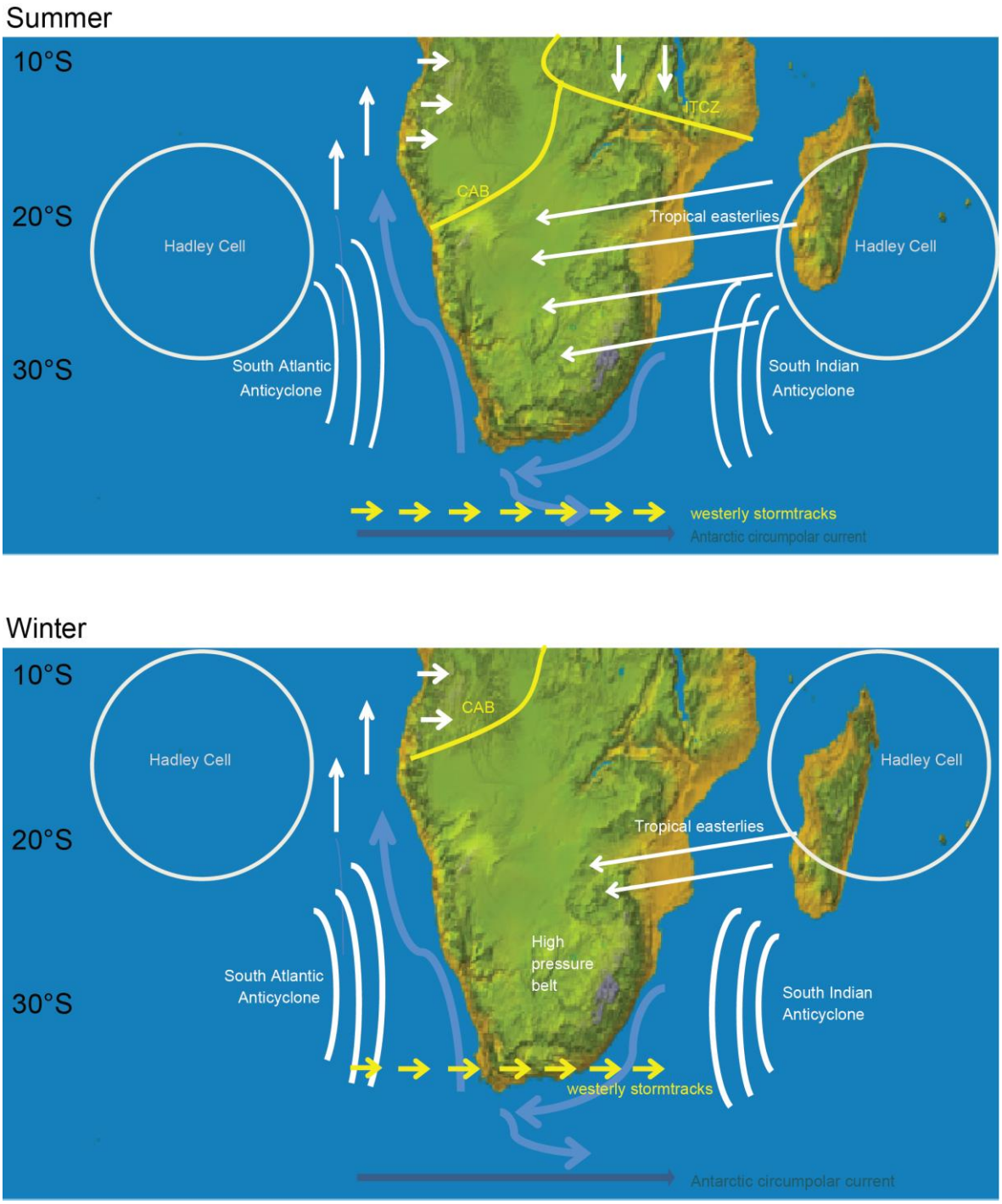

Figure 2.1: Modern climate system over southern Africa during summer (upper part) and winter (lower part). Blue arrows are ocean currents (Bengula and Agulhas current), white and yellow labelling are atmospheric and wind systems. During the austral summer, central and eastern southern Africa have low pressure over land which attracts more moist air easterlies. The ITCZ is in the southern hemisphere, the westerlies are south of continent. In winter, the ITCZ, CAB, Hadley cells and westerlies migrate northwards. Stronger Anticyclones and high pressure over land then lead to less easterly moisture reaching the interior.

A major factor effecting climate and weather over southern Africa is the feedback between the atmosphere and the oceans, which happens on multiple timescales and in both directions (Tyson and Preston-Whyte 2000). One of the ocean-atmosphere interactions which affects the southern African rainfall is the Walker circulation, which is responding to SST changes in the Pacific and Indian Ocean, which leads to ENSO (El Niño Southern Oscillation; large-magnitude, slowly-evolving SST anomalies in the Pacific); other effects are influenced by the SSTs from the currents around the continent (Fig. 2.1; Tyson and Preston-Whyte 2000). Main drivers that have been suggested as influencing the climate in South Africa are: the ITCZ, the CAB, Indian Ocean SSTs, the westerly storm tracks, Antarctic ice volume, Northern Hemisphere ice volume, global temperatures, orbital forcing, upwelling of the Agulhas and the Benguela currents, ENSO and land atmosphere feedbacks (Nicholson 2000, Tyson and Preston-Whyte 2000). This multiplicity emphasizes the confusion and lack of consent on this topic. A review of current hypotheses on drivers of rainfall over Africa includes: 1) Interhemispheric symmetry (e.g. Partridge et al. 1997), 2) Expansion and contraction of the ITCZ rainbelt (Collins et al. 2011), 3) Influence of the CAB (e.g. Tierny et al. 2011b, Tierny and deMenocal 2013) and 4) Indian Ocean SST control on southern African rainfall (Schmidt et al. 2014), including movement of the winter rainfall zone inland (van Zinderen Bakker 1976, Cockcroft et al. 1987, Stuut et al. 2004, Chase and Meadows 2007). The most likely explanation is that multiple forcing mechanisms are working on different sites (Singarayer and Burrough 2015). One problem is that there are few well dated, high resolution environmental records in the southern hemisphere. The terrestrial record is patchy, incomplete and especially lacks sequences where different lines of palaeoclimatic evidence can be compared.

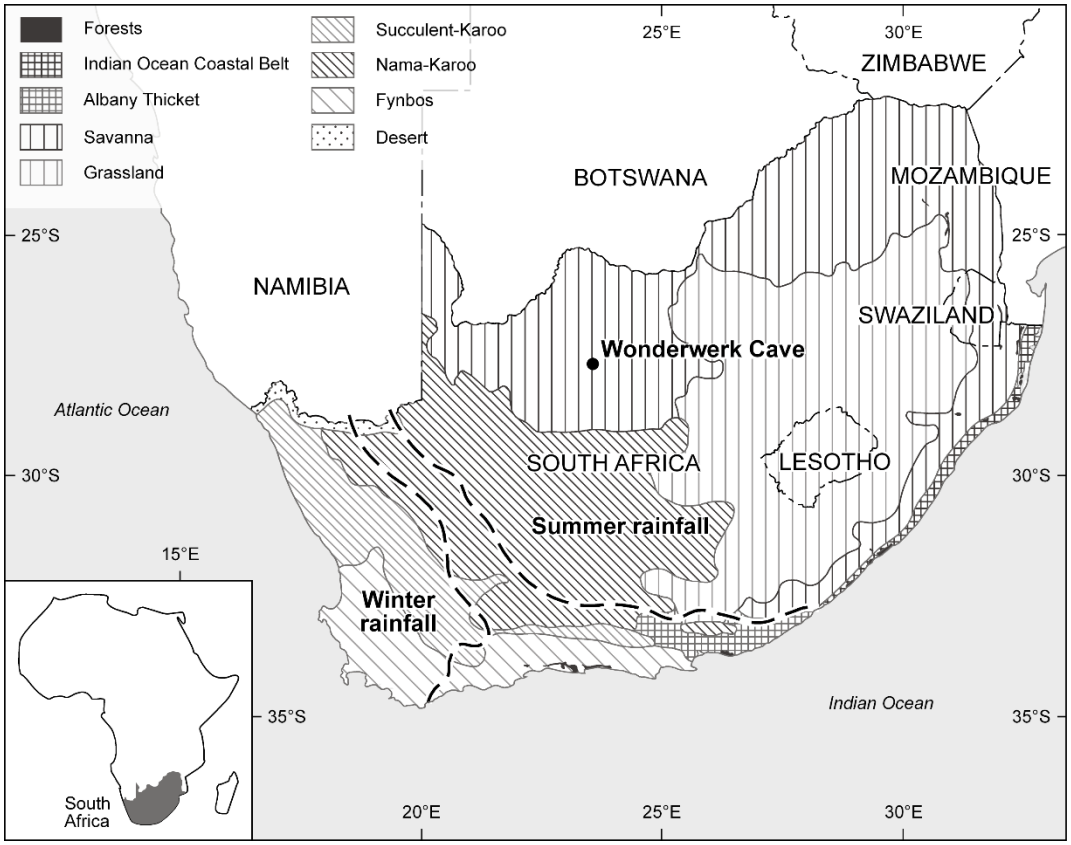

Figure 2.2: Map of Southern Africa, showing the biome types within the modern state of South Africa, as well as the extent of the winter and the summer rainfall zones (from Ecker et al. 2015). Wonderwerk Cave is located within the savannah biome, in the summer rainfall region.

2.2 Modern savannah environments of southern Africa

The rainfall pattern is the major influence on creating the diverse biomes in South Africa. Wonderwerk Cave is located in the savannah biome (Fig. 2.2) (Mucina and Rutherford 2006). It is the most widespread biome in Africa, and in South Africa it meets the Nama-Karoo biome to the south and the grassland biome to the east of Wonderwerk Cave. The South African savannah biome is situated mostly below 1500m asl, with mean annual precipitation (MAP) from 200mm to 1350mm and a coefficient of variation (CV) from 35% to 25% (Mucina and Rutherford 2006). Most rain falls in a short period in summer. In the context of this thesis, the definition of savannah is a tropical or subtropical C_4 grassland

with scattered bushes and deciduous trees, after Shorrocks and Bates (2014). Important influences on the type of savannah and its maintenance are the length and severity of the wet and dry season (Shorrocks and Bates 2014), fire for refreshing the vegetation layer and interaction with a variety of herbivore fauna on all levels (Mucina and Rutherford 2006).

Savannahs support rich large mammal faunas, mainly ungulates. There are also large and diverse quantities of birds, although their impact on the environment as single individuals is less than large herbivores (Mucina and Rutherford 2006). Carnivores are mainly small, with 90% of species less than one metre tall (exceptions are, for example, cheetah (*Acinonyx jubatus*), leopard (*Panthera pardus*), lion (*Panthera leo*), spotted hyena (*Crocuta crocuta*) and wild dog (*Lycaon pictus*)). Primates do not in general inhabit the savannah biome, except for vervet monkeys (*Chlorocebus pygerythrus*), baboons (*Papio ursinus*) and humans. Rodents in Africa in general include squirrels (Sciuridae), spring hare (*Pedetes capensis*), gundis (Ctenodactylidae), dormice (*Graphiurus* sp.), blesmols (Bathyergidae), porcupines (Hystricidae), cane-rats (*Thryonomys* sp.), jerboas (Dipodidae) and murids (Muridae) (Shorrocks and Bates 2014). Changes in climate over time changes the faunal and floral composition of the savannah biome, or expands and contracts biomes, as shown in the next section.

2.3 Trends in climate and environment during the last two million years in southern Africa

Palaeoclimate research uses the principles of modern climatic research to understand physical causes of variation. The methods used are reliant on the analysis of geochemical or biological proxy records revealing past temperature, precipitation and wind. Quaternary palaeoenvironmental reconstructions in Africa are based on a range of marine and terrestrial proxy data sources. Marine sediment cores provide high-resolution climate

records including terrestrial material, e.g. aeolian dust and pollen, and marine archives, e.g. marine shells and sediment within any one marine core (Thomas and Burrough 2012). One of the main challenges in marine cores is to determine the catchment area contributing to the sediment build up. Due to the lack of long, high-precision terrestrial records, marine cores are a major source of evidence for the past of southern African environment. Terrestrial archives on land include lake sediment, speleothems, pollen, charcoal, tree rings, large mammals, micromammals and stable isotopes in a variety of material. Appendix 1 lists major terrestrial proxy archives from southern Africa discussed in this chapter, predominantly from the summer rainfall zone. One problem is the different timescales represented by the different proxies and archives. As all proxies have their advantages and flaws, it is ideal to have multi-proxy records per site. Local and regional records can then ultimately be compared to global records, e.g. ice cores. The Epica Dome C ice core from Antarctica is the reference for temperature changes in the southern hemisphere, reaching back 800,000 years (Jouzel et al. 2007).

Pleistocene climate and environment

The global Pleistocene climate record is dominated by the changes between glacial and interglacial cycles. These have a strong effect in the Northern Hemisphere, whereas insolation and obliquity are major drivers of rainfall and vegetation change in southern Africa (e.g. Hopley et al. 2007a). The conventional model was first proposed by van Zinderen Bakker (1976): during glacials the climate system reacted more extremely than in today's winter season, with a further northward shift of all systems, including the ITCZ, Hadley cells, the westerlies and Anticyclones. Glacial conditions are expected to have weakened inter-hemispheric thermal contrast, which should in turn limit seasonal displacement of the ITCZ. This would bring arid conditions to the summer rainfall zone in glacials, and increased moisture delivery during interglacials (Nicholson and Flohn 1980).

Additionally, expansion in Antarctic sea ice volume would have displaced the westerlies northwards, bringing wetter conditions to the winter rainfall zone and possibly extending it (van Zinderen Bakker 1976). Many proxy records seem consistent with this model (e.g. Meadows and Baxter 1999, Parkington et al. 2000, Shi et al. 2001, Stuut et al. 2002, review in Chase and Meadows 2007), but other research proposes movement, expansion or decrease of the winter rainfall zone (e.g. Lee-Thorp and Beaumont 1995, Partridge et al. 1999, Burrough et al. 2009). There are further critical reviews on the movement of the ITCZ and the westerlies (e.g. Collins et al. 2011, Kohfeld et al. 2013) and what degree of influence obliquity minima and maxima, SSTs in the surrounding oceans and expanding sea-ice had on the climate system over southern Africa (Chase and Meadows 2007); as well as its impact in comparison to Northern Hemisphere insolation (Dupont et al. 2011). Many more high-resolution terrestrial records from the different parts of the continent are needed to solve those questions. In the following, key Pleistocene proxy records from the southern African summer rainfall region are discussed.

Few records from southern Africa go back as far as the onset of the Walker circulation (~ 1.7Ma). One is the Buffalo Cave speleothem, which shows a major episode of C_4 grass expansion at ~1.7Ma (Hopley et al. 2007a). Lee-Thorp et al. (2007) also place the largest shift to open grassy conditions at Sterkfontein and Swartkrans, based on enamel stable isotope analysis, shortly after 2Ma, possibly in connection with the onset of the Walker circulation. Evidence for conditions in the southern Kalahari come from a section in the Mamatwan Mine. A rapid replacement of the basin fill happens around 1Ma, helping to establish the modern savannah environment. For at least 420ka previously to that event, a permanent water body persisted in the region, which has been arid ever since (Matmon et al. 2015). At ~ 0.8Ma, the glacial-interglacial cycles changed from a 41,000 year cycle to a 100,000 year cycle with more extreme glacials and interglacials and faster transitions due

to larger ice sheets in the northern hemisphere. This is known as the Mid Pleistocene Transition (MPT), leading to more rapidly changing and unstable climate conditions afterwards. One potential local source of environmental information during this time are tufas along the Ghaap Escarpment. The pilot study shows a gradual increase in $\delta^{18}O$ from the Plio-Pleistocene to the middle Pleistocene and to the Holocene (Doran et al. 2015). A similar trend is evident in the Makapansgat valley speleothems (Hopley et al. 2007a+b). In the faunal record, the time span 1Ma to 700ka is characterised by the Cornelian Land Mammal Age (LMA), which is a mixture of modern grassland fauna with remnants of woodland and closed habitat fauna (Hendey 1974). It is also the first LMA that develops a character distinct from East Africa. The following Florisian LMA (700ka-10ka) shows more developed mammal forms, the appearance of immigrant species and species which indicate wet environments (Brink 2005). While a mixed wooded grassland environment is coherent with the proxies described above, there is little local evidence for wet phases 700-200ka besides the faunal record.

One of the longest proxy records in South Africa is Tswaing Crater (~ 200ka) (Partridge et al. 1997). It is interpreted as showing low rainfall around 200ka, and wet conditions at the MIS6/7 interface. The Florisbad fauna and pollen too suggest a wet initial occupation of the glacial MIS6 and a rainfall maximum at 157ka, but also modern sub-arid conditions in later MIS6 (Brink 1988, van Zinderen Bakker 1989). Pollen from marine core GeoB1711-4 off Namibia show cool and moist conditions in MIS 6, interpreted as an extension of the winter rainfall zone (Shi et al. 2001). The following interglacial MIS5 saw rising sea levels reaching their highest stand in MIS5e, and Tswaing Crater shows higher than present rainfall (Partridge et al. 1997). Fluctuating conditions dominate towards the MIS4 glacial, with an insolation minimum and possibly very dry conditions in the summer rainfall zone (Chase and Meadows 2007). Towards the Last Glacial Maximum (LGM), Tswaing Crater

shows lower rainfall levels (Partridge et al. 1997), with some wet spells mirrored at Wonderkrater at 50-30ka. The LGM is another phase where an expansion of the winter rainfall zone is proposed by reduction in summer insolation, intensification and equatorward movement of westerlies and, therefore, more rain in the interior (Chase and Meadows 2007). Marine core leaf wax isotopes are interpreted as showing a wetter LGM over southern Africa (Collins et al. 2014). This is opposed to Gasse et al. (2008) who suggest more site variation and a drier rather than wetter LGM. This is supported by the southern coast Uitenhage Aquifier (Heaton et al. 1986) and Cango Cave stalagmites (Talma and Vogel 1992), both indicating lower rainfall over southern South Africa 21-18ka. Warming after the LGM is disturbed by the Younger Dryas around 12.9ka in the northern hemisphere (Rasmussen et al. 2006), a short period of return to near glacial conditions. The Younger Dryas signal is not found consistently in records in southern Africa, sparking debates about its severity and possible lag compared to the northern hemisphere. Many records show arid conditions, while others show moisture instability (e.g. Holmgren et al. 2003, Chase et al. 2011, Truc et al. 2013, Green et al. 2015). In the Northern Cape, pollen sequences, including Wonderwerk Cave and Equus Cave, indicate dry woodland and lower temperatures before 17ka and warmer conditions after. Moisture oscillations appear 23-11ka, with peaks at 17ka, 14.6ka and 12.6ka. The records show consistent dry conditions during the Younger Dryas. These northern interior proxy records often display opposite patterns to eastern savannah sites like Wonderkrater and Tswaing Crater (Scott et al. 2012).

Holocene climate and environment

A systematic review of the Holocene climate in the interior, including data from Rose Cottage Cave, Equus Cave and Florisbad finds that conditions were generally warm and/or arid after the Younger Dryas; with warmer and wetter conditions 7-5ka and an aridification trend after 5ka (Scott and Lee-Thorp 2004). A number of specialist grazer species go extinct

at the end of the Pleistocene and the start of the Holocene in South Africa, including *Antidorcas bondi*, *Equus capensis*, *Megalotragus priscus* and *Damaliscus niro* (Brink 2005). Increased aridification, leading to a lower net production of the ecosystem, has been proposed as a reason for the extinctions (Brink and Lee-Thorp 1992), leading to increased competition between grazer species (Thackeray 1984). The Holocene fauna of southern Africa is similar to the Florisian fauna, without the wetland species and the large number of specialist grazer species (Brink 2005).

A recent review of pollen data showed two sets of contrasting records in the summer rainfall zone, with increase in rainfall during the Holocene (e.g. at Wonderkrater, Tswaing Crater) in one set of records, and another set showing dry periods 5-7 cal. BP (e.g. at Blydefontein, Braamhoek, Equus Cave, Florisbad, Lake Eteza) (Chevalier and Chase 2015). There is limited evidence for an Altithermal (climatic optimum) in the mid-Holocene in South Africa (~7000-4500 BP) with higher temperatures than today and increased summer rainfall, the opposite result of the pollen review. Another review of pollen records using different methods of reconstruction proposes signs of increased moisture at 7-8ka at several sites, and cooler temperatures after 6ka in the Holocene. Around 2ka most records show a dry event with reduced summer rainfall (Scott et al. 2012).

In general, the Holocene climate conditions seem highly variable. Modern rainfall data over the last millennia show synchronicity between the northern and southern hemisphere rainfall zones (Nicholson 2000). It follows the timescales of the global ENSO system and SST variations, showing the connections across the southern hemisphere. The late Holocene and the last centuries have seen a consistent aridification trend in the summer rainfall region (Nicholson 2001, Scott et al. 2012). In the Northern Cape, proxy records show the early Holocene (11-7.5ka) was relative arid, warm and open. The following 7.6 to 5.1ka records have evidence of increased moisture, but the drivers are unclear. The

Northern Cape shows further variability with a warm wet spell 4.3-3.2ka and a dry cool spell 3.2-2.6ka. Evidence of increased C_4 grasses might be related to further concentration of rainfall in the summer (Scott and Lee-Thorp 2004). The following part 2.4 will show which archaeological developments happen in South Africa during the climate and environment changes discussed above. The biome, faunal and aridity changes clearly changed the resources available for hominins, but connections between cultural and environmental change are far from being proven.

2.4 The Stone Age archaeology of South Africa

South Africa has a long tradition of archaeological research. Stone artefacts have been collected in South Africa since the 1850s, and the first excavations took place in the 1880s, led by amateurs (Deacon 1990). John Goodwin was, from 1923 onwards, the first trained archaeologist working in South Africa. The terms Early Stone Age (ESA), Middle Stone Age (MSA) and Later Stone Age (LSA) were first proposed by Goodwin and van Riet Lowe (1929) and still provide the framework for South African archaeology today. This chapter provides an overview of the current state of research in South African archaeology for the time periods relevant to this thesis, with an emphasis on the archaeology of the interior and the Northern Cape. Hominin fossils from the ESA time period in South Africa are *Australopithecus sediba* (Berger et al. 2010), *Paranthropus robustus* (Thackeray et al. 2001) and *Homo ergaster/erectus*. Although all might have made stone tools, the conventional view is to associate *Homo* species with lithics. During the MSA, the modern *Homo sapiens* develops (Klein 2009).

2.4.1 Early Stone Age (ESA)

Lithics appear around two million years ago in South Africa, attributed to the Oldowan industry (Lombard et al. 2012). Archaeological sites in the Northern Cape with Oldowan

artefacts include Wonderwerk Cave (Chazan et al. 2012) and Kromdraai A (Kuman et al. 1997), whereas Sterkfontein Member 5 in Gauteng has currently the oldest dated Oldowan assemblage in southern Africa (Granger et al. 2015). The Oldowan technology consists of cores, core tools and flake tools with little retouch as well as hammerstones and manuports. Handaxes, cleavers and other bifacially worked tools are characteristic of the Acheulean which followed, and are found in Strata from around 1.5 million years ago onwards (Lombard et al. 2012). Other characteristic Acheulean tools are cleavers, large flakes, and some first retouched flakes. A transition to more refined and smaller handaxes appears in the late Acheulean after 600ka (Chazan et al. 2008).

Evidence for the earliest intentional use of fire by hominins comes currently from Wonderwerk Cave (Chapter 3; Berna et al. 2012). Art is not known from the ESA, but mineral pigments (ochre) have been introduced by hominins in Acheulean sites such as Wonderwerk Cave, Kathu Pan and Duinfontein 2 in the Northern Cape (Cruz-Uribe et al. 2003, Beaumont and Vogel 2006). Conclusions as to the origins of hunting behaviour, as opposed to scavenging, and the volume of meat in the diet of hominins remain contested, especially for the Oldowan time periods. Most faunal remains at ESA sites are more likely to reflect natural accumulations rather than hunting remains. It is generally assumed that *Homo ergaster/erectus* played a more active role in hunting than earlier hominins, although the oldest evidence for hunting comes from Europe (Klein 2009). Stable carbon isotopes on *Homo ergaster/erectus* teeth from Swartkrans Cave show a considerable breadth of diet, which could include seeds, fruits, nuts, insects, and meat (Lee-Thorp et al. 2000, van der Merwe et al. 2003). The proportion of meat versus plant food cannot be determined with this method.

The transition to the following Middle Stone Age (MSA) is evident in assemblages dating to 200-300ka, comprising of a mix of large blades and points, Levallois technology, bifaces

and scrapers (Lombard et al. 2012). The terms Fauresmith and Sangoan have been used to describe those transitional industries (Underhill 2011), but their characterization is quite unclear. Notably, many ESA sites in South Africa are situated in the interior and few along the coastline, compared to later time periods, although changing sea levels have to be considered (Compton 2011).

2.4.2 Middle Stone Age (MSA)

The transition from handaxe dominated lithic technology (Mode 2 technology) to the use of Levallois technique (Mode 3 technology) took place between 300,000 and 130,000 years ago in Southern Africa. Rarity of sites provides some explanation for why so little is known about the lithic technology at the beginning of the MSA. Artefacts are made mainly with discoidal or Levallois flake technology, with some blades from volumetric cores (Lombard et al. 2012). Main tool types are scrapers, points and denticulates (Klein 2009). Theories about the MSA succession were long dominated by the sequence published by Singer and Wymer (1982) from their excavations at Klasies River as well as following frameworks by Volman (1981) and Wurz (2002). Those frameworks are based on a division of the MSA stone tool technology on morphological similarities between sites (Table 2.1). Despite the availability of more direct dates and more sites, they remain a major influence on how to divide the MSA in South Africa.

Singer and Wymer 1982	Volman 1981	Wurz 2002	Lombard et al. 2012	Characteristics in lithic technology
	MSA 1		Early MSA	Few formal tools, short broad flakes
MSA I	MSA 2a	Klasies	Klasies River	Few formal tools, mostly denticulates, scrapers, bifacial points; quartzite dominates
MSA II	MSA 2b	Mossel Bay	Mossel Bay	More retouched pieces, unifacial and bifacial points
			Pre-Still Bay	Currently undetermined
		Still Bay	Still Bay	bifacial, leaf-shaped points
Howiesons Poort	Howiesons Poort	Howiesons Poort	Howiesons Poort	Backed pieces; more fine-grained rocks as raw material
MSA III	MSA 3	Post-Howiensons Poort	Sibudu	Heterogeneous assemblages, often unifacial levallois points, Sibudu type points
MSA IV	MSA 4		Final MSA	High regional variability

Table 2.1: Comparison of different proposed frameworks for the MSA.

Of particular research interest in current years were the two very short and innovative industries that appeared within the MSA in the period 80-60ka, namely: the Still Bay and the Howiesons Poort. The reasons for their appearance and sudden disappearance are enigmatic. So far, the Still Bay seems to be restricted to South Africa's coast and little is known about this time period from the interior. The Howiesons Poort industry occurs in archaeological sites throughout southern Africa and is characterised by backed or truncated flakes and blades or segments, often on exotic raw materials. With the international research focus on Still Bay and Howiesoons Poort in recent years, the following MSA

periods have been largely neglected. Often assemblages are heterogeneous and consist of unifacial points, scraper or knives and are often associated with changes in raw material.

Modern behaviour, meaning the behaviour of anatomically and/or cognitively modern humans is indicated by finds from coastal sites >100ka in South Africa (McBrearty and Brooks 2000), including engraved ochre (Henshilwood et al. 2002, Mackey and Wetz 2008), "art workshops" (Henshilwood et al. 2011), shell beads (d'Errrico et al. 2005, d'Errico et al. 2008), the use of bedding material (Wadley et al. 2011), incised ostrich eggshell (Texier et al. 2010), and incised bone and bone tools (Henshilwood et al. 2001, d'Errico et al. 2012). Coastal sites also show the emerging use of marine resources by MSA foragers through shellfish, fish, and marine mammal remains. A further characteristic of the MSA includes hunting of all sizes of bovids (Deacon and Deacon 1999). Most of the rare sites in the interior from this time period are not fully analysed and published yet (e.g. Erfkroon, Churchill et al. 2000; Wonderwerk, Beaumont and Vogel 2006), so little is known about the appearance of modern humans or the transition to LSA lithic technology.

The transition to the Later Stone Age is marked by regional differences, and includes the appearance of microlithic tools (Lombard et al. 2012). Some sites show a dominance of hollow-based points (Sibudu, Wadley 2005b; Umhlatuzana, Kaplan 1990), or bipolar technology (Klein Kliphuis, Mackay 2006, 2010; Umhlatuzana, Kaplan 1990). The transition took place during the MIS3 to MIS2 interglacial-glacial phase. A population bottleneck due to an inhospitably cold and dry climate have been discussed at times in connection with MIS3, however with little environmental data to support such a claim (Mitchell 2008). About two thirds of MIS3 sites in South Africa are in the grassland or mixed woodland biome, a clear shift from the greater focus on coastal sites during earlier MSA periods.

2.4.3 Later Stone Age (LSA)

The start of the LSA in South Africa comprises assemblages broadly between 40-20ka (Lombard et al. 2012). Early LSA assemblages are not well understood and there are no formal classifications of industries. The stone tools in most sites are microlithic and made on quartz, although some non-descriptive non-microlithic assemblages exist. A proposed water deficit in southern Africa around the Last Glacial Maximum has been proposed as one possible reason for the uneven distribution of sites (Wadley 1993). As in Chapter 2.3, there is contradicting environmental evidence as to whether the LGM was a wet or arid period in the interior.

Orton 2014	**Lombard et al. 2012**	**Humphrey&Thackeray 1983**
Early LSA	Early LSA	Early LSA
Late Pleistocene microlithic	Robberg	Robberg
Terminal Pleistocene/early Holocene non-microlithic	Oakhurst	Kuruman Industry
Holocene microlithc	Wilton	Wilton complex
Late Holocene assemblages	Final LSA Ceramic final LSA	

Table 2.2: Comparison of different frameworks for the LSA. Orton (2014) and Lombard et al. (2012) refer their classification to the whole of South Africa, whereas Humphrey&Thackeray (1983) use this classification especially for the Kuruman Hills and Ghaap Escarpment area of the Northern Cape.

The first formal technological group in the LSA is the Robberg, featuring microlithic tools made of bladelets and bladelet cores, which allow more advanced composite tools. Backed tools and ground stone work also occurs in some sites, e.g. at Umhlatuzana, Rose Cottage Cave and Elands Bay Cave (Wadley 1993). Still, those assemblages are generally small, scarce and not well dated, especially in the interior (Thackeray 1981). Archaeological visibility increases after 13ka, which is interpreted as colonization of previously

uninhabited areas and/or high population pressure with the transition to the Holocene (Wadley 1993). The Oakhurst (Sampson 1974) is the first Holocene LSA industry, a non-microlithic, bladelet-poor industry (Wadley 1993). The dominant raw materials are coarse-grained rocks, e.g. banded ironstone, quartzite, hornfels, dolerite, or dolomite. The few formal tools include variants of scrapers and adzes; blades are rare (Humphrey and Thackeray 1983). Regional variants result in a long time span published for the Oakhurst, from around 12 to 7bp. They are sometimes called Albany (southern and eastern Cape, Deacon 1984), Lockshoek (Karoo and Free State, Sampson 1974), and Kuruman (Northern Cape, Humphreys and Thackeray 1983).

The Wilton (Goodwin and van Riet Lowe 1929) is characterised by microlithic tools. The dominant tool types are small scrapers, backed blades and segments. Tool production is more standardized, with a wide repertoire of tool types including adzes, points, borers and notched artefacts. The wider use of fine-grained rocks, e.g. chert, chalcedony, jasper or quartz, is another visible difference to the Oakhurst (Mitchell 2005). This industry is much more visible over South Africa, but the best described assemblages are again from the southern and eastern Cape (Humphrey and Thackeray 1983, Lombard et al. 2012). Changes occur in the tool types and frequencies within the Wilton itself, with a higher percentage of backed blades and different raw materials after 6-4ka (Humphrey and Thackeray 1983, Barham and Mitchell 2008). Bone working is more abundant than in the MSA or early LSA assemblages, as well as the frequent presence of decorated OES fragments and OES beads, shell beads, engraved stones and rock paintings.

Ceramics were introduced into the Wilton shortly before 2000 years before present (Mitchell 2005). In the Northern Cape, this introduction has taken place without visible breaks in the lithic technology (Humphrey and Thackeray 1983). Only three areas in the Northern Cape have been studied intensively for the LSA so far: the Kuruman Hills and the

Ghaap Escarpment (Humphrey and Thackeray 1983), the Orange River (Sampson 1974) and the Namaqualand region (Orton 2012). These isolated areas show differences between each region and compared to other areas of South Africa. One of the reasons could be that there is no unique definition of the term 'microlithic', resulting in different categories used for the same artefact group by different authors (Orton 2014). Another reason is that the meaning of 'Wilton' changed since the first excavation of Wilton Rockshelter by Hewitt in 1921, and is only used for part of this assemblage today. Table 2.2 shows the different proposed frameworks and terms resulting from discussions in the last years (Lombard et al. 2012, Orton 2014). In this thesis I follow the framework used in most publications about Wonderwerk Cave itself; and closest to Lombard et al. (2012). These terms should be treated as flexible and not as separating different groups of people or drawing a strict line to other parts of the country. The archaeozoological record shows a trend to the hunting of more dangerous animals in the LSA compared to the MSA. Most hunted fauna is migratory plains game, with a trend for increased hunting of browsers. Tortoises, marine resources, fish and small game is exploited more intensively (Klein and Cruz-Uribe 1987, Klein 2009). By this time, hunting with bow-and-arrow has become widespread (Deacon 1995). Although the origins of this technology have been discussed for earlier times (Lombard and 2012), its use at this time is proposed to correlate with increased hunting of individual small browsing antelopes rather than hunting of large herbivores in herds.

2.5 Summary

The paucity of terrestrial archives and the fragmentary nature of existing records prevents a cohesive summary of past climate in southern Africa and its environmental changes. Equally, there is no consensus on the importance and interaction of the possible drivers. Most reconstructions rely in large part on data from marine cores, global climate archives

and computer models. Between 2Ma and 200ka, the general trend is a spread of C_4 grasses to establish the modern vegetation in the summer rainfall zone and a gradual aridification trend. The larger amount of late Pleistocene data, mainly from pollen and speleothem isotopes, highlights regional differences. The eastern sites like Wonderkrater and Tswaing Crater are still the longest and most cited by palaeoclimatologists and archaeologists, and are subject to ongoing research (Backwell et al. 2014, Schmidt et al. 2014). New data from Wonderwerk Cave and other northern interior sites will clarify the regional picture, as the trends in one region do not appear to always be mirrored in other regions of southern Africa. The lack of terrestrial archives is also reflected in the lack of well-dated archaeological sites. Although Southern Africa's interior has many ESA sites, most do not span long sequences. Many are karstic infill sites or open air sites with poor preservation of organic material. The interior lacks the fine-layered MSA sites that are found along South Africa's south coast, and so little is known about the timing and distribution of important innovations, as well as regional variations. Research into the Northern Cape LSA sites has been neglected over the last 20 years, and is in need of more investigations with modern excavation techniques and analytical methods. It is therefore essential for archaeology, environmental and climate science to work together to fill the gaps and illuminate more of southern Africa's rich past.

Chapter 3 - The site of Wonderwerk Cave

This chapter introduces the site of Wonderwerk Cave, from which the material in this thesis was recovered in archaeological excavations. Described are the setting of the site in the surrounding landscape, its history of research and the current state of analysis of cultural remains. Special emphasis is placed on introducing the stratigraphy and dating to provide a framework for the following radiocarbon and isotope samples analysed in this thesis, as well as on environmental proxies from the site as comparison to my own results.

3.1 Location and description

Wonderwerk Cave is located in the Northern Cape province of South Africa, at the eastern flank of the Kuruman Hills, 1660m above sea level (27°50'46''S, 23°33'19''E). It is halfway between the modern towns of Kuruman and Danielskuil, about 45km from each town (Fig. 3.1) (Beaumont 1990a). Wonderwerk Cave is on the geological border between the Ghaap plateau dolomites and the banded ironstone, jasper and chert of the Kuruman hills. Those hills are up to 400m high (relative to the plain) and run north-south. Outcrops of banded ironstone are visible on their slopes. The valleys are filled with aeolian sediment from the Kalahari (Matmon et al. 2011). Wonderwerk Cave is located at the base of a 121 metre high conical hill (Humphrey and Thackeray 1983). Considering the wider region, Wonderwerk Cave is located west of the Vaal-Harts river valleys, the Ghaap Escarpment and the Ghaap Plateau (Fig. 3.1). To the south is the Postmasburg/Sishen Area with known specularite deposits. To the west are the Langeberg Mountains and northwest the southern edge of the Kalahari.

The cave is 140m long and 10 – 26m wide, with a height above the modern floor between seven and three metres, comprising about 2400m^2 (Fig. 3.2). The only entrance is 24m wide

and overlooks the Ghaap Plateau in north-northwest direction (Fig. 3.3A) (Beaumont 1990a). The entrance probably extended further forward in the past (Rüther et al. 2009, Brook et al. 2015). The cave is situated in dolomites of the Late Archaean-Early Proterozoic Ghaap Group, which is overlain by banded ironstones of the old Ghaap Plateau (Goldberg et al. 2015). It formed as a solution cavity in the dolomitic limestone. Roof weaknesses are indicated by calcareous nodes and little stalagmites, which are inactive nowadays. The largest is a stalagmite 20m into the cave from the modern entrance (Fig. 3.3B) (Beaumont 1990a). The natural vegetation cover around the cave today is dry savannah, with no permanent water source nearby (Fig. 3.3D). The nearest known water sources are a spring zone on a hill slope 5km to the south and a sinkhole called Boesmansgat 12km to the southeast (Fig. 3.1). A stream channel exists in front of the cave 5-6m below the level of the modern entrance. Remnants of fan gravels, possibly from a former pan, were found 120m north of the site (Goldberg et al. 2015).

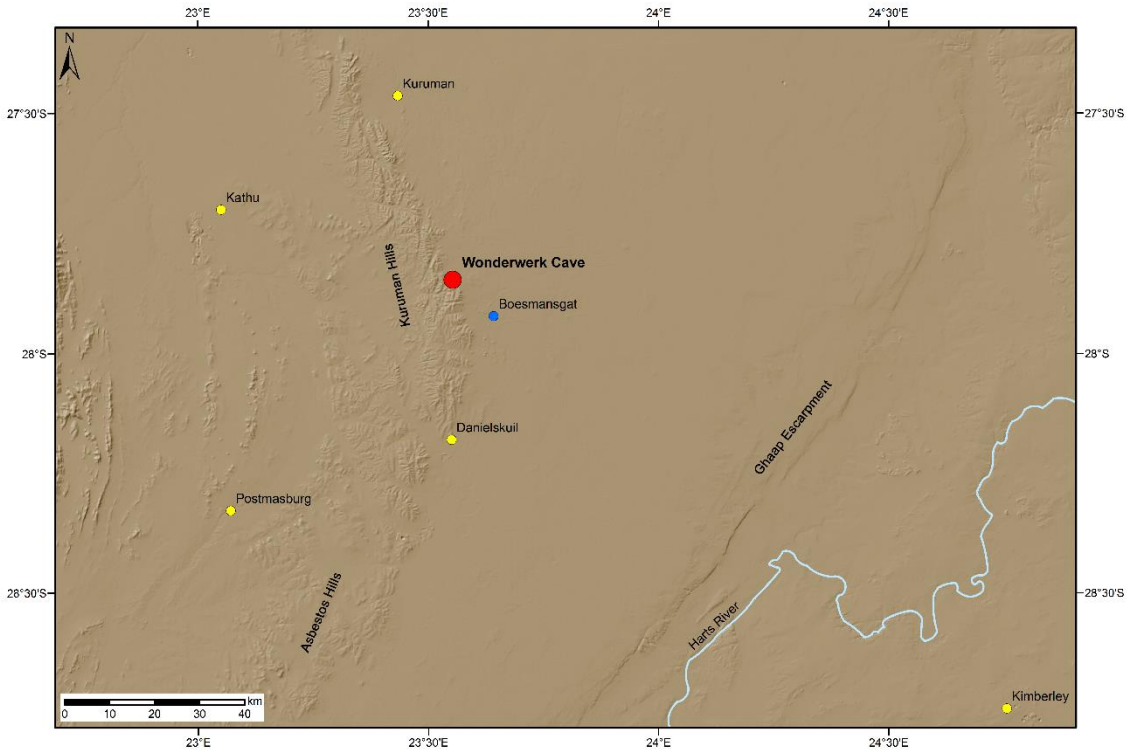

Figure 3.1: Map of the local area with Wonderwerk Cave highlighted in red, modern towns in yellow and the closest permanent water source, the Boesmansgat, in blue (Map created by C. Green).

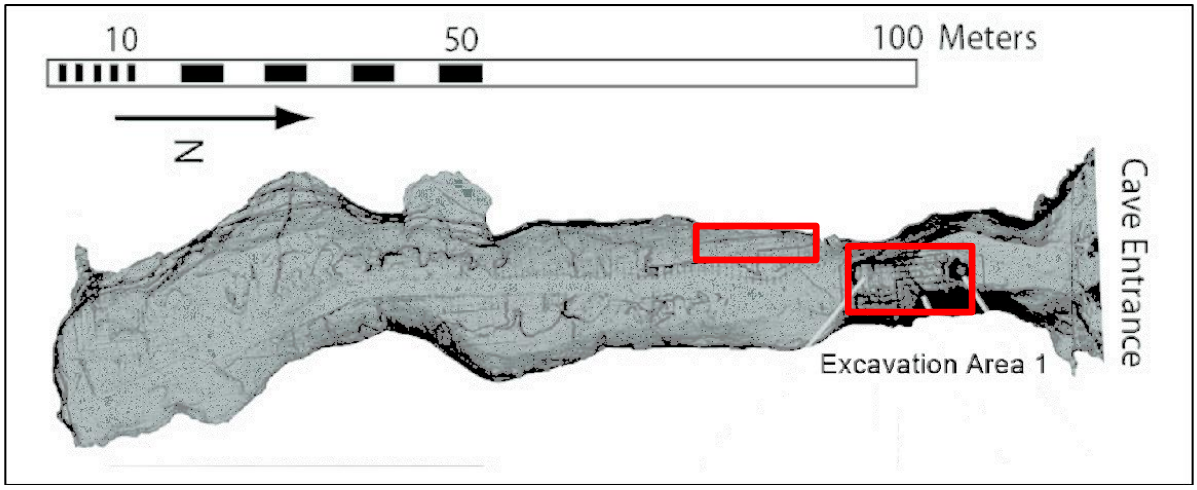

Figure 3.2: Scan of Wonderwerk Cave, after Chazan et al. (2012). Red boxes highlight Excavation area 1 (right) and 2 (left).

3.1.1 Modern climate

Wonderwerk Cave is on the southern edge of the Kalahari, in today's summer rainfall region. The boundary with the winter rainfall region is 450km to the west. Mean daily temperatures are 24°C in January and 10°C in July. The site is located just west of the 400mm isohyet (van Zinderen Bakker 1982). Meteorological data collected at Wonderwerk farm shows mean annual rainfall (MAR) in the years 1957 - 1979 to be 421mm. Most rainfall occurs January to March, when thunderstorms are common. Winters are cold and dry, with moderate frost (Beaumont 1990a). The nearest station with meteorological data on both temperature and rainfall is at Kuruman. It is also the location of a permanent spring, called the 'Eye of Kuruman'. The region has water deficiency all year round, but springs and pans fill up after heavy rainfall.

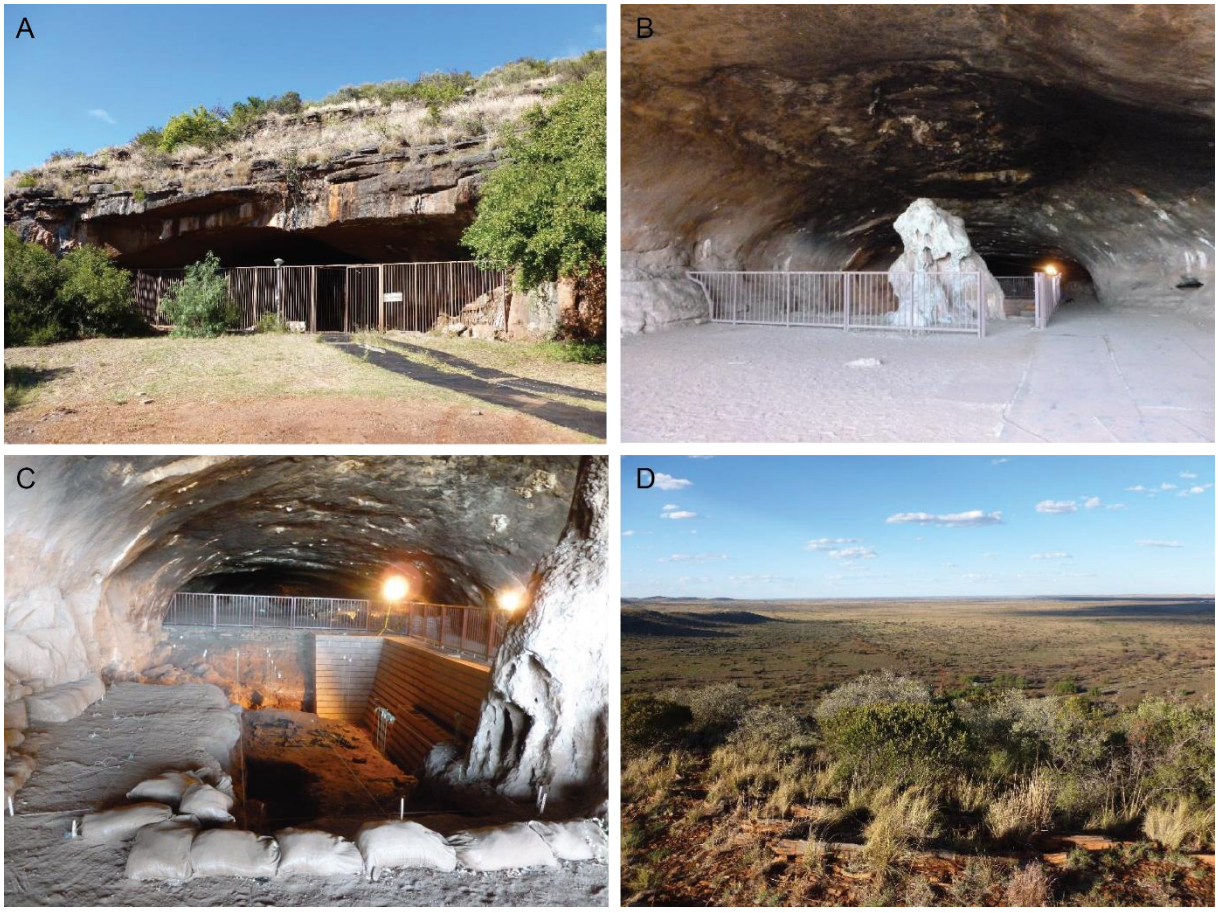

Figure 3.3: A: Modern entrance to Wonderwerk Cave. B: In the entrance area, looking into the cave towards Excavation 1. Notice the large stalagmite in the middle. C: View

into Excavation 1. D: View from the top of Wonderwerk Cave to the northeast, over the Ghaap Plateau. The Kuruman Hills are at the left side of the picture.

3.1.2 Modern vegetation

The vegetation around Wonderwerk Cave is classified as belonging to the savannah biome according to Mucina and Rutherford (2006), further specified as Kuruman mountain bushveld (SVk 10). On the plain to the east of Wonderwerk open shrub-bushveld occurs (SVk 8, Kuruman Vaalbosveld) with a dominance of *Tarchonanthus camphoratus*, as well as some *Acacia*, *Rhus ciliate* and *Grewia flava*. River courses often have dwarf shrub vegetation (Van Zinderen Bakker 1982, Mucina and Rutherford 2006). Some areas have 'bush clumps' with *Olea africana* concentrations as well as *Acacia karroo, Acacia trotilis, Rhus* sp., *Grewia flava* and *Boscia albitrunca* (Werger 1978). Effects of overgrazing are visible, resulting in a dominance of *Rhigozum trichotomum* and *Tarchonanthus camphoratus*. To the north the vegetation changes to Kuruman Thornveld (SVk 9), while farther to the west it grades into Kuruman Bushveld (SVk 12) (Mucina and Rutherford 2006).

Pollen collection on surfaces in the wider Wonderwerk area by van Zinderen Bakker (1982) shows consistency with vegetation surveys by Thackeray (1984), T. Anderson (1991) and a short survey in 2013. In December 2013, Marion Bamford (University of the Witwatersrand) and I conducted a small plant survey in front of Wonderwerk Cave and up the left-hand site of the Wonderwerk hill. All plants were identified by M. Bamford. There is no significant difference visible between the Ghaap plateau and the Kuruman hills vegetation, although the plain might have proportionally more *Acacia, Rhus* and more varieties of grass species. The results of our survey are listed in Table 3.1. All are indigenous species adapted to arid, open or rocky habitat. Wonderwerk is in an area that supports both grazers and browsers due to its mosaic of open shrub- and grassland, small

trees and rocky slopes as well as flat plains. The trees show a mixture of small to medium sized species. This is in no way an extensive or systematic survey. The species found also overlap with the list of tree, shrub and grass species in the Northern Cape by Thackeray (1981).

Latin name	Common name
Trees and Shrubs	
Acacia sp.	Acacia / Thorn tree
Asparagus sp.	Asparagus
Croton gratissimus	Lavender Croton
Diospyros sp.	Ebony tree family
Euclea sp.	Guarri
Euclea undulata	Common Guarri
Grewia sp.	Raisin bush / Brandy bush
Justicia sp.	Daisy bush
Labeckia sp.	Bushman's thorn tree
Maytenus heterophylla	Common spike-thorn
Olea africana	Wild Olive
Rhus burchelli (Searsia burchelli)	Karee
Rhus ciliate (Searsia ciliate)	Sour Karee
Rhus lancea	Karee
Tarchonanthus camphoratus	Camphor bush
Ziziphus mucronata	Buffalo thorn
Grasses	
Cymbopogon sp.	Lemon grass
Eragrostis sp.	Love grass
Poaceae family	Bunchgrass
Setaria sp.	Broad leaf grass

Table 3.1: Latin and common names of flora identified during a plant survey around Wonderwerk Cave in 2013.

3.1.3 Modern fauna

Historic records by early travellers in the 19th century passing through the area describe carnivores like lion (*Panthera leo*), hyena (*Crocuta crocuta*) and jackal (*Canis mesomelas*), as well as large game like zebra (*Equus burchelli*), quagga (*Equus quagga*), white rhinoceros (*Ceratotherium simum*), giraffe (*Giraffa camelopardalis*), wildebeest (*Connochaetes* sp.), roan (*Hippotragus equinus*), hartebeest (*Alcelaphus buselaphus*), buffalo (*Syncerus caffer*), eland (*Taurotragus oryx*) and ostrich (*Struthio camelus*) (Thackeray 1981). The biomass today is significantly lower due to modern development and farming. Only smaller mammals are spotted in the Kuruman hills today, e.g. jackal (*Canis mesomelas*), springhare (*Pedetes capensis*), porcupine (*Hystrix africaeaustralis*), duiker (Cephalophinae), hyrax (*Procavia capensis*), warthog (*Phacocherus* sp.), bushpig (*Potamochoerus larvatus*) and steenbok (*Raphicerus campestris*) (survey by C. Anderson 1991). Modern game farms in the area stock mainly springbok (*Antidorcas marsupialis*), gemsbok (*Oryx gazella*), hartebeest (*Alcelaphus buselaphus*), wildebeest (*Connochaetes* sp.), zebra (*Equus* sp.), kudu (*Tragelaphus strepsiceros*) and eland (*Taurotragus oryx*) (Humphrey and Thackeray 1983, Beaumont 1990a, pers. observations).

3.2 Research history

The first description of the cave was given by Methuen (1846), a traveller who noted the 2.5m high stalagmite a few metres into the cave and the Holocene rock art on the walls. In the first half of the 20th century, the cave was used as a living space (1909-1911) and sheep shelter (till the 1930s) by P. E. Bosman, the farm owner. His brother, N. J. Bosman, also dug up to 2.5m deep in the back of the cave in search of guano to sell between 1940 and 1944 (Beaumont and Vogel 2006).

First archaeological investigations began with a visit in 1940 by B.D. Malan and a one week test excavation in 1943 by B.D. Malan and L.H. Wells (Malan and Cooke 1941, Malan and Wells 1943). Some further excavation work was undertaken by the University of California Expedition in 1948 (Fig. 3.4) (Camp 1948). K.W. Butzer (University of Chicago) studied sediment collections and the sections of Wonderwerk between 1974 and 1977 (Butzer et al. 1978, Butzer 1984a, b). The most extensive excavations were carried out by P. Beaumont from 1978 onwards, joined by J.F. and A.I. Thackeray for two seasons in 1979, and carried on until 1996 (Thackeray et al. 1981, Humphreys and Thackeray 1983, Thackeray 1984, Beaumont 1990a, 2004a, Beaumont and Vogel 2006). Altogether, seven excavation areas were opened in different parts within the cave, the largest being Excavation 1, followed in size by Excavation 6 at the back of the cave (Beaumont and Vogel 2006). Questions of palaeoclimate and palaeoenvironment were always investigated parallel to the archaeological analysis through pollen, microfauna and macrofauna analysis, which are described below (paragraph 3.5).

New investigations of an international research team under M. Chazan (University of Toronto) and L. K. Horwitz (The Hebrew University of Jerusalem) started in 2004 with the aim of obtaining new samples for absolute dating and geomorphological analyses, and analysing cultural material from Beaumont's excavations (Chazan et al. 2012). In 2013 the project was expanded to also include new excavations.

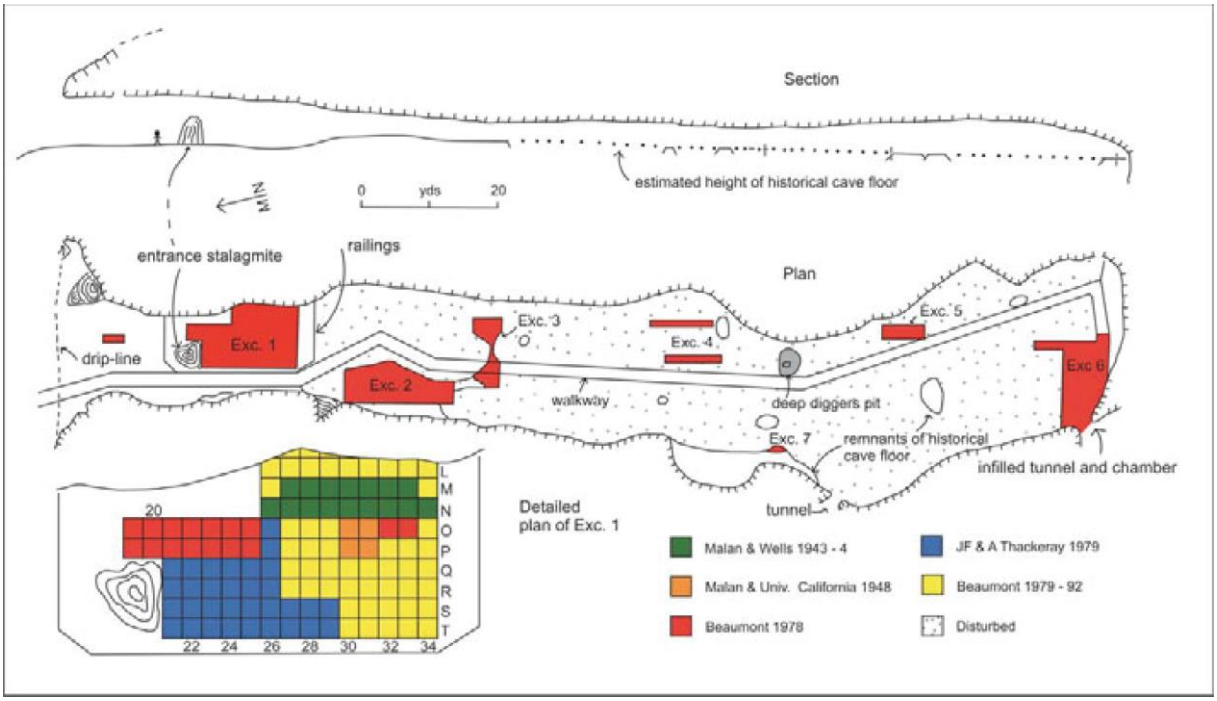

Fig. 3.4: Excavation areas in Wonderwerk Cave and detailed plan of previous work in Excavation 1 by excavator (from Beaumont and Vogel 2006, Fig. 2).

3.3 Stratigraphy and dating

The focus in this chapter is on Excavation areas 1 and 2, where the material for this thesis is from. Excavation 1 consists of up to 3m of Holocene deposits and approximately 4m of Pleistocene deposits. Correlations of Beaumont and Thackeray's excavations are possible; there is more uncertainty in correlating with Malan's excavation squares. Due to the significant time gap between the Holocene and Pleistocene strata, and the different excavators and dating methods used accordingly, both sections are described separately.

Excavation 1 Holocene

The stratigraphy of Strata 1 to 5 are described in Table 3.2 (Thackeray 1981, 2015; Beaumont 1990a). During the excavation, natural layers were divided into spits of 50mm, following the natural slope. Spits were given Roman numbers, e.g. 4aI, 4aII (Humphrey and Thackeray 1983; Table 3.3).

Stratum	Description	Lithic industry
1a	modern sheep and cattle dung	
1b	stone rubble from guano diggers, dung	
1a-c	general use of cave as a shelter after 1911	
2a	built floor, probably by Bosman when he lived in the Cave in 1910	
2b	dung and twigs in dark brown sand	Ceramic LSA/Wilton
3a	soft dark brown sand	Ceramic LSA/Wilton
3b	guano and minor roof spall in soft dark brown sand	Wilton
4a	red brown soft sand	Wilton
4aLH	high concentration of artefacts in reddish sand (LH=Living horizon)	Wilton
4b	red-brown sand	Wilton
4c	travertine sheets with interbedded beige sand	Wilton
4d	red brown to orange sand, roof spall, ash lenses, slabs	Oakhurst
5a	small subangular pebbles in a compact matrix	?
5b	small subangular pebbles in a softer matrix	?

Table 3.2: Stratigraphy of the Later Stone Age Strata in Excavation 1 after Thackeray (1981, 2015).

All Strata thin out backwards of the stalagmite (Fig. 3.5). The origin of the pebbles in Stratum 5 is unsolved, but the Stratum slopes towards the dripline. Therefore, fluvial transport or frost have been suggested as its origin. The stalagmite broadens at its base, with the maximum extent in Strata 4c/4d (Beaumont 1990a). Features include a modern rubble pit, probably from the guano diggers in squares O24-25, P23-25, Q24-35 and R25 as well as two postholes from a tent in square R22, Stratum 2a (Humphrey and Thackeray 1983). Another feature-like element is Stratum 4aLH, which does not extend throughout all squares, and was thought originally to be a living horizon (Thackeray 2015).

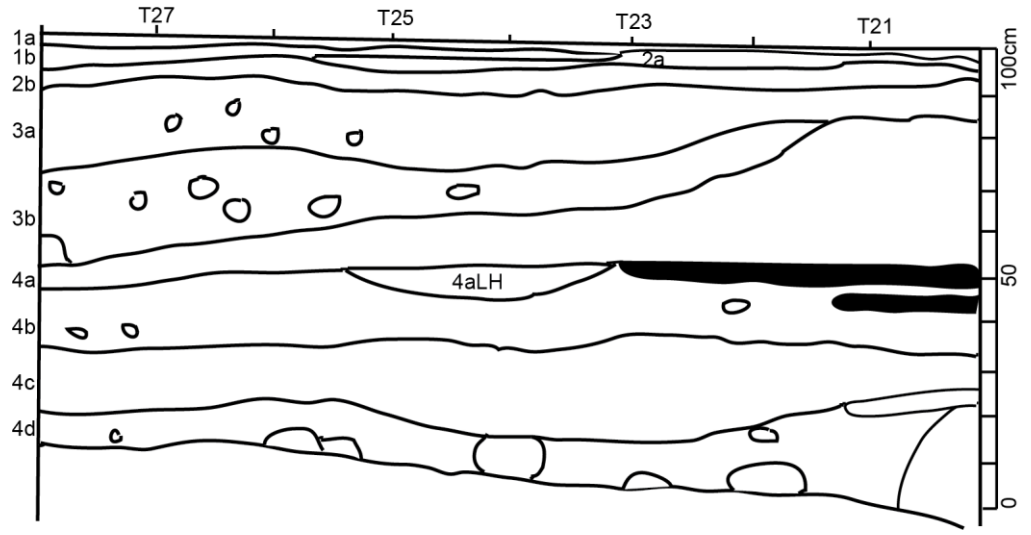

Figure 3.5: Re-drawn profile from Thackeray (1981) of the Holocene Strata in Excavation 1 along the T-line. Note varying thickness of strata. Black areas indicate flowstones next to the stalagmite.

The LSA sequence is dated by radiocarbon dating. The dates and a full discussion follow in Chapter 4. One U-series date from a stalagmite gave an age of 4.1 ± 1.2 ka (Beaumont and Vogel 2006), but we could not pinpoint from which Stratum it derived exactly. There are three so far unpublished OSL dates from the LSA strata, which agree with the radiocarbon dates (L. Horwitz, pers. comm.)

Beaumont	Thackeray (1981)	Lee-Thorp and Ecker (2015)
1	1	Modern
2	2a	Modern
3 UP	2b	2b
3 MID	3aI, 3aII	3a
3 LR	3b	3b
4aUP	4aI, 4aII	4aI
4a MID	4aIII, 4aIV	4aII
4a LR	4aLH	4aLH
4b Tufa 5	4bI	4bI
4b Tufa 6	4bII	4bII
4b RS 6/7	?	-

4c UP	4cI	4cI
4c LR	4cII	4cII
4d	4dI, 4dII	4dI, 4dII
5	5I, 5II	5I
5	5III, 5IV	5II

Table 3.3: Correlation of Excavation 1 Holocene spits.

Excavation 1 Pleistocene

Two test excavations in 1943 were dug in a guano digger pit 200m into cave and in what is now Excavation 1 in squares M33, N34 and N33 (Table 3.4). The diggers' pit yielded lithics made with Levallois technique, cores and scrapers on grey chert, overlain by LSA deposits. Lithics from Excavation 1 were attributed to the Fauresmith overlain by a rough, probable Levallois industry of weathered and partially water-worn chert. The overlaying LSA was attributed to the Smithfield A culture, including rich deposits of artefacts and OES with incisions (Malan and Wells 1943). An excavation by Malan and Wells for one month in 1944 in squares M-N 26-32 to a maximum depth of about two metres was never published. Malan and the University of California African expedition, Southern Part, excavated three weeks in 1948 in O-P 30-1, and reached bedrock in square P31. This is also largely unpublished other than a note in Camp (1948), but unpublished reports exist for both ventures. 25 handaxes were recovered 1943-44 by Malan from various areas in the cave (Beaumont 1990a).

Stratum	Square	Excavator
1	S+T 29-34, O 32-33, K-P 26-28, Q-R 26-34, O-P 19-24, P 32-33	P. Beaumont
2	S+T 29-34, O 32-33, K-P 26-28, Q-R 26-34, O-P 19-24, P 32-33	P. Beaumont
3	S+T 29-34, O 32-33, K-P 26-28, Q-R 26-34, O-P 19-24, P 32-33	P. Beaumont
4a	S+T 29-34, O 32-33, K-P 26-28, Q-R 26-34, O-P 19-24, P 32-33	P. Beaumont
4b	S+T 29-34, O 32-33, K-P 26-28, Q-R 26-34, O-P 19-24, P 32-33	P. Beaumont
4c	S+T 29-34, O 32-33, K-P 26-28, Q-R 26-34, O-P 19-24, P 32-33	P. Beaumont
4d	S+T 29-34, O 32-33, O-P 19-24, P 32-33	P. Beaumont
5	O 21-23, S+T 29-34, O 32-33, P 32-33	P. Beaumont
6	O21-23, S+T 29-34, O 32-33, P 32-33	P. Beaumont
ESA strata	P 32-33; O 32-33	P. Beaumont
1-4d	Q 21-23, R 21-24, S 21-28, T 21-28	A. and F. Thackeray
1-5b	O 25, P 25, Q 24-25, R 25, O 24, P 24	A. and F. Thackeray
~ 2 meters	M 33, N 34, N 33; M-N 26-33	B.D. Malan and L.H. Wells
Various	O-P 30-31	U. of California
12	Q 32, S 32, R 32	M. Chazan et al.

Table 3.4: Excavated squares in Excavation 1 of Wonderwerk Cave by Strata and excavator.

Subsequently P. Beaumont excavated into the ESA Strata in 1978-1982, 1985-1986 and 1989 (Table 3.4). Beaumont continued until 1993, extending Excavation 1 into one large area due to low artefact density. Until 1996, he and his teams worked on clearing out all the guano diggers' backdirt to establish correlations throughout the cave and follow Strata

using six smaller excavation pits. From 1997 until 2002, sorting continued of the sieved material in the McGregor Museum, including post-excavation artefact washing and labelling work (Beaumont and Vogel 2006).

Beaumont sub-divided his Pleistocene Strata with letters, e.g. a-c, but did not describe on what basis, so only full Strata are used in this thesis. He also used site-wide Major Units (MU) in publications (Table 3.5), but they are not based on detailed lithic, faunal, botanical analysis, continuous profiles or absolute dates, and are not used in recent publications (Berna et al. 2012). Malan and Wells (1943) established a grid system in square yards, which was kept by all subsequent excavators until 2013, when M. Chazan and team established a new digital grid system in metres, which is possible to correlate with the old system. All references to squares in this thesis follow the square yard system, as only material from excavations before 2013 was analysed. Measurements were taken in metres. There is one established metre point on the wall above Excavation 1, in other areas measurements were taken from the estimated historical surface (Beaumont and Vogel 2006). Beaumont divided Strata more than 10cm thick into 5 or 10cm spits, following the natural slope of the deposits. As the Strata are of differing thickness in the excavation area, and are slightly sloping, it is difficult to compare spits. Buckets were screened through 1mm mesh sieves (Beaumont 1990a).

The labelling of the Strata continued from the LSA section (Strata 1-5), therefore the ESA comprises Strata 6 to 12. All together the LSA deposits are of a more anthropogenic nature than the ESA strata. Strata 6-8 thin out south to north (towards the cave entrance). Strata 6 and 7 were originally differentiated on the basis of different roof debris content, but were considered subunits of MU4 later (Beaumont and Vogel 2006). Strata 9-12 were intensively studied by Goldberg et al. (2015). They divided archaeological Strata 9-12 into lithostratigraphic units 1-10 for micromorphology and FTIR work (Table 3.3). K. Butzer

provided the first sedimentological analysis of the Wonderwerk ESA strata. He notes the presence of wood ash throughout this sequence and the presence of well-sorted sands of exotic, sub-rounded, oxide-coated quartz of aeolian origin (Butzer 1984b), but his units cannot be correlated directly to the modern stratigraphy. Further detailed sedimentological descriptions can be found in Goldberg et al. (2015). Sediments in Wonderwerk are made of reddish, powdery, bedded silt and sands. The majority of sediment components are quartz and silty clay aggregates (Goldberg et al. 2015). Areas of roof fall are common. Some levels are diagenetically altered and dissolved, for example with calcite cements or secondary precipitation of phosphate. The sand fraction in the sediments is derived from the Kalahari, although it could have rested outside the cave thousands of years before being blown into it (Matmon et al. 2011). The silty clay aggregates are also wind-blown. Their source is possibly a pan or basin close by. Only Stratum 12 bottom shows fine laminations which are signs of water transport (Goldberg et al. 2015). Sheet-flow is a likely explanation for this deposit (Berna et al. 2012). A sterile deposit of bedded silts and clays has only been reached in Square 32 so far and this represents the base of the Wonderwerk sequence. Some centimetre-sized insect burrows and to a lesser extent some horizontal rodent burrows were identified in the sample section. It is therefore assumed that material was not moved more than possibly a few centimetres vertically (Birkenfeld et al. 2015). The analysis was done only on a very small profile and there are high degrees of variability in every stratigraphic unit. It is important to consider the sharp erosional contacts between many units, which show that sedimentation was not continuous (Goldberg et al. 2015).

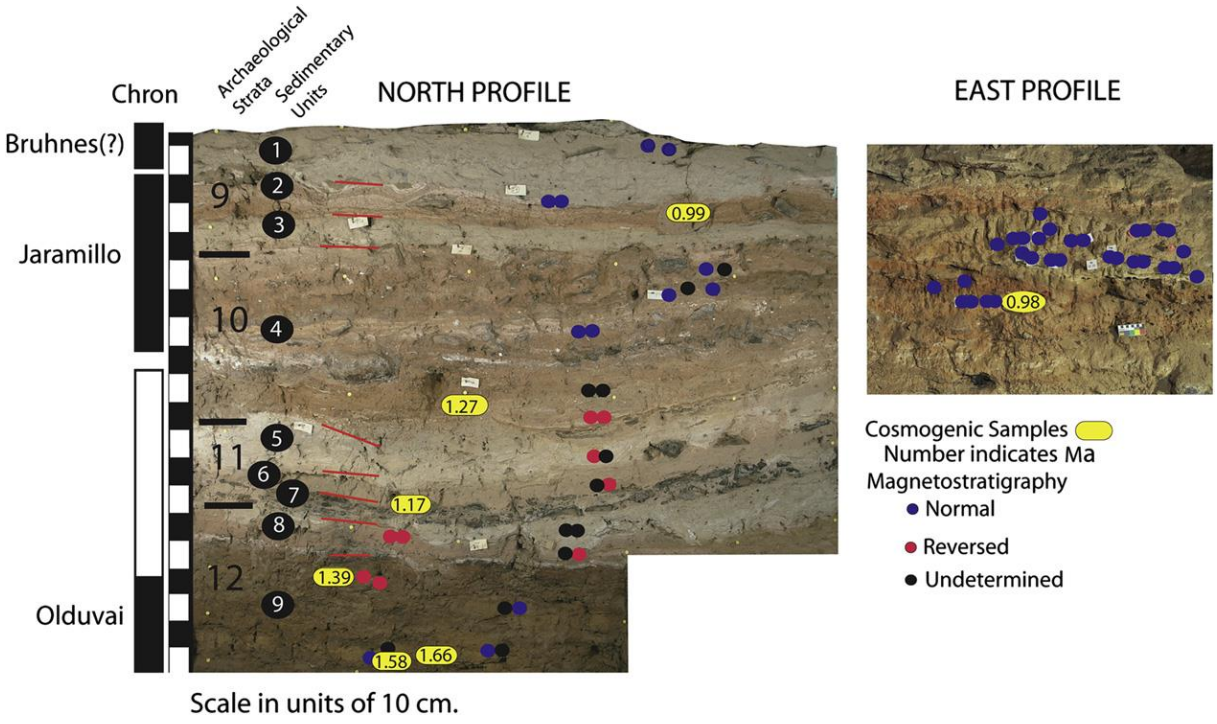

Figure 3.6: Excavation 1 dated profile Strata 9 to 12, including the position of dating samples (from Chazan et al. 2012).

The Wonderwerk ESA Strata are constrained chronologically by cosmogenic burial dating and palaeomagnetism (Table 3.6 and Fig. 3.6). There are additionally some OSL, U-series and U-Pb dates. It is important to remember that the different methods report different events. While radiocarbon dates on archaeological material date when humans used the cave, cosmogenic burial and OSL date when the sediment initially entered the cave. Palaeomagnetism shows when the sediment settled down and a stable magnetic signal was established, sometime after the initial entry. Considering this, offsets between dates from different methods are expected.

U-series dating on small 5-20cm stalagmites includes two dates in Excavation 1 Stratum 6 of < 349ka and <350ka, which are considered minimum ages (Beaumont and Vogel 2006). One OSL date from the top of Stratum 9 was beyond the saturation of quartz. Its calculated age of 256±21ka is a minimum age (Chazan et al. 2008). Two speleothems from Stratum 10 were dated by U-Pb dating, with ages of 0.734±0.069 and 0.839±0.026 Ma (Pickering

2015). Palaeomagnetic analysis was first performed by K.L. Verosub in 2001 in Excavation 1, followed by re-sampling in 2004 by H. Ron. The palaeomagnetic sequence of N>R>N>R>N has since been revised to N>R>N/N (N = normal polarity, R = reversed polarity) (Beaumont and Vogel 2006, Chazan et al. 2008, Matmon et al. 2011). Seven samples from the Excavation 1 dating profile (lithostratigraphic Strata 9, 6, 4 and 2) and six samples from Excavation 6 were analysed with cosmogenic two-isotope burial dating ($^{26}Al/^{10}Be$), magnetostratigraphy and grain-size distribution analysis. Simple burial period ages range between 2.6Ma and 1.6Ma. If corrected for the exposure rate, calculated from a transect of samples in the area of the cave, the burial ages of the sediment are between 1.85±0.23 Ma and 0.78±0.18Ma (Matmon et al. 2011). Uncertainties exist about the initial Al/Be ratios when sediment reached the cave and about how long sediment moved in the cave before reaching its final resting point. There are further uncertainties in comparing this method to the magnetism measurements. The maximum age is constrained to 2.58Ma, based on the occurrence of lithics, and that the cave mouth probably was not open before. These arguments and further archaeological finds favour an interpretation using minimum ages (Table 3.6), which implies Stratum 12 represents the end of the Olduvai subchron (1.96-1.78Ma). In upper Stratum 12 a magnetic reversal appears, continuing in Stratum 11. Stratum 10 is normally oriented and attributed to the Jaramillo subchron, leaving Stratum 11 to be dated between the Olduvai and the Jaramillo subchron (Matmon et al. 2011). A sedimentary break in Stratum 9 leaves the upper part of the ESA sequence still undated, somewhere between 350ka and 780ka. Current Amino Acid Racemisation dating on OES from the Pleistocene Strata of Excavation 1 shows a wide range of dates, some contradicting the current interpretation of strata ages (Penkman et al., pers. com.). This reflects the problems in the stratigraphy of Excavation 1 and we treat all dates as broad timespans rather than definite dates.

Exc. 1	Exc. 2	Exc. 3	Exc. 4	Exc. 5	Exc. 6	Major Unit	Lithostratigraphic units Exc. 1	Lithic association
1-4d	1	1		1		1		LSA
	2 a-b	2, 3		2	3 UP	2		MSA
5 a-b	3,4 a-e	4-6	4		3LR, 4	3		?
6,7 a-b	5				5	4		Acheulean
8a-e						5		Acheulean
9a-f						6	1,2,3	Acheulean
10 a-b						7	4	Acheulean
11						8	5,6,7	Acheulean
12a-c						9	8,9	Oldowan

Table 3.5: Stratigraphy of excavation areas in Wonderwerk Cave. Modified after Beaumont and Vogel (2006), with information from Berna et al. (2012) and Chazan et al. (2012).

Excavation 2

Excavation 2 is further into the cave beyond Excavation 1. Both areas are divided from each other by the modern walkway. Excavation 2 is on the right site of the walkway and substantially smaller than Excavation 1 (Fig. 3.2 and 3.7). Squares W-X 49-53 were excavated in 1981 (Beaumont 1990a) and comprise five strata. Stratum 1 is a thin LSA deposit, preceeded by a MSA level (Goldberg et al. 2015). Roof spall rubble are part of the sediment in Stratum 3, and major rockfall occurs in Stratum 4 (Fig. 3.7) (Beaumont and Vogel 2006). The MSA Strata is dated to between ~70 and >220ka on twelve U-series readings. Strata 3 and 4 upper (before the roof spall) are dated to 276-286 ka on three U-series measurements (Beaumont and Vogel 2006, Beaumont 2011). Stratum 4, after the roof fall, is currently undated. Stratum 5 is archaeologically sterile so far, and has one U-Pb date of ~500ka (Pickering 2015).

Excavation 6

Excavation 6 is the second largest excavation area with ~25m^2 and 2m depth, and is excavated into 3 large steps, and a little tunnel at the bottom leading to a recess in the cave

wall. A single U/Th date on a fragment of stalagmite recovered within the Fauresmith deposits gave a minimum age of 187±8ka (Beaumont and Vogel 2006). A palaeomagnetic sequence of the steps yielded R -> N, based on eight samples, but cannot be related with the cosmogenic burial ages in this part of 0.97±0.19 to 0.78±0.18Ma (Chazan and Horwitz 2009, Matmon et al. 2011).

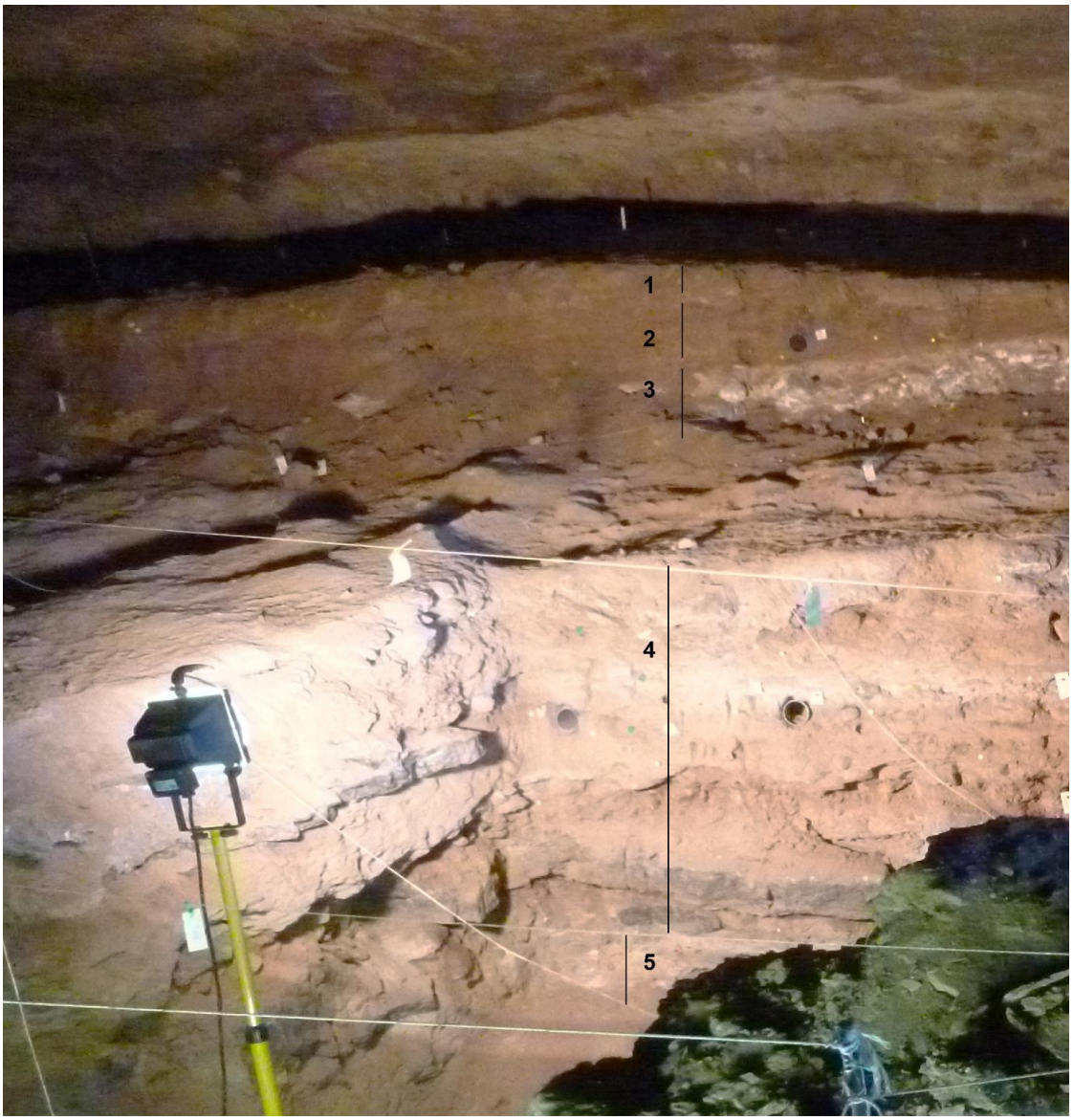

Figure 3.7: Picture of Excavation 2 squares X-Y 40-41, Strata 1 to 5 labelled in profile. Note the step between Strata 1-3 and Strata 4-5; and the major rockfall in lower Stratum 4.

Archaeological Strata	Paleomag. Signal	OSL & U/Pb Ages	Cosmogenic Burial Dating			Global Paleomagnetic timescale
			Sample #	Burial age based on local correction	Simple burial age	
Str 8-7-6	?	OSL top of 9 >256 ±21				?Bruhnes 0.78
Str 10-9	Normal	U/Pb 0.734±.069 0.839±0.02	Cos 5	0.98±0.19	1.76±0.11	Jaramillo 1.07-0.99
			Cos 6	0.99±0.19	1.77±-0.11	
Str 12 top, Str 11, Str 10 bottom	Reverse		Cos 2	1.39±0.19	2.17±0.11	1.78-1.07 Matuyama
			Cos 3	1.17±-0.19	1.95±0.12	
			Cos 4	1.27±-0.19	2.05±0.11	
Str 12	Normal		Cos 1	1.66±0.19	2.44±-0.13	Olduvai 1.96-1.78
			WWD-1	1.58±-0.19	2.36±0.12	

Table 3.6: Earlier Stone Age Strata in Excavation 1 and dating correlations; all ages in mya (from Horwitz et al. *in press*).

3.4 Cultural material

3.4.1 Lithic artefacts

Excavation 1 Holocene

LSA lithics from the excavations 1978 - 1979 were studied by A. Thackeray for her PhD thesis (Thackeray 1981). Strata 1 to 2a were disturbed in modern times and their lithic assemblages are not described here. Strata 2b and 3a are assigned to the Ceramic LSA, part of the Wilton which follows in Strata 3b to 4c. Stratum 4d is a local variant of the Oakhurst (Thackeray 1981, Beaumont 1990a). The richest Strata with artefacts are 2b to 4c, with the highest proportions of finds in 4aLH. More than 80% of the lithics are unretouched, about 4% are retouched tools and 10-15% utilized. Cores are mostly irregular, with bladelet cores most abundant in 3a to 4aLH (25% of core assemblage). All Strata have more flakes than blades. Flakes have plain platforms. Few blades appear in in Strata 5 and 4d, with the majority of blades from Strata 3 to 4aLH. Flakes and blades have a low percentage of cortex, suggesting that primary core reduction must have been outside the excavation area. The largest group of Wilton tools are scrapers and backed tools; the second largest are blades and segments (Fig. 3.8B). Backed artefacts are numerous in Strata 3a, 3b, 4b, and

dominant in 4a and 4aLH. Oakhurst Strata 4d has no backed artefacts. Wilton Stratum 4c to 3b has gradual changes occurring within, the causes of which are unknown (Thackeray 1981), but which have been noted for other Wilton assemblages in South Africa previously (Deacon 1982). The change is in the percentage of tools, towards more blades and backed artefacts in Strata 4aLH to 3b than before, coincides with chert becoming a more dominant raw material. Scrapers are the most numerous tools type again in the youngest Strata (Thackeray 1981).

The retouched component in Stratum 4d is mainly large scrapers on banded ironstone, and irregular forms (Fig. 3.8A). The Oakhurst lithic assemblage seems different from the overlaying Wilton in artefact form, scraper morphology, raw material, tools and associated non-lithic artefacts (Humphrey and Thackeray 1983). Raw material used is local and dominated by banded ironstone (layers 2b, 3a, 4b, 4c and 4d) or chert (layers 3b, 4a and 4aLH); quartz (~5%), dolomite and others play a lesser role. Chunk includes large quartz crystals (Thackeray 1981).

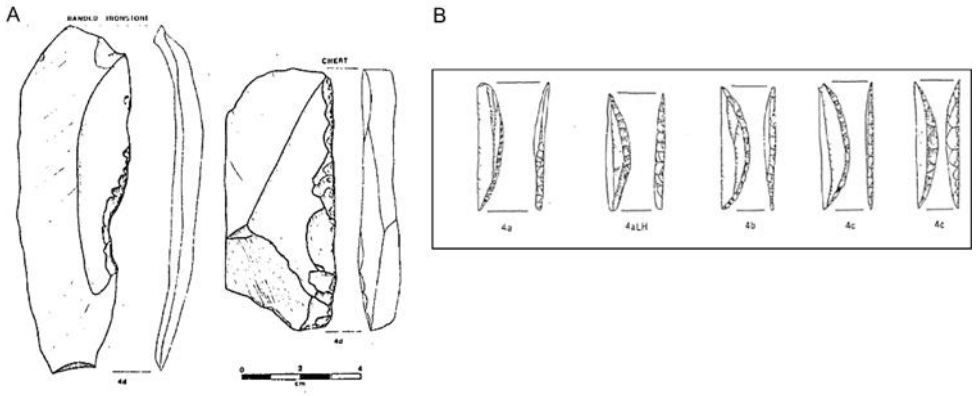

Figure 3.8: Lithics from the Holocene Strata in Excavation 1. A: Scrapers from Stratum 4d (from Thackeray 1981). B: Chert segments from several Holocene Strata (from Thackeray 1981).

Stratum 5 has some irregular cores and flakes of poor-quality chert, in general many pieces are broken and damaged. Occasionally prepared platform cores made Malan assign this

Stratum to the MSA, whereas Beaumont assigned it to the Robberg on the basis of rare bladelets (Beaumont 1990a). He later revised this first impression on the basis of older intrusive material (Beaumont and Vogel 2006) and the cultural association of the lithic assemblage in Stratum 5 is currently unknown. Other lithic material artefacts from the Later Stone Age in Wonderwerk include six ground stone ring fragments, four palette fragments and three chert pendant fragments.

Excavation 1 Pleistocene

The ESA Strata in Excavation 1 are characterised by a low find density and the use of local banded ironstone as the dominant raw material (Chazan et al. 2008). Based on lithic finds, Beaumont has assigned Strata 6 to 8 to Early, Middle and Late Fauresmith stages, Strata 9 to 11 to the Acheulean, and concluded that Stratum 12 might be Oldowan (Beaumont and Vogel 2006, Chazan et al. 2008). New analysis of the whole ESA assemblage by M. Chazan shows Strata 6 to 11 correlate best with the Acheulean (Mode 2 Technology). The assemblage has many bifaces but few cores and flakes (Fig. 3.9); there is no evidence for prepared core technology and no Levallois or large flake-blade production. There are no immediately visible trends in biface morphology through time. One preliminary tendency is that bifaces get more refined (decrease in thickness, increase in length-to-thickness ratio) from Stratum 9 upwards (Chazan et al. 2008). Strata 8 and 9 contain several cleavers made using the Victoria West technique. They also have bifaces with flat invasive removals for thinning. Stratum 10 has seven bifaces with non-invasive retouch, 36 flakes, 15 cores and 23 modified slabs. The lithic assemblage of Stratum 11 consist of only two bifaces and 19 tools in total. Stratum 12 has 65 artefacts: 44 flakes, three flake fragments and 18 cores. Chert is the dominant raw material in this stratum. The technology is similar to the Sterkfontein Member 5B lithic assemblage (Chazan et al. 2008, Berna et al. 2012, Chazan et al. 2012).

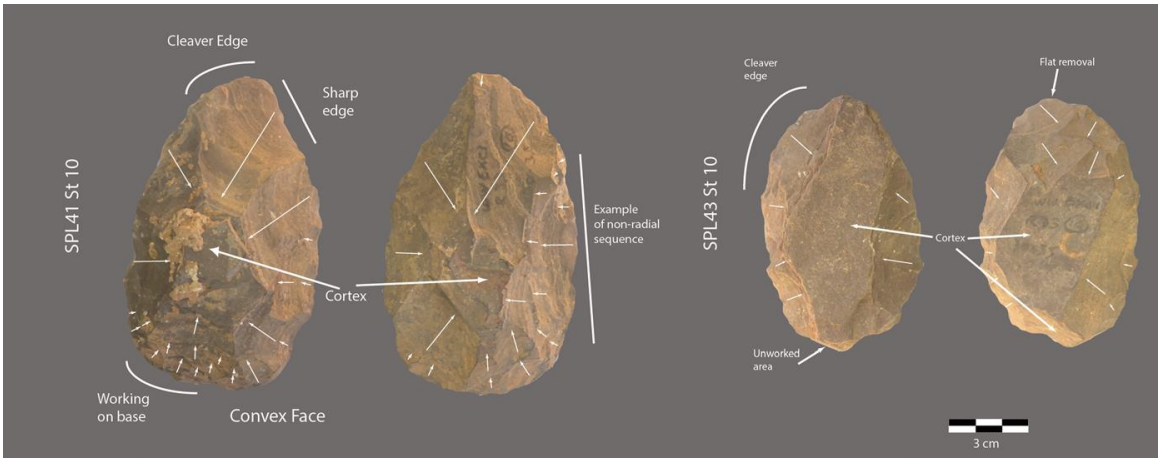

Figure 3.9: Handaxes with non-invasive, shaping flake removals from Wonderwerk Cave Excavation 1 Stratum 10 (from Chazan 2015).

Excavation 2

The Later Stone Age lithic assemblage in Excavation 2 (Stratum 1) is largely unpublished. The MSA lithic sample (Stratum 2) includes prepared cores, blades, Levallois points, unifacial and bifacial points. Stratum 3 includes prepared cores, blades, Levallois points, bifaces and convergent scrapers on banded ironstone, and has been assigned to the 'Late Fauresmith'. Underneath is a 'Middle Fauresmith' with a similar lithic assemblage as well as convex scrapers and small, refined handaxes on banded ironstone (Beaumont and Vogel 2006).

Excavation 6

Excavation 6 has higher find densities than Excavation 1 and a lithic assemblage characterised as Fauresmith with blades, handaxes, Levallois points and manuports (ironstone slabs and quartz crystals, both local). A full study of the material is yet to be published. There is no evidence for underlying earlier ESA Strata in this part of the cave (Chazan et al. 2008, Chazan and Horwitz 2009).

3.4.2 Faunal remains

This section describes the previously identified macrofauna from Wonderwerk Cave. Details on sampled species for this thesis and their diet, habitat, physiology can be found in Chapter 6. For description of microfauna from Wonderwerk Cave see below (paragraph 3.5).

Excavation 1 Holocene

The first study of large faunal remains from Wonderwerk was undertaken by Cooke, who identified 23 horn cores and 173 teeth from the guano digger inspections. He noted the fragmentary nature of the bone assemblage. Species present in his collection were: *Hystrix africaeaustralis* (porcupine), *Syncerus caffer* (buffalo), a large extinct Alcelaphine, *Alcelaphus camaa* (red hartebeest), *Connochaetes* sp. (wildebeest), *Damaliscus pygargus* (blesbok), *Antidorcas marsupialis* (springbok), *Hippotragus* sp. (roan), *Taurotragus oryx* (eland), *Phacochoerus* cf. *aethiopicus* (warthog), *Ceratotherium simum* (white rhinoceros), as well as many Equid teeth, which he identified to five *Equus* species, including the extinct *Equus capensis* (Malan and Cooke 1941).

The large mammal remains from the Strata 1 to 5 in Excavation 1 were analysed by F. Thackeray in his PhD thesis (Thackeray 1984). His conclusion is that no large changes are visible in the large mammal record, other than a dominance of grazer species after Stratum 4d. A rise in the percentage of Equids, Alcelaphini and springbok from the late to the middle Holocene and again to the later Holocene was interpreted as a rise in grazer numbers and therefore an increase in grassland. Humans are identified as the main accumulators, although there are cutmarks on less than 1% of the faunal remains. There is little carnivore or porcupine damage on the material. All skeletal elements of ungulates are present, with ribs and thoracic elements most numerous, but no identification or detailed study was done

on the long bone fragments. Smaller ungulates are more numerous and possibly brought to the cave whole; large animals might have been butchered at the kill site and only parts brought into the cave. The percentage of burnt bone is less than 4.2%, with no burnt bone at all in Strata 4b and 5 (Humphrey and Thackeray 1983, Thackeray 1984, 2015).

The following taxa were identified in Excavation 1 Strata 1 to 5 (Thackeray 2015):

Primates: *Papio ursinus* (Baboon)

Carnivores: *Panthera pardus* (leopard), *Hyaena/Crocuta* (hyaena), *Canis* cf. *mesomelas* (jackal), *Felis lybica* (wildcat) and *Viverridae* (small carnivores).

Ruminants: *Oreotragus oreotragus* (klipspringer), *Raphicerus campestris* (steenbok), *Sylvicapra grimmia* (duiker), *Ovis/Capra* (sheep or goat – limited to Strata 1-2), *Redunca fulvorufula* (reedbuck), *Antidorcas marsupialis* (springbok), *Equus quagga/burchelli* (zebra), *Alcelaphus/Connochaetes* (hartebeest or wildebeest), *Phacochoerus aethiopicus* (warthog), *Taurotragus oryx* (eland), *Syncerus caffer* (buffalo), *Hippotragus equinus* (roan) and *Kobus ellipsiprymnus* (waterbuck).

Other: *Lepus* (hare), *Procavia capensis* (hyrax), *Hystrix africaeaustralis* (porcupine), *Orycteropus afer* (aardvark), *Testudo* (tortoise) and *Pyxicephalus* (bullfrog).

Extinct fauna identified includes *Equus capensis* (a large zebra – one M_2 and one P^4 in Stratum 4d) and *Megalotragus priscus* (a large Alcelaphine – one M^3 in Stratum 4cI) (Thackeray 1984).

Excavation 1 Pleistocene

Three horncores from Malan's excavations were identified as *Damaliscus niro*, having been published as ibex horncores first (Malan and Wells 1943). The keratin was preserved, allowing radiocarbon dating (OxA 2333) on one of the horncores, which gave an age older

than 40ka. The metric measurements and comparisons to other South African sites predict a Middle Pleistocene age. Carbon isotopes on the keratin of the dated horncore (UCT 3257) gave a result of $\delta^{13}C$ -7.2‰ (Thackeray 1990, Thackeray and Brink 2004).

Parts of the macrofauna from Beaumont's ESA excavations until 1990 were analysed by R. Klein (University of Chicago), who noted 18 taxonomic identifications as well as the presence of OES. The low number of samples resulted in an MNI for all species per Strata of one. The sample included: jackal sized *Canis* sp., mongoose-sized carnivore sp., *Procavia capensis* (hyrax), *Equus* sp. (zebra), four size classes of Bovidae, *cf. Bunolagus monticularis* (bushman hare) and *Hystrix africaeaustralis* (porcupine) (Beaumont 1990a). A further publication of the Acheulean fauna with a higher number of samples also included *Leporidae* (hares), *Pedetes capensis* (springhare), *Canis mesomelas* (jackal) and *?Connochaetes gnou* (black wildebeest) (Klein 1988).

Subsequently, analysis of all the Pleistocene fauna has been started by L.K. Horwitz and J. Brink. The focus so far has been on Strata 12-10. Stratum 10 yielded 80 teeth and 595 complete and splintered bone fragments. 43.7% show traces of burning, through all squares and in all spits (Berna et al. 2012). Stratum 12 yielded 260 and Stratum 11 180 identifiable bones and tooth fragments, dominated by bovids (Brink et al. 2015). Stratum 12 includes the extinct hyrax species *Procavia transvaalensis* and *Procavia antiqua*. Both are found in other South African Plio-Pleistocene sites, e.g. Sterkfontein (Berger et al. 2002). All together the Stratum 12 fauna is of the Makapanian Land Mammal Age (~3-1Ma). Another extinct mammal present is a large caprine. The most complete fragment recovered is a jawbone of a new-born individual in Stratum 11, which is larger than *Makapania broomi*, but cannot be identified to species. *Hipparion* is present, but could not be identified further to species level. No cutmarks were observed, but porcupine and carnivore damage are present, as well as burnt bones and teeth (Chazan et al. 2012, Brink et al. 2015). In detail,

macrofauna identified in Stratum 12 include tortoise, snakes, reptilians, ostrich (OES), *Hystrix* sp. (porcupine), *Pedetes* sp. (springhare), *Lepus capensis* (Cape hare), *Pronolagus* sp. / *Bunolagus* sp. (red rock hare) and other Lagomorpha; *Cercopithecidae* indet.; Primate indet., Canidae in all size classes and small-medium felids; Equidae and *Hipparion* sp., Bovidae including Alcelaphini, Antilopini, *Pelea capreolus* and fragments of all size classes. The total number of identified specimens (NISP) is 441 (Chazan et al. 2012, Brink et al. 2015).

Excavation 2

Klein's analysis of the fauna from the MSA Stratum include Leporidae (hares), *Hystrix africaeaustralis* (porcupine), *Papio ursinus* (baboon), *Canis mesomelas* (jackal), *Procavia capensis* (hyrax), *Equus capensis* (zebra), *Phacochoerus aethiopicus* (warthog), *?Taurotragus oryx* (eland), *?Pelea capreolus* (grey rhebok), *Damaliscus dorcas* (bontebok) and *Raphicerus* sp. (steenbok). It was not specified where the MSA level is situated in the cave in this publication, we assume it is Excavation 2 Stratum 2. All species are represented in low quantities, with no MNI over one (Klein 1988).

3.4.3 Other artefacts and features

This part will give a brief overview of other archaeological material and features found in Wonderwerk Cave, that have no direct connection to the research questions. The disturbed Strata 1 and 2 yielded metal, glass and European porcelain. Small plain body sherds of pottery were found in Strata 1 to 3b. Complete and partial bone points and tools, two bone beads and bone fragments with incised lines were found in the Wilton levels. The LSA Strata had plain as well as decorated OES fragments, OES beads and pendants, and flask mouth fragments (Humphreys and Thackeray 1983, Beaumont 1990a). Pieces of specularite are found in the LSA and MSA strata, as well as locally available haematite

down into the ESA strata. Pebbles of quartz, chalcedony and other exotic manuports were found from Stratum 10 and younger (Beaumont 1990a, Beaumont and Vogel 2006).

Art

Rock art, as well as portable art, is known from Wonderwerk Cave. Rock paintings are visible on the cave walls from the entrance until about 40m into the cave, when the light becomes dim. Depicted are geometric designs and various animals including water fowl, elephants, ostrich, eland and antelope in black, white, yellow and red monochromes, as well as red antelope depictions with black outlines. The rock art has been damaged by graffiti from visitors over the last centuries (Malan and Cooke 1941, Thackeray et al. 1981, Beaumont 1990a).

Engraved stones were discovered in the Holocene Strata 3a, 3b, 4a, 4b, and 4d of Excavation 1. All are dolomite, except for one haematite sample. They show incised lines, mostly random, parallel or in grids. The most clearly identifiable is the hind leg of a zebra. It also has traces of red ochre and fine engraved incisions only visible under the microscope. All stones but one are unfinished and broken. They are among the earliest representatives of rock engravings in southern Africa (Thackeray et al. 1981, 1983, Thackeray 2013, 2015). Slabs with parallel incised lines have also been found in some MSA and ESA Strata in the cave (Beaumont and Vogel 2006), but a study using non-destructive neutron tomography on four of those slabs from Excavation area 6 showed that the incisions are all natural (Jacobson et al. 2011, 2012).

Fire

The archaeological evidence for when during human evolution the control of fire was mastered is disputed. Currently, Wonderwerk Cave is the site with the oldest evidence for fire at a well-stratified archaeological cave site. Beaumont first mentioned evidence of fire

from all Strata in Excavation 1 and several other areas in the cave (Beaumont and Vogel 2006). Potlid fractured artefact surfaces, burnt faunal remains and ash lenses were listed. He also concluded that the fire could not have come from the outside or be spontaneously lit guano or plant remains (Beaumont and Vogel 2006, Beaumont 2011).

More evidence of fire in Stratum 10 of Excavation 1 was published by Berna et al. (2012). Micromorphology and Fourier transform infrared microspectroscopy (mFTIR) were used on sediment from the dating section. Micromorphology showed fragments of micritic pseudomorphs of plant tissue and burned bone and pot-lid fractures on banded ironstone. Several lines of evidence suggest fires of up to 500°C *in situ*. Wildfires, transport of fire or spontaneous inflammation of guano were excluded as explanations (Berna et al. 2012). Further samples from fieldwork in 2011 show again potlidded and burnt lithics and more burnt bone in Strata 9 and 10. It was proposed that some of the original identified ashes in Berna et al. (2012) could be calcified plant tissue (Goldberg et al. 2015). A project by M. Thibodeau (Simon Fraser University, Canada) is currently under way to develop new methods to distinguish between ash and calcified plants. There are burnt macro- and microfauna in all ESA Strata of Excavation 1, including Stratum 12, but no evidence for defined features or *in situ* ash was found from micromorphological analysis so far. Therefore, the question of the origin of the burnt fauna is at the moment unresolved and is part of further research (Chazan et al. 2012).

3.5 Environmental analyses at Wonderwerk Cave

From the start of Beaumont's excavations, environmental proxy analyses were undertaken by specialists. The Holocene Strata are well studied, whereas there was little investigation into the Pleistocene. With the new team and new methods available, palaeoenvironmental reconstructions are a main focus of the Chazan and Horwitz investigations (Horwitz et al.,

in press). Table 3.7 provides an overview of the current state of analyses in Excavation 1. The different proxies are presented in detail below.

Material	**Section**	**Status**	**Published**
Micro-morphology and geology of sediments	Holocene	no modern analysis	Butzer 1984b, Thackeray 2015
	Pleistocene	Str 12-7 analysed	Chazan et al., 2008, 2012; Matmon et al., 2012; Goldberg et al. 2015
Micro-fauna	Holocene	Strata 1-4d analysed	Avery 1981
	Pleistocene	Str. 12 and 11 analysed; Str. 10 through 7 being analysed	Avery, 2007; Fernandez-Jalvo and Avery 2015
Macro-fauna	Holocene	Analysed; **Re-analysis of teeth during this thesis**	Thackeray 1984, 2015
	Pleistocene	Strata 12-11 fully analysed; Strata 10 through 7 partially analysed, **all teeth analysed for this thesis**	Brink et al. 2015, *in press*
Stable light isotopes ($\delta^{18}O$ and $\delta^{13}C$) - ostrich eggshell	Holocene	analysed	Lee-Thorp and Ecker 2015, **this thesis**
	Pleistocene	analysed	Ecker et al. 2015, **this thesis**
Stable light isotopes ($\delta^{18}O$ and $\delta^{13}C$)- tooth enamel	Holocene	analysed	Thackeray and Lee-Thorp 1992, **this thesis**
	Pleistocene	analysed	**This thesis**
Macro-botanicals	Holocene	Strata 4d and 5 analysed, 1-4c ongoing	Bamford 2014, 2015
	Pleistocene	Strata 12-7 fully analysed	Bamford 2015

Phytoliths	Holocene	ongoing	
	Pleistocene	Strata 12-7 fully analysed	Rossouw and Scott 2015
Pollen	Holocene	analysed	Van Zinderen Bakker 1982, Brook et al. 2010, Scott and Thackeray 2015
	Pleistocene	Strata 12-7 examined, absent to rare	Chazan et al., 2012

Table 3.7: Palaeoenvironmental sources found in Excavation 1 at Wonderwerk Cave (modified after Horwitz et al. *in press*).

Pollen

The stable temperature and humidity in the cave might have helped to preserve pollen compared to the open veld and pollen are found in all the Holocene strata, but not below. The pollen reaching the sections might be biased by factors like the stalagmite blocking the way, distance from the cave entrance, wind, and the introduction of pollen by animals and human occupants (e.g. burrowing bees, people bringing in plants for bedding). The first pollen study on Wonderwerk Cave material was undertaken by van Zinderen Bakker (1982). He was given 34 sediment samples from the Thackeray excavation. Only 8 samples yielded enough material for analysis, with 150-300 pollen grains per sample. He found high percentages of *Compositae* in Strata 4b to 4d. Strata 3b-4a were dominated by *Gramineae* pollen. Strata 2a to 3a showed higher aboreal pollen than before, with still high *Gramineae* and medium *Compositae* percentages. Van Zinderen Bakker interpreted the results as meaning that the start of the Holocene had an open savanna, with warmer and wetter conditions than today, similar to modern northern Botswana. The dominance of grass pollen in 4a and 3b suggested a treeless dry grassveld and limited summer rain to him. A possible wetter episode with tree growth occurred at 2900 BP. The late Holocene still has

high percentages of grasses, but with slightly more humid conditions. Due to the paucity of this pollen evidence, L. Scott re-sampled the Holocene sequence (Scott and Thackeray 2015) and compared the results with van Zinderen Bakker 1982 and pollen from the stalagmite and dung records in the cave (see below). The results show consistently more *Poaceae* pollen from the mid-Holocene onwards, together with a decline in *Asteraceae* pollen species. This can be read as a spread of grassland (Scott and Thackeray 2015). Details of the pollen record in the cave speleothem (Brook et al. 2010) are discussed in the next section.

Speleothems

A 60cm horizontal core was drilled into the large speleothem at the entrance to Excavation 1 (Brook et al. 2010). Petrography, stable isotopes and pollen were analysed from the drilled core. The stalagmite, rising 2.5 m above today's cave floor, is made of calcite, with an outermost layer of aragonite. Three fabrics were visible within the core: layered fabric, microstromatolitic fabric and concretionary fabric. The latter was interpreted as representing moister conditions than the other two, coinciding with reduced carbon isotope values. Chronology was established by 14 conventional radiocarbon and three AMS dates, the results reported as calibrated in OxCal. The age of the speleothem sample is 35ka to present, with hiatus or slow deposition 33-23ka, and 13-4ka. The carbon and oxygen stable isotope values from the core were interpreted as lower values indicating cooler and wetter conditions with increased winter rainfall. From this interpretation and gaps in the growth of the stalagmite, wetter conditions were inferred for 33, 23-17 and 4-0ka. Drier conditions therefore prevailed 17-13, 33-23 and 13-4ka, with the late Holocene being the driest period. A gap in the stalagmite record from 13 to 4ka means that most of the Later Stone Age sequence analysed in this thesis is not covered by stalagmite analysis. The pollen spectra from the stalagmite as well as two samples from small mammal dung deposits (dated by

^{14}C to about 12ka and 13-14ka cal. BP) deeper within the cave were studied. *Poaceae* dominates throughout, but the last 4ka had more than the pre-Holocene. The Holocene samples also included tree pollen (e.g. *Olea*), sedge pollen (*Cyperaceae*) and *Chenopodaceae*. In the pre-Holocene, shrub-elements like *Passerina* and *Asteraceaea* are dominant. Dry karroid and marginal fynbos elements suggest a cool and sub-humid Last Glacial Maximum (Brook et al. 2010). Recently, a further core from the large stalagmite and a tufa deposit in the cave entrance area have been analysed, providing information about late Holocene conditions of the last 3500 years (Brook et al. 2015). In this study, northern hemisphere Late Holocene warm periods appear to correspond with moist climate intervals in the summer rainfall zone of southern Africa while cold northern hemisphere periods are often associated with dry climate intervals (Brook et al. 2015). The authors then linked moist periods to first appearances, e.g. of domesticated animals, and dry periods to cultural decline, e.g. the fall of Great Zimbabwe, but encompass the whole summer rainfall region of southern Africa in those assumptions.

Macro plant remains

Beaumont (1990a) noted well-preserved plant remains and charcoal in the Holocene strata, but the identification is still ongoing. Seeds from the 1977 excavation were identified by E.J. du Plessis, and listed as unpublished in a table in Beaumont (1990a). His list of seeds identified in Strata 1 - 4d is similar to the modern vegetation around Wonderwerk (Chapter 3.1.3). The modern mixed Strata 1 and 2 included *Acacia sp. Euclea* sp. *Olea* sp., *Ziziphus* sp., *Schinus* sp., *Elephantorrhiza elephantia, Prosopis* sp., *Prunus armeniaca, Diospyros* sp., *Datura inoxia, Grewia* sp., *Ceratonia* sp., *Euphorbiaceae, Pisum sativum, Citrullus* sp. and *Cucumis* sp. Strata 2a to 3b also showed a great variety, with slightly different species: *Euclea* sp., *Olea* sp., *Rhus* sp., *Elephantorrhiza* sp., *Diospyros* sp., *Grewia* sp., *Echium* sp., *Lithospermum* sp., *Rumex* sp., *Teucrium* sp., *Commelina* sp., *Solanum* sp., *Asclepias* sp.,

Citrullus sp., *Cucumis* sp., *Cenchrus* sp., *Andropogon* sp., cf. *Eragrostris tef,* cf. *Eleusine* and, *Zea mays*. The Strata below (4a to 4d) yielded only 3 species: *Euclea* sp., cf. *Olea* sp. and *Diospyros* sp. This only represents a small fraction from just a few squares excavated in 1977.

Charcoal and plant remains from the whole Excavation 1 sequence are currently being analysed by M. Bamford (University of the Witwatersrand). Preliminary results for the charcoal in Stratum 4d include *Searsia lancea, Commiphora* cf. *schimperi, Strychnos* sp. and *Dombeya rotundifolia*. This indicates a more mesic climate in Stratum 4d compared to today (Bamford 2015). Charcoals from Stratum 5 (n=134) were identified into eight wood species: *Ozoroa paniculosa, Sersia lancea, Ehretia rigida, Commiphora* sp., *Dombeya rotundifolia, Olinia ventosa, Berchemia discolor* and *Halleria lucida*. Most species occur in the region today, except *Olinia ventosa* and *Berchemia discolor*, which indicate a moister environment (Bamford 2015). In the micormorphological analysis of Stratum10 the absence of large remains of wood charcoal was noted. Calcified microbotanical remains include grass culms, sedge culms and dicot stems (Berna et al. 2012, Bamford 2015).

Phytoliths

Sixteen soil samples from Strata 12 to 9 were sampled for grass phytoliths. Comparisons with phytolith profiles from the National Museum Bloemfontein database show positive correlation of C_4 grass phytolith abundance and <500mm annual summer rainfall. Stratum 12 indicates a savannah to Nama-Karoo type grassland, warm, locally mesic to dry and with arid summer rainfall. Starting at the top of lithostratigraphic unit 8 and continuing in archaeological Stratum 11 trapeziform shaped morphotypes indicate succulent karoo vegetation with cooler conditions and possible winter rainfall influence (Chazan et al. 2012). The change in Stratum 11 continues in lower Stratum 10, before fluctuating back to

warmer C_4 grassland conditions in upper Stratum 10 and Stratum 9 (Fig. 3.10) (Horwitz et al., *in press*).

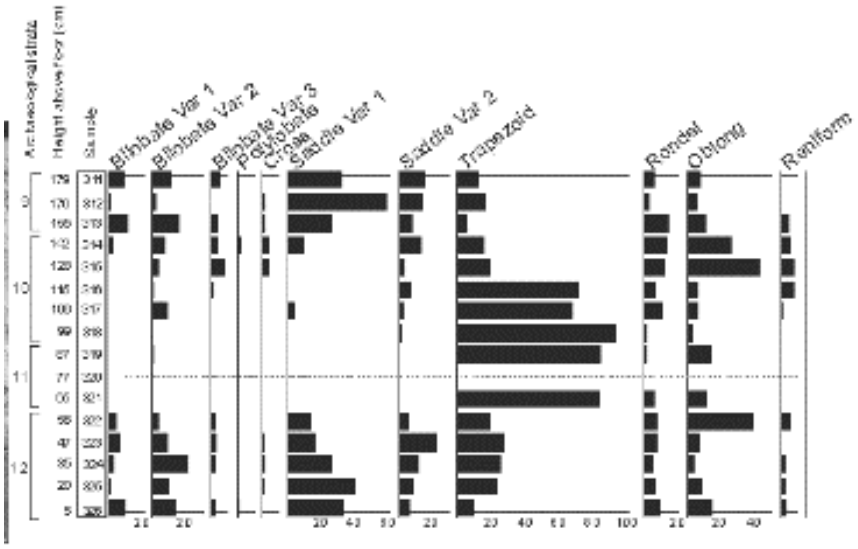

Figure 3.10: Percentage diagram of grass silica short-cell phytoliths retrieved from Strata 12 through 9 of Excavation 1. Counts were normalized as percentages of the short-cell sum for each sample, based on the total count of all the morphotypes per slide (from Horwitz et al. *in press*).

Micromammals

The Strata in Wonderwerk Cave have abundant micromammal remains brought in mainly by barn owl (Avery 2007). The Holocene Strata 1-4d of Excavation 1 yielded 3,731 individuals from at least 33 species in 30 genera, including Macroscelidiae (shrews, 7 species), Chiroptera (bats, 7 species), Rodentia (rodents, 17 species of mice, rats, gerbils). Stratum 5 yielded no microfauna. Changes in relative abundance of those species were used for palaeoenvironemental reconstruction. They show Stratum 4d with a dry climate and open scrub landscape, with few trees on drainage lines and no great evidence for bushes or grass. Stratum4c is slightly less dry, with more bushes and trees, developing in Stratum 4b into a woodland savanna. Stratum 4aLH has an emphasis on grass, while Stratum 4a also shows an expansion of grassland but with change within the grassland structure. More open

and dry grassland might be an explanation. Afterwards (Strata 3b to 1) drier conditions with short grass and scrub prevail; Stratum 3b shows signs of slightly wetter climate with more vegetation cover. It was suggested that at no time in the Holocene sequence was rainfall under 200mm/year, or did bushes and/or trees disappear completely (Avery 1981). F. Thackeray (1984) used the abundance of three distinct micromammal species for further environmental reconstructions (*Desmodillus auricularis* for dry environment, *Mystromy albicaudatus* for grasslands and *Soccomostus campestris* for wooded savannah environments), which show similar results (Fig. 3.11). His results show a semi-arid to arid early Holocene, and increased rainfall in Strata 4c-4d. The Mid Holocene has more grassland savannah, with woodland areas remaining. Temperatures appear to decrease in Strata 4c to 3. The Late Holocene sees an expansion of open grassland (Thackeray 1984). A moisture index created from the Holocene micromammal data indicates a dry early Holocene, becoming moister in the mid-Holocene, and more in the late Holocene (Thackeray 1987).

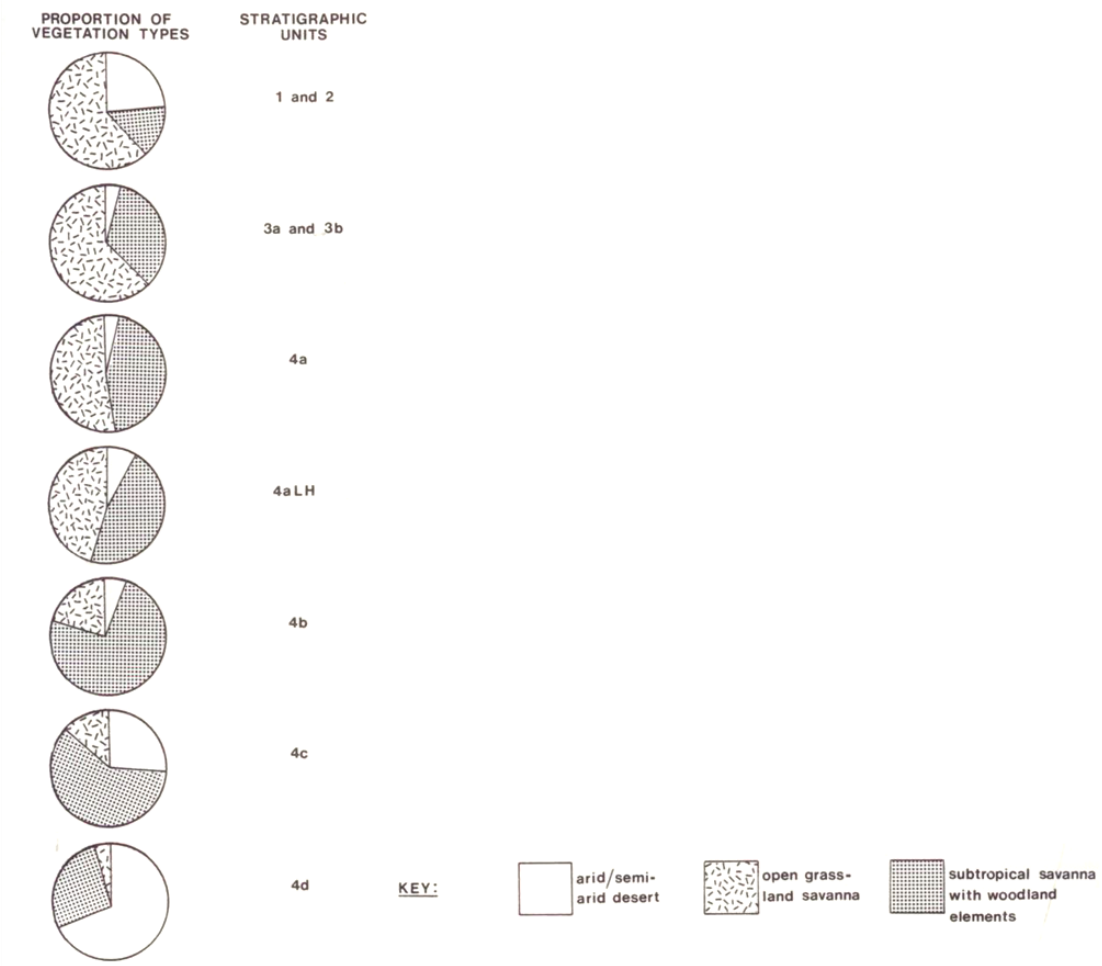

Figure 3.11: Temporal changes in habitat reflected by temporal variability in the relative abundances of desert (*D. auricularis*), grassland (*M. albicaudatus*) or savannah woodland (*S. campestris*) taxa (modified from Thackeray 1984).

The ESA micromammal assemblage is large and with a high degree of breakage. So far maxillae and mandibulae were separated for identification work. Subsamples from all Strata are analysed, including for Excavation 1 Stratum 6 (37 samples, MNI 2,345), Stratum 7 (34 samples, MNI 4,143), Stratum 8 (3 samples, MNI 747), Stratum 9 (24 samples, MNI 8,448), Stratum 10 (35 samples, MNI 12,131), Stratum 11 (1 sample, MNI 365) and Stratum 12 (18 samples, MNI 785) (Avery 2007). They include 35 genera. Best represented are Rodentia (rodents) with 20 genera, followed by Soricidae (shrews) and smaller abundances of Chrysochloridae (golden moles) and Chiroptera (bats) (Avery 2007). The majority of taxa inhabits flat topography with grass dominating (25%), although scrub and

trees and bushes were other preferred vegetation zones. Relationships between different ecological variables were modelled, showing trends through time. In the lower ESA, a more closed and moist, subtropical signal exists, followed by drier and more open habitat. Looking at the general proportion of micromammal genera, Stratum 12 is more dry and open, while Stratum 11 shows moist and cool conditions due to higher frequency of *Soricidae* (Fernandez-Yalvo and Avery 2015, Horwitz et al. *in press*).

Stable light isotopes

Equid teeth samples from excavations in 1979-1980, from Strata 2a through to 4d, were analysed for carbon and nitrogen isotopes (Thackeray and Lee-Thorp 1992). On dentine, 18 carbon samples and ten nitrogen samples were successful. Additionally, the carbon isotopes of eleven enamel apatite samples from the same specimens were analysed. The results show a collagen $\delta^{13}C$ range of 3.7‰. The carbon results show prevailing C_4 grasslands throughout the Holocene (Thackeray and Lee-Thorp 1992). Thackeray and Lee-Thorp (1992) relate the $\delta^{15}N$ results to rainfall and created a rainfall index. This index shows significance, but is based on only ten samples. It shows dry conditions becoming moister in the middle and late Holocene. Although $\delta^{15}N$ correlations with rainfall gradients are published (e.g. Gröcke et al. 1997), there is reason for caution as other studies show no relationship and much development has taken place in recent years concerning the nitrogen cycle and its influences. Lee-Thorp has also undertaken carbon and oxygen stable light isotope analysis on ostrich eggshell from the Holocene levels of Excavation 1 in Wonderwerk Cave. Those results are summarized in Chapter 5 and in Lee-Thorp and Ecker (2015).

3.6 Summary

Wonderwerk Cave is a unique archaeological site. Due to its long sequence, it is an exceptional site to explore changes in human behaviour as well as environmental and climatic changes through time. The good preservation in the dry climate allows several proxies to be explored and compared. Wonderwerk Cave has well-dated Early Pleistocene, less well dated Middle as well as Late Pleistocene strata, and well constrained Holocene strata, although gaps remain (Chapter 4). Currently, Wonderwerk Cave has the earliest evidence for hominin occupation of a cave environment, the earliest evidence for use of fire by hominins and evidence of early art and manuports. Its location makes it ideal to fill the gaps in the environmental and human history of Southern Africa's interior.

Chapter 4 - Radiocarbon dating of the Holocene Strata at Wonderwerk Cave

The overarching aim of this chapter is to set a framework for the Holocene Strata of Wonderwerk using radiocarbon dates, which will constrain them and help with the subsequent interpretation of the stable isotope results. Without a secure chronology provided through radiocarbon dating of the Wonderwerk Holocene sequence it is impossible to understand what drives climate and environment in South Africa's interior and what degree of variability is possible, even for this more recent period. The chapter starts by introducing the principles of radiocarbon dating and previous radiocarbon work at Wonderwerk Cave, then outlines the material and methods of the new dates within the framework of this thesis. It further outlines the Bayesian model developed to calibrate and constraint the dates within the Wonderwerk archaeological strata. This allowed a re-structuring of the Holocene record. The implications of the results on the LSA in Wonderwerk, in particular, and the LSA in South Arica's interior, in general, are discussed.

We rely on the Holocene as a basis for understanding those changes in the Pleistocene, where the record is much more fragmentary. The existing radiocarbon dates are too coarsely distributed to evaluate environmental changes in the Holocene sequence, and the chronology suffers significant gaps. A small set of new dates were chosen to provide a firmer chronological footing for interpreting cultural, environmental and biological shifts at Wonderwerk Cave. These were combined with existing dates in a Bayesian model. Particular interest was placed on solving the following questions:

(i) Resolve the chronology of independently observed shifts in the lithic assemblage and resolve the chronology of the 'wet' phase, as determined by various proxies.

(ii) Establish the last appearance date of *Antidorcas bondi* and last local appearance of *Damaliscus pygargus*, at this site, by directly dating the tooth dentine collagen of these two specimens. These remnants of Pleistocene faunal communities provide important clues about the local environment. The two dates will also fulfil the function of strengthening the chronological model. Although Wonderwerk already has a number of radiocarbon dates published, significant gaps remain and are closed with the new dates before being able to answer the research questions in this study.

4.1. Background

Thirty radiocarbon dates for the Holocene Strata of Wonderwerk Cave have been obtained independently by several researchers between 1978 and 1995, measured on charcoal, ostrich eggshell and travertine (Butzer et al. 1978, 1979a, b; Humphrey and Thackeray 1983; Beaumont 1990; Vogel et al. 1986, Lee-Thorp pers. comm.). Hypothetically then, Wonderwerk has the best radiocarbon record for the Northern Cape. However, the dating program was disorganized and uncoordinated, resulting in the clustering of dates in certain strata, and gaps in the chronology in other phases. Although Beaumont and Morris (1990) listed most of the dates, they were never published all together in a peer-reviewed and accessible journal. They were also never calibrated, making it difficult to compare proxy records from these Strata with environmental proxies like speleothem records or deep sea core records. My aim was to establish a higher resolution chronology for the Holocene levels at Wonderwerk Cave, Excavation 1, using nine radiocarbon dates on charcoal and two on tooth dentine. The pretreatment, combustion and graphitization of the samples was carried out at the Oxford Radiocarbon Accelerator Unit, Research Laboratory for Archaeology and the History of Art, University of Oxford.

4.1.1 Principles of radiocarbon dating

Radiocarbon (^{14}C) is produced mainly in the upper atmosphere, where cosmic rays interact with the nitrogen atoms in air; and is lost through radioactive decay with a half-life of approximately 5730±40 years (Godwin 1962). In living organisms, organic matter is in equilibrium with the atmospheric concentration of ^{14}C. When an organism dies, no more ^{14}C enters an organism and it decays to ^{14}N (Michels 1973). The two major ways of measuring this phenomenon are decay counting and accelerator mass spectrometry (AMS). In the case of the latter, the radiocarbon atoms are detected directly, requiring therefore smaller sample sizes (Bronk Ramsey 2008). A number of corrections are needed in the process. The $^{13}C/^{12}C$ ratio is measured in a mass spectrometer to correct for the natural fractionation that occurs as the carbon isotopes progress from the atmosphere into the organic matter; one of the main discriminators being photosynthesis. After this correction, the measured ratio is compared to standards of known age. AD 1950 is used as year zero for computing dates (Bronk Ramsey 2008). Tree-rings of known age provide the main record of variation in the atmospheric concentration of radiocarbon (McCormac et al. 2004; Reimer et al. 2004) back into the Late Glacial, lake varve counting being one method to estimate values beyond that into deeper time.

Each uncalibrated radiocarbon date has a standard deviation, which arises because of the statistical uncertainty of estimating the exact $^{14}C/^{12}C$ ratio in any sample. The fundamental limitation on the precision of a radiocarbon date is the number of atoms present; thus, standard deviations are greatest for samples many thousands of years old, as so few ^{14}C atoms remain. Further ground-breaking developments in radiocarbon dating over the last decade are advances in chemical pretreatment, which have allowed older samples to be measured more accurately and free of contamination, and statistical developments using

computer models. The most common statistical application is Bayesian modelling. This approach allows for dates to be constrained using independently obtained information, e.g. the stratigraphic relationships of archaeological strata. It is still unusual for archaeologists working in southern Africa to publish calibrated radiocarbon dates (Barham and Mitchell 2008) and most dates available in the literature are measured by the decay counting method. AMS dates are increasingly widely used and the majority of new dates are gained using AMS. At the same time, Bayesian modelling is being used more widely, especially in cave/rock shelter contexts.

4.1.2 Previous radiocarbon dating work at Wonderwerk Cave

In the late 1970s and early 1980s, 26 radiocarbon dates were obtained for the Holocene layers of Wonderwerk Cave. The dates from the different authors are comparable today because almost all come from Excavation 1 and, although excavation techniques and labelling varied between excavators, all samples can be assigned the layers named by Thackeray.

Several authors submitted material for dating independently (Table 4.1):

- Humphrey and Thackeray (1983) reported 7 dates from the 1979 excavation of Anne Thackeray, Francis Thackeray and Peter Beaumont.
- 3 OES samples from Malan and Peabody's excavation 1948 were submitted for dating by Peter Beaumont in 1977, and reported in Vogel et al. (1986).
- after the 1981/1982 excavation Peter Beaumont submitted 7 more samples of charcoal and OES, reported in Vogel et al. (1986).
- Butzer reported 5 dates he commissioned in Butzer (1978), Butzer et al. (1979a), (1979b).

- Francis Thackeray obtained 4 dates on travertine lenses in 1980, which were excluded in this analysis because of the unclear stratigraphic position of the lenses and their questionable material (Vogel et al. 1986).

- Julia Lee-Thorp submitted 4 charcoal samples in 1995 (collected by Peter Beaumont), reported in Lee-Thorp and Ecker (2015).

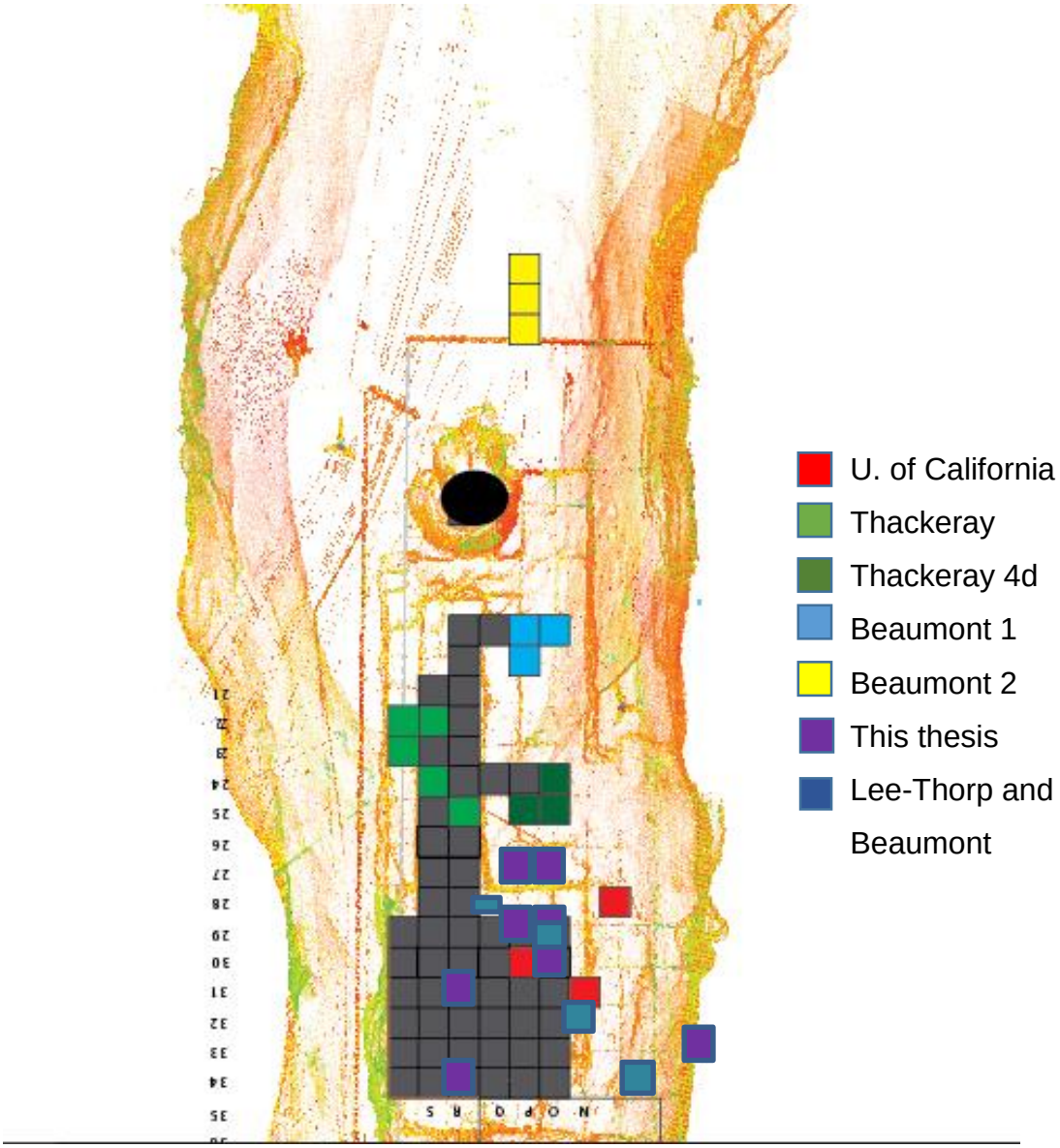

Figure 4.1: Location of ^{14}C samples in Wonderwerk Cave Excavation 1 and entrance trench. Colours show who excavated and/or submitted the samples respectively. Number of samples submitted per square varies.

Lab Code	^{14}C Measurement		Stratum	Square	Material	Reference	Modelled Date Range (cal BP, 95% probability)
	Date (^{14}C yrs BP)	Uncertainty (1σ)					
Pta-2779	1210	50	2b	T22/23	charcoal	Humphrey&Thackeray 1983	1276-985
Pta-2542	1890	50	3a	O19/P20	charcoal	Beaumont 1990	2001-1630
Pta-6873	2120	80	3a	S22	charcoal	Lee-Thorp&Ecker 2015	2330-1900
Pta-2543	2910	60	3b	O19/P20	charcoal	Beaumont 1990	3329-2848
Pta-2785	3990	60	3b	R25	charcoal	Humphrey&Thackeray 1983	4616-1870
Pta-2541	4240	60	4a	P20/21	charcoal	Beaumont 1990	5030-4621
Pta-2797	4890	70	4aLH	T22/S22	charcoal	Humphrey&Thackeray 1983	5745-5484
Pta-2544	5180	70	4b	O19/P20	charcoal	Beaumont 1990	6703-5756
Pta-2545	5970	70	4cI	O19/21	charcoal	Beaumont 1990	8802-6715
Pta-2798	7430	60	4cI	S24/25, T24/25	charcoal	Humphrey&Thackeray 1983	8386-8048
Pta-2546	9130	90	4dI	O19/22	charcoal	Beaumont 1990	11810-10205
Pta-2852	9760	120	5a	O24	charcoal	Humphrey&Thackeray 1983	12132-11440
Pta-2790	10000	70	4dII	O25/O25	charcoal	Humphrey&Thackeray 1983	11715-11300
Pta-2786	10200	90	4dII	O25/P25	charcoal	Humphrey&Thackeray 1983	11868-10263
Pta-6872	10120	120	4dII	P26	charcoal	Lee-Thorp&Ecker 2015	11728-11306

Pta-6871	10120	100	4dII	Q23	charcoal	Lee-Thorp&Ecker 2015	11726-11310
Pta-6884	10080	100	5a	N28	charcoal	Lee-Thorp&Ecker 2015	12057-11461
Unmodelled dates							**Cal. BP**
Pta-3427[1]	5800	70	3a	P8	charcoal	Vogel et al. 1986	6730-6405
Pta-3426[1]	2310	60	3a	P7	charcoal	Vogel et al. 1986	2430-2098
Pta-2139[2]	3060	40	3	P30	OES	Butzer et al. 1978	3350-3074
Pta-2140[2]	5930	50	4c	M28	OES	Butzer et al. 1978	6855-6558
Pta-3425[1]	6840	80	4cI	P7	charcoal	Vogel et al. 1986	7826-7507
Pta-3366[1]	8000	80	4cII	P9	OES	Vogel et al. 1986	9012-8596
Pta-3439[1]	9030	90	5a	P7/9	OES	Vogel et al. 1986	10372-9745
Pta-2141[2]	12380	100	5	N31	OES	Vogel et al. 1986	14920-14020
Pta-3441[1]	12400	180	5	P7	OES	Vogel et al. 1986	15124-13855

Table 4.1. Published and calibrated radiocarbon dates (Pretoria Laboratory) from Wonderwerk Cave using OxCal version 4.2 (Bronk Ramsey 2013) and the ShCal13 calibration curve for the southern hemisphere (Hogg et al. 2013) as described in the text. The table includes dates used in the Bayesian model, and those excluded because of (1) unreliable stratigraphic position in the entrance trench, or (2) being excavated by the University of California Expedition in 1948 and argued as having an unreliable stratigraphic position.

Following recalibration and Bayesian modelling of the existing radiocarbon dates, outlined below, the chronology suffers significant gaps and is too coarse to precisely pinpoint the timing of distinct episodes evident in the stable oxygen isotope record. To improve the Bayesian model, all determinations with unknown stratigraphic positions (e.g. from the

1948 excavation), and those conducted using unknown material were removed, and concentrated only on those remaining for Excavation 1. Besides charcoal and OES, two established datable materials, the material dated in Wonderwerk includes "branch fragment", "travertine lenses", "carbonaceaous soil" and "grass". Samples that were thought to be mixed in by the excavators, and samples from other areas than Excavation area 1 (e.g. a trench in the cave entrance) were also excluded. The 17 remaining charcoal dates (listed in Table 4.1) were calibrated to construct a Sequence model in OxCal version 4.2 (Bronk Ramsey 2009; Bronk Ramsey et al. 2013), with Strata represented as Phases within the Sequence model.

The model was run against the SHCal13 curve (Hogg et al. 2013) for the southern hemisphere. In order to obtain better time constraints on the spits in each stratum, Phases with blank dates were built into the model to act as boundaries for the known radiocarbon dates. The model was run several times, with and without the outlier model function, showing similar results with the outputs not varying by any more than a few decades. This gave us confidence in our modelled time ranges. Pta2852 and Pta3439 are reported as coming from the mixed LSA/MSA industry from Stratum 5, but have poor agreement. When placed into layer 4d in the model, they obtain good agreement. Beaumont and Vogel (2006) also state that there is intrusive material in layer 5 upper part, confirmed through the OES fragment radiocarbon ages. This could mean the Layer 4d / Layer 5 boundary from the excavation is not completely clear, as also noted by Anne Thackeray (1981). It became clear that there is no reliable date for Stratum 5 available and we concluded that it must be older than 12,000 cal. BP[1]. This work is published as part of a report on the existing

[1] In this thesis, cal. BP is used for calibrated and/or modelled dates from OxCal, although the majority of South African LSA literature uses BC/AD to describe dates for assemblages. One reason is that this thesis spans a much longer time than the LSA, and dates for the MSA and ESA are reported in BP. Also, the radiocarbon dating in Wonderwerk Cave goes back to the Holocene/Pleistocene boundary, where BC/AD becomes irrelevant. Another possibility would have been to report all dates in the discussion uncalibrated, to

palaeoenvironmental record in Lee-Thorp and Ecker (2015). The calibrated sequence model clearly shows that there are blanks in the stratigraphic sequence. The period around 4aLH and 4bI is the main focus because of the secure identification of a moist phase (Chapter 5 and 6). At the same time, this is the phase in the Holocene with only one radiocarbon date for the stratum. The new dating program, therefore, focused particularly on this period.

4.2 Material and methods

4.2.1 Sample selection

During sorting of the faunal material in preparation for sampling for isotopic analysis, the project's archaeozoologist, James Brink, and I discovered an *Antidorcas bondi* (Bond's springbok) specimen in Stratum 4c, a Stratum with a calibrated age of 5960-9800 cal BP according to the first model. Few *A. bondi* individuals survived into the Holocene and even fewer are directly dated; presently the most recent (last known appearance) specimen is thought to be ca. 7500 years BP (Plug and Engela 1992). This Wonderwerk specimen could therefore be the most recent, and hence represent the last known appearance of this species, but at present the 95.4% confidence range for Stratum 4c is far too broad to allow any firm conclusions. The sequence was also found to contain a *Damaliscus pygargus* (Blesbok) specimen, which today lives in the open grasslands to the east and northeast of the interior, and is unknown in the savannah biome around Wonderwerk. The specimen comes from layer 3a associated with the Ceramic LSA, where its occurrence suggests that it was in the area when the first ceramic technology arrived, and shortly afterwards, the earliest domestic livestock were introduced. Again, however, the age of last local appearance cannot be

allow for new developments in calibration curves and easier comparisons with articles that do not report calibrations. However, calibration is vital for the future of radiocarbon dating in South Africa's archaeology and other researchers have started to follow this approach.

assigned precisely based on the broad chronological range for Stratum 3a (1200-2700 cal. BP).

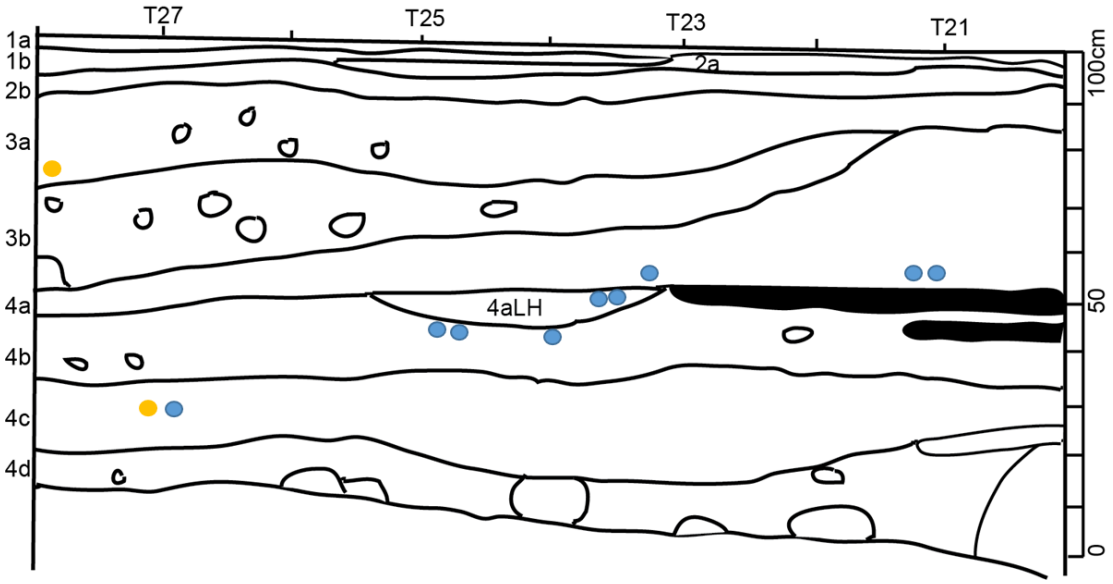

Figure 4.2: Location of new ^{14}C samples, projected on the T-Line section drawing from Thackeray (1981). Blue filled circles are charcoal samples, and yellow filled circles are (from lower to higher levels) the *Antidorcas bondi* specimen and the *Damaliscus pygargus* specimen, respectively.

For the faunal samples, the two relevant teeth from the two species, *A. bondi* and *D. pygargus*, were documented with photographs, 3D scans (L. Grossman, Institute of Archaeology, The Hebrew University of Jerusalem, Israel) as well as descriptions and measurements. E. Boaretto (Weizmann Institute, Israel) conducted a test to predetermine that well-preserved collagen was present from the tooth dentine. Charcoal is abundant and well preserved throughout the Holocene record of Wonderwerk Cave. Sample selection was based on the distribution of the existing dates and the position of the samples, as well as larger-size fragments to facilitate identification to species. All charcoal samples were identified, photographed and weighed by M. Bamford (University of the Witwatersrand, South Africa). As the results were expected to be younger than 8000 cal BP. Acid Base Acid (or "ABA") was chosen as being a sufficient pretreatment method.

Figure 4.1 shows all new samples in stratigraphic context. The existing radiocarbon dates, measured from the 1970s to 1990s, were done without the advanced pretreatment and AMS technology available today. They are regarded as robust, however, as they were all done in the same reputable laboratory (Pretoria) and are consistent with each other, in relation to the stratigraphy, as well as in the Bayesian model. The selected samples are close in space horizontally (Figure 4.2) to the majority of former ^{14}C samples (Table 4.1). This improves trust in their stratigraphic position. Problems with charcoal or collagen preservation were not expected. The dry cave interior and fine sediment has preserved the fauna and charcoal well. Good collagen preservation has been previously demonstrated in a study of carbon and nitrogen isotopes in Equid teeth (Thackeray and Lee-Thorp 1992), and more recently by successful DNA extraction from Equid teeth (Orlando et al. 2009). Charcoal preservation is good and we have chosen large pieces (between 0.16 and 0.91g). The cave occupies a savannah and thornbush shrub environment, with no long-lived trees present; therefore there is little danger of the use of old wood for fuel by prehistoric hunter-gatherers.

Sample ID	Species	Stratum	Square	Lab ID	14C Measurement (1 σ uncertainty)	$\delta^{13}C$	Calibrated Date (unmodelled, cal BP, 95% probability)	Modelled date (cal BP, 95% probability)
Dentine samples								
8346	*Antidorcas bondi*	4c	K27	37276	n/a			
8238	*Damaliscus pygargus*	3aIII	T28	37277				
Charcoal samples								
Q23 A	*Ochna pulchra*	4aII	Q23	OxA-30566	4459±30	-22.8	5275-4866	5257-4872
Q21 B	*Searsia Lancea*	4aII	Q21	OxA-30567	4427±29	-25.5	5210-4856	5213-4868
R21 A	*Vitex mombassae*	4aII	R21	OxA-30568	4207±30	-27.1	4832-4577	5076-4644
R23 A	*Heteromorpha trifoliata*	4aLH	R23	OxA-30638	5340±33	-23.3	6192-5945	6188-5431
R23 D	*Vitex mombassae*	4aLH	R23	OxA-30639	4887±33	-23.9	5655-5475	5655-5477
Q24 A	*Searsia lancea*	4bI	Q24	OxA-30640	5627±33	-23.5	6439-6297	6504-6308
T25 C	*Vitex mombassae*	4bI	T25	OxA-30641	5771±34	-24.8	6637-6415	6664-6454
T25 B	*Searsia lancea*	4bI	T25	OxA-30642	5915±34	-22.6	6790-6566	6830-6377
K27 A	*Searsia lancea*	4c	K27	OxA-31897	5063±30	-23.6	5893-5658	9072-6773

Table 4.2: The results for submitted radiocarbon dates determined in this thesis. The teeth samples did not yield enough collagen to be dated. The charcoal samples are recorded uncalibrated in radiocarbon years BP (using the half life of 5568 years), and calibrated in OxCal 4.2 (Bronk Ramsey 2013) using the ShCal13 calibration curve for the southern hemisphere (Hogg et al. 2013) as described in the text. $\delta^{13}C$ values are reported relative to VPDB.

4.2.2 Sampling, pretreatment and AMS measurement

Pretreatment of radiocarbon samples is necessary to remove sedimentary carbonates, organic acid contaminants and possible dissolved atmospheric carbon dioxide (Brock et al. 2010). The tooth and charcoal samples followed standard pretreatment protocols published in Brock et al. (2010). The crushed teeth were soaked in 0.5M HCl at room temperature for two hours. The tubes were then centrifuged, and the liquid decanted. This was repeated two times, whereas the third time the samples were left overnight in the HCl. The next day it was clear that sample 37276 had completely dissolved, and we would therefore not be able to collect any collagen from it. The remaining sample was centrifuged, and washed 3 times with ultrapure MilliQ^{TM} deionized water, followed by a base wash (0.1M sodium hydroxide (30 min.)), with three ultrapure MilliQ^{TM} deionized water washes afterwards. Filled with pH3, the sample was left for 20 hours at 75°C to gelatinize. The next day the gelatin solution was decanted and filtered using Ezee-filters^{TM}. The liquid was then transferred into an ultrafilter and centrifuged. The liquid gelatinized collagen was then pipetted out into a tube for freeze-drying. In the end, the second tooth, sample number 37277, did not produce enough collagen to process it any further.

The charcoal samples were left in 1M HCl in a heating block (80°C) for 1 hour, before being rinsed 3 times with ultrapure MilliQ^{TM} deionized water and separated by Ezee-filters^{TM}. This was followed by a base wash with 0.2 M NaOH, which was repeated six to eight times per sample until the solution showed a light brown colour. After three rinses with ultrapure MilliQ^{TM} deionized water and being separated by Ezee-filters^{TM} again it was left in 1 M HCl in a heating block (80°C) for one hour, followed by three more washes. The samples were frozen and then dried in a VaCo 5 freeze-dryer. Portions (2.5 - 3.5 mg) of the freeze-dried charcoal samples were then weighed into tin capsules and combusted in

an elemental analyser (Carlo-Erba NA 2000) coupled to a gas source isotope ratio mass spectrometer (Sercon 20/20) in order to measure their carbon and nitrogen stable isotopic compositions. The $\delta^{13}C$ values produced are reported in Table 4.2. The remaining CO_2 gas was transferred using a splitter and collected cryogenically for graphitization and dating. Sample graphitization followed Dee and Bronk Ramsey (2000). This meant the collected CO_2 was transferred into rigs with an iron catalyst. Hydrogen gas was added and the whole mixture heated for 6 hours (Brock et al. 2010). Finished samples were pressed into graphite targets and measured on the ORAU HVEE AMS system. See Bronk Ramsey et al. (2004) for details and discussion of precision. Three Oxford laboratory known-age standards underwent the same pretreatment and measurement procedure for quality control: pig ribs from the Mary Rose ship-wreck (AD 1545); fossil wood (~ 180Ma) and charcoal from a Buddleia burned in 2002 (all from the UK) (Brock et al. 2010).

4.2.3 Calibration and model specifications

The nine new radiocarbon dates were used to substantially improve the model outlined in section 4.1.2. The new model is again a Sequence model, with Boundaries between the archaeological strata, and Phases within the Boundaries. If the dates could be divided into spits in a stratum, each spit is built as its own Sequence within the Boundaries, and thus allowed to overlap. The earlier model had transition Boundaries which assumed all the spits followed each other in time, but the indistinct nature of some of the Boundaries, and the fact that the samples came from different parts of Excavation 1, meant that it was more realistic to model the site as comprising independent but potentially overlapping spits. No blank Phases were used this time, as the new dates filled those spaces. I did not include depth information in our model for several reasons. Firstly, after establishing how the different excavators labelled their Strata and spits, I concluded that it was not certain how

the excavators measured the depth of the samples. Beaumont, for example, established one fixed point on the cave wall above Excavation 1, but measured some of the strata, especially the Pleistocene ones, from the top of the Excavation trench. Secondly, that would mean excluding some of the Lee-Thorp and Beaumont dates as they do not have depth information, and I would have been more limited in the selection of new samples. Another reason is that the focus of this thesis is not only to gain palaeoenvironmental information in a well-dated context, but also to explore the influence of environmental change on the archaeology from Wonderwerk Cave. Therefore a sequence model with the spit system was used rather than a depth model.

OxCal Difference functions were used in two ways: to calculate hiatus times between the strata, and to calculate duration of each strata. Difference functions estimate the time span between different points in a Sequence (at 95.4% probability). In this case, the outlier model was set to the commonly used probability of 5%. The purpose of the outlier model is to reduce the impact of inconsistent results. It therefore checks the compatibility of each date with the other dates in its Phase and the Sequence as a whole. The Date function was used in each phase to give a summary distribution for the likely age of each strata, which is clearer than showing the start and end Boundary for each one. The spits within a given Strata could overlap, but the Date function only gives results for the full strata, which are definitely separate in time. Again, the model was run on the SHCal13 curve (Hogg et al. 2013) for the southern hemisphere. Several versions were run, with and without Stratum 5, and with and without spits in Stratum 4d and with and without separating Stratum 3 into substrata 3a and 3b. This was to test how dates with slightly unclear stratigraphic position or poor agreement behaved. It is important to consider that the model presented in the following (Appendix 5.1 model code) and its results are only one possible way to model the results, and the following is what I think is the best interpretation considering

stratigraphy, distribution of dates and the model constrains. The modelled radiocarbon date ranges are presented at 95.4% probability. The ages are given in cal. BP.

4.3 Results

The results of the dating program are listed in Table 4.2 (see also Appendix 2.2 for individual plots of the results). As outlined above, the two teeth did not yield enough collagen to be dated. Table 4.2 also gives the calibrated time ranges for those dates, as well as the newly modelled dates. There is no striking difference between the calibrated Oxford dates, modelled or unmodelled. Several dates stood out in this new model as having bad individual agreement indices (Index A = a measure of agreement between the modelled and unmodelled data), including both dates from Stratum 4dI:

- Pta-2546 (Stratum 4dI) 16.1% agreement, 88% posterior outlier probability in outlier model.
- Pta-2786 (Stratum 4dI) 29.9% agreement, 14% posterior outlier probability in outlier model.

As well as:

- Pta-2852 (Stratum 5a) 9.3% (59.5% agreement when in Stratum 4dII), 28% posterior outlier probability in outlier model.
- Pta-2545 (Stratum 4c) 33.3% agreement, 62% posterior outlier probability in outlier model.
- OxA-31897 (Stratum 4c) 5.5% agreement, 100% posterior outlier probability in outlier model.
- OxA-30638 (Stratum 4aLH) 24.7% agreement, 80% posterior outlier probability in outlier model.

All other dates have more than 60% agreement, most of them over 100%. The three new Oxford dates for upper Stratum 4b (4bI) are slightly older than expected from the previously available data, and Pta-2545, which follows directly afterwards, is therefore too young to be in good agreement with the new dates. On the other hand, the new date OxA-31897 in 4c is younger than the other 4c dates, which already cover a wide range, and seems to be an outlier. Pta-2852 is labelled 5a, but fits much better with Stratum 4dII in the model. Although there are two dates labelled 5a, one is more likely from 4dII, and both do not span the whole depth of Stratum 5. The age for Stratum 5 is therefore a minimum age. Pta-2786 showed poor agreement in spit 4dI, as well as when not included in a spit but just run as part of 4d. Compared to the earlier version of the model, both versions give similar ages and age boundaries for the uppermost Strata 4a-2b. This considerably strengthens the basis for interpreting these sections of the model. OxA-30638 is slightly older than the other two dates in this stratum, therefore Stratum 4aLH is now considered older than before, and 4b has a longer time span. In general, there is little time difference between Stratum 4dI, 4dII and 5a (Fig. 4.3). The three dates from Stratum 4c are not consistent and in agreement, resulting in an enlarged span between boundaries for Stratum 4c. Strata 4b, 4aLH and 4a on the other hand are closer together again, spanning roughly 300 years all together and are well constrained. Another, younger set of dates is from Stratum 3 and 2b. The modelled durations of the Strata shows short spans of less than 500 years for Strata 2b, 4aLH, 4d and 5a (Fig. 4.5). This coincides with Strata 2b, 4d and 5a yielding lower amounts of archaeological material and are thinner Strata than the mid-Holocene ones. Strata 4a and 4b show longer durations with a mean between 500 and 1000 years. Stratum 3, although having a lot of archaeological material, but less than 4a, shows the longest duration. The calculated duration for Stratum 4c is long and uniform, which is a corollary of the imprecision of its associated boundaries. The calculation of hiatus length showed that often

no significant time elapsed between strata, and where they did occur their duration was less than 500 years (Fig. 4.6). It is especially interesting that the shortest possible hiatus is between 4d and 5, which confirms our concerns about the stratigraphic boundary. The only exception is between Strata 4d and 4c, where a hiatus seems likely, although the probability function is wide and probably elongated the 4c dates. The modelled Strata ages from the Date function (Fig. 4.4, Table 4.3) are within the wider boundaries for each Strata and in agreement with the difference function results.

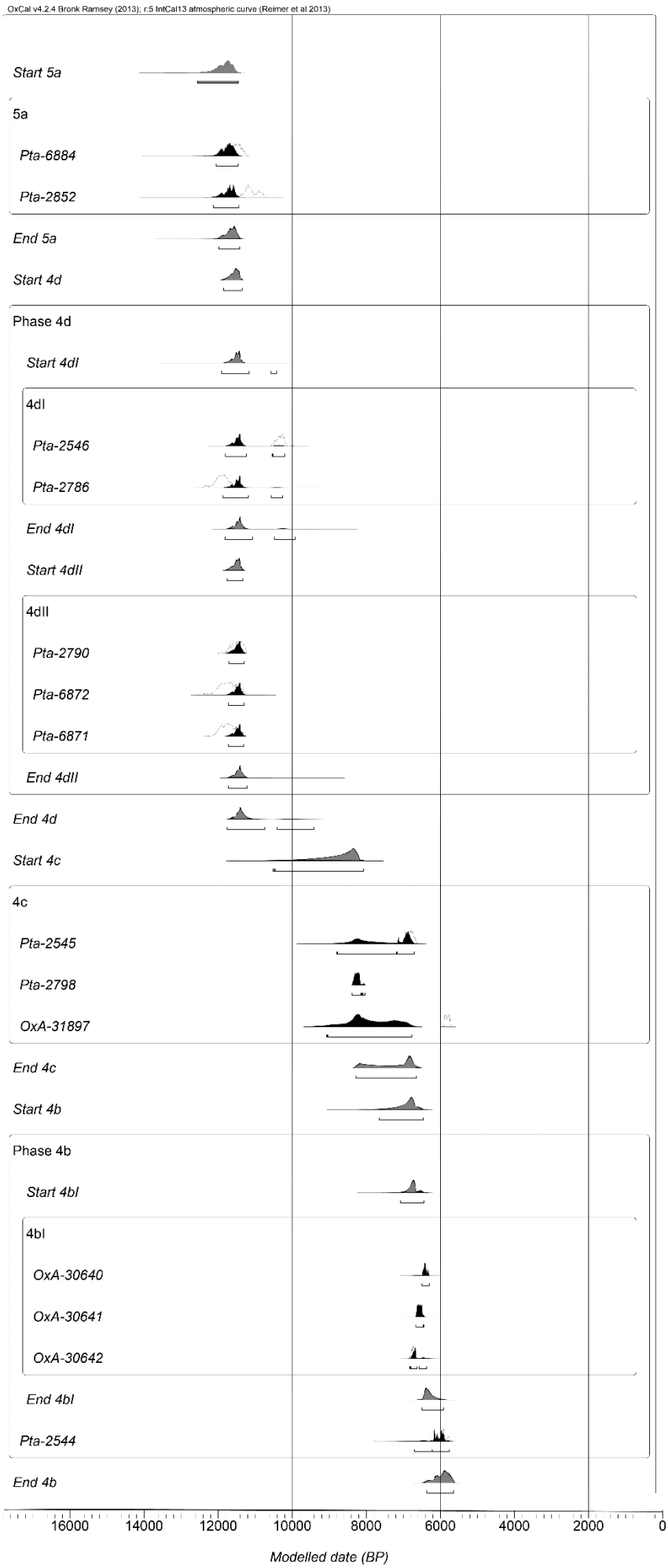
OxCal v4.2.4 Bronk Ramsey (2013); r:5 IntCal13 atmospheric curve (Reimer et al 2013)
Start 5a
5a
Pta-6884
Pta-2852
End 5a
Start 4d
Phase 4d
Start 4dI
4dI
Pta-2546
Pta-2786
End 4dI
Start 4dII
4dII
Pta-2790
Pta-6872
Pta-6871
End 4dII
End 4d
Start 4c
4c
Pta-2545
Pta-2798
OxA-31897
End 4c
Start 4b
Phase 4b
Start 4bI
4bI
OxA-30640
OxA-30641
OxA-30642
End 4bI
Pta-2544
End 4b
16000
14000
12000
10000
8000
6000
4000
2000
0
Modelled date (BP)

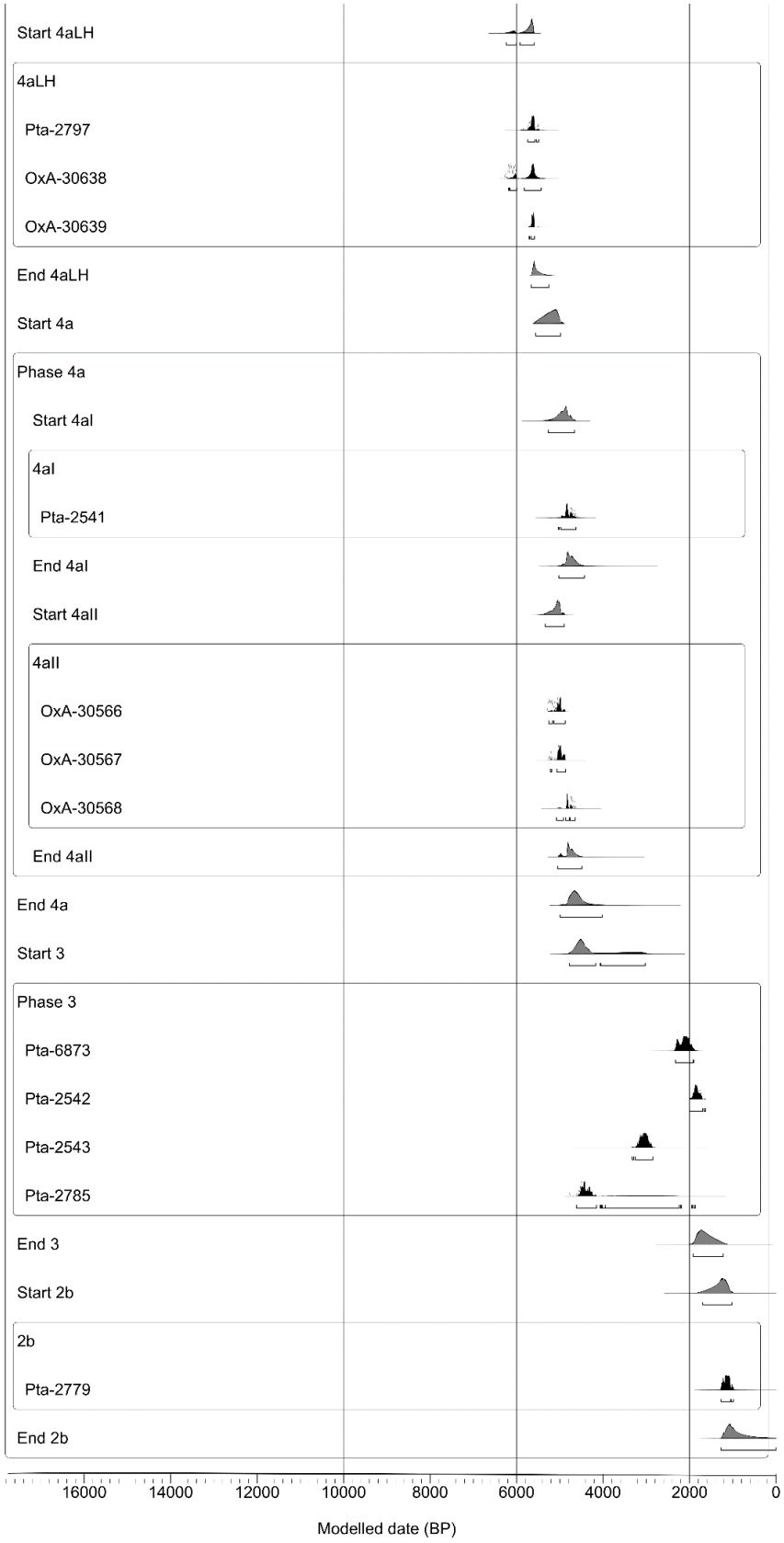

Figure 4.3: Plot of modelled dates (in black) from the OxCal program, ordered from oldest to youngest dates. Modelled boundaries between phases in light grey, all ages in cal BP.

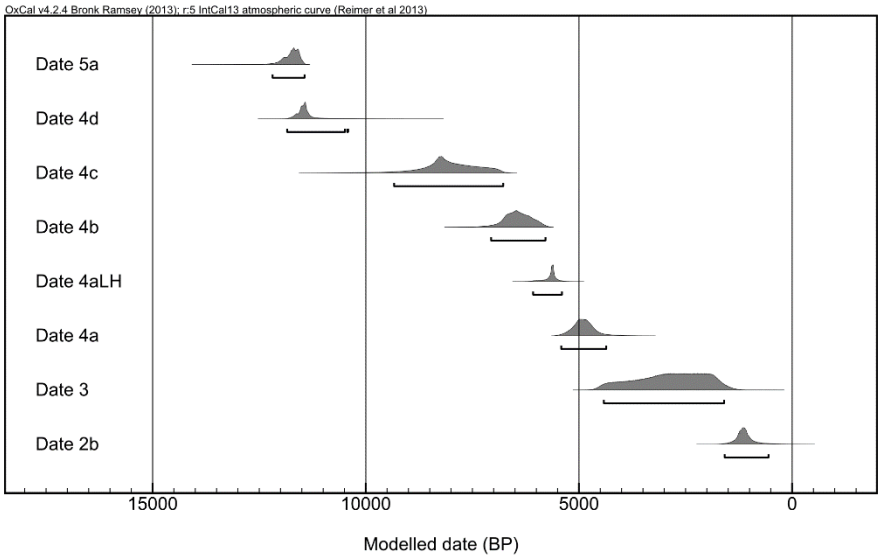

Figure 4.4: Summary statistics of the Strata ages, as a result of the Date-function (ages in cal BP).

4.4 Discussion

Later Stone Age chronology of Wonderwerk Cave

The model data provides a chronology that extends from over 12 000 years cal. BP to less than 1000 years cal. BP. Thus, calibration and Bayesian modelling indicates a rather longer sequence than radiocarbon years alone, and greater resolution for the cultural phases. It allows the construction of a chronological sequence with estimates for all Strata and the spits within a stratum. The Oakhurst (Stratum 4d) is the first Holocene industry in Wonderwerk Cave. The dates can be divided into two phases following the spit labelling system. The older one, 4dII has an age range (at 95.4% confidence level) from 11.2-11.8ka cal. BP, and the younger overlapping from 9.9-11.9ka cal. BP. The Wilton Strata (4c through to 3b) begin before 9ka cal. BP. This places the start of the Wilton at the site rather earlier than previously thought. Thackeray (1981) concluded in her study of the Excavation 1 lithics, that the Oakhurst cannot be a predecessor industry of the Wilton and therefore

Stratum	Lithic technology	Boundary age (cal. BP)	Boundary age (cal. BP); Incl. new dates	Date function age (cal. BP)); Incl. new dates	Beaumont spits	Thackeray spits
2b	Ceramic LSA	2b-3a: 190-2700	3-1700	553-1583	3UP, 3MID	2b, 3aI, 3aII
3	Wilton (backed bladelets/chert)	3b: 2060-4800	1240-4800	1598-4416	3LR	3b
4aI	Wilton (backed bladelets/chert)	4300-5070	4400-5260	4362-5417	4aUP	4aI, 4aII
4aII	Wilton (backed bladelets/chert)	4500-5400	4500-5300		4aMID	4aIII, 4aIV
4aLH	Wilton (backed bladelets/chert)	4900-5890	5260-6240	5400-6075	4aLWR	4aLH
4bI	Wilton (scrapers/ ironstone)	5550-6200	5900-7090	5786-7061	4bTUFA5	4bI
4bII	Wilton (scrapers/ ironstone)	5700-6500	5650-7660*		4bTUFA6	4bII
4cI-4cII	Wilton (scrapers/ ironstone)	5960-9800	6660-10500	6777-9336	4cUP, 4cLR	4cI, 4cII
4dI	Oakhurst	8600-11600	9900-11900	10416-11844	4d top	4dI
4dII	Oakhurst	10550-12200	11200-11800		4d base	4dII
5a	?	n/a	11400-12560	11436-12187	5a	5I

Table 4.3: Archaeological Strata in Excavation 1 showing associated stone tool technology. Correlations of the Strata names with the corresponding spits in both the Beaumont (Beaumont 1990, Beaumont pers. comm.) and the Thackeray (Thackeray 1981, Thackeray 1984) excavations are given. The modelled age boundaries at 95.4% confidence for each of the Strata (rounded) are shown based on the Bayesian modelling of existing radiocarbon dates (Table 4.1). Modelled start and end boundaries between Strata including the new Oxford dates (Table 4.2) are shown in column 4, and the results of the date function statistical analysis in column 5. *boundaries for the whole of 4b.

may have been made by different groups of people. The calculated hiatus between those Strata seems to strengthen that argument. The scrapers in Stratum 4c are described as the lower ones more resembling Stratum 4d scrapers, and the upper ones more resembling Stratum 4b scrapers (Thackeray 1981). It is proposed that this shows that Stratum 4c has two phases, but no change to the assigned Strata boundary was ever made (Thackeray 1981). This could explain the long span (6777-9336 cal. BP) and disagreement of the Stratum 4c ages.

A cultural shift within the Wilton industry is marked by Stratum 4aLH (Chapter 3), with boundaries between 5.3ka and 6.2ka cal. BP, between Strata 4bI and 4aII. The more recent Wilton phase, marked by higher proportions of backed bladelets now occurs within the Stratum boundaries of 4.4ka to 5.3ka cal. BP. The last phase of the Wilton occurs in Stratum 3b, with rather broad boundaries from up to 4.4ka indicate that this phase may have begun as early as 2.7ka cal. BP. In the different model versions run, it was not possible to separate dates from Strata 3a and 3b with one described as coming from the boundary. For this reason, the model presented here does not distinguish 3a from 3b, and the start of the Ceramic LSA cannot be determined more precisely. The new radiocarbon dating has resulted in improved age certainty for levels 4a, 4b and 4aLH. We can now confidently constrain a moist episode within 4aLH to less than 650 years, which stands out in the otherwise arid signal of the Wilton phase, coinciding with a shift in dominant raw material and tool type. For further discussion see Chapter 8.

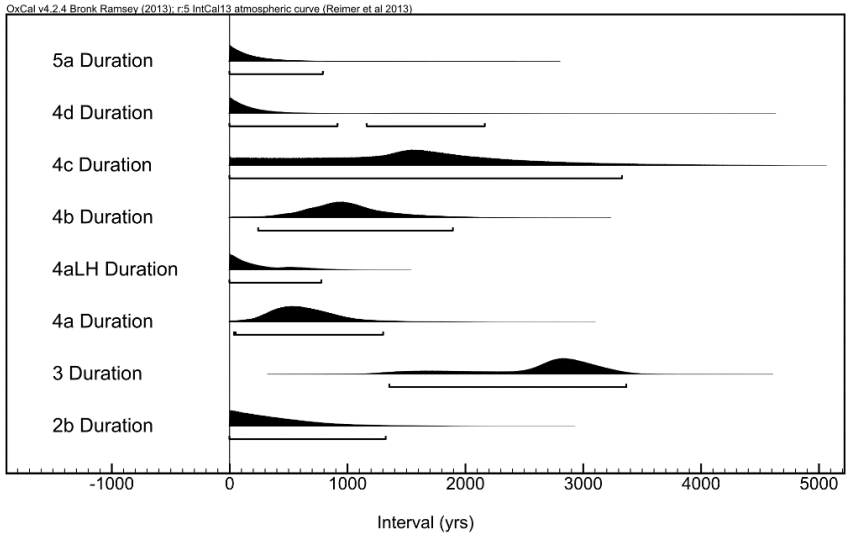

Figure 4.5: Results of modelled duration of Strata in Excavation 1 using the Difference function.

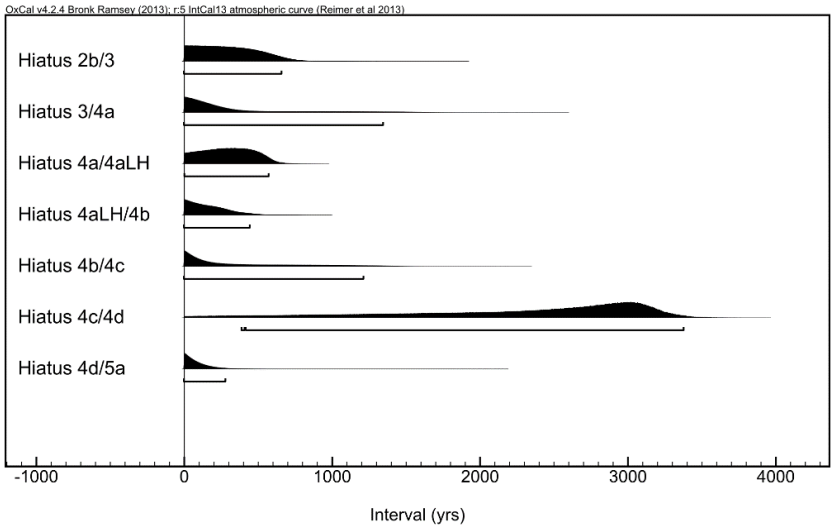

Figure 4.6: Results of modelled intervals of hiatus length between Strata in Excavation 1 using the Difference function.

The *Antidorcas bondi* and *Damaliscus pygargus* teeth were bracketing Stratum 3a and 4c (Fig. 4.1), and although one was replaced later with a charcoal sample from the same square, we have no better resolution for those earlier and later phases of the Holocene

sequence. As the OxA-31897 date did rather expand than constrain Stratum 4c, the aim to have direct dates for the *Antidorcas bondi* and *Damaliscus pygargus* specimen was not achieved. If A. Thackeray's conclusion is taken into account, that Stratum 4c might have two phases based on the scraper assemblage (Thackeray 1981), the new OxA-31897 date, as the youngest, might represent the earlier phase of 4c. Coming from the same square as the *A. bondi* specimen, it is possible, although not proven, that *A. bondi* survived in the Northern Cape till about 6000 cal. BP.

Implications for the Later Stone Age of South Africa's interior

Without doubt, Wonderwerk Cave has currently one of the best-dated Holocene sequences in South Africa. This sequence can be used as an anchor to compare with other LSA sites in the interior to. Unfortunately, there has not been much research into the LSA of the Northern Cape in recent years (Sadr 2013), excluding Namaqualand (Orton 2013). It is commonly assumed that the Wilton-like technology spread from Zimbabwe and Namibia through the interior to the coast (Mitchell 2013). The calibrated dates set the start of the Wilton at Wonderwerk possibly early compared to coastal sites, which might confirm this theory. On the other hand, the wide spread of dates in the first Wilton stratum, 4c, makes it impossible to determine the most likely start date with much confidence.

Similarly, pottery and domestics, either independently or through diffusion, are supposed to have moved from East Africa south (Orton 2012), so it is not surprising that Wonderwerk also shows early dates for pottery, whereas domestic sheep/goat and cattle are only found in Strata 1-2a, which are disturbed from more recent use of the cave last century. The earliest Stratum with pottery is 3a. Looking at the two dates from Stratum 3a, pottery was in the region since at least 2000 cal. BP (380 BC). It will require more well-dated early pottery sites in the interior to determine dispersal routes. The rock art on the Wonderwerk

walls remains undated, but the incised slabs are recovered from Strata 4d through to 3a, from Strata with radiocarbon dates (Thackeray et al. 1981). Therefore, being at least 11,000 years old, Wonderwerk is still a place with one of the oldest rock engravings in southern Africa, certainly for the LSA, which is otherwise quite poor in artistic expressions before the Wilton complex.

Although we could not date the samples directly, the charcoal date from Square K27 (5063±30ka) indicates that *A. bondi* survived until more recently than expected in this region. Remains of another extinct animal, *Megalotragus priscus* are from the same Stratum (Stratum 4c) and are therefore also the youngest example of this species in Africa (Faith 2014). Maybe some species survived longer in the more remote areas of the arid interior like Wonderwerk Cave, but more directly dated specimens from the sub-continent are needed to address the question of latest appearance with confidence.

4.5 Conclusion

The new radiocarbon dates, in connection with existing dates, when calibrated show Stratum 5 and 4d are comparable short phases before 10ka cal. BP, and could include late-Pleistocene climate extremes previous to the final warm stage of the early Holocene. Strata 4a and 4b are also close together in time, with 4aLH as a short but prominent phase in between. Strata 3 and 4c clearly comprise material from a wider time span and would need further field work to establish distinct levels within these strata. Altogether, a better dating program and the more widespread use of calibration is needed in South African archaeology. The introduction of the first calibration curve for the southern hemisphere that goes beyond 10 000 years into OxCal version 4.2 in 2013 (Bronk Ramsey et al. 2009, Hogg et al. 2013) is certainly a step in simplifying calibration of dates from South African archaeological sites.

Chapter 5 - Ostrich eggshell as a climatic proxy in Wonderwerk Cave

Stable light isotope analysis of ostrich eggshell provides a proxy of humidity changes over time. This chapter introduces ostriches as a species and especially OES as a material. It is followed by a description of the OES material from Wonderwerk Cave and the methods used to analyse it. The results are discussed in the light of C_4 intake in the ostrich diet through time, changes in humidity, and a comparison to other OES work in southern Africa. A particular focus is on comparison of Pleistocene and Holocene data from the Wonderwerk sequence. A detailed discussion of the OES results in the context of other environmental proxies from Wonderwerk Cave is given in Chapter 7.

5.1 Introduction to ostrich ecology and OES

5.1.1 Ostrich ecology

Ostriches, *Struthio camelus* (Order *Struthioniformes*, Family *Struthionidae*), are the largest living flightless birds. From early periods in prehistory onwards they have been exploited by humans for their meat, skin, feathers and eggs (Brown 1982, Williams et al. 1993). The oldest engraved OES containers known to have been recovered so far were found in a 60,000 years old layer at Diepkloof Rock Shelter, Western Cape, South Africa (Texier et al. 2010). Ostrich eggshell beads appeared for the first time in southern Africa in levels around 42,000 years ago at Border Cave (D'Errico et al. 2012). Other MSA sites in South Africa with OES beads are Spitzkloof Rockshelter (Dewar and Stewart 2012), Cave of Hearths (McNabb and Sinclair 2009), Bushman Rockshelter (Plug 1982), Kathu Pan (Beaumont 1990b), and Boomplaas Cave (Deacon 1995), but none of this material is directly dated. At the same time OES beads have appeared in East African sites like Mumba Cave and Kisese II Rockshelter, Tanzania and Enkapune ya Muto, Kenya (Klein 2009,

d'Errico et al. 2012). Currently the oldest directly dated OES beads are from MSA strata about 30 to ~50ka years old at Magubike Rockshelter, Tanzania (Miller et al. 2014). Ostrich eggshell fragments and ostrich skeletal remains are extremely rare in published Plio-Pleistocene faunal lists from southern Africa pre-dating the Middle Stone Age. Exceptions are Swartkrans Member 5, where nine fragments of eggshell (as well as an ostrich phalanx) were identified and attributed to *Struthio* sp. (Watson 1983), and Kromdraai B, where sparse ostrich eggshell fragments and bones were found (Brain 1981). Besides its archaeological significance, OES is also used by several other scientific disciplines. Ratite stable light isotope ratios have been used to indicate vegetation and hydrological changes from the Miocene through to the Holocene (eg. Stern et al. 1994, Johnson et al., 1997, Ségalen et al., 2006, Kingston, 2011). Ostrich eggshell is directly dateable by Radiocarbon, Amino Acid Racemization and U-series methods, making it a useful material for establishing chronologies (Johnson et al. 1998).

There are several subspecies of *Struthio camelus*: *Struthio camelus molybdophanes* and *Struthio camelus massaicus* can be found in East Africa while *Struthio camelus camelus* lives in North and West Africa. There is also the extinct subspecies *Struthio camelus syraicus*, which inhabited Arabia. In Southern Africa, the subspecies *Struthio camelus australis* is found in the wild today, although before the influence of humans reduced its habitat, this species was widespread and also inhabited the area around Wonderwerk Cave (Brown 1982; Chapter 3.1.3). All ostrich eggshell fragments recovered in Wonderwerk Cave belong to *Struthio camelus australis* (Ecker et al. 2015). Female ostriches lay an average of eight eggs and a maximum of 13 eggs per clutch. As several females lay their eggs into one nest, not all of them will be incubated (Brown 1982, von Schirnding et al. 1982). Eggs are laid mostly within a few weeks of the beginning of a rainy season (Sauer and Sauer 1966, Williams et al. 1993). The ostrich breeding cycle and seasonally changing

availability of plants are to be considered as the stable isotopes in the eggshell show only the environmental signal of the breeding season.

Habitat

Ostriches prefer short-grass plains and semi-deserts, as well as deserts with annual grasses. *Struthio camelus australis* is also seen occasionally in open woodland and scrub vegetation (Brown 1982). They forage in green vegetation patches in arid environments. Gravel plains are better suited for ostriches than rocky slopes or stony landscapes. Ostriches will spend some time in washes to feed (Williams et al. 1993).

Water dependency

Ostriches are particularly arid-adapted. They are non-obligate drinkers and have limited water excretion; in general, they can remain without drinking for days if there is enough green food available. Their main water intake is from plant water rather than environmental water sources, and they recycle metabolic water (Williams et al. 1993). Their bodywater pool is therefore strongly influenced by ^{18}O enrichment in plants due to evapo-transpiration. Subadult birds have a slightly higher water intake than adult birds. Ostriches only forage during daylight and appear to remain in one place during the night (Williams et al. 1993). Unlike other mammals, adult ostrich birds do not seek shade even in the desert during the day (Sauer and Sauer 1967).

Diet

Ostriches are hind-gut fermentors with a digestive efficiency comparable to large herbivores (Swart 1988). Their diet is vegetarian, although insects, shell, resin, and antelope faecal pellets were found in small amounts in ostrich stomachs (Milton et al. 1994). They consume a wide range of C_3, C_4 and CAM plants. Plant tenderness is the over-riding factor, as they have no teeth. Ostriches prefer green plants over dead or woody plant material and

avoid toxic plants (Milton et al. 1994). Their preferred foods are dicotyledonous plants, herbs and grasses (Willimas et al. 1993). Additionally, they are one of the few species that feeds on succulents, but they show no preference for this vegetation type (Milton et al. 1994). During feeding they also ingest stones and grit from the ground which assist with digestion in the stomach and contribute calcium to the body (Brown 1982).

5.1.2 OES formation and composition

Structure

Bird eggs consist of a yolk, which is covered in layers of albumen in shell membrane and shell carbonate. Compared to diet, yolk lipid is depleted by -2.6‰; albumen is 1.5‰, shell membrane is 3.6‰ and shell carbonate is about 15‰ enriched (Hobson 1995). The shell contains 95% inorganic fraction, formed from blood carbonate, resulting in a dense carbonate matrix that is extremely resistant to decay processes (Brooks et al., 1990, Miller et al., 1992, Johnson et al. 1998). The remaining 5% includes approximately 3.5% organic fraction and 1.5% water (von Schirnding et al. 1982). The organic fraction of OES is mainly protein fibres throughout the calcite crystals and is enriched in carbon by 2‰ compared to diet. The enrichment in ^{15}N is 3‰, similar to bone collagen enrichment. The inorganic fraction is mainly the stable polymorph of calcium carbonate/calcite. There are also up to 2% magnesium carbonate and 1% tricalcium phosphate. Large calcite crystals, as long as the egg is thick, form a mammillary cone (Fig. 5.1). The isotopic difference to the organic carbon fraction is about 14‰. Pores of 0.02-0.05mm thickness pass all the way through the eggshell, which is covered on the outside with a transparent film called cuticle (Fig. 5.1) (von Schirnding et al. 1982, Hobson 1995, Johnson et al. 1997, Johnson et al. 1998).

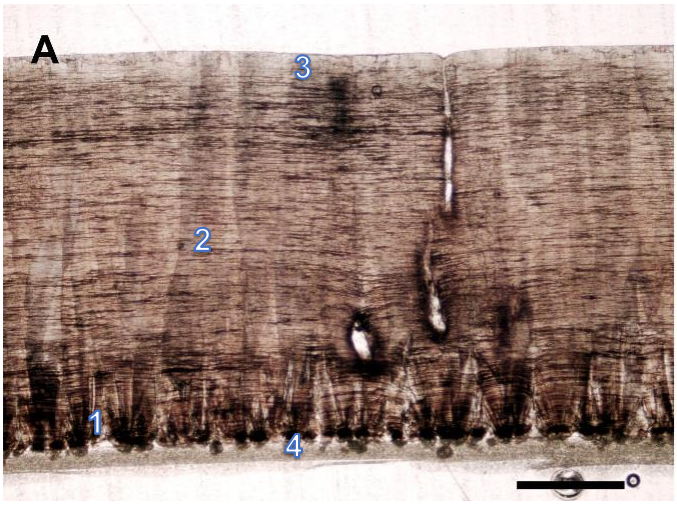

Figure 5.1: Transverse sections of eggshell microstructure of a modern *Struthio camelus*. (1) mammillary cone, (2) pore channel, (3) cuticle, (4) shell membrane. Scale bars = 500 µm (picture courtesy of J. Botha-Brink).

Stable isotopes in OES

The fractionation between the plant diet and eggshell $CaCO_3$ is about 15‰ for $\delta^{13}C$. Based on typical values for C_3 and C_4 plants, of -26‰ and -12.5‰ respectively, an ostrich feeding on C_3 plants alone would produce eggshell with $\delta^{13}C$ values of -11‰, while at the opposite end, those feeding on C_4 plants alone, would produce values of 2.5‰. Given that ostriches eat a range of plants, eggshell $CaCO_3$ isotopic composition reflects the proportions of C_3, C_4 and CAM in local vegetation that the ostrich finds palatable rather than a measure of the actual proportions of C_4 (or CAM) plants in the total local plant biomass.

Oxygen isotope fractionation between bodywater and $CaCO_3$ is about 30‰ (following the standard fractionation from H_2O to $CaCO_3$; Sharp 2007). Ostriches' bodywater pool is influenced by ^{18}O-enrichment in plants due to evapotranspiration. Eggshell $\delta^{18}O$ values ($\delta^{18}O_{CaCO3}$) reflect the influence of low humidity or relative humidity (RH) conditions, over and above the regional controls exerted by meteoric water $\delta^{18}O$ values ($\delta^{18}O_{mw}$). Modern studies suggest that OES $\delta^{18}O_{CaCO3}$ is highly correlated with mean annual relative humidity (MARH) and with mean annual precipitation (MAP) via their influence on

evapotranspiration in plants (Ségalen 2003). Therefore, in the Wonderwerk context, a preponderance of ^{18}O-enriched OES fragments reflects a phase of enhanced aridity (also expressed as lower MAP), while ^{18}O-depleted OES reflects greater humidity (higher MAP). As a result of the short interval represented by eggshell formation during egg-laying (3-5 days), the building of nests over several weeks, the contribution of more than one female to the clutch (Sauer and Sauer 1966; von Schirnding 1982) and the marked intra- and inter-seasonal variability in moisture conditions that typically pertains in arid zones, OES isotopic values can be highly variable even at one time and place (eg. Johnson et al. 1997). Each eggshell, and thus each fragment in a site, reflects a much shorter glimpse of time compared to that reflected in teeth or bone (von Schirnding et al. 1982; Johnson et al. 1997, 1998). Therefore, most authors suggest a minimum of three and a good mean of five to ten OES samples per layer at one site (von Schirnding et al. 1982, Johnson et al. 1998). We followed this advice when collecting samples from Wonderwerk Cave and used >10 samples per Stratum where possible.

Diagenesis

Ratite (struthionid or aepyornithid) eggshells occur in many palaeontological and archaeological sites. Although it was at one time feared that ostriches' habit of swallowing stones including limestone fragments might impart a radiocarbon reservoir effect, or shift $^{13}C/^{12}C$ ratios, no such effects have been observed and ^{14}C determinations show that shell carbonate remains a closed system (e.g. Long et al. 1983). In archaeological sites, the most important taphonomic constraint is burning or heating of fragments, as occurs for OES in contact with heated sediments near hearths. It has been shown, however, that colour and smell are good guides as to whether fragments have been heated or not (Crisp 2013).

5.2. Material and Method

Sampling strategy

The OES samples for this thesis were chosen and sent to Oxford by L. Horwitz during 2012 and 2013. Additionally, I selected samples from the Wonderwerk boxes in the Kimberly museum in April 2013 (SAHRA export permit ID. 679, Case ID 2169). Samples from the Holocene were not analysed (except Stratum 4d), as this is already covered by sufficient samples from Lee-Thorp and Ecker 2015, analysing Excavation 1 Strata 1-5, using between 7 and 24 samples per stratum. The method and analysis used is highly similar to the approach used in this thesis, so the results are comparable. The only exception is Stratum 4d, as this had the lowest number of samples, which was improved with new samples of spits 4dI and 4dII. All together 256 OES pieces from Excavation 1 and 2 were available, from which a selection was sampled (n= 186) and a further selection chosen to analyse (n=158).

Altogether, 102 OES fragments from eight archaeological Strata (Strata 12 to 6 and 4d) in Excavation 1 were measured for carbon and oxygen stable light isotopes of the inorganic fraction, as well as 56 OES from 5 Strata in Excavation 2. It was not possible to analyse the same number of samples per stratum. More than 20 samples per Stratum would be excessive, so a maximum of 20 was analysed when possible. Small pieces were excluded if the number of samples in the layer was high enough, to avoid completely destroying samples. Nevertheless, some samples needed to be crushed whole. Due to the expected large variation between ostrich eggshell fragments, >10 samples per Stratum were measured where possible. Other reasons for not sampling and/or analysing all available OES were visible signs of diagenesis, burning, abrasion and the cost of measurements.

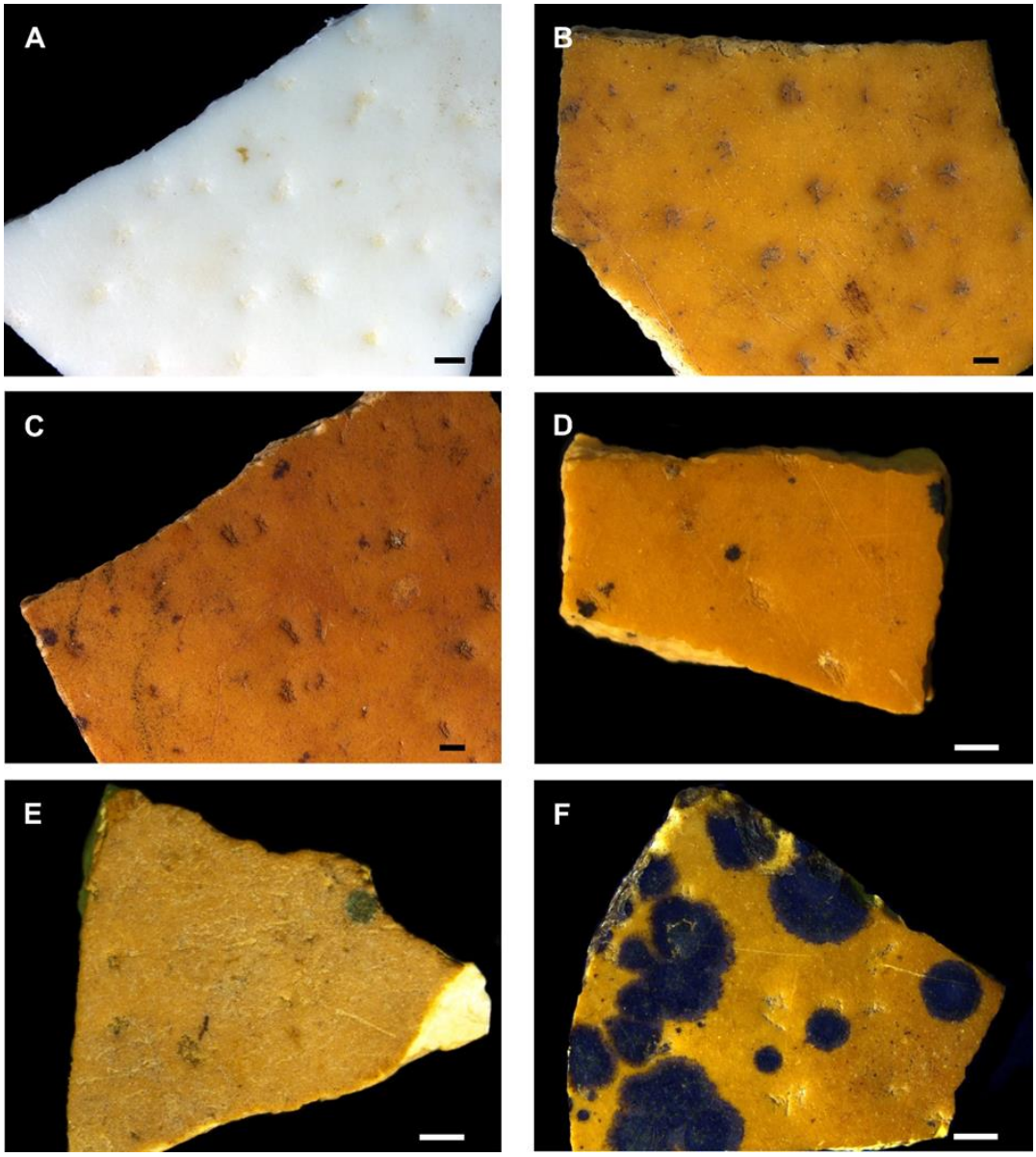

Figure 5.2: Examples of OES from Wonderwerk Cave and modern standard. (A) *Struthio camelus* modern standard, (B) Str. 2 R23, (C) Str. 4 R29, (D) Str. 7 #4524, (E) Str. 7 #4548, (F) Str. 8 #4468. Scale bars = 1 cm (picture courtesy of J. Botha-Brink).

Sampling and Pretreatment

OES sampling took place in the Research Laboratory for Archaeology and the History of Art at Oxford University. The first step was to take pictures of all samples prior to sampling, which are uploaded to the SAHRIS system as a requirement for the export permit (www.sahra.org.za/sahris/node/126022/objectschildren - link from 3/7/2015). One small corner of each fragment was removed with a diamond tipped saw blade in a handheld drill.

The fragment was then cleaned with an aluminium-oxide blaster and finely crushed in an agate mortar and pestle. Visible signs of burning (colour change brown-grey-black; and smell) during sampling or crushing were reported (Appendix 5.1). No chemical pretreatment was used on the samples, as a test of pretreated and untreated pieces of modern OES showed no differences in the outcome (Lee-Thorp, pers. comm.).

Measurement

Samples were analysed at Bradford University, using a Finnigan Gasbench II, connected to a Thermo Delta V Advantage continuous flow isotope ratio mass spectrometer. The carbonate fraction of each sample was reacted with phosphoric acid (100%) at 70°C to release CO_2, for measurement of $^{13}C/^{12}C$ and $^{18}O/^{16}O$ ratios. The reference gas was calibrated against three international (NBS 19, CO-1, CO-8), and two laboratory carbonate standards (MERCK $CaCO_3$, OES), which were interspersed in all runs (Appendix 4.2). The results for both isotopes are expressed as per mil (‰) in the delta (δ) notation versus the international VPDB and VSMOW standard respectively, as follows: $\delta^{13}C_{VPDB} = (R_{sample} - R_{ref})/R_{ref}$ x 1000 where $R=^{13}C/^{12}C$. $\delta^{18}O_{VSMOW} = (R_{sample} - _{Rref})/R_{ref}$ x 1000, where $R=^{18}O/^{16}O$. Analytical precision as determined from multiple replicates of the OES laboratory standard, was better than 0.1‰ for $\delta^{13}C$ and 0.2‰ for $\delta^{18}O$.

Quality control

The variation of the measured international and laboratory standards within a run and between all OES runs is ≤0.5‰ in carbon and ≤0.1‰ oxygen isotopes (Appendix 4.2), indicating measurement consistency. Burnt OES could be a problem, especially above 200°C, where values start to gradually shift and clear alteration occur at the 500°C black stage. The $\delta^{18}O$ value should be more influenced than the $\delta^{13}C$ value (Lee-Thorp. pers. com.). In another study, heating of a modern OES fragment slowly up to 500°C lead to

minimal depletion in the $\delta^{13}C$, less than is expected as natural variation (Johnson et al. 1998). Both heating studies used only one sample respectively. Besides the colour, which could also come from sediment staining or weathering, smell is an indicator of burning (Crisp 2013). When sampling the Wonderwerk OES, exclusion of brown or blackish OES was not strict, because the source of the colour change was unclear. Colour and smell were recorded (Appendix Table 5.1). The smell does not always, but often, occur in black or dark brown OES. There are only one red and two grey OES pieces. It is feasible to consider the smelly ones unreliable. I tested mean values per Strata with and without possible burnt samples. $\delta^{13}C$ and $\delta^{18}O$ mean values tend to be both lower unburnt compared to burnt samples, but only in a few Strata is the difference more than one per mill. A systematic offset cannot be inferred. The mean values all together are more close to the "unburnt only" value. There should be no significant influences to the results, except perhaps in Excavation 2 Stratum 4 and 5, were all/the majority of samples are black and smelly. The large spread in $\delta^{13}C$ values in Stratum 10 cannot be explained by burnt OES influencing values. In another test, samples were plotted on the excavation grid with the values per square. There is no clustering of values in a particular area for Excavation 1 and 2.

Statistics

To test for homogeneity of variance, a Levene's test in R (version 3.0.1) was used for Excavation 1 and 2 results, as well as for the Holocene result from Lee-Thorp and Ecker (2015) to allow statistical comparison. This test confirmed the null hypothesis that all Strata variances are equal, except for $\delta^{13}C$ in Stratum 10. Statistically significant differences in $\delta^{18}O$ between all Strata were tested, including between and against all of the Holocene data from Lee-Thorp and Ecker (2015). A one-way ANOVA with Tukey's HSD *post-hoc* test in R (R Core Team 2013), with $p<0.05$ regarded as significant, was used. In Stratum 10, a

Kruskal-Wallis test as well as a Mann-Whitney test between all Strata was used for carbon isotope results (Appendix 6.1).

5.3. Results

Excavation 1 Holocene

The results for the Stratum 4d samples are consistent with the 4d samples from Lee-Thorp and Ecker (2015). The variation is higher in $\delta^{18}O$ than in $\delta^{13}C$. There is no significant difference between the spits 4dI and 4dII. Basic statistics of the results are listed in Table 5.1, with a full list of results in Appendix 5.1.

Stratum	**n**	**$\delta^{13}C$**	**Sd**	**min**	**max**	**$\delta^{18}O$**	**sd**	**min**	**max**
4dI	9	-8.4	1.7	-9.8	-4.7	39.8	2.9	37.0	45.2
4dII	5	-8.0	0.5	-8.5	-7.4	39.0	2.3	36.0	41.8
All	14	-8.3	1.4	-9.8	-4.7	39.5	2.6	36.0	45.2

Table 5.1 Descriptive statistics for OES results of Stratum 4d, including number of samples (n), mean values, standard derivations (sd), minimum (min) and maximum (max) values.

Excavation 1 Pleistocene

Basic statistics of the results from Excavation 1 Pleistocene Strata are listed in Table 5.2. All results are listed in Appendix 5.1. Figures 5.3 and 5.4 show the distribution of mean and median values and well as individual values graphically.

Stratum	n	$\delta^{13}C$	Sd	min	max	$\delta^{18}O$	sd	min	max
6	11	-8.4	1.0	-9.7	-6.7	40.0	3.5	35.2	47.6
7	19	-8.5	0.9	-10.4	-7.0	39.1	3.2	34.1	47.2
8	20	-8.7	0.8	-10.5	-7.7	38.8	2.9	32.9	45.5
9	16	-8.3	1.2	-10.6	-6.6	38.7	3.7	33.6	47.8
10	16	-7.5	2.5	-10.0	-1.5	36.0	2.2	32.8	40.8
11	1	-10.0	-	-	-	35.2	-	-	-
12	5	-8.6	0.3	-8.9	-8.1	39.4	1.8	36.4	41.1

Table 5.2 Descriptive statistics for OES results per Stratum from the Pleistocene of Excavation 1, including number of samples (n), mean values, standard derivations (sd), minimum (min) and maximum (max) values.

The $\delta^{13}C$ mean values range from -10‰ to -8.4‰. Therefore, the ostrich diet was largely dominated by C_3 plants, with a small but consistent contribution of C_4. There is a visible shift between Strata 12/11 and Stratum 10. Stratum 10 has the widest distribution of carbon isotope values, ranging from a predominantly C_3 (minimum value -10‰) to a predominantly C_4 diet (maximum value -1.5‰). Statistical tests confirmed that Stratum 10 is significant different in $\delta^{13}C$ from all other Excavation 1 Pleistocene Strata. The mean value of -7.5‰ is the second highest, so the extreme C_4 values indicate short spells within the long time span covered by this stratum. Values for Strata 9 to 6 cluster tightly, with similar means, maximum values, minimum values and standard derivations.

Overall, the oxygen isotope data for the early/mid-Pleistocene sequence indicate a generally arid setting for Wonderwerk Cave with many $\delta^{18}O$ values near or above 35‰. The $\delta^{18}O$ data are more variable than the $\delta^{13}C$ data. The lowest individual value is 32.8‰, and the maximum individual value is 47.8‰. The means range by 4.8‰, from 35.2‰ to 40.0‰. Stratum 12 shows ^{18}O-enriched values, indicating arid conditions. However, the sample size for Stratum 12 is small (n=5) and the results might therefore not cover the full range of variation. This is also the case for Stratum 11, where only one sample was available

for analysis. This sample yielded low $\delta^{18}O$ and $\delta^{13}C$ values indicating moister conditions and C_3 plant foods. Although an isolated specimen, this result is consistent with phytolith analysis which shows a change from a more arid environment in Stratum 12 to more humid conditions with more C_3 grasses in Stratum 11 (Chazan et al., 2012; Chapter 3). Mean values for oxygen isotopes increase from Stratum 11 upwards, and especially from Stratum 9 upwards, and the data indicate drier conditions (or at least more frequent dry spells). As is the case for the $\delta^{13}C$ findings, Stratum 10 differs from the other Strata, showing a lower median value indicating moister conditions. These results suggest a highly variable environment with large shifts in moisture within the time span represented. When the data are divided by sublevels (Beaumont's a, b, c, d, e), the only visible differences within a Stratum are: 9c-e are lower in $\delta^{18}O$ (35.6‰) than 9a-b (39.9‰ and 39.5‰ respectively). Samples labelled 10a are lower in carbon and oxygen than samples only labelled Stratum 10. As explained in Chapter 3, the sub-level divisions are not consistent enough to be used reliably. The values seem to follow in parts the lithostratigraphic division of the early Pleistocene Strata.

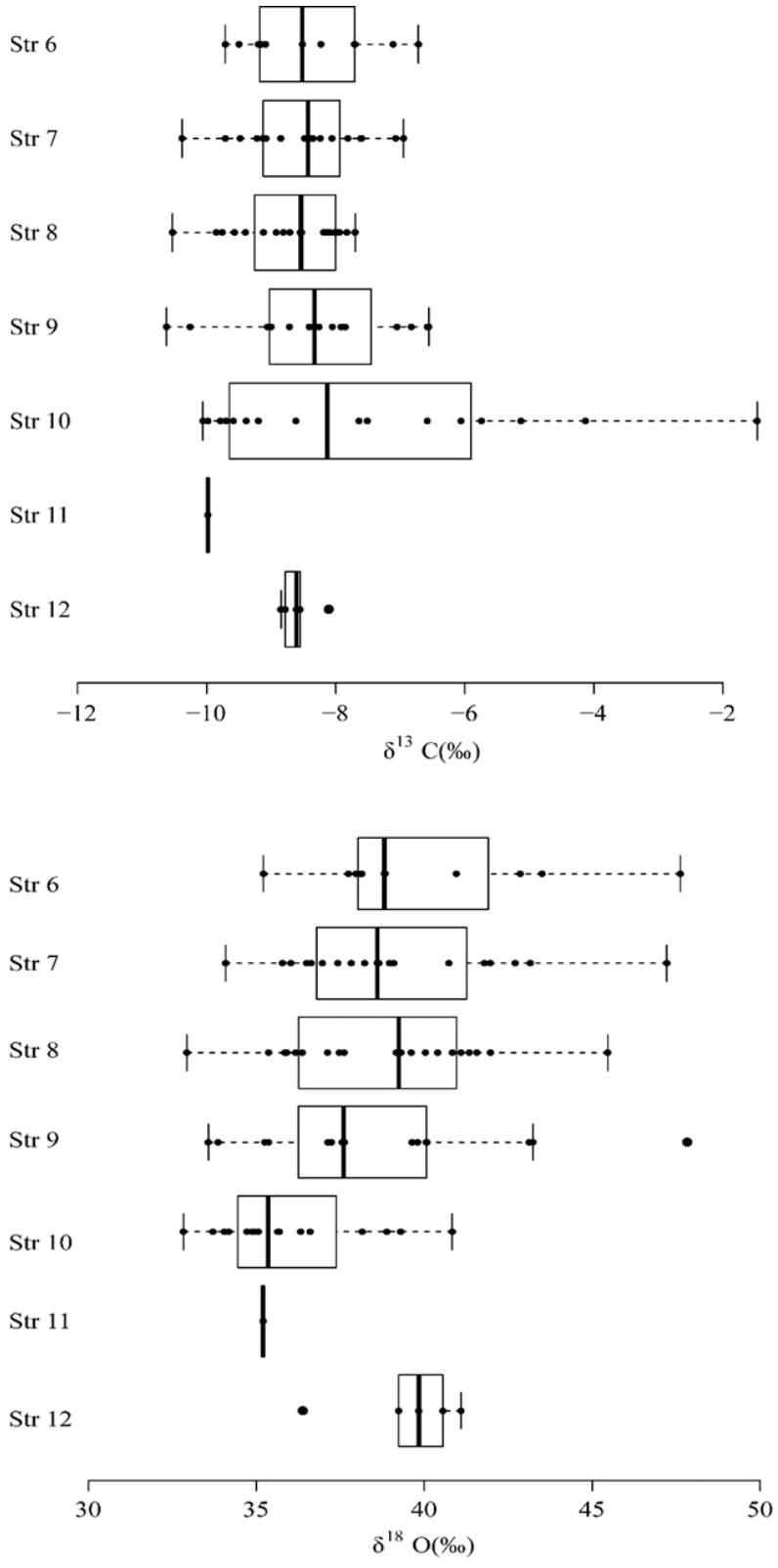

Figure 5.3: Boxplots showing the distribution of $\delta^{13}C_{VPDB}$ (above) and $\delta^{18}O_{SMOW}$ (below) isotope data for Wonderwerk Strata 6-12. Black line represents the median, dots represent the individual measured values.

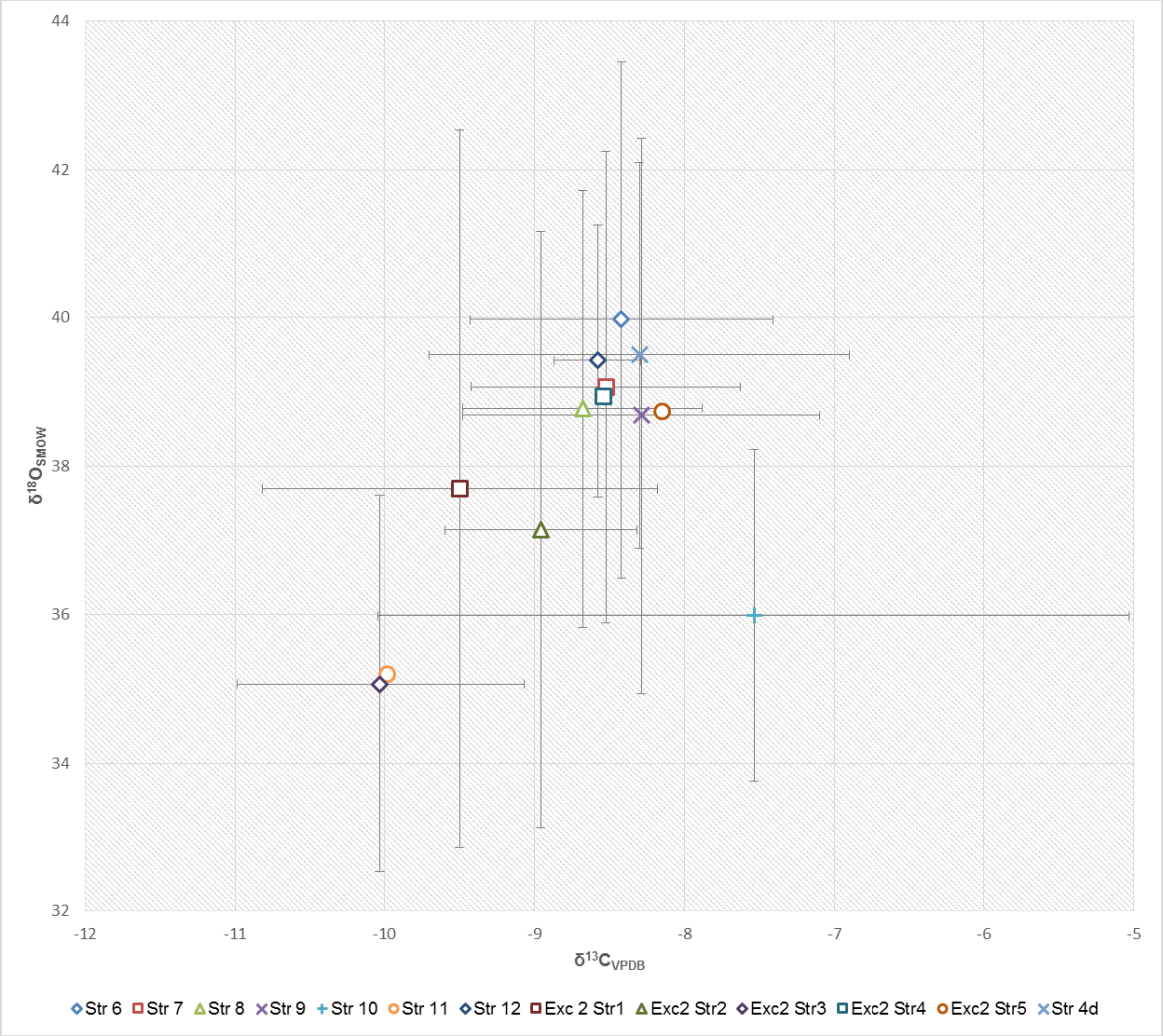

Figure 5.4: Scatter plot of OES $\delta^{13}C$ and $\delta^{18}O$ mean value per stratum. Error bars represent two sigma standard derivations.

Excavation 2

Descriptive statistics of OES stable light isotopes from Excavation 2 are listed in Table 5.3. A full list of results is available in Appendix 5.1. Stratum 1, the LSA level, shows a considerably wide span of values, especially in oxygen isotopes. Its median, on the other hand, is highly similar to the uppermost Holocene Strata of Excavation 1 in carbon and oxygen isotope values (Figure 5.5). In Stratum 2, the early MSA, the carbon clusters quite tightly around -9‰. The mean $\delta^{18}O$ values on the other hand are more negative than most Strata in Excavation 1 except Strata 10, 11 and 5I. It also shows a spell or spells towards more negative values. This continues in Stratum 3, where the $\delta^{18}O$ is less spread, but more

negative, with a mean value of 35.1‰, than in any other Stratum in Wonderwerk. The $\delta^{13}C$ values follow the trend in Stratum 3 and show a mean of -10‰. Stratum 4 is slightly more positive in both, although we only have two samples from this stratum. The five samples from Stratum 5 show large variations, with lower $\delta^{18}O$ values and enriched carbon isotope values, but those might not be reliable due to burning.

Stratum	**Age**	**n**	**$\delta^{13}C$**	**sd**	**min**	**max**	**$\delta^{18}O$**	**sd**	**min**	**max**
1	LSA	15	-9.5	1.3	-11.2	-7.7	37.7	4.8	31.6	45.0
2	MSA	18	-9.0	0.6	-10.2	-7.4	37.1	4.0	30.8	48.4
3	undated	17	-10.0	1.0	-11.0	-8.2	35.1	2.5	32.6	40.0
4	undated	2	-8.5	0.8	-9.1	-8.0	38.9	2.1	37.5	40.4
5	undated	4	-8.2	0.3	-8.5	-7.8	38.7	2.9	36.2	41.3

Table 5.3: Descriptive statistics for OES stable light isotope results per Stratum from Excavation 2, including number of samples (n), mean values, standard derivations (sd), minimum (min) and maximum (max) values.

A Levene's test confirmed the null hypothesis that all Strata variances are equal for $\delta^{18}O$ and $\delta^{13}C$ within Excavation 2. In a test using all data from Excavation 1 and 2, $\delta^{13}C$ shows again no equal Strata variances, except when Stratum 10 is excluded from the dataset. A one-way ANOVA with Tukey's HSD *post-hoc* test, showed significances within Excavation 2 between Stratum 2/3, 3/5 and 1/5 in carbon.

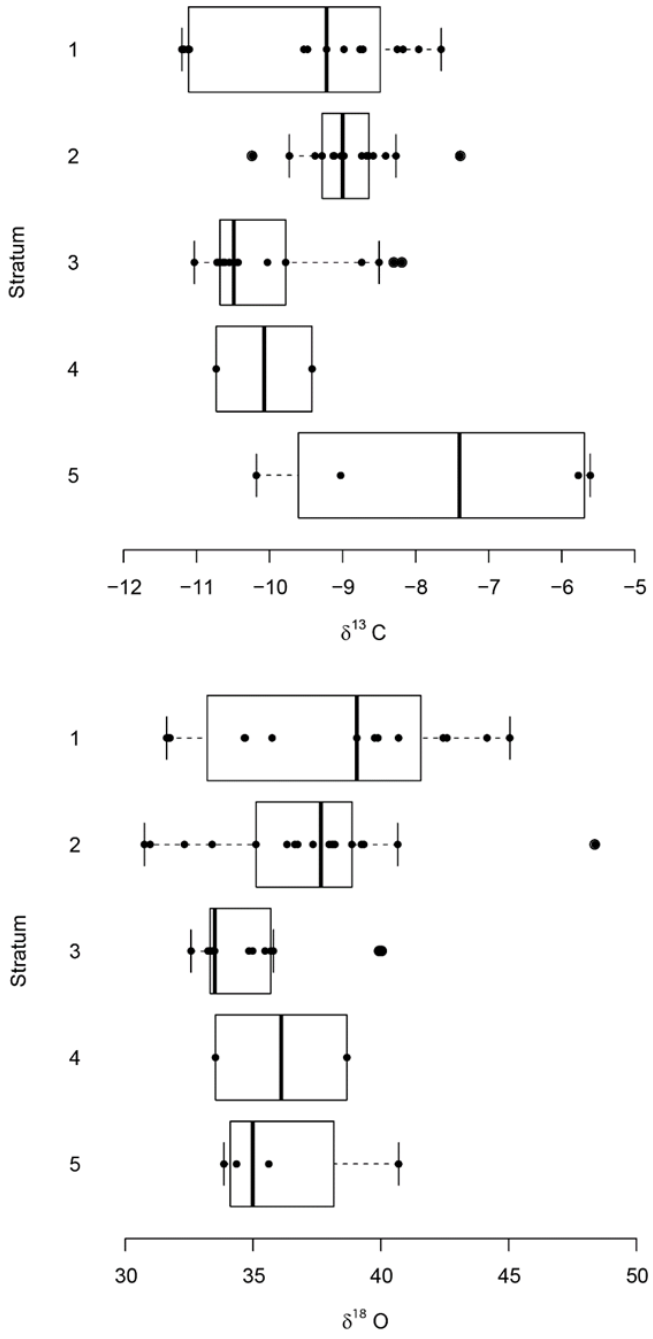

Figure 5.5: Boxplots showing the distribution of $\delta^{13}C_{VPDB}$ (above) and $\delta^{18}O_{SMOW}$ (below) isotope data for Wonderwerk Excavation 2. Black line represents the median, dots represent the individual measured values.

5.4. Discussion

Mixing model

To estimate how much C_4 plants the ostrich ingested, a two-endmember mixing model was calculated. Using -11‰ and 2.5‰ as endpoints, the results for the mean values as well as maximum and minimum values per Strata are in Table 5.4. The results from Lee-Thorp and Ecker (2015) are included for the Holocene Strata as comparison. Based on mean values, the overall C_4 in ostrich diet is about 20% and does not vary greatly over time (Figure 5.6). Exceptions are lower percentages in Excavation 1 Strata 4dI, 5I, 5II, 11 and Excavation 2 Strata 3. The highest C_4 percentages are in Strata 10 and 4aII.

Stratum	**%C_4**	**Min**	**Max**	**%C_3**
Excavation 1				
1+2a	14.7	3.3	63.3	75.3
2b	14.0	3.3	65.3	76.0
3a	17.3	1.3	50.7	72.7
3b	18.7	12.0	54.7	71.3
4aI	15.3	0.0	56.0	74.7
4aII	22.0	8.7	44.0	68.0
4aLH	15.3	6.7	64.7	74.7
4bI	18.7	8.7	54.7	71.3
4bII	17.3	2.7	63.3	72.7
4cI	15.3	3.3	64.0	74.7
4cII	16.7	7.3	62.7	73.3
4dI	10.7	4.0	80.0	79.3
4dII	19.3	7.3	69.3	70.7
5I	2.7	-5.3	75.3	87.3
5II	11.3	0.7	69.3	78.7
6	17.3	8.7	61.3	72.7
7	16.7	4.0	63.3	73.3
8	15.3	3.3	68.0	74.7

9	18.0	2.7	60.7	72.0
10	23.3	6.7	26.7	66.7
11	6.7			83.3
12	16.0	14.0	70.7	74.0
Excavation 2				
1	10	-1	68	80
2	13	5	66	77
3	7	0	71	83
4	17	13	70	73
5	19	17	69	71

Table 5.4: Calculated percentage of C_4 and C_3 plants in the ostrich diet per stratum using the mean value per stratum in a two endmember mixing model. Including minimum and maximum percentage intake from individual minimum and maximum stable isotope values per stratum.

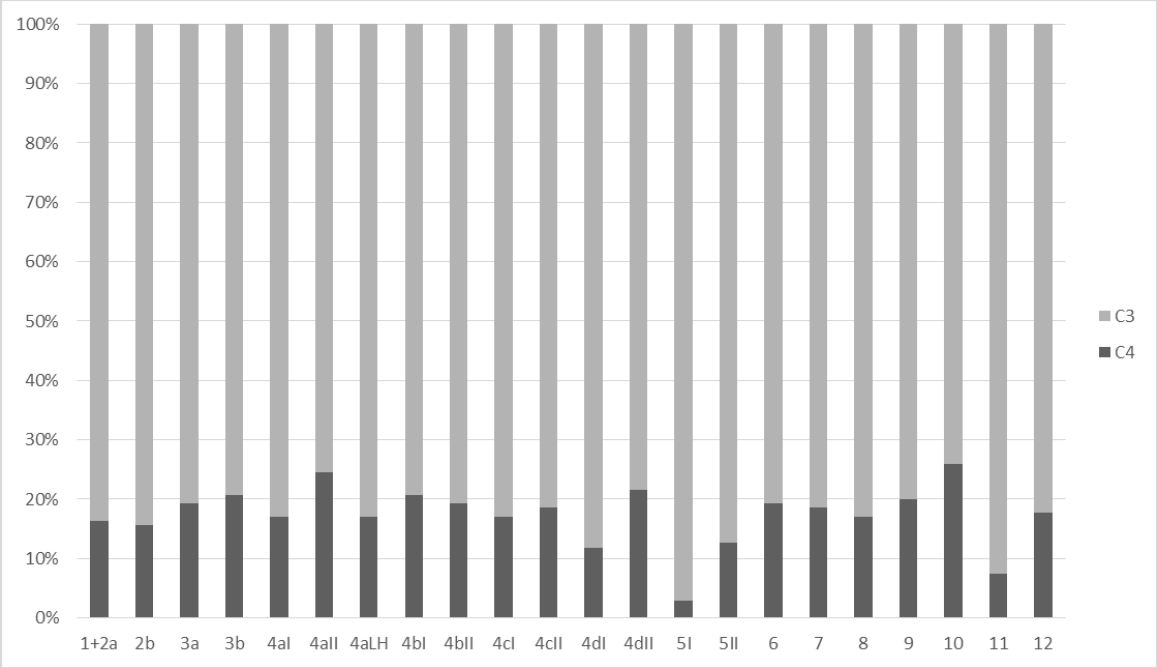

Figure 5.6: Results of mixing model for Excavation 1. Dark colour percentage of C_4 in the ostrich diet, light grey colour percentage of C_3, calculated from Strata mean values (includes data from Lee-Thorp and Ecker 2015).

Evaluating the whole sequence

Combining data from this thesis with Lee-Thorp and Ecker (2015), it is possible to explore and compare the OES results over the whole Wonderwerk sequence. For the Holocene, the overall mean for $\delta^{13}C$ is -8.6±1.2‰, and individual values range between -11.8‰ and -4.1‰, spanning a dietary range from C_3 to large amounts (> 50%) of C_4 plants. The mean for all $\delta^{18}O$ values is 39.0±3.2‰, but the variation of individual values across all Strata is extremely high, from 29.4‰ to 50.3‰. These data suggest highly variable but mostly arid conditions throughout the sequence. Mean values in the Holocene are in general higher in both $\delta^{13}C$ and $\delta^{18}O$ compared to the Pleistocene Strata. Considering the complete Excavation 1 sequence, Stratum 5 is significantly different in $\delta^{13}C$ to all Strata with high C_4 mean values, and in $\delta^{18}O$ to Strata with high means. This is mainly driven by spit 5I. Stratum 10 is significantly different in $\delta^{18}O$ against the arid Strata 3a and 3b (Appendix 6.1). Four moist phases are clear in Excavation 1: Stratum 11, Stratum 10, Stratum 5 and 4aLH/4bI. Stratum 2 in Excavation 2 is similar in both $\delta^{13}C$ and $\delta^{18}O$ to the one OES value from Stratum 11. According to lithics and preliminary radiometric dating, it should be younger than Stratum 11, so both might present similar C_3 dominated conditions, suggesting similar conditions re-appearing throughout the two million years. Stratum 10 is comparable, but with a striking cluster of extreme high $\delta^{13}C$ values. Statistically, compared with Excavation 1, Excavation 2 Stratum 3 is significantly different in $\delta^{13}C$ and $\delta^{18}O$ from mid-Holocene Strata; as well as Stratum 10 and 9 in $\delta^{13}C$ and Stratum 6 in $\delta^{18}O$. Excavation 1 Stratum 5I and Excavation 2 Stratum 2, which have been identified as 'wet' from proxies like faunal abundances, microfauna, geological features and botanical remains in Wonderwerk, but are less depleted in both isotopes than Excavation 1 Stratum 11 and Excavation 2 Stratum 3 (Fig. 5.4).

It may be concluded that the carbon and oxygen isotope data for Wonderwerk Cave OES fragments follow independent trends (e.g. Stratum 4aLH). This is not entirely surprising as they reflect different environmental variables. It is often assumed that C_4 plants suggest greater aridity, as they thrive in warm climates and open vegetation. Ostriches might therefore increase their intake in C_4 grasses if the environment becomes dominated by it. On the other hand, they will only eat the fresh green sprouting grass, and no coarse dry specimen. The reverse happens if an environment has increasing numbers of C_3 plants, but they are woody and thorny, not palatable for ostriches. $\delta^{13}C$ OES is therefore not suitable to closely tracking vegetation changes. Oxygen reflects aridity, as plants under water stress close their stomata and change fractionation against ^{18}O with this step. Aridity will therefore lead to higher $\delta^{18}O$ values, but $\delta^{13}C$ values will only increase at the same time if there is also enough fresh green grass expanding.

Comparison to other OES analyses at Wonderwerk Cave

The ostrich eggshell from Wonderwerk was used by L.K. Horwitz and J. Botha-Brink to investigate pore density and thickness. Furthermore, samples were analysed with a Scanning Electron Microscope (SEM) and with histological sections (see Ecker et al. 2015 for details). Studies of modern bird eggshell have shown a correlation between eggshell permeability and nesting environment conditions. When conditions are hot and/or arid, the eggshell tends to be thicker, but also with more pores to allow gas exchange. Horwitz and Botha-Brink found that pore density and shell thickness are significantly different between LSA and ESA Strata in Wonderwerk (Ecker et al. 2015). This correlates with the mean values in oxygen isotopes for OES from LSA and ESA, which are separated too, although not statistically significant when excluding depleted $\delta^{18}O$ phases like Stratum 11 and 10. Thicker eggshell in the late Holocene is associated with an increase in pore density indicating more arid conditions in the more recent periods.

Comparison to other OES studies in Southern Africa

Isotope studies based on OES from archaeological sites are sparse, with the exception of Equus Cave (Johnson et al. 1997), western Lesotho (Mitchell 2000) and a shorter Blydefontein Rock Shelter sequence (Bousman 2005) in the interior, and on the west coast, a sequence for Elands Bay Cave (Lee-Thorp and Talma 2000). New studies from the south coast from the MSA sites Pinnacle Point (Lee-Thorp and Marean, in progress) and Blombos Cave (Roberts 2013) are currently unpublished and show lower variability in the isotope values than Wonderwerk Cave.

The closest comparison for the Wonderwerk OES results is the sequence established by means of Isoleucine (Ile) epimerisation ratios for individual fragments, and based on $\delta^{13}C$, $\delta^{15}N$ and $\delta^{18}O$ values for OES samples from Equus Cave, in the Ghaap Escarpment (Johnson et al. 1997). In that record, the $\delta^{13}C$ values change little in the Holocene, and the most notable $\delta^{15}N$ shift (on which interpretations of aridity were based) occurs between the late Glacial and the Holocene. Although interpreted as indicating shifts in temperature, high $\delta^{18}O$ variability occurs within the Holocene. Based on the Ile ratios, data are sparse in the early Holocene, but the grouped $\delta^{18}O$ data after about 6000 years suggest lower values near 4000 years and higher values at ca. 1-2ka. The Wonderwerk OES $\delta^{18}O$ data are consistent with the Equus Cave data for 1-2ka, where both overlap in time and indicate aridity in the last two millennia. Additionally, mean values for the disturbed Strata 1 and 2a in Wonderwerk are similar to modern values obtained by Johnson et al. (1998) for Kimberley.

The much shorter Blydefontein Rock Shelter $\delta^{13}C$ record for OES indicates a shift incorporating more C_4 plants after 2000 years BP in the Karoo (Bousman 2005). Spanning the last glacial-interglacial transition and the Holocene, Elands Bay Cave on the Western Cape coast shows increasing $\delta^{18}O$ throughout with a depleted episode ca. 12.5ka. The

oxygen isotope record shows variability within the Holocene, interpreted as arid episodes at 4.2-3ka and 1-0.5ka followed by humid spells. As this site is in the winter rainfall region, the climatic conclusions might not be relevant for Wonderwerk Cave in the summer rainfall region. The $\delta^{13}C$ values from Elands Bay are slightly higher when the $\delta^{18}O$ values are higher, which can mean more CAM plants in this environment rather than large proportions of C_4 grasses (Lee-Thorp and Talma 2000). Ségalen et al. (2006) show an offset of 4-5‰ in $\delta^{18}O$ between the summer and winter rainfall regions in Namibia using ratite eggshells. This reflects the generally lower $\delta^{18}O$ values of winter rainfall. Its influence is a possible explanation for Wonderwerk Strata with lower $\delta^{18}O$ values.

5.5 Conclusion

The $\delta^{18}O$ record from OES at Wonderwerk reveals mostly arid but highly variable conditions, with a few distinct phases of increased humidity. The general trend is towards greater aridity towards as well as within the Holocene. Excavation 1 Strata 11and 10 show humid, cool conditions, while most Strata in Excavation 2 also show low $\delta^{18}O$ values. The $\delta^{13}C$ values show that the proportions of C_3 and C_4 plants in ostrich diets remained broadly similar throughout the last two million years, with a few notable exceptions: Excavation 1, Stratum 11 and 10 and in Excavation 2 Strata 2-4. Results from stable light isotope analysis from enamel of large mammal species (Chapter 6) will be used to create a much more detailed picture of vegetation changes than the rather opportunistic feeding ostriches. The oxygen and carbon isotope sequences do not appear to always shift in concert, a result that does not lend support to notions that increases in proportions of C_4 grasses necessarily denote increased aridity.

Chapter 6 - Enamel stable isotopes in the Wonderwerk fauna

This chapter deals with the core of the thesis, the application of stable light isotope analyses of tooth enamel to a diachronic series of mammalian faunal samples from Wonderwerk Cave. As background, the chapter first describes how mammal teeth can be used to inform about diet based on isotopic composition. The Wonderwerk dental sample studied is described, along with criteria for sample selection and documentation procedures. A description of the methods is followed by the respective results. The discussion part explores dietary changes through time in the analysed species as well as physiological differences between species. A short note on the use of aridity indices concludes the chapter.

6.1 Stable isotopes in enamel

The mineral fraction of enamel is a highly crystalline material and more resistant to diagenesis than bone and dentine. For this reason, it is a highly suitable material for stable isotope analysis (Lee-Thorp and van der Merwe 1991, Koch et al. 1997). This section will explain the properties of enamel and how it is used in stable isotope research, before the analysis of enamel from Wonderwerk Cave is described. The four types of mammalian teeth (incisors, canines, premolars, molars) consist of an enamel crown and one or more roots made of dentine. Both might be covered by varying proportions of cementum. Both dentine and cementum have a large organic component made up mainly of collagen fibres (Hillson 2005). The major mineral fraction in teeth is biogenic apatite. Enamel is composed of over 99% apatite, with the remaining being small amounts of water and trace amounts of organic compounds (LeGeros et al. 1978). Enamel apatite has a flexible composition of calcium, phosphor, carbon and to a lesser extent chloride, fluoride and micronutrients (Elliot 1997). All molecules can be replaced by other ions, apatite can therefore have

changing compositions, although the main structure remains the same (LeGeros 1981). Carbon ions in bioapatite occur as substitutes in the phosphate position or as adsorbed carbonate (as CO_3^{2-} and HCO_3^- ions) on surfaces and in hydration layers (LeGeros et al. 1967, Poyart et al. 1975). The formation of enamel is called amelogenesis, in which ameloblasts first produce a matrix during the earliest stage of tooth development known as the bell stage. In the second stage, named maturation, the protein and remaining water are removed and the structure is mineralized (Weinmann et al. 1942, Sakae and Hirai 1982).

Tooth enamel forms incrementally from crown to base. This means that the oldest enamel is on the occlusal surface of the tooth and the youngest near the roots (Zazzo et al. 2005). In contrast to bone, which is remodelled constantly during an individual's lifetime, enamel is not rebuilt. Therefore, enamel retains the isotopic signature from the mammals' diet at the time of its formation (Zazzo et al. 2005). Most mammals, including the species sampled in this thesis, have two sets of teeth: The deciduous, or milk teeth, are replaced by the second set of permanent teeth. Replacement times vary greatly. Some rodent species, including species sampled in this study, have either ever-growing incisors or a complete set of ever-growing teeth (Ungar et al. 2010). For stable isotope analysis, the time of mineralization of the enamel is most important (but complex, Hoppe et al. 2004), not the eruption age (where the gingival emergence is most commonly used as marker). After eruption, a tooth begins to wear down from grinding against other teeth and against food. Worn parts vanish and thus are not available for stable isotope analysis (Hillson 2005, Wang et al. 2008).

Several mechanisms can change the isotopic values of biogenic apatites. Possibilities are through addition of exogenous material, e.g. precipitation of secondary minerals or adsorption of ions on the surface of crystals. Another mechanism would be isotopic exchange reactions with surrounding fluids (Sponheimer and Lee-Thorp 1999b, Zazzo et

al. 2004). Chemical pretreatments are used routinely to eliminate remaining organics and possible secondary carbonates (Chapter 6.4.2). Of importance for this thesis are changes occurring during burning of enamel, which leads to water loss, resulting in fracturing and cracking (Shipman et al. 1984). Teeth burn in a similar manner to bone, depending on temperature and duration as well as whether they are permanent or deciduous teeth. Stages of incineration are visible as colour changes from brown/black to blue-grey and finally chalky white (calcination) (Schmidt 2008). Water loss changes the apatite lattice irreversibly at temperatures of 200°C and higher, whereas over 500°C loss of CO_3 occurs (LeGeros et al. 1978, LeGeros 1981). At calcination, most water and protein will have burned and evaporated (Schmidt 2008).

The uptake of isotopic signals from diet is tissue specific (DeNiro and Epstein 1978). The carbon isotopic signal derives through the food chain from the plants eaten by herbivores, and reflects the CO_2 fixation in the plants. Other than collagen, which mostly reflects protein consumption, $\delta^{13}C$ in enamel carbonate reflects the whole diet (Ambrose and Norr 1993). Isotope enrichment of carbon in tooth enamel to diet is 13.3‰ to 14.6‰ for medium to large sized ungulate mammals. Studies on modern captive and wild animals with known diet showed that the number varies with animal size, digestive system and quality of diet (Tieszen 1994; Cerling and Harris 1999, Passey et al. 2005). One theory is that ruminants produce more methane than non-ruminants which leads to slightly different enrichment factors between diet and apatite (Cerling and Harris 1999), but this is physiologically yet unproven. In this study I have used 14.1‰ for enrichment in carbon isotopes in all taxa (following Cerling et al. 2015), as this is the most common used enrichment factor in studies with African large herbivores.

In mammalian tissues, oxygen is bound in the phosphate and the carbonate of the bioapatite. $\delta^{18}O$ enamel carbonate values are derived from blood biocarbonate, and therefore

ultimately from ingested water at the time of tissue formation, reflecting climatic conditions (Dansgaard 1964, Rozanski et al. 1993). The water could be taken in through drinking, reflecting meteoric water, or food, reflecting humidity, or both. The enrichment of oxygen isotopes from drinking water is 26‰ (Tieszen 1994). Bodywater in large mammals is at a constant temperature, so no further temperature-dependent fractionation occurs when the oxygen is incorporated into carbonate or phosphate (Longinelli et al. 1984, Bryant et al. 1996). Fractionation occurs only during inhalation, respiration, sweating and loss through water vapour. The majority of the O_2 intake/loss in mammals is through non-fractionating drinking and diet, as well as faeces and urine, which determines the isotopic composition preserved in fossil material (Koch 2007). Other influences are body cooling mechanisms like panting (depleted compared to sweat; Wong et al. 1988), and feeding habits. Nocturnal feeders, which feed at night and mostly on the roots and other underground storage organs of plants, have depleted $\delta^{18}O$ values (Sponheimer and Lee-Thorp 1999a). Browsers should be enriched if they eat mainly evapotranspirated plant leaves compared to grazers and carnivores (Kohn et al. 1996, Cerling et al. 1997, Sponheimer and Lee-Thorp 1999a).

It is disputed if maternal milk changes the isotopic signature to more positive carbon and/or oxygen isotope values (Franz-Odendaal et al. 2003, Camin et al. 2008, Metcalfe et al. 2010). Every species has a different time line of tooth formation, development and eruption, and teeth can start mineralizing before birth (Table 6.1). Independent of weaning, there are compositional differences between different teeth from a jaw and within an individual tooth. The same tooth from different individuals of the same population can vary by up to 3‰. One main factor causing intra-tooth and intra-jaw differences is seasonality of diet (Kohn et al. 1998).

6.2 The Wonderwerk dental assemblage

The complete available faunal collection from the Wonderwerk Cave excavations was examined in order to select suitable teeth for enamel samples. The goal was to sample a wide variety of species to represent the different possible ecological niches. The sampled species in this chapter include ungulates, rodents and hyrax (the latter represented by one sample). Too few suitable carnivore samples were available from any of the layers (only two possible hyena teeth) and so no carnivores were sampled. There were large numbers of *Papio* sp. (Baboon) teeth in the Holocene levels, but as most were deciduous, too immature for isotope analysis, they were not sampled. Not sampled were any of the domestic animals (one *Bos taurus* and five *Ovis/Capra* in the disturbed Stratum 1-2a) nor microfauna, tortoise remains or reptiles. The ostrich eggshell material is described in Chapter 5.

The Pleistocene sample is restricted due to a high degree of burning as well as extreme fragmentation, and contains a large number of deciduous teeth (especially in equids). It was impossible to avoid first molars because of the small sample size available. Similarly, it was not possible to limit samples to those located near the dated excavation profile, rather they derive from the whole of Excavation 1 and 2. All deciduous teeth, clearly burnt tooth fragments and enamel fragments that could not be identified to family level (except for Stratum 4d – due to extremely small sample size) were excluded. Strata 9 and 10 had especially high numbers of burnt teeth, limiting the sample sizes for those Strata. Excavation 2 Stratum 2 yielded two teeth of rhinoceros, and a high proportion of deciduous equids teeth as well as hyrax remains. In the Holocene Strata, the faunal material is found in significantly greater numbers and is better preserved, with complete teeth more common than in the Pleistocene samples.

Species	Permanent tooth formula	Age of weaning	Permanent tooth development	Comments	References
Bovidae					
Alcelaphini					
Alcelaphus buselaphus (Hartebeest)	I 0/3, C 0/0, P 3/3, M 3/3	Completed at ~ 7 months	n/a		Skinner & Chimimba 2005, Florisbad collection
Connochaetes taurinus (Blue Wildebeest)	I 0/3, C 0/1, P 3/2, M 3/3	Up to 8 months	M_1 5-1m, M^1 6-8m, M2 12-16m, M3 18-24m, P3-4 28-32m	Not enough information for *C. gnou*	Attwell & Jefferey 1981, Skinner & Chimimba 2005
Damaliscus pygargus (Blesbok)	I 0/3, C 0/1, P 3/3, M 3/3	4 months	M1 6m, M2 9m, M3, I 18m, completed 33m		Skinner & Chimimba 2005
Tragelaphini					
Tragelaphus strepsiceros (Greater Kudu)	I 0/3, C 0/1, P 3/3, M 3/3	3-6 month	I+C 21-24 m, P+M 29m		Skinner & Chimimba 2005, Shorrocks & Bates 2014
Taurotragus oryx (Eland)	I 0/3, C 0/1, P 3/3, M 3/3	~ 4 months	M1 6-8m, M2 14-20m, M3 24-27m, P2-4 36-37m.		Attwell & Jefferey 1981, Skinner & Chimimba 2005
Antilopini					
Antidorcas sp., incl. *A. marsupialis, A. bondi* (Springbok)	I 0/3, C 0/1, P 2/2, M 3/3	4 months	M1 1-4m, M2 7-9m, M3 10-22m, P3-4 16-19m		Rautenbach 1971, Skinner & Chimimba 2005
Neotragini					
Raphicerus campestris (Steenbok)	I 0/3, C 0/0, P 3/3, M 3/3	n/a	n/a		Skinner & Chimimba 2005, Kingdon et al. 2013
Oreotragus oreotragus (Klipspringer)	I 0/3, C 0/0, P 3/3, M 3/3	4-5 months	n/a		Cueno 1965, Skinner & Chimimba 2005, Kingdon et al. 2013
Reduncini					

Redunca fulvorufula (Mountain Reedbuck)	I 0/3, C 0/0, P 3/3, M 3/3	~ 3 months	M1 3m, M2 9m, M3 2y, P4 2.5y		Skinner & Chimimba 2005, Kingdon et al. 2013
Kobus leche (Lechwe)	I 0/3, C 0/0, P 3/3, M 3/3	6-7 months	n/a		Skinner & Chimimba 2005
Pelea capreolus (Grey rhebok)	I 0/3, C 0/0, P 3/3, M 3/3	n/a	n/a		Skinner & Chimimba 2005, Kingdon et al. 2013
Perissodactyla					
Equids, incl. *Equus quagga burchelli* (Plains zebra), *Equus quagga quagga* (extinct)	I 3/3, C 1/1, P 3/3, M 3/3	After 8-12 months	M1 9-12m, M2 1-1.5y, M3 3-5y, P2-3 2-3y, P4+C 3.5y, I3 4y		Smuts 1974, Skinner & Chimimba 2005
Ceratotherium simum (White rhinoceros)	I 0/0, C 0/0, P 3/3, M 3/3	After 1 year	P2 3-4y, P2-4 4-8y, M1 3y, M2 4-7y, M3 8-16y		Hillmann-Smith et al. 1986, Skinner & Chimimba 2005
Rodentia					
Hystrix africaeaustralis (Cape porcupine)	I 1/1, C 0/0, P 1/1, M 3/3	After 4 weeks	I at birth, M1 2-3m, M2 5-6m, M3 11m, P 2y.	M do not grow continously	Skinner & Chimimba 2005
Pedetes capensis (Springhare)	I 1/1, C 0/0, P 1/1, M 3/3	After 6-7 weeks		All teeth ever-growing	Skinner & Chimimba 2005
Suidae					
Phacochoerus africanus (Common warthog)	I 1/2-3, C 1/1, P 3/2, M 3/3	Start 9 weeks, could suckle until 5 months	C 1m, M_1 3m, M2 9-11m, I+P after 1y, P 20-22m, M 36m.	M3 grows permanently	Skinner & Chimimba 2005, Shorrocks and Bates 2014
Procaviidae					
Procavia capensis (Cape hyrax)	I 1/2, C 0/0, P 4/3, M 3/3	At 1-5 months	M1 5-7m, I 8-19m, M2 11-16m, M3 20-23m, completed 5y		Steyn & Hanks 1983, Skinner & Chimimba 2005

Table 6.1 Permanent tooth formula, weaning age and permanent tooth development (commonly eruption ages) of the sampled species, including references.

Ungulates were traditionally classified into two groups, the perissodactyls and artiodactyls, based on their digestive system, hindgut fermentation and rumination respectively (Shorrocks and Bates 2014). Another feeding distinction that has arisen in ungulates is that between grazers, browsers and mixed feeders (Hofmann 1968, Estes 1991). Grazing ungulates feed on monocotyledonous plants (grasses, but also reeds and rushes), while browsers feed on dicotyledonous plants (tree foliage, but also fruits and herbs). Mixed feeders ingest both graze and browse, often switching their foraging activity between the wet season (grass) and the dry season (foliage). The adaptation is evident in the teeth, as the upper incisors and canines have been lost and the premolars and molars show complex folds and sharp ridges for grinding vegetable matter. Some grazers have evolved high-crowned (hypsodont) teeth to resist grinding. In the Wonderwerk sample, grazers, browsers and mixed-feeders were sampled to obtain a complete picture of the local ecology. Information on diet and habitat of all sampled species is summarized in Appendix 3.

Bovidae are the largest family of mammals in the Wonderwerk assemblage in all Strata. Tribes present include Alcelaphini, Tragelaphini, Antilopini, Neotragini and Reduncini. Therefore, the whole range of modern grazing, browsing and mixed-feeding bovids is present, as well as all size categories from the small *Raphicerus campestris* (~10 kg) to the largest bovid, the eland (~500 kg). Perissodactyla are represented by Equidae, and one sample from a white rhinoceros. The two rodent species *Pedetes capensis* and *Hystrix africaeaustralis* are both present throughout the sequence, and offered the chance to build a comparative sequence on smaller, less mobile mammals. A few samples from the warthog *Phacochoerus africanus* and one Hyrax sample complete the analysed assemblage.

6.4 Methods

6.4.1 Sampling

All samples were identified by Dr. James Brink (JB) and the author (ME) at the Florisbad Quaternary Research Station, National Museum Bloemfontein, South Africa, using their reference collection. After identification of the tooth type, position of tooth represented and species, we carefully documented the condition of the samples. Pleistocene samples were given a code for burning (Scale 0-5, unburnt to white). Holocene samples were measured for length of crown, width of crown, mesial breadth of lobe and distal breadth of lobe by JB, while the Pleistocene samples were measured using the same criteria by ME prior to sampling. Sampling directly on measurable edges was avoided. All samples were photographed with a digital camera with macro function on a photographic stand with a scale before and after sampling. Buccal, lingual and where appropriate occlusal pictures were taken. Any obvious features, e.g. wear stage, glue adhering or missing parts were noted. First, the outer surface was cleaned with a brush if necessary and then removed using a diamond-tipped drill. Clean enamel powder (4-10mg) was collected subsequently onto weighing paper, and stored in a microcentrifuge tube. Bulk samples covered the full length of the enamel wherever possible to obtain a sample representing its entire development. When a tooth was too fragmented, a small piece of the enamel was removed for subsequent crushing in an agate mortar and pestle. Some of the Holocene teeth had been glued during post-excavation analysis. Researchers regularly comment on excluding samples because of adhering glue that might influence the carbon isotope values (Clayton et al. 2006, Lee-Thorp et al. 2010), whereas other studies found no influence of bone glues on stable isotope values (Lopez-Polin 2012). In this study, all glue was drilled off before sampling. Ideally, to avoid sampling the same individual more than one time, the same tooth on the same side should always be used. To avoid nursing or weaning effect, teeth that grow late in the life

of an individual should be preferentially chosen. Furthermore, as there can be intra-tooth variation in the stable isotope values, always choosing the same sampling spot in every species is desirable. Due to the nature of the Wonderwerk enamel assemblage described above, it was not possible to fulfil these strict sampling criteria. However, careful quality control was used to assure the high quality of the results (Chapter 6.4.4).

All samples were given unique ME numbers. This was necessary as not all samples have SPF numbers (a unique number given to diagnostic samples at Wonderwerk by Horwitz and Brink). Pre-sampling pictures of all samples were uploaded to the SAHRIS webpage (http://www.sahra.org.za/sahris/node/171538/objectschildren) as a requirement for the export permit.

Species	**N Exc 1 Holocene**	**N Exc 1 Pleistocene**	**N Exc 2 Stratum 2**
Alcelaphini indet.	51 (53)	24 (28)	1 (1)
Alcelaphus buselaphus (Hartebeest)	41 (45)		1 (1)
Connochaetes sp. (Wildebeest)	14 (14)		2 (2)
Damaliscus sp.	4 (6)	2 (2)	3 (3)
Tragelaphini indet.	11 (41)	4 (4)	
Tragelaphus strepsiceros (Greater kudu)	34 (34)	4 (4)	3 (3)
Taurotragus oryx (Eland)	7 (7)	2 (2)	
Bovid indet.	5 (19)	0 (1)	
Antidorcas sp. (Springbok)	17 (19)	13 (13)	2 (2)
Raphicerus campestris (Steenbok)	34 (34)	3 (3)	2 (2)
Oreotragus oreotragus (Klipspringer)	1 (1)		
Redunca fulvorufula (Mountain reedbuck)	17 (17)	1 (1)	

Kobus leche (Lechwe)		2 (2)	2 (2)
Pelea capreolus (Grey rhebok)	3 (4)	1 (1)	3 (3)
Equus sp. (Zebra) / *Hipparion* sp.	22 (28)	26 (32)	3 (4)
Ceratotherium simum (White rhinoceros)			1 (1)
Diceros bicornis (Black rhino)		0 (1)	
Hystrix africaeaustralis (Cape porcupine)	25 (27)	14 (16)	2 (3)
Pedetes capensis (Springhare)	22 (25)	6 (6)	
Phacochoerus africanus (Common warthog)	6 (7)		
Procavia capensis (Cape hyrax)	1 (4)		
ALL	**315** (385)	**102** (116)	**26** (28)

Table 6.2: Number of enamel samples from Wonderwerk Cave, with number of identified teeth in parentheses. Excavation 1 Stratum 5 is included in the Pleistocene column.

6.4.2 Pretreatment

Pretreatment in the Research Laboratory for Archaeology and the History of Art, University of Oxford followed the laboratory standard protocol, modified after Sponheimer (1999). Enamel powders were soaked in ~1.8 ml NaOCl solution (~2%) for 30 minutes to remove organics. During this time the samples were mechanically shaken several times, then centrifuged for five minutes at 13 000 RPM speed and the liquid removed with a pipette. The first batches (one batch = 12-16 samples) of samples were started with 2-3 min centrifuge at 13 000 RPM, but sample size, calculated sample loss (on 55 random samples, Appendix 4.1) and clearness of the liquid led to increase the centrifuge time for the remaining samples. Thereafter, all samples were centrifuged for five minutes at maximum speed. The tube was refilled with distilled water, and the process repeated three times. Due to the small amount of enamel in some samples, only two washes after the NaOCL were carried out, but care was always taken to removing all liquid each time. Samples were then

soaked in 0.1M Acetic Acid (CH_3COOH) for ten minutes, including the centrifuge time of five minutes, to remove any exogenous carbonate. Samples were decanted and washed with distilled water as described above, three times. Tubes were closed with parafilm and freeze dried overnight.

6.4.3 Measurement

Samples were analysed at Bradford University, using a Finnigan Gasbench II, interfaced with a Thermo Delta V Advantage continuous flow isotope ratio mass spectrometer. After purifying with helium, the carbonate fraction of each sample reacted with 100% phosphoric acid at 70°C to release CO_2, for measurement of $^{13}C/^{12}C$ and $^{18}O/^{16}O$ ratios. The reference gas was calibrated against three international standards (NBS 19, CO-1, CO-8), three laboratory carbonate standards (MERCK $CaCO_3$, BES, OES), and two Oxford lab standards (MAM, WILD), which were interspersed in all runs (Appendix 4.2). The standards were chosen to span the whole expected range of carbon and oxygen isotope values. The results for both isotopes are expressed as per mil (‰) in the delta (δ) notation versus the international VPDB and VSMOW standard respectively, as follows:

$\delta^{13}C_{VPDB} = (R_{sample} – R_{ref})/R_{ref}$ x 1000 where $R = ^{13}C/^{12}C$

$\delta^{18}O_{VSMOW} = (R_{sample} – R_{ref})/R_{ref}$ x 1000, where $R = ^{18}O/^{16}O$

Analytical precision as determined from multiple replicates of the laboratory standards was approximately 0.1‰ for $\delta^{13}C$ and 0.2‰ for $\delta^{18}O$.

6.4.4 Quality control

Both standard deviation per individual measurement (ten measurements per sample) and $CaCO_3$, which are both values provided by the mass spectrometer, are influenced by a number of parameters. Unusual high and low $CaCO_3$ values were checked against the

isotope results per Stratum and species, and no trend was observed. The variation of the standards in all runs was plotted to reveal outliers. The variation of the measured international and laboratory standards within a run and between all runs is less than 0.2‰ in carbon and less than 0.6‰ in oxygen (Appendix 4.2). Besides the standards, other possible signs of diagenetic influences were investigated. During sampling, some samples were marked as possibly burnt, but clearly burnt samples were excluded from sampling. In scatterplots per species that included the possibly burnt samples, no marked difference or trend was visible compared to the unburnt pieces (except excluded pieces, see below) (Appendix 4.3). It can be therefore assumed with confidence that the isotopic values have not been influenced by burning. A comparison of results by tooth type to detect possible weaning effect was not possible for the Pleistocene samples as they were mostly too fragmented to identify the exact tooth type. A case study on 37 *Alcelaphus buselaphus*, 13 *Raphicerus campestris* and 18 *Hystrix africaeaustralis* Holocene samples showed no trend for higher values in M1s compared to other tooth types (Appendix 4.3). First, second and third molars, as well as premolars, showed similar variability. Due to the wide and uneven spread of samples in Excavation 1 and 2, it was a question if certain isotope values would cluster in one area of the Excavations and therefore might reveal inconsistency within a stratum. Test plots and statistical tests showed no correlation between squares and isotope values (Appendix 4.3).

Measurements of individuals

Five pairs of samples (ME228/ME344; ME336/ME371; ME475/ME517; ME306/ME305; ME 241/ME242) could possibly be from the same individual, as they derive from the same species in the same stratum, spit and square, as well as showing similar dental wear stages. One pair of samples (ME537/ME540) is certainly known to be from the same individual. The difference between the *A. marsupialis* samples ME537 and ME540 is 0.8‰ in carbon

and 0.7‰ in oxygen, a difference that can be expected for two samples from different tooth types of one individual. The other pairs show higher differences, especially in the oxygen (up to 3.6‰). They are less likely to be from the same individuals but we cannot be certain.

Re-Runs

After analysis of the enamel results, nine samples were identified as outliers and run again on the same machine at Bradford University, including all samples with $\delta^{18}O$ values above +40‰ (ME247, ME317, ME532, ME619). The values for the re-run samples were all close to the original measurement, confirming those results, and especially confirming the $\delta^{18}O$ values above 40‰ (Appendix 4.4). The mean values of the first measurement and the re-run are used for both carbon and oxygen isotope results in all the graphs and statistical analysis.

6.4.5 Statistics

To test for homogeneity of variance in the Excavation 1 and 2 results, a Levene's test in R (version 3.0.1) was performed, with the null hypothesis that all Strata variances are equal. Tests were conducted within each species over time (Strata) and within each Stratum on their own; and then with the species within the Strata. Furthermore, statistical differences between all Strata were tested for each species using one-way ANOVA with Tukey's HSD *post-hoc* test in R (R Core Team 2013), with $p<0.05$ regarded as significant. As ANOVA can only be undertaken with parametric values, a Kruskal-Wallis test was used for datasets where the Levene's test failed. This is an alternative test to ANOVA if the data are not normally distributed, but it has less possibilities for post-hoc testing. Both tests were run for differences between all species within each Stratum throughout the sequence respectively.

6.5 Results

Descriptive statistics for all species per Strata can be found in Table 6.3 (Excavation 1 Holocene), Table 6.4 (Excavation 1 Pleistocene) and Table 6.5 (Excavation 2 Stratum 2). Bivariate plots of the results can be found in Figure 6.1 (all results Excavation 1 Holocene), Figure 6.2 (all results Excavation 1 Pleistocene), Figure 6.3 (mean values per Strata) and Figure 6.4 (Boxplots per species per Stratum). $\delta^{13}C$ values of all samples range from 100% C_3 (minimum -14.1‰) diets to 100% C_4 diets (maximum 3.9‰). $\delta^{18}O$ values of all samples are expressed in SMOW and range from a minimum of 20‰ to a maximum of 41.4‰. In general, $\delta^{13}C$ and especially $\delta^{18}O$ values are higher in the Holocene compared to the Pleistocene Strata. Only mid-late Holocene Strata show a distribution of carbon isotope values that fall within the range expected from modern studies of the sample species (e.g. Gagnon and Chew 2000, Sponheimer et al. 2003, Codron et al. 2008).

	$\delta^{13}C$					$\delta^{18}O$			
Species	**mean**	**sd**	**min**	**max**	**n**	**mean**	**sd**	**min**	**max**
Stratum 1-2a									
Alcelaphini	-0.5	1.4	-1.9	0.9	2	31.8	2.2	29.6	34.0
Equus sp.	-6.3	0.8	-7.1	-5.4	2	31.0	0.6	30.5	31.6
H. africaeaustralis	-6.7	0.6	-7.4	-6.0	4	30.3	0.9	29.2	31.7
Stratum 2b									
Alcelaphini	1.7	0.3	1.5	2.0	2	32.0	0.4	31.5	32.4
A. marsupialis	-9.8	0.8	-10.7	-8.8	3	31.7	0.4	31.2	32.2
R. fulvorufula	1.1	1.2	-0.6	2.0	3	32.6	1.5	31.2	34.6
O. oreotragus	-11.7				1	35.0			
Tragelaphini	-8.6	1.1	-10.3	-7.2	5	32.4	1.5	30.6	35.0
Equus sp.	-0.8	0.8	-1.8	0.2	3	30.4	2.1	27.7	33.0
P. africanus	0.0				1	31.5			
Procavia capensis	-4.3				1	41.4			
Stratum 3a									
Alcelaphini	1.9	0.8	0.2	3.0	20	33.6	1.7	30.5	36.7
>A. buselaphus	2.2	0.6	1.4	3.0	9	33.0	1.4	30.5	35.3
>C. taurinus	1.2				1	31.6			

>*D. pygargus*	0.3				1	32.0			
A. marsupialis	-6.8	2.0	-9.0	-2.9	6	33.1	1.3	31.3	35.2
R. campestris	-12.8	1.3	-14.1	-11.4	2	35.4	0.4	35.0	35.8
R. fulvorufula	1.9	0.6	1.3	2.5	2	32.6	1.4	31.1	34.0
Tragelaphini	-9.8	1.0	-11.3	-8.1	9	32.9	2.5	28.1	36.5
>*T. strepsiceros*	-9.7	1.1	-11.3	-8.1	4	34.5	1.8	31.9	36.5
Equus sp.	-0.3	0.8	-2.1	0.9	9	31.7	1.2	29.9	33.6
H. africaeaustralis	-11.6	1.5	-13.0	-10.1	2	28.7	0.4	28.3	29.1
Stratum 3b									
Alcelaphini	1.7	1.6	-3.5	3.5	20	33.5	2.1	29.2	36.5
>*A. buselaphus*	2.0	0.6	1.1	2.8	8	33.2	2.5	29.2	36.1
>*Connochaetes* sp.	2.5	0.4	2.2	2.9	2	32.0	0.6	31.4	32.5
A. marsupialis	-9.8	1.0	-10.8	-8.9	2	32.7	1.8	30.9	34.5
R. campestris	-10.8	1.1	-12.8	-9.3	7	35.2	2.9	28.5	37.8
R. fulvorufula	2.1	0.8	1.1	3.1	4	33.2	1.3	31.6	35.1
Tragelaphini	-9.1	1.0	-10.7	-7.4	18	34.0	1.7	31.3	38.1
>*T. strepsiceros*	-9.3	1.0	-10.3	-8.0	4	35.4	1.8	33.1	38.1
Equus sp.	-1.6				1	33.7			
H. africaeaustralis	-11.4	0.7	-12.3	-10.3	4	28.7	1.9	25.7	30.8
P. capensis	-0.9				1	27.2			
Stratum 4a									
Alcelaphini	2.2	0.9	-1.2	3.7	36	33.5	2.4	29.7	39.2
>*A. buselaphus*	2.4	0.5	1.4	3.1	15	33.0	1.9	30.8	36.7
>*Connochaetes* sp.	2.3	0.9	0.6	3.7	7	33.6	1.0	32.0	35.0
A. marsupialis	-5.1	1.9	-7.0	-3.2	2	31.8	1.4	30.4	33.2
P. capreolus	-6.1	0.1	-6.2	-5.9	2	33.8	1.2	32.6	35.0
R. campestris	-9.3	0.9	-10.7	-7.9	10	34.4	1.8	31.1	37.0
R. fulvorufula	1.7	1.5	-1.6	2.9	6	34.6	2.4	31.3	37.9
Tragelaphini	-7.5	1.8	-9.6	-4.3	14	34.1	1.9	31.6	38.1
>*T. strepsiceros*	-7.8	1.5	-9.4	-4.3	10	34.0	1.6	31.6	37.6
Equus sp.	0.2	0.8	-0.9	0.9	3	33.0	1.3	31.7	34.7
P. africanus	1.0	0.5	0.4	1.9	5	33.0	2.4	30.5	37.2
H. africaeaustralis	-6.8	4.0	-11.5	-0.2	5	29.9	1.5	28.1	31.8
P. capensis	-0.5	0.6	-1.2	0.3	8	28.6	1.8	24.3	30.3
Stratum 4aLH									
Alcelaphini	2.3	1.0	0.0	3.3	8	34.3	2.2	31.0	38.3
>*A. buselaphus*	1.9	1.0	0.0	2.8	5	34.0	2.0	31.0	36.4
A. marsupialis	-7.0	0.1	-7.1	-6.9	2	31.0	0.4	30.6	31.4
P. capreolus	-11.9				1	35.2			

R. campestris	-11.4	0.4	-11.9	-11.0	3	36.1	4.2	32.9	42.0
R. fulvorufula	3.5				1	37.4			
Tragelaphini	-9.2	1.1	-10.0	-7.4	4	35.3	2.4	32.6	38.1
Equus sp.	2.9				1	37.1			
H. africaeaustralis	-9.4				1	31.5			
P. capensis	-0.1	0.0	-0.1	0.0	2	30.6	0.9	29.7	31.5
Stratum 4b									
Alcelaphini	1.5	2.0	-2.1	3.9	5	33.5	1.2	32.0	34.7
>A. buselaphus	0.8	2.1	-2.1	2.5	3	34.4	0.4	33.9	34.7
A. marsupialis	-7.7				1	35.0			
R. campestris	-9.1	1.0	-10.7	-7.6	8	34.5	2.9	31.7	39.5
Tragelaphini	-8.1	1.0	-9.5	-6.5	5	34.4	1.8	32.7	37.8
Equus sp.	0.5	0.6	-0.2	1.1	2	33.0	1.4	31.7	34.4
H. africaeaustralis	-0.8				1	29.1			
P. capensis	0.1	1.0	-1.5	1.4	5	29.3	1.3	27.7	30.7
Stratum 4c									
Alcelaphini	1.8	0.8	0.7	3.7	10	33.1	1.1	31.6	34.6
>A. buselaphus	2.3	1.4	0.8	3.7	2	33.3	1.3	32.1	34.6
>C. taurinus	1.9	0.1	1.8	2.0	3	33.5	1.3	31.6	34.4
A. bondi	-2.5				1	31.4			
R. campestris	-9.5	0.8	-10.7	-8.7	3	35.6	3.2	33.0	40.1
Tragelaphini	-9.0	0.9	-10.9	-7.8	17	35.6	1.9	31.6	39.6
>T. strepsiceros	-8.9	0.9	-10.5	-7.8	8	34.9	2.3	31.6	39.6
Equus sp.	0.7				1	33.0			
H. africaeaustralis	-8.0	1.7	-10.8	-6.1	4	29.7	1.0	28.9	31.4
P. capensis	-0.7	1.0	-2.3	0.6	6	29.0	1.1	27.5	30.5
Stratum 4d									
Alcelaphini	0.0	1.7	-1.4	2.7	4	33.8	1.0	32.6	35.3
Tragelaphini	-10.0	0.6	-10.5	-9.0	4	35.2	1.5	32.8	36.7
H. africaeaustralis	-9.2	1.5	-10.6	-6.9	4	29.4	1.6	27.1	31.4

Table 6.3: Descriptive statistics (mean values, standard deviation, minimum and maximum values) of enamel isotope results Excavation 1 Holocene. N is the number of samples per species.

	$\delta^{13}C$					$\delta^{18}O$			
Species	**mean**	**sd**	**min**	**max**	**n**	**mean**	**sd**	**min**	**max**
Stratum 5									
Alcelaphini	-1.3	4.5	-5.8	3.2	2	35.3	2.1	33.8	36.8
A. marsupialis	-8.9				1	32.6			
A. bondi	-1.6	1.8	-5.0	0.6	6	30.7	1.9	28.8	33.4
R. campestris	-10.0	1.0	-11.1	-8.8	3	34.4	2.5	30.8	36.4
Equus sp.	-1.6	1.0	-2.9	-0.4	3	31.2	0.9	29.9	32.0
H. africaeaustralis	-7.8	3.9	-11.8	-3.9	2	28.7	1.7	27.0	30.3
Stratum 6									
Alcelaphini	-7.2				1	29.1			
Antidorcas sp.	-12.0	0.4	-12.4	-11.6	2	36.1	0.4	35.8	36.5
P. capensis	-1.6	0.1	-1.6	-1.7	2	26.8	0.5	26.3	27.3
Stratum 7									
Alcelaphini	-2.9	4.2	-8.7	2.1	6	32.1	1.8	30.6	35.8
A. marsupialis	-8.7	1.7	-10.4	-7.0	2	30.9	2.6	28.3	33.6
A. bondi	-3.4				1	29.3			
Tragelaphini	-10.0				1	30.9			
E. quagga	-6.8				1	31.1			
H. africaeaustralis	-9.8				1	27.9			
P. capensis	-2.7				1	28.4			
Stratum 8									
Alcelaphini	0.6	0.0	0.6	0.6	2	29.0	1.0	28.0	30.0
Tragelaphini	-10.7				1	31.9			
Equus sp.	0.2				1	31.0			
H. africaeaustralis	-9.9	1.5	-11.4	-7.9	3	26.2	1.8	24.4	28.7
Stratum 9									
Tragelaphini	-6.2				1	27.1			
Equid*	-2.9	0.3	-3.2	-2.6	2	30.9	0.5	30.4	31.4
H. africaeaustralis	-10.4	0.5	-10.9	-9.9	2	25.0	0.4	24.6	25.4
Stratum 10									
Alcelaphini	-5.3	0.8	-6.1	-4.5	2	31.7	2.5	29.3	34.2
Antidorcas sp.	-9.3				1	29.6			
K. leche	-4.1	2.7	-6.8	-1.4	2	30.1	1.1	29.1	31.2
P. capreolus	-8.5				1	29.4			
R. fulvorufula	-12.6				1	33.5			
Tragelaphini	-9.1	1.7	-11.0	-6.1	6	30.1	0.7	28.9	30.9
Equid*	-6.1	2.2	-9.1	-3.0	5	30.0	1.9	27.6	32.0
H. africaeaustralis	-10.2				1	28.7			

Stratum 11									
Alcelaphini	-6.8	3.7	-10.3	-0.7	4	28.8	2.6	25.6	31.6
Tragelaphini	-10.6				1	30.5			
Equid*	-5.8	2.6	-8.1	-1.8	4	26.2	1.7	24.1	28.6
Stratum 12									
Alcelaphini	-7.2	2.3	-9.9	-2.5	8	30.6	3.0	26.1	36.0
Equid*	-5.7	2.6	-8.8	-0.9	10	28.2	2.8	22.7	32.5
H. africaeaustralis	-8.4	3.7	-12.0	-1.5	5	26.3	2.6	21.8	29.3
P. capensis	-7.4	3.0	-10.4	-4.4	2	25.7	4.1	21.7	29.8

Table 6.4: Descriptive statistics (mean values, standard deviation, minimum and maximum values) of enamel isotope results Excavation 1 Pleistocene. N is the number of samples per species. **Equus* sp. and possible *Hipparion* sp.

	$\delta^{13}C$					$\delta^{18}O$			
Species	**mean**	**sd**	**min**	**max**	**n**	**mean**	**sd**	**min**	**max**
Excavation 2 Stratum 2									
Alcelaphini	-1.2	1.8	-3.5	2.3	7	31.0	2.1	28.6	35.3
>C. taurinus	-2.0	1.5	-3.5	-0.5	2	29.6	1.0	28.6	30.6
A. marsupialis	-9.1	0.8	-9.9	-8.4	2	34.9	6.0	28.9	41.1
P. capreolus	-11.7	0.1	-11.8	-11.6	2	35.1	0.3	34.9	35.4
R. campestris	-13.0	0.0	-13.0	-13.0	2	31.2	2.4	28.8	33.7
K. leche	-3.7	3.7	-7.4	0.0	2	30.0	3.4	26.6	33.4
Tragelaphini	-10.7	0.9	-11.5	-9.5	3	33.3	0.9	32.0	34.2
C. simum	-7.8				1	20.0			
Equus sp.	-1.5	0.9	-2.6	-0.4	3	32.7	0.9	31.5	33.4
H. africaeaustralis	-9.4	1.2	-10.6	-8.2	2	26.9	3.2	23.6	30.1

Table 6.5: Descriptive statistics (mean values, standard deviation, minimum and maximum values) of enamel isotope results Excavation 2 Stratum 2. N is the number of samples per species.

Changes to species identification

Five samples were initially identified as bovids, and assigned a size-class. The isotope results make it possible to reconsider the species identification of those samples. Sample ME284 is a large-medium bovid from Stratum 4b. Its $\delta^{13}C$ value of -2.1‰ shows that is almost exclusively a grazer, possibly from the Alcelaphine tribe. It was excluded from

analysis as a possibly burnt sample. ME490 was identified as small-medium bovid in Stratum 3a. Its $\delta^{13}C$ value of 1.5‰ shows a specimen with an entirely C_4 diet. In this size range, it could belong to the Alcelaphini or Reduncini tribe. Samples ME208 and ME209 were both large-medium bovids from Stratum 4d. Their $\delta^{13}C$ values of -10.3‰ and -10.5‰ make it most likely that both are Tragelaphini. As there are only limited samples from Stratum 4d, they were included in the analysis as Tragelaphines. ME207 is a large-medium bovid from Stratum 4d. Its $\delta^{13}C$ value of -1.4‰ is in the grazer range, and Alcelaphini are the only large grazers in this assemblage. As we have only limited samples from 4d, it was included in the analysis as Alcelaphine.

Samples ME287, ME219 and ME222 were all identified as Alcelaphines. Although Alcelaphines show slightly more C_3 intake in the early Holocene in our analysis, the $\delta^{13}C$ values of these three individuals show values of a dominant C_3 to a full C_3 diet. We therefore challenge the identification and rename these samples 'bovid' to avoid confusion. In Excavation 2 Stratum 2, sample ME607 was identified as *Pelea* cf., but showed a $\delta^{13}C$ value of -2.0‰. As *Pelea* is normally a browser, this shows either extreme behaviour of one individual, or it is a similar sized grazer like *Redunca* or *Damaliscus* with a wrong identification due to fragmentation of the material. It was reclassified as a small-medium bovid and excluded. In Excavation 1 Stratum 9 sample ME641, identified as Alcelaphine, has a $\delta^{13}C$ value of -12.9‰, which is a 100% C_3 diet. Although the Alcelaphini show more mixed-feeding in the Pleistocene compared to the Holocene, this value is completely in the C_3 diet range and may indicate wrong identification. Therefore, it was renamed 'large bovid' but excluded from further analysis.

Samples excluded from further analysis

After measurement of the carbon and oxygen isotope values, the following samples were excluded from all further analysis (graphs, statistics, interpretation, comparisons) for the reasons outlined below. Sample ME682 (*Pedetes capensis,* Stratum 10). It only had 0.1mg of material to measure after pretreatment. Its standard deviations are high, and therefore it is possibly an unreliable measurement due to small sample size. Sample ME224 is a possible Alcelaphine from Stratum 4c with a $\delta^{13}C$ value of -11.0‰, much lower than the other Holocene Alcelaphine specimens. The tooth was described as burnt and a smell was noted while sampling. ME468 (*Redunca fulvorufula,* Stratum 3b) has a $\delta^{13}C$ value of -9.8‰, which is low for a *R. fulvorufula* in the Holocene. The tooth was described as possibly burnt and a smell was noted while sampling. ME257 is a *Taurotragus oryx,* marked as *cf* – it is therefore an uncertain identification - from Stratum 4c with an unusually high $\delta^{13}C$ value of -1.1‰. The sample was noted as having thin brittle enamel, possibly from burning, and was excluded as unreliable.

6.5.1. Bovidae

Alcelaphini

Within the Bovidae, Alcelaphines are the largest group represented in the Wonderwerk faunal remains, present in all analysed Strata, with clearly more samples in the Holocene (n=110) compared to the Pleistocene Strata (n=33). Due to the fragmentary nature of teeth in the Pleistocene of Excavation 1, those samples that could not be identified with certainty to species level and were grouped as *Alcelaphini*. This possibly includes the same species as occurring in the younger samples, i.e. the direct evolutionary predecessors of the Holocene species, as well as similar adapted but extinct species from this tribe, e.g. *Megalotragus priscus*.

In the Holocene samples of Excavation 1 and late Pleistocene Excavation 2, the hartebeest *Alcelaphus buselaphus* (Pallas 1766) is the most commonly identified Alcelaphine (n=42). Hartebeest formerly occurred widely over most of Africa and the Middle East. The red hartebeest is the subspecies represented in the Wonderwerk Cave area (Apps 2012). *Alcelaphus buselaphus* is more flexible in habitat than other Alcelaphini as long as the habitat is open; it can be found in moist or dry grasslands, savannas, shrubland and open woodlands. It accepts higher grass or more wooded areas than other Alcelaphini and fundamentally they are highly mobile animals (Kingdon 1982, Skinner and Chimimba 2005). The hartebeest is a grazer with a coarse grass diet; accounts of the seasonal intake of browse range from 5-40% (Gagnon and Chew 2000). Studies on modern specimens gave $\delta^{13}C$ values between 1‰ and 2‰ (Sponheimer et al. 2003). Although arid adapted in its metabolism, it can only remain a limited time without drinking surface water (Skinner and Chimimba 2005).

Connochaetes species were identified from Excavation 2 (n=2) and the Holocene Strata (n=14) of Excavation 1. There are several possible explanations why they are not present in the earlier Strata. The fragmented nature of the samples could mean their remains were placed in the general Alcelaphini category. Another explanation is that at times, Wonderwerk Cave was not a suitable habitat for this specialised grazer. Most of the identified enamel samples belong to *Connochaetes taurinus* (Burchell 1823), the Blue Wildebeest. Three samples are identified as possibly belonging to *Connochaetes gnou* (Zimmermann 1780), the black wildebeest, a species endemic to South Africa. Today the range of the two wildebeest species is separate, with the black wildebeest inhabiting the grasslands of South Africa's interior and the blue wildebeest the northerly areas of southern Africa. The species may however have overlapped in the past (Brink 2005). Wildebeest occur in open grasslands, plains and dry shrub- and woodland. *Connochaetes* sp. are

predominantly grazers preferring short growth (Gagnon and Chew 2000, Apps 2012). This is reflected in $\delta^{13}C$ values of modern wildebeest in southern Africa of 0‰ to 4‰ (Codron et al. 2008). They are water dependent, and need to drink especially in the dry season at least every second day (Kingdon 1977). Wildebeest are known from Eastern Africa for their long migrations in large herds. With modern fences restricting habitats, it is impossible to estimate how far southern African wildebeest would have migrated.

The third Alcelaphine species is *Damaliscus* (n=9). Considering the location of Wonderwerk, the samples most likely belong to *Damaliscus pygargus* (Pallas 1767), commonly known as the blesbok. It disappeared from this area sometime in the mid-Holocene, but was widespread in the neighbouring grassland highveld and the northern Karoo (Apps 2012). The youngest certain identification of *D. pygargus* is from Stratum 4c (n=1). The species lives in open grass- and shrublands. Today, they are predominantly grazers on short to medium tall grass and are dependent on water (Gagnon and Chew 2000, Apps 2012). Carbon isotope values are expected to be in the range of -2‰ to 4‰ (Sponheimer et al. 2003, Codron et al. 2008). Another possible *Damaliscus* species in the Wonderwerk assemblage could be the Tsessebe, *Damaliscus lunatus* (Burchell 1823). The Tsessebe is an exclusive grazer, whose diet can include medium-taller grass but prefers burnt areas and needs shelter in its habitat (Apps 2012).

Alcelaphini molars and premolars were sampled from the Wonderwerk assemblage. The $\delta^{13}C$ values show that the Alcelaphini diet in the Holocene is, as expected, almost entirely made up of C_4 plants. Alcelaphini have mean $\delta^{13}C$ values between -0.5‰ and 2.3‰ in the Holocene Strata with the lowest individual value being -3.5‰ and the highest individual value being 3.9‰. As a trend, the $\delta^{13}C$ are lower in Strata 4d to 4b (means 0.0‰ to 1.8‰) compared to the mid-late Holocene (Strata 2b to 4LH; means 1.7‰ to 2.3‰). In Excavation 1 Strata 5-8, the $\delta^{13}C$ mean values are between -7.2‰ and 0.6‰, which is in general lower

than in the Holocene Strata. Individual values range from -8.7‰ to 3.2‰. In contrast, Strata 10 to 12 have means between -7.2‰ and -5.3‰, with individual values ranging between the extremes of pure C_3 (-10.3‰) and pure C_4 (-0.7‰) diet. In Excavation 2 Stratum 2, the Alcelaphini have a mean of -1.2‰, and the two *C. taurinus* specimen a mean of -2.0‰.

The mean $\delta^{18}O$ values in the Holocene range from 31.8‰ to 34.3‰, with the lowest individual value being 29.2‰, and the highest individual value being 39.2‰, therefore showing a range over 10‰. The highest oxygen isotope values are in the mid-Holocene. Stratum 2 Excavation 2 has lower $\delta^{13}C$ and $\delta^{18}O$ values than the Holocene samples, with the $\delta^{18}O$ mean values of 31.0‰ and 29.6‰ respectively. There are no large differences within Pleistocene Strata mean $\delta^{18}O$ values, with Strata 5-8 $\delta^{18}O$ means are 29.1‰ to 32.1‰ and Strata 10-12 29.8‰ to 31.7‰. The lowest individual value in the Pleistocene of Excavation 1 is 25.6‰ and the highest individual value is 36.8‰.

In Strata with enough individual *Alcelaphus buselaphus* samples in the Holocene, the $\delta^{13}C$ means range from 0.8‰ to 2.4‰ and the $\delta^{18}O$ means from 33.0‰ to 34.4‰. *Connochaetes taurinus* and *Connochaetes gnou* specimen have a tighter range of values. Their $\delta^{13}C$ means range between 1.2‰ and 2.5‰ and are never below 0‰; the $\delta^{18}O$ means range from 31.6‰ to 33.6‰, but this low range might be influenced by the low number of wildebeest samples. Wildebeest are pure grazers and their tight $\delta^{13}C$ range reflects little dietary flexibility. There is no statistical difference in $\delta^{18}O$ between *Alcelaphus buselaphus, Damaliscus* sp. and *Connochaetes* sp. throughout the sequence (Appendix 6.2). Statistical differences in Alcelaphini between all Strata are large (p-value $4.017e^{-08}$, Kruskal-Wallis test), driven by Pleistocene-Holocene differences. Between the tribes the difference is also significant, with *Connochaetes* sp. having higher $\delta^{13}C$ values than the other Alcelaphini in the Holocene (p-value 0.004, Kruskal-Wallis test). **Summary:** All species of Alcelaphini have a diet composed of C_4 grasses in the Holocene, whereas some specimens in the early Pleistocene

show a mixed-diet $\delta^{13}C$ value. $\delta^{18}O$ values are in agreement with that for large ungulates that regularly drink, with the highest values in the mid-Holocene.

Tragelaphini

Both Tragelaphini species of southern Africa, kudu *Tragelaphus strepsiceros* (Pallas 1766) and eland *Taurotragus oryx* (Pallas 1766) are present in the Pleistocene (n=13) and Holocene Strata (n=52) in Wonderwerk. The kudu (n=41) is more numerous than the eland (n=9) which is often identified based on its larger size. Some authors include the eland in Tragelaphus as *Tragelaphus oryx*, while others keep the separate genera names. Modern genetic studies confirm the inclusion of *Taurotragus* in the *Tragelaphus* tribe (Skinner and Chimiba 2005). Both can be used synonymously. I follow the previous papers on mammal assemblages from Wonderwerk Cave, and use the traditional division. Tooth fragments that could not be identified to species level were grouped as Tragelaphini. They range over most of East and Southern Africa in arid grasslands, shrub- and woodlands (Apps 2012, IUCN SSC Antelope Specialist Group 2008a). Especially the kudu needs some vegetation cover. Small differences have been reported in preferred browse, where the kudu concentrates on higher quality forage, and the eland is more generalist, including some grass and dry forage in its diet (Gagnon and Chew 2000). This is evident in modern published $\delta^{13}C$ values of around -13‰ for kudu and lower values of -8‰ to -11‰ for eland (Sponheimer et al. 2003, Codron et al. 2008).

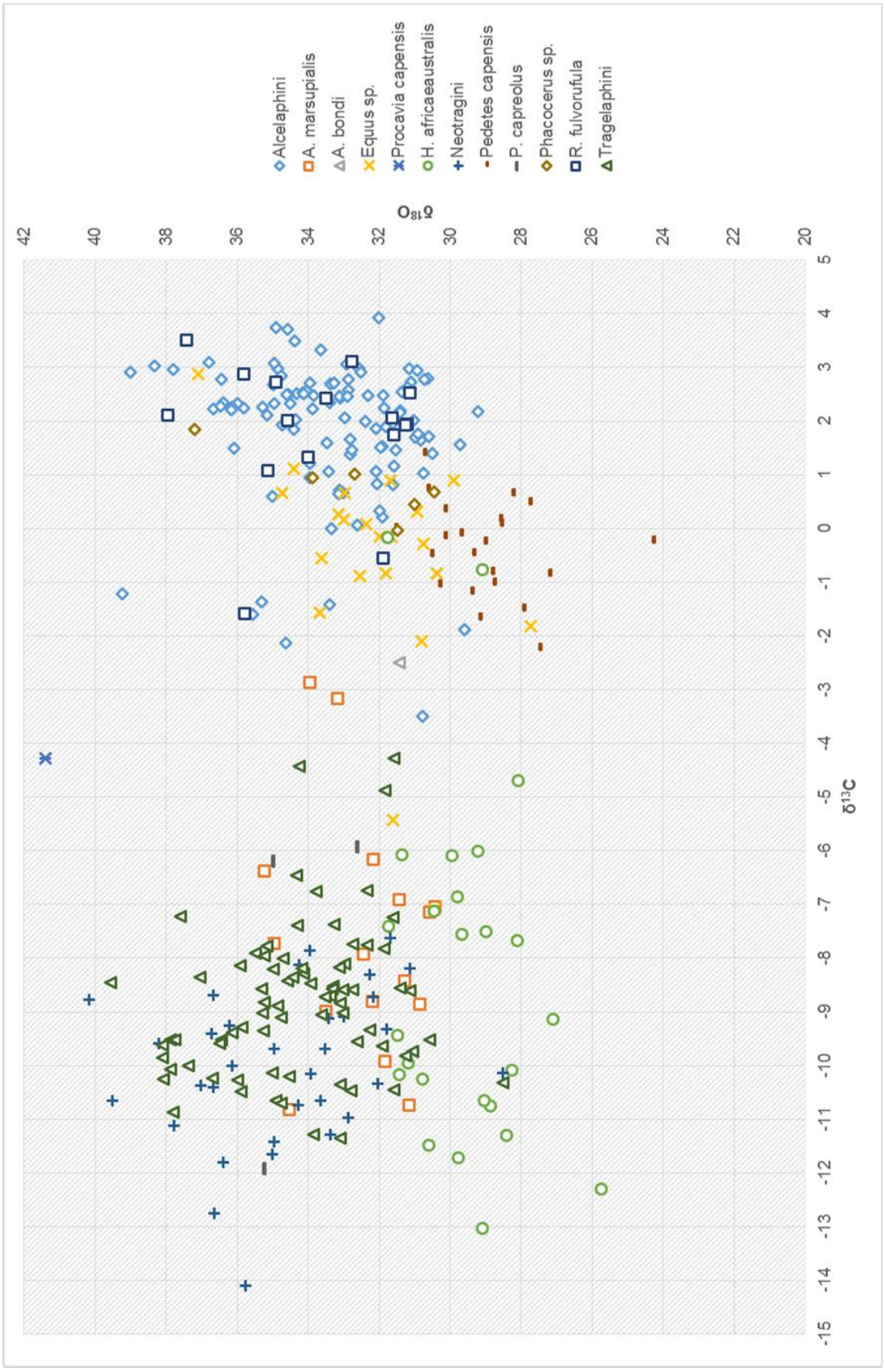

Figure 6.1: Bivariate plot of all results in Excavation 1 Holocene (Strata 1 to 4d).

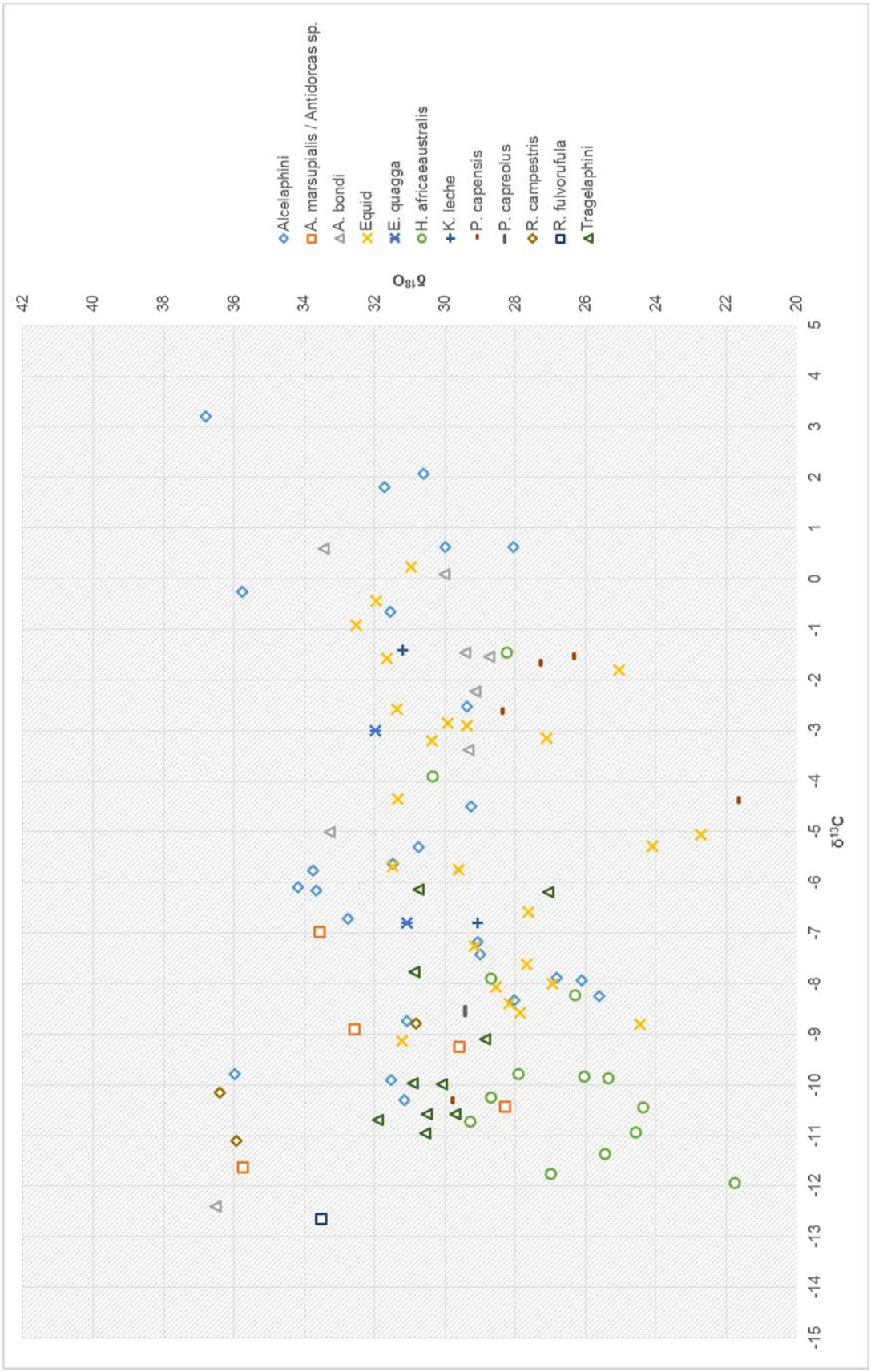

Figure 6.2: Bivariate plot of all results in Excavation 1 Pleistocene (Strata 5 to 12).

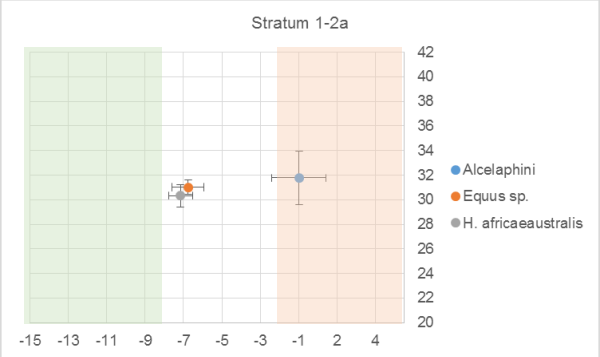
Stratum 1-2a
Alcelaphini
Equus sp.
H. africaeaustralis

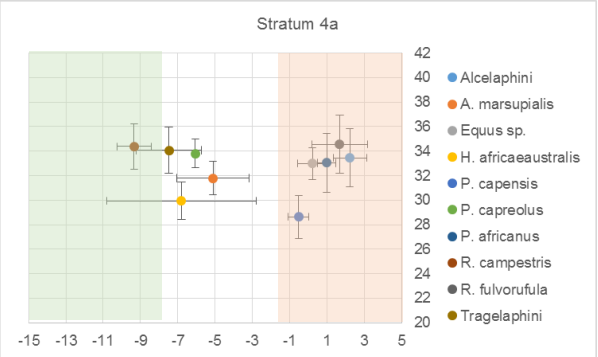
Stratum 4a
Alcelaphini
A. marsupialis
Equus sp.
H. africaeaustralis
P. capensis
P. capreolus
P. africanus
R. campestris
R. fulvorufula
Tragelaphini

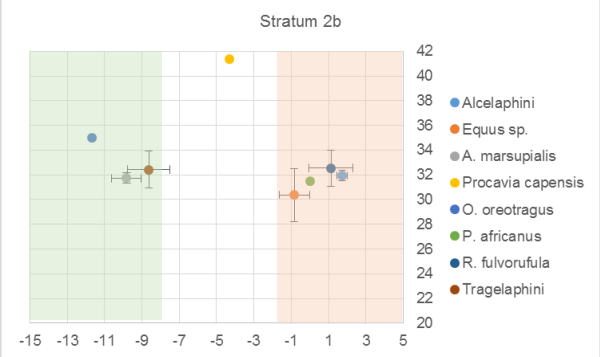
Stratum 2b
Alcelaphini
Equus sp.
A. marsupialis
Procavia capensis
O. oreotragus
P. africanus
R. fulvorufula
Tragelaphini

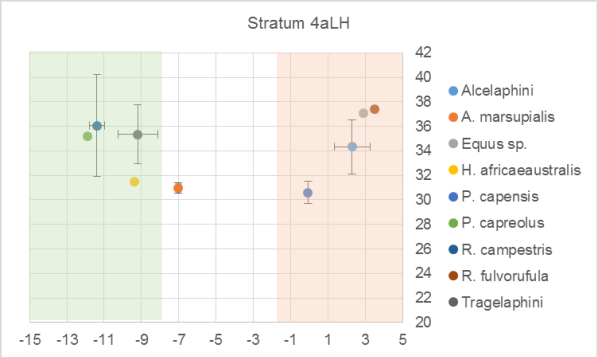
Stratum 4aLH
Alcelaphini
A. marsupialis
Equus sp.
H. africaeaustralis
P. capensis
P. capreolus
R. campestris
R. fulvorufula
Tragelaphini

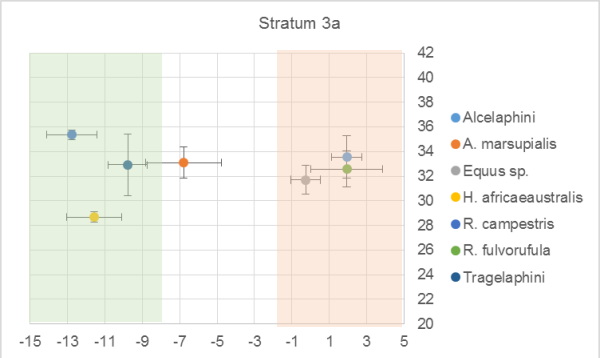
Stratum 3a
Alcelaphini
A. marsupialis
Equus sp.
H. africaeaustralis
R. campestris
R. fulvorufula
Tragelaphini

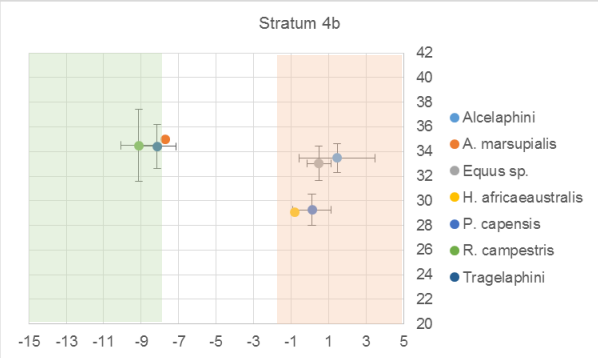
Stratum 4b
Alcelaphini
A. marsupialis
Equus sp.
H. africaeaustralis
P. capensis
R. campestris
Tragelaphini

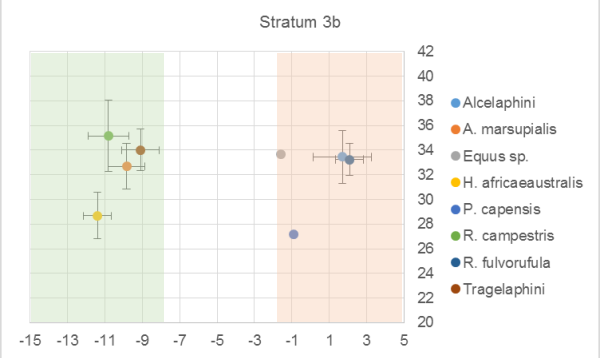
Stratum 3b
Alcelaphini
A. marsupialis
Equus sp.
H. africaeaustralis
P. capensis
R. campestris
R. fulvorufula
Tragelaphini

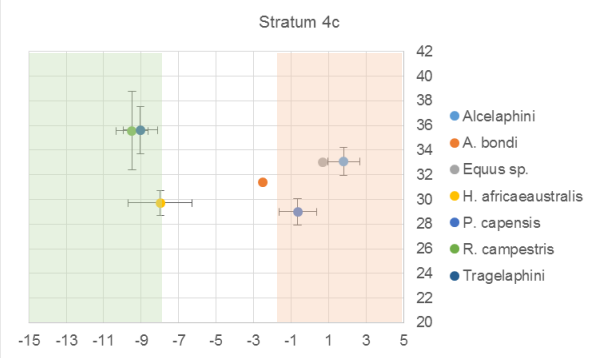
Stratum 4c
Alcelaphini
A. bondi
Equus sp.
H. africaeaustralis
P. capensis
R. campestris
Tragelaphini

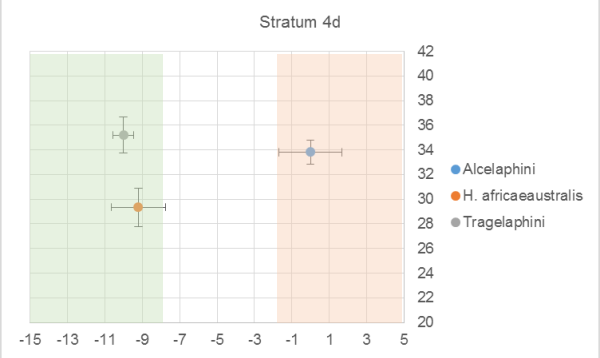
Stratum 4d
Alcelaphini
H. africaeaustralis
Tragelaphini

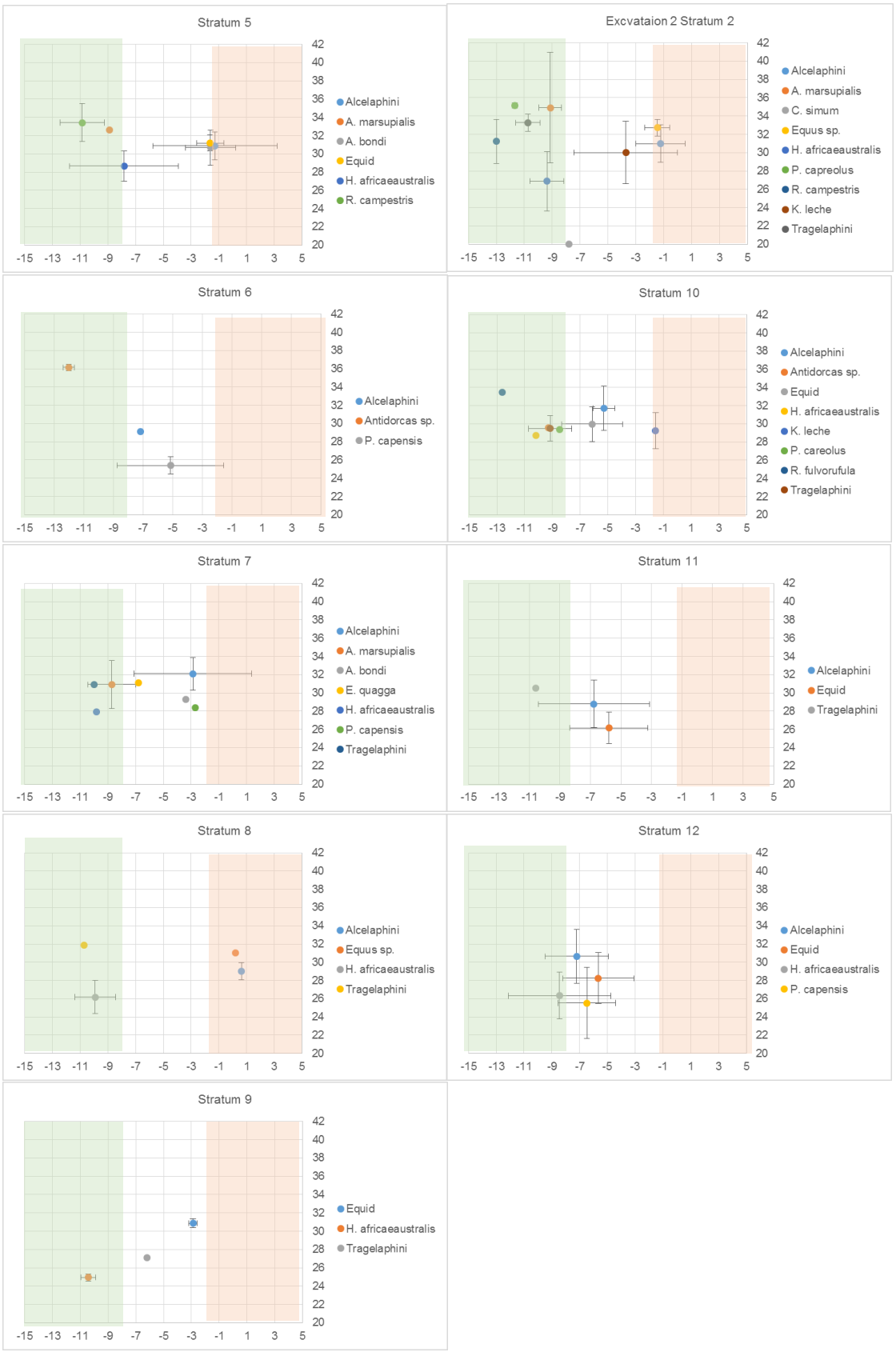

Figure 6.3: Bivariate plots of mean value of all species per stratum. $\delta^{13}C$ values are on the x-axis, $\delta^{18}O$ values on the y-axis. Error bars show the standard derivations. Green shaded

areas indicate >70% C_3 plant consumption, red shaded areas indicate >70% C_4 plant contribution.

There is no statistically significant difference in the Wonderwerk results in $\delta^{13}C$ or $\delta^{18}O$ values between *Tragelaphus strepsiceros* and *Taurotragus oryx* (Appendix 6.2). The differences between these species in eating habits as described above do not show up isotopically. Both species are therefore pooled as Tragelaphini in the following analysis and discussion. The Tragelaphini show $\delta^{13}C$ values of a pure C_3 diet with a small C_4 intake for individual specimens. In the Holocene, mean $\delta^{13}C$ values are -10.0‰ to -7.5‰, (range 2.5‰). The individual values span a larger range, with the lowest individual value of -11.3‰ and the highest individual value of -4.3‰. Standard derivations are low and between 0.6‰ and 1.1‰ per stratum. The values in the Pleistocene Strata are similar, with means of -10.7‰ to -6.2‰ and individual values spanning from -11.5‰ to -6.2‰. Only Stratum 10 and Excavation 2 Stratum 2 have more than one sample per Stratum in the Pleistocene, which limits the possibility of assessing variability between the tribes.

Both species are diurnal, browsers, and independent of water if enough green forage is available (Kingdon 1982, Skinner and Chimiba 2005). As a trend, Holocene $\delta^{18}O$ values are generally higher than Pleistocene ones. The Holocene means are between 32.4‰ and 35.6‰, with individual values in a wide range of over 11‰ spanning from the lowest (28.1‰) to the highest (39.6‰) value. In the Pleistocene (including Excavation 2), mean $\delta^{18}O$ values are between 27.1‰ and 33.3‰, with individual values ranging from 27.1‰ to 34.2‰. **Summary:** The Tragelaphini species are flexible browsers, with varying small amounts of C_4 in their diet. As a general trend, $\delta^{18}O$ values are lower in the Pleistocene compared to the Holocene.

Antilopini

Springbok species are known in southern Africa since the Pliocene, including the extinct *Antidorcas recki*, *Antidorcas australis* and *Antidorcas bondi*. The extant springbok *Antidorcas marsupialis marsupialis* (Zimmermann 1780) is represented in the Holocene and Pleistocene levels of Wonderwerk. Two samples from Stratum 10 and 7 could not be identified to species but only to genus (*Antidorcas* sp.). *A. marsupialis* lives in arid scrub and grassland and are recorded in historical records as having migrated in large herds (Skinner and Chimiba 2005, Apps 2012). Springbok are mixed-feeders, ingesting more graze in summer and more browse in winter (Gagnon and Chew 2000, Apps 2012). In Wonderwerk, *A. marsupialis* has $\delta^{13}C$ values between a pure C_3 diet and mixed-feeding throughout the sequence. The means range in the Holocene from -9.8‰ to -6.8‰ and in the Pleistocene from -12.0‰ to -8.7‰. Individual $\delta^{13}C$ values range in the Holocene from -10.8‰ to -2.9‰ and in the Pleistocene from -12.4‰ to -7.0‰. Springbok are highly arid adapted and independent of water (Skinner and Chimiba 2005). Mean Holocene oxygen values range from 31.7‰ to 35.0‰, with individual values ranging from 30.4‰ to 35.2‰. Pleistocene oxygen values are highly variable, with means from 29.6‰ to 36.1‰ and individual values of 28.3‰ to 41.1‰.

The other springbok species present is *Antidorcas bondi* (n=9). Only one example is from the Holocene, Stratum 4c (6.7-9.3 cal BP, Chapter 4). *A. bondi* was thought to have become extinct about 7000 years ago. It fed on newly grown shoots as a specialized grazer (Brink and Lee-Thorp 1992). Therefore, following previous studies, *A. marsupialis* and *A. bondi* are expected to have distinct carbon isotope values of -4‰ to -12‰ and -2‰ respectively (Brink and Lee-Thorp 1992, Sponheimer et al. 2003, Codron et al. 2008). Indeed, there are isotopic differences in $\delta^{13}C$ between the antelope species *A. marsupialis* and *A. bondi* (Fig. 7.8) in Wonderwerk. This is confirmed by statistical tests (p-value of $5.78e^{-05}$, ANOVA test

with Tukey-HD post-hoc testing). There are no statistically meaningful differences in oxygen between these two species. The one Holocene *A. bondi* has values of $\delta^{13}C$ -2.5‰ and $\delta^{18}O$ 31.4‰. This fits with the Pleistocene *A. bondi* mean values of $\delta^{13}C$ -1.6‰ to -3.4‰ and $\delta^{18}O$ 29.3‰ to 30.7‰. Individual carbon values are -5.0‰ to 0.6‰, a significant enrichment compared to *A. marsupialis*. In Stratum 6 are two samples, one was identified as a probable *A. marsupialis* and one as *A. bondi*, but as both show C_3 dietary $\delta^{13}C$ values, both could be *A. marsupialis*.

Antidorcas marsupialis hofmeyri is a subspecies living today in Namibia and Botswana and is commonly called the Kalahari springbok (IUCN SSC Antelope Specialist Group 2008b). Three teeth from the Holocene Strata 3b, 4a and 4b showed characteristic morphological features and larger size of *A. m. hofmeyri*, suggesting that they could belong to this subspecies, but there was not enough material to be certain of this identification. The three samples show no difference isotopically to *A. marsupialis*. Though it is possible that both subspecies had no dietary and/or isotopic differences, it is also possible that the quantity of samples analysed was too small. **Summary:** *Antidorcas marsupialis* is a browser to mixed feeder throughout the sequence, clearly distinct from the extinct grazer *Antidorcas bondi*. The $\delta^{18}O$ values of both species are variable but comparable.

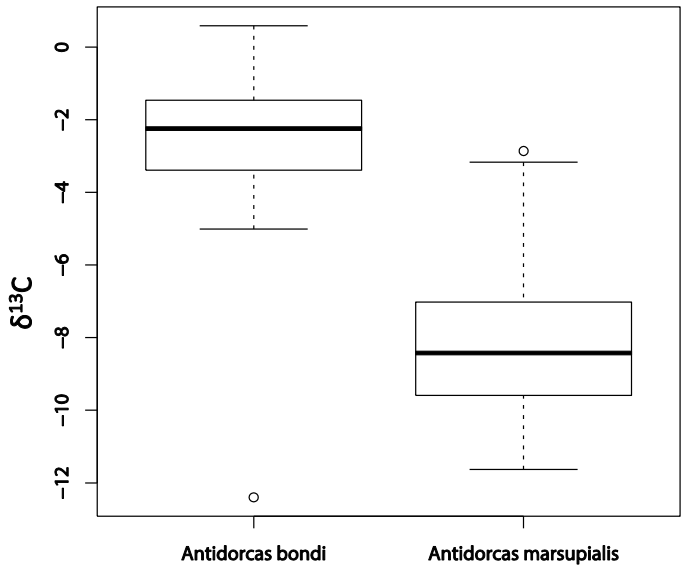

Figure 6.4: Box and whisker diagram of *A. bondi* and *A. marsupialis* (of all Strata), showing *A. bondi* has higher carbon isotope values compared to *A. marsupialis*. The difference is statistically significant (Appendix 6.2).

Neotragini

Raphicerus campestris

The steenbok, *Raphicerus campestris* (Thunberg 1811) is present throughout the Late Pleistocene (n=3) and Holocene (n=34) of Excavation 1 as well as Excavation 2, Stratum 2 (n=2). It is present in both East and South Africa today, although as two geographically unconnected populations (IUCN SSC Antelope Specialist Group 2008c). The steenbok is widespread in different biomes and occupies grasslands, savannahs, semi-desert, open woodland and shrublands. It does not like rocky areas but needs cover possibilities (IUCN SSC Antelope Specialist Group 2008c). Although classified as an intermediate grazer-browser by Gagnon and Chew (2000), it has been proven in other studies (e.g. Du Toit 1993) that *Raphicerus campestris* is predominantly a browser: it feeds on high-quality tubers, roots, leaves, flowers, pods and berries located near ground level and is largely water independent. $\delta^{13}C$ values of -9‰ to -12‰ and high $\delta^{18}O$ values, compared to regular drinkers are expected from studies of modern specimen (Sponheimer et al. 2003, Codron

et al. 2008). The $\delta^{13}C$ values reveal a pure C_3 diet throughout the sequence, with means range from -12.8‰ to -9.1‰. Individual values range from a minimum of -14.1‰, which is also the lowest carbon value of the whole study, to a maximum individual value of -7.6‰. In the Pleistocene, there are only samples from Stratum 5 and Excavation 2 Stratum 2. Means are -13.0‰ to -10.0‰, with individual values ranging -13‰ to -8.8‰, showing a narrower range than in the Holocene, but perhaps influenced by sample size. *R. campestris* is quite variable in its range of oxygen values. The means are close together (34.4‰ to 36.1‰) in the Holocene, but the individual values range from 28.5‰ to 40.1‰. In the Pleistocene, means are 31.2‰ to 34.4‰, lower than in the Holocene but also close together. The individual values on the other hand span 28.8‰ to 36.4‰, and there are large standard derivations (up to 3.2‰) per stratum. **Summary:** In the Wonderwerk assemblage, *Raphicerus campestris* has the lowest $\delta^{13}C$ and highest $\delta^{18}O$ values of any species, agreeing with a specialised, water-independent browser.

Oreotragus oreotragus

There is only one identified tooth of klipspringer (left M_1), *Oreotragus oreotragus* (Zimmermann 1783) in this study, from Stratum 2b. Wonderwerk Cave is a suitable habitat for the klipspringer, which needs rocky terrain and ground cover, but comes out into the open dry grassland, savannah or woodland to feed (Kingdon 1982, Hilton-Barber and Berger 2004). It is a generalist browser with a diet of large amounts of berries, fruit and flowers. Independent of water, it will drink if water is available (Kindgon 1977, Gagnon and Chew 2000, Apps 2012). Stable isotope values are expected to be similar to *R. campestris* due to a similar diet and physiology. The sample from Stratum 2b has values of $\delta^{13}C$ -11.7‰ and $\delta^{18}O$ 35.0‰. The animal therefore falls, as expected, well within the browser and pure C_3 dietary range. The $\delta^{18}O$ value of this specimen is the most positive in this stratum, except for the Hyrax (see below). This might reflect its habitat on higher, well-

drained slopes and hills and a diet of plant leaves which are subject to high evapotranspiration. **Summary:** *Oreotragus oreotragus* consumed a C_3 diet, and expresses a high $\delta^{18}O$ value for a bovid in the Wonderwerk assemblage, but the sample size is too small to explore intra-species variability.

Reduncini

Redunca fulvorufula

Redunca fulvorufula fulvorufula (Afzelius 1815), the southern subspecies of the mountain reedbuck, is present in the Holocene of Excavation 1 (n=17, from Stratum 4aLH upwards) and in Pleistocene Stratum 10 (n=1). As expressed in its English name, its preferred habitat is hills, ridges and rocky terrain. It needs bush or tree cover in dry grass- and shrublands, and is dependent on water (Kingdon 1982, IUCN Red List 2014). *R. fulvorufula* are obligate grazers and $\delta^{13}C$ values are therefore expected to be in the range of 1‰ to 2‰ (Gagnon and Chew 2000, Sponheimer et al. 2003). The Holocene $\delta^{13}C$ means range like expected between 1.1‰ and 2.1‰, and individual values range from -1.6‰ to 3.5‰. This shows a pure C_4 diet and reflects the high grazing specialisation of these animals. The Holocene $\delta^{18}O$ mean values are from 32.6‰ to 34.6‰, with individual values showing a range from 31.1‰ up to 37.9‰. The one Pleistocene sample from Stratum 10 has a carbon value of -12.6‰. Because of lack of more samples, it is impossible to say if this is an error in identification (the value would fit well with the similar sized *R. campestris*) or if *R. fulvorufula* changed its diet during the Pleistocene. The $\delta^{18}O$ value of 33.5‰ is high for the Pleistocene compared with other Pleistocene bovids. **Summary:** *Redunca fulvorufula* is a specialised grazer in the mid-late Holocene of Wonderwerk Cave. It is not possible from this study to infer the Pleistocene diet of this species.

Kobus leche

The lechwe, *Kobus leche* (Gray 1850) would not be able to survive in the Wonderwerk area today as it only occurs in the wetlands of Botswana, Namibia, Angola, Zambia and Congo today (IUCN SSC Antelope Specialist Group 2008e). It was, however, present in the past, represented by two teeth in Excavation 1 Stratum 10 (M_2 and $M_{2/3}$) and two teeth in Excavation 2, Stratum 2 (M^1 and P^4). Its foremost habitat requirement is standing bodies of water. Lechwe are predominantly grazers, feeding on grasses and sedges on floodplains (Gagnon and Chew 2000, Aps 2012), resulting in mixed-feeding values in modern stable isotope studies (Sponheimer et al. 2003, Codron et al. 2008). The results for the four *K. leche* specimens show mean values similar to each other with high variation in individual values. The means in carbon are -4.1‰ and -3.7‰ respectively (individual values range -7.4‰ to 0.0‰) and in oxygen 30.1‰ and 30.0‰ (individual values range 26.6‰ to 33.4‰). **Summary:** The Pleistocene *K. leche* from Wonderwerk Cave has a mixed diet of C_3 and C_4 plants, much like modern specimens.

Pelea capreolus

Skinner and Chimimba (2005) include the grey rhebuck *Pelea capreolus* (Forster 1790) in the Reduncini, according to morphological (Vrba et al. 1994, Vrba and Schaller 2000) and mtDNA data research (Gatesy et al. 1997, Matthee and Robinson 1999). This thesis follows this classification. *Pelea capreolus* is a small bovid endemic to southern Africa. It inhabits hills, slopes, mountains and grassland plateaus and browses on forbs and broad-leaf plants (Kingdon 1982, Gagnon and Chew 2000). The small sample of *P. capreolus* (n=7) reveals in two Strata a pure C_3 diet (Pleistocene Excavation 2 Stratum 2 and Holocene Stratum 4aLH) and in the two other Strata a more mixed diet (Holocene Stratum 4a and Pleistocene Stratum 10), with $\delta^{13}C$ mean values range from -6.1‰ to -11.9‰. It obtains enough water through its food to be water independent (Kingdon 1982). $\delta^{18}O$ mean values range from

29.4‰ to 35.2‰. **Summary:** *P. capreolus* has a flexible browser diet, with $\delta^{18}O$ values similar to the other small browsers *R. campestris* and *O. oreotragus*.

6.5.2. Perissodactyla

Two families of Perissodactyla are present in the Wonderwerk dental assemblage, Equidae and Rhinocerotidae.

Equidae

Equids are numerous in the Wonderwerk faunal assemblage, with more Equid teeth in the Pleistocene (n=29) than the Holocene Strata (n=22). The *Equus* line is supposed to be present in South Africa from 1.8 Ma onwards till the present day. In the early Pleistocene Strata of Excavation 1 (Strata 9 to 12), the Equid species could be three-toed *Hipparion* or the single-toed *Equus* sp. *Hipparion* has a long evolutionary history from the Miocene till its extinction around 0.78 Ma (Kingdon 1979). The last record of *Hipparion* in southern Africa comes from a level dated to ~1Ma at the site of Cornelia-Uitzoek (Brink et al. 2012). There is only one tentatively identified *Hipparion* tooth in Stratum 11. As it is extinct, the diet and habitat preferences of *Hipparion* are unknown, but it is assumed to have been similar to today's Equids; it was a water dependent grazer living on grassy plains and steppes (Hilton-Barber and Berger 2004). The term Equid is used here for the lower Pleistocene Strata to include the possibility of both *Hipparion* and *Equus* remains.

Of the genus *Equus*, the species could be *Equus capensis*, *Equus quagga quagga* or *Equus quagga burchelli*. The latter two co-existed over the same time span from around 1.8 Ma until modern times and are genetically more recent developed subspecies of the plains zebra (Leonard et al. 2005, Lorenzen et al. 2008). Wonderwerk is situated near the southern limit of *Equus quagga burchelli* and near the northern limit of *Equus quagga quagga* in classical distribution maps. A morphometric study on teeth from museum specimen by Thackeray

(1984) found no difference. Modern DNA work, including Equid teeth from Wonderwerk Cave (Orlando at al. 2009), showed indistinguishable mtDNA. The quagga went extinct in the wild in 1878. It was a grazer adapted to the grasslands and shrubland of the interior of South Africa. There are two certainly identified *E. quagga quagga* samples in Strata 7 and 10. All other samples are *E. quagga quagga/burchelli*. Following the international rules of zoological nomenclature, *E. quagga* has precedence. It can live in a range of habitats of savannah, woodland and scrubland and is a selective grazer, with occasionally eating herbs, twigs, leaves, shrubs and fruit (Apps 2012). Stable isotope values of modern zebra are in the range of 0‰ to 2‰ (Codron et al. 2008).

The two *Equus* sp. in the Holocene Stratum 1 have lower $\delta^{13}C$ values than the other Holocene *Equus* sp. samples, a mixed-feeding signal with a mean of -6.3‰. As this is the disturbed level from when the cave was inhabited last century there are several possible explanations for this signal. These specimens were not complete enough to be identified to species, and could be domestic horses that were fed by humans, being brought in from another environment, or reflecting changing ^{13}C in the atmosphere in the last centuries. These values should therefore not be taken as representing a wild modern zebra population. Without the values for Strata 1+2a, Holocene $\delta^{13}C$ mean *Equus* values range from -1.6‰ to 0.7‰ (individual values range from -2.1‰ to 1.1‰), a clear C_4 diet signal. In the early Pleistocene Strata, the one probable *Hipparion* tooth from Stratum 11 has values of $\delta^{13}C$ -1.8‰ and $\delta^{18}O$ 25.5‰. This is higher in $\delta^{13}C$ than the other Equid samples in this level, and similar to Holocene values. Two *E. quagga* samples (Stratum 7 and 10) have values of $\delta^{13}C$ -3.0‰ and -6.8‰, and $\delta^{18}O$ 31.1‰ and 33.0‰. There is no other Equid for comparison in Stratum 7 while in Stratum 10 the specimen is higher in carbon compared to the other Equid samples from this Stratum. There is not enough positively identified material to test if different Equid species had different diets during the Pleistocene.

Statistically, the $\delta^{13}C$ values of the Strata 10-12 Equids are significantly dissimilar to those of other Equids, especially compared to the mid-late Holocene. In Strata 5-9, and including Excavation 2 Stratum 2, mean $\delta^{13}C$ values are -2.9‰ to 0.2‰ (individual values -3.2‰ to -0.4‰), showing a C_4 dominated diet, only slightly lower than the Holocene Strata. The $\delta^{13}C$ values for Strata 10 to 12 are characteristic mixed-feeders: $\delta^{13}C$ means of between -5.7‰ and -6.1‰ (individual values spanning -9.1‰ to -0.9‰).

Equids are highly mobile, but as an obligate drinker depend on daily access to water. The Holocene $\delta^{18}O$ mean values range from 30.4‰ to 33.7‰, with not too much variability, and individual values from 27.7‰ to 34.7‰. This is in the range of other large grazers, but slightly lower than some of the water-independent browsers, e.g. *Raphicerus campestris*. The only exception is Stratum 4aLH, with higher $\delta^{13}C$ of 2.9‰ and $\delta^{18}O$ of 37.1‰ compared to the other Strata. The Pleistocene $\delta^{18}O$ mean values (30.9‰ to 32.7‰, individual values 25.9‰ to 33.4‰) are similar to the Holocene ones. The $\delta^{18}O$ means range from 26.2‰ to 30.0‰. **Summary:** Equids were feeding on C_4 grasses in the Holocene, but have variable mixed-feeding values in the Pleistocene before 0.78Ma. The $\delta^{18}O$ values show no significant difference in the mean values between Pleistocene and Holocene, and reflect a regular drinker.

Rhinocerotidae

Ceratotherium simum (Burchell 1817), the white rhinoceros, is represented by a single third premolar from Excavation 2 Stratum 2. *C. simum* is found in open flat grassland and savannah with short grass, where it takes up to 99% unselective graze (Apps 2012), which should in theory be reflected in a carbon isotope value above 0‰. In contrast, the $\delta^{13}C$ result for this tooth is -7.8‰, the signal of a mixed-feeder. *C. simum* is dependent on water for drinking and to wallow in to cool down, and is therefore never found too far from

standing water (Kingdon 1979). The analysed $\delta^{18}O$ value is the lowest in the whole dataset of Excavation 1 and 2 with a value of 20.0‰. This possibly represents its dependency on daily drinking water, but might not completely explain the low value. **Summary:** *Ceratotherium simum* in Excavation 2 Stratum 2 was taking in more C_3 browse than is expected from modern observations of its feeding patterns. The sample size is too small to explore the reason behind its low $\delta^{18}O$ value.

6.5.3 Rodentia

Hystrix africaeaustralis

The Cape porcupine *Hystrix africaeaustralis* (Peters 1852) was sampled throughout the entire analysed sequence. The species is widespread in Africa south of the Sahara, which is reflected in their wide range of suitable habitats, with forests being the only exception. In the absence of natural shelters, they dig holes (Grubb, P. 2008). Porcupines are nocturnal and feed on fruits, bulbs, roots, bark and seeds (Apps 2012). They sometimes gnaw bones, but this has no influence on the stable isotope values, which are expected to be in a mixed-feeder range. The *Hystrix* incisors, already erupted at birth, are ever-growing, but not so the molars (Skinner and Chimimba 2005). Premolars and molars were analysed (n=39), and two incisors. Holocene mean $\delta^{13}C$ values range from -0.8‰ to -11.6 ‰, with individual values between -0.2‰ to -13.0‰, spanning the complete C_3 to C_4 diet range. Standard variations within Strata are large (up to 4‰). In the Pleistocene Strata, $\delta^{13}C$ mean values range from -7.8‰ to -10.4‰, again with large individual variations between -12.0‰ to -1.5‰, showing a similar mixed signal like in the Holocene Strata. $\delta^{18}O$ values are low compared to the larger herbivores in Wonderwerk Cave. Mean $\delta^{18}O$ Holocene values are 29.1‰ to 31.5‰, with individual values ranging from 25.7‰ to 31.8‰. Pleistocene means are between 25.0‰ and 26.9‰, which is quite a tight range, but with an individual minimum of 21.8‰ and a maximum of 30.3‰. **Summary:** *Hystrix africaeaustralis* is a

flexible mixed-feeder, with no clear trends in its diet apparent through time. Its $\delta^{18}O$ values are lower than the large ungulates from the same Strata, possibly reflecting night-time feeding on underground storage organs.

Pedetes capensis

The springhare, *Pedetes capensis* (Forster 1778), is another rodent found throughout the sequence, but absent in Excavation 2 Stratum 2. One main habitat requirement determining their range is light sandy soils to burrow. They are known e.g. from pans, overgrazed land and floodplains, and do not need heavy vegetation cover (Butynski and De Jong 2008). Springhares are nocturnal and feed on the roots of grasses, as well as seeds and sometimes grass leaves (Apps 2012). Only a small proportion of the diet is browse in the form of tubers and seedlings (Skinner and Chimimba 2005). *Pedetes capensis* teeth are all ever-growing (Skinner and Chimimba 2005). Stable isotope values will therefore, in contrast to the larger mammal samples, show a bulk result of the last weeks/months in the springhare's life, rather than their childhood. No modern springhare stable isotope value was found in the literature.

The Holocene *Pedetes capensis* specimens (n=22) in Wonderwerk have $\delta^{13}C$ mean values of -0.9‰ to 0.1‰, with individual values ranging between -2.3‰ and 1.4‰. This shows a dominance of C_4 in the springhare Holocene diet. In the Pleistocene Strata 6 and 7 (n=3), the $\delta^{13}C$ values are lower compared to the Holocene (2.7‰ and -1.6‰), and even lower, reaching the mixed-feeder range in Stratum 12 (-7.4‰). The variation in Stratum 12 is large (n=2), with the minimum $\delta^{13}C$ value (-10.4‰) characteristic of a pure C_3 diet, and the maximum $\delta^{13}C$ value (4.4‰) a pure C_4 diet. Springhares do not drink water, but obtain sufficient moisture from rain drops, food and oxidation of hydrogen from ingested food. Oxygen isotope values are lower in Wonderwerk, similar to *H. africaeaustralis*. Holocene $\delta^{18}O$ mean values are 27.2‰ to 30.6‰, with individual values from 24.3‰ to 31.5‰. In

Stratum 6 and 7, $\delta^{18}O$ values are low (26.8‰ and 28.4‰), in Stratum 12 even lower (25.7‰). Again, Stratum 12 has large variation within, with the lowest value 21.7‰ and the highest value 29.8‰, therefore spanning over 8‰ in this stratum. **Summary:** *Pedetes capensis* in the Holocene has a pure C_4 diet, whereas it incorporated more C_3 food in the Pleistocene. Its $\delta^{18}O$ values are lower than the large ungulates from the same strata, possibly reflecting night-time feeding on underground seedlings.

6.5.4 Suidae

Phacochoerus africanus

The common warthog *Phacochoerus africanus* (Gmelin 1788) lives in moist and dry mosaic habitats - African savannah grasslands, open woodland and shrubland, often near water (Cumming, D.H.M. 2008). Five molars and one premolar from Strata 4a and 2b, were analysed. Although a 'normal' cheek dentition is developed, the M3 is constantly growing through the animal's life and slowly enlarges and replaces the other cheek teeth. Impressive, enlarged tusk-like canines erupts already after one month (Hillson 2005, Skinner and Chimimba 2005, Shorrocks and Bates 2014). This diurnal Suid is mainly a selective grazer, and includes roots, sedges, invertebrates and small animals in its diet (Skinner and Chimimba 2005, Apps 2012). Modern $\delta^{13}C$ values for warthog are -2‰ to 0‰ (Codron et al. 2008). The Wonderwerk Holocene $\delta^{13}C$ mean values are similar with 0.0‰ and 1.0‰ (range of individual values 0.0‰ to 1.9‰). Warthogs need to drink daily (Kingdon 1979). $\delta^{18}O$ mean values are 31.5‰ and 33.0‰. All $\delta^{18}O$ values cluster around 30‰ except for sample ME401 with 37.2‰. **Summary:** *Phacochoerus africanus* from the Holocene Strata in Wonderwerk is a grazer that drinks regularly.

6.5.5 Hyracoidea

Procavia capensis

The Cape rock hyrax *Procavia capensis* (Pallas 1766) is found all over Africa and into the Arabian Peninsula and the southern Levant wherever suitable habitat occurs (Barry et al. 2008) and is present in Wonderwerk in all Strata of Excavation 1 in low quantities. It takes five years for the whole permanent dentition to develop, erupt and be in wear, which is about half its lifespan (Steyn and Hanks 1983). One molar/premolar from Stratum 2b was analysed. Hyraxes need shelter, so they are often found in outcrops or cliffs, but are otherwise present in most habitats (Kingdon et al. 2013). It is an opportunistic feeder eating a mixed diet of grass, forbs, shrubs, fruit and berries (Skinner and Chimimba 2005, Apps 2012, Kingdon et al. 2013). Mainly browse is consumed, with seasonally larger quantities of grass, which is reflected in the mixed-feeder $\delta^{13}C$ value (-4.3‰) of the Stratum 2b specimen. Hyrax are not water dependent if they can consume sufficient green food. Due to its water-concentrating physiology, $\delta^{18}O$ values are expected to be higher compared to large ungulates. The $\delta^{18}O$ value is 41.4‰, which is the highest $\delta^{18}O$ value of any species analysed in the assemblage. **Summary:** *Procavia capensis* is like expected a mixed-feeder, independent of water.

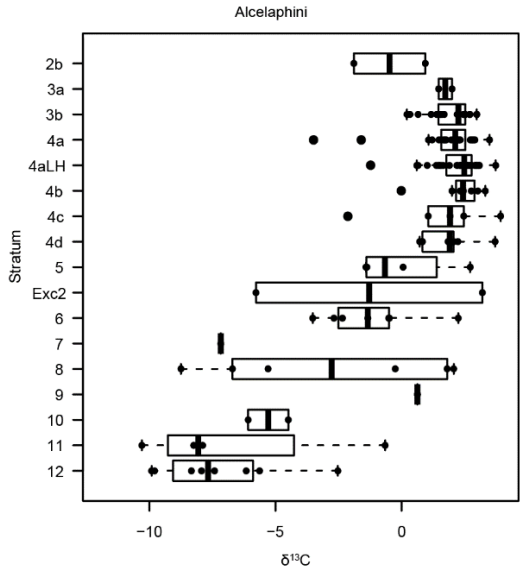
Alcelaphini
Stratum
2b
3a
3b
4a
4aLH
4b
4c
4d
5
Exc2
6
7
8
9
10
11
12
−10
−5
0
δ13C

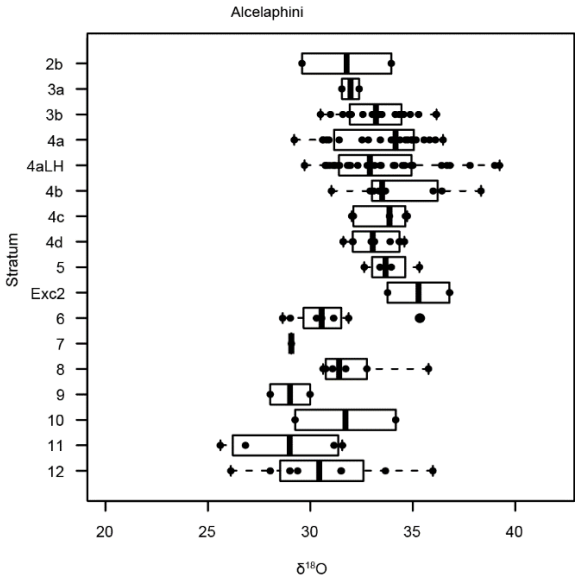
Alcelaphini
Stratum
2b
3a
3b
4a
4aLH
4b
4c
4d
5
Exc2
6
7
8
9
10
11
12
20
25
30
35
40
δ18O

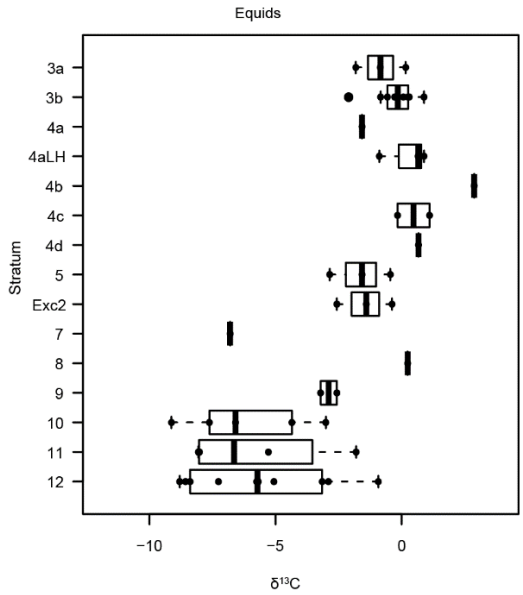
Equids
Stratum
3a
3b
4a
4aLH
4b
4c
4d
5
Exc2
7
8
9
10
11
12
−10
−5
0
δ13C

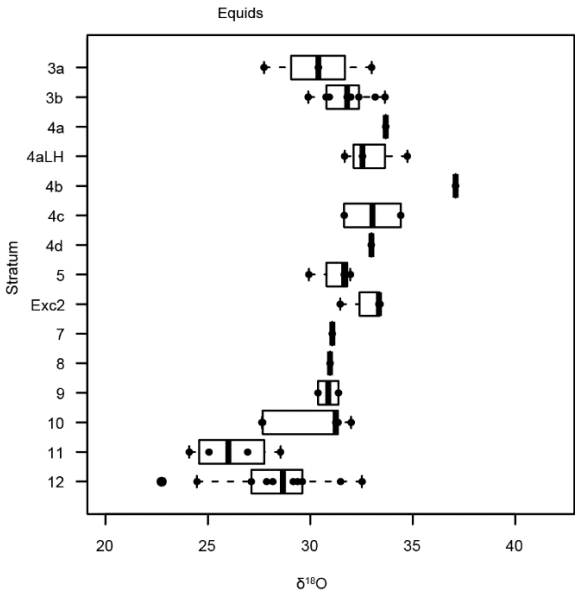
Equids
Stratum
3a
3b
4a
4aLH
4b
4c
4d
5
Exc2
7
8
9
10
11
12
20
25
30
35
40
δ18O

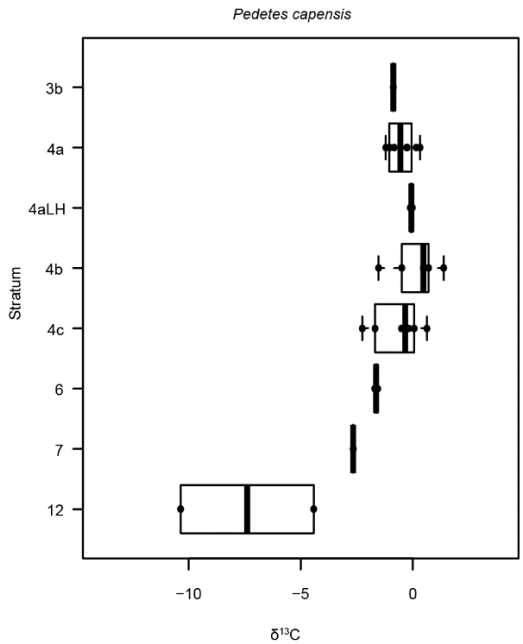
Pedetes capensis
Stratum
3b
4a
4aLH
4b
4c
6
7
12
−10
−5
0
δ13C

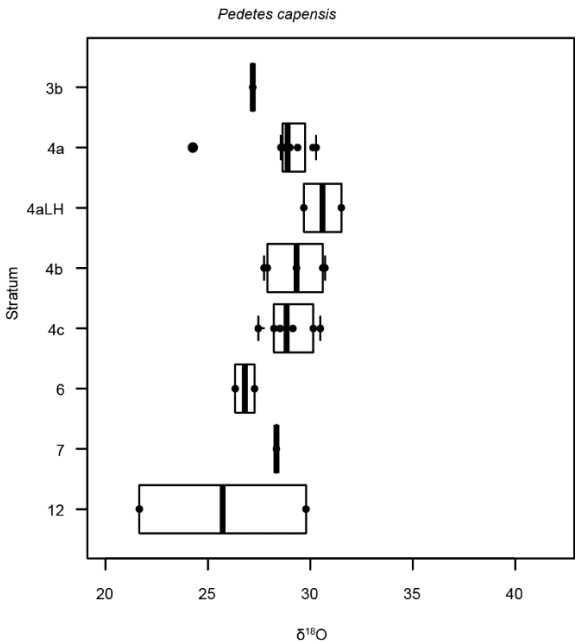
Pedetes capensis
Stratum
3b
4a
4aLH
4b
4c
6
7
12
20
25
30
35
40
δ18O

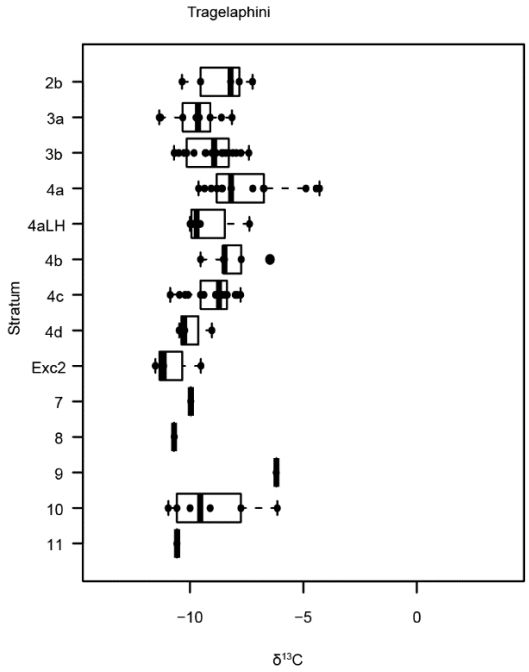
Tragelaphini
Stratum
2b
3a
3b
4a
4aLH
4b
4c
4d
Exc2
7
8
9
10
11
−10
−5
0
δ13C

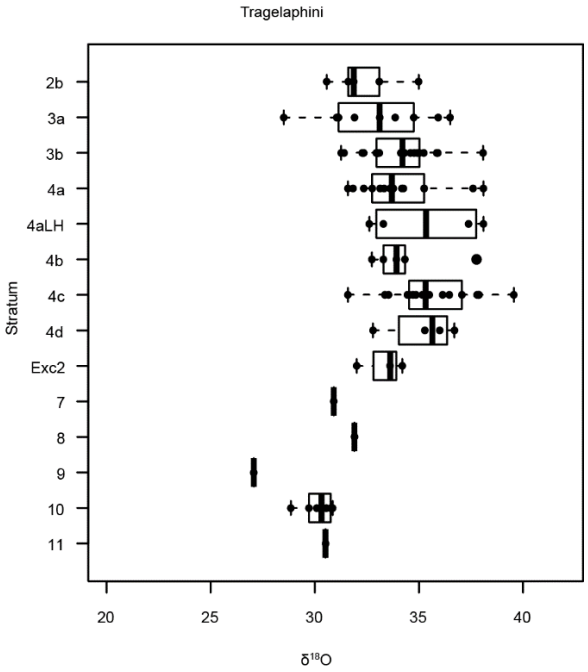
Tragelaphini
Stratum
2b
3a
3b
4a
4aLH
4b
4c
4d
Exc2
7
8
9
10
11
20
25
30
35
40
δ18O

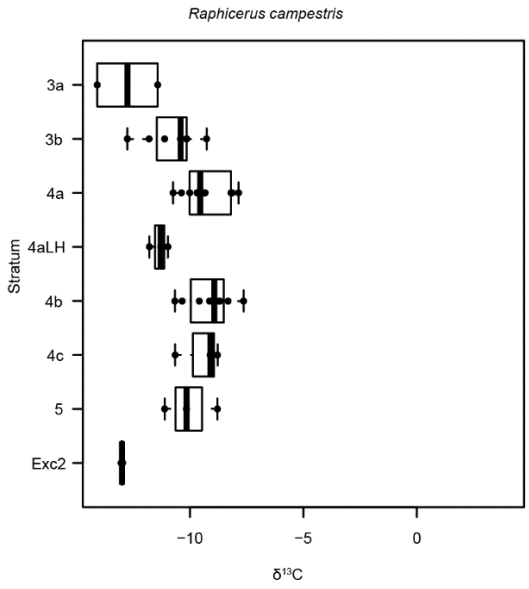
Raphicerus campestris
Stratum
3a
3b
4a
4aLH
4b
4c
5
Exc2
−10
−5
0
δ13C

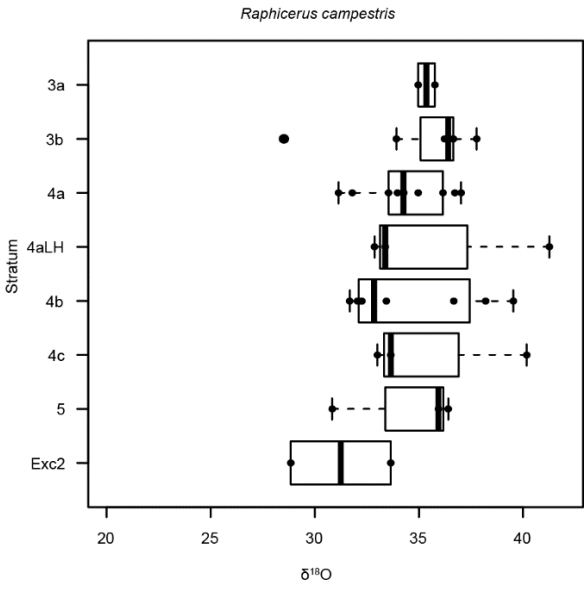
Raphicerus campestris
Stratum
3a
3b
4a
4aLH
4b
4c
5
Exc2
20
25
30
35
40
δ18O

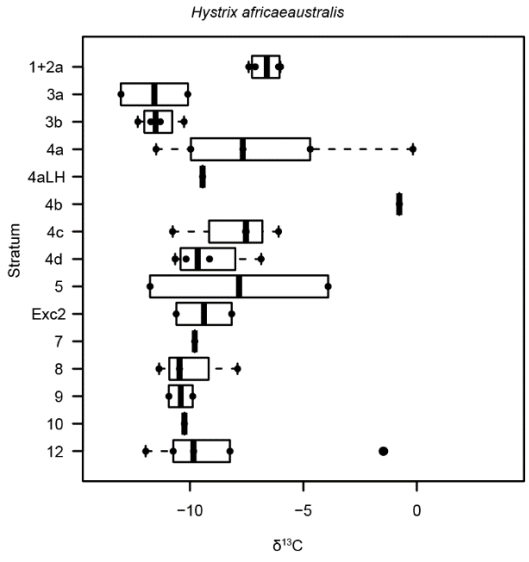
Hystrix africaeaustralis
Stratum
1+2a
3a
3b
4a
4aLH
4b
4c
4d
5
Exc2
7
8
9
10
12
−10
−5
0
δ13C

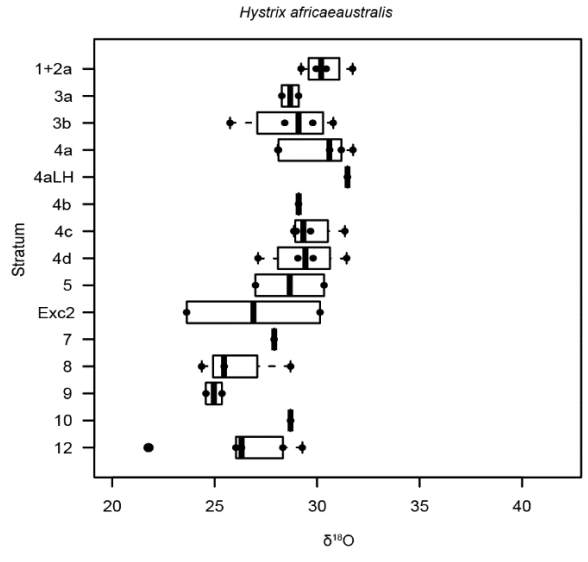
Hystrix africaeaustralis
Stratum
1+2a
3a
3b
4a
4aLH
4b
4c
4d
5
Exc2
7
8
9
10
12
20
25
30
35
40
δ18O

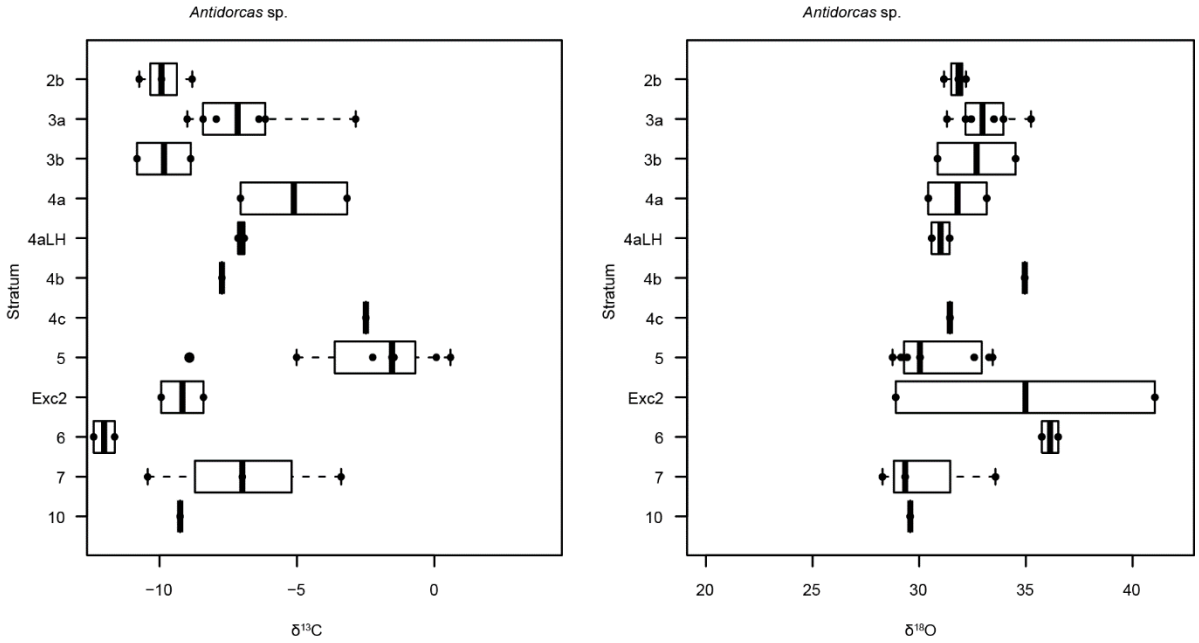

Figure 6.5: Box and whisker plots of $\delta^{13}C$ and $\delta^{18}O$ per Stratum for Alcelaphini, Equids, *Pedetes capensis*, Tragelaphini, *Raphicerus campestris*, *Hystrix africaeaustralis* and *Antidorcas* sp. Thick black line is the median, the box represents the third percentile. The points are all the individual measurements.

6.6 Discussion

6.6.1 $\delta^{13}C$ values and dietary change through time

Comparing the results found in this study with $\delta^{13}C$ values from the limited literature on modern $\delta^{13}C$ of South African mammals (Sponheimer et al. 2003, Codron et al. 2008), most species in the Holocene Strata of Wonderwerk are within the expected $\delta^{13}C$ ranges, as shown above. Furthermore, based on $\delta^{13}C$ values, there is a clear separation of species into grazers and browsers in the Holocene Strata. At the one extreme is the browser *Raphicerus campestris* with a diet of 100% C_3 (average $\delta^{13}C$ values of <-12‰ in Stratum 3a). At the opposite end of the spectrum are hypograzers like *Connochaetes* sp. with 100% C_4 diet (average $\delta^{13}C$ >2‰). Few species fall into the mixed-feeder range (means of -9‰ to -3‰), a characteristic noted for modern African ecosystems (Codron et al. 2008). This is in marked contrast to the Pleistocene Strata of Excavation 1 and 2, where most specimens fall

within the mixed-feeder range. Figure 6.6 shows the percentage of taxa that are predominantly grazers (mean >-3‰), browser (>-9‰) and mixed-feeders (-9‰ to -3‰) per stratum. A change from 50-60% mixed feeders in Stratum 10-12, to 20-40% in the Middle Pleistocene and early Holocene is evident, with the lowest percentage (16%) of mixed-feeders in Stratum 4aLH. While the percentage of browsers remains broadly similar at 20 to 50% throughout the Pleistocene and Holocene sequence, the C_4 grazers increase over time. They increase from 5-22% in Stratum 10-12, to 30-47% in the Middle Pleistocene and early Holocene and make up over 60% of samples in late Holocene Strata 4a and 3a. This shows that browser diet remained constant over the last two million years, while previously mixed-feeding species like Alcelaphines, Equids and springhare become specialized grazers. Statistical analysis (Appendix 6.2) confirms this observation. There is no statistical difference in $\delta^{13}C$ values between Tragelaphini and Alcelaphini in the Pleistocene of Excavation 1 Strata 6 to 12. In the Holocene Strata, Tragelaphini and Alcelaphini have significantly different $\delta^{13}C$ values (e.g. Stratum 4d Alcelaphini-Tragelaphini p=0.02). The same applies for the other grazer and browser species (Appendix 6.2).

Where individual species and tribes are concerned, the diet of both Alcelaphini and Equidae in Strata 10-12 is made up of 40-50% C_4 vegetation[1]. This becomes variable in the following Strata, and reaches 80-90% C_4 in the early Holocene, before showing values of a "100%" C_4 diet in the mid-Holocene. Alcelaphini have consistent slightly higher C_4 intake than Equids, which was also noticed in other similar isotope studies (Cerling et al. 2015). There are fewer samples of *Pedetes capensis* than for the large herbivores, but values for this modern grazer are consistent with the observed trend with mixed feeder values in Strata

[1] Using the endpoints for grazers (mean >-3‰), browser (mean >-9‰) and mixed-feeders (mean -9‰ to -3‰).

12 and 10 shifting to grazing in the Middle Pleistocene, and to an even higher C_4 intake in the Holocene. Tragelaphini on the other hand remain at 60-80% C_3 intake throughout the sequence. The smaller C_3 browsers (*R. campestris, H. africaeaustralis*) show surprisingly little dietary variation through time. *A. marsupialis* is the only species which has a mixed and highly variable diet throughout the last one million years, with a preference for more C_3 in some strata. The only trend from C_3 to more mixed-feeding can be seen in *H. africaeaustralis*, between the Pleistocene and the Holocene. In Excavation 2 Stratum 2, the full specialization into grazers and browsers is already developed. The isotope values show the modern differentiation into the grazing and browsing clade, with little mixed-feeders. The only exception is *C. simum*, which is described as a pure grazer today (Apps 2012), but, as shown in other studies in South and East Africa (Spohnheimer et al. 2001b, Zazzo et al. 2000), has a mixed C_3-C_4 diet in the Pleistocene. It is one more example that it is insufficient to project the diet of modern mammals into the past, as significant changes have taken place.

The observed change can reflect either a shift from C_3 tree/shrub food to C_4 grass, or a change from C_3 grasses to C_4 grasses. C_3 grasses are not a component of the local vegetation today, but might have been a part of the local vegetation in the past, if conditions would have been unsuitable for C_4 plants (e.g. winter rainfall, low growing season temperatures and/or low pCO_2). It is impossible to determine the plant type with stable light isotope analysis alone, but the second option is more likely from an ecological perspective. It is implausible that genera in the Artiodactyla as well as in the Perissodactyla and Rodentia should all change their dietary specialization at about the same time. Biogenic factors like diagenetic change in the enamel or an increase in the isotope enrichment factor are unlikely explanation, as only today's grazer species are influenced.

Alcelaphines, Equids and *Pedetes capensis* have a grazer tooth morphology, including hypsodonty, developed by 2Ma, despite the C_3-C_4 mixed isotope signal in the Pleistocene. A chronological offset between diet and dental morphology has been noted by Lister (2013) for African proboscideans, but in this case the diet change occurred long before the morphological change in the teeth. In the case of the Wonderwerk grazers, the intake of only part of C_4 in their diet, or C_3 grasses, might have put enough pressure on the organism to develop this specialised morphology. Another explanation could be that the Wonderwerk record only catches phases when grazers had lower C_4 grass intake than at other times during the Plio-Pleistocene. Further research is needed to define the selective forces behind the discrepancy between diet, environment and morphology.

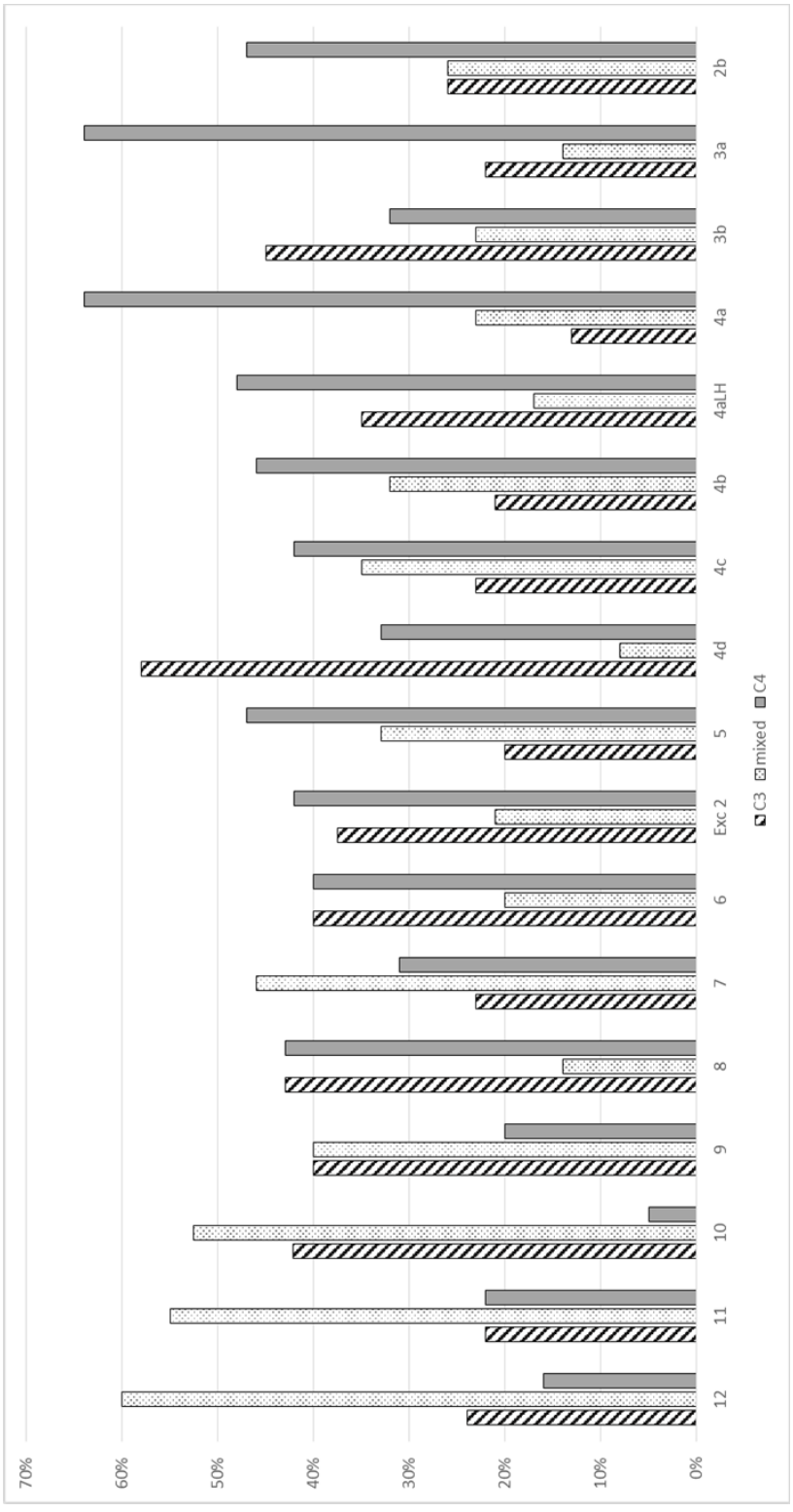

Figure 6.6: Histogram of the percentage of predominantly C_4, mixed and C_3 feeders per Stratum after stable carbon isotope results. Note the low number of mixed-feeders in the Holocene, and the rise of C_4 feeding specimen from Strata 9-10 upwards, and again in the mid-late Holocene.

6.6.2 $\delta^{18}O$ values and species drinking habits

$\delta^{18}O$ can inform about drinking behaviour, which is one ecological factor that cannot be explored with $\delta^{13}C$. $\delta^{18}O$ values in mammals derive from ingested water from food and meteoric water, which itself is influenced by climate. Additionally, drinking behaviour, diet and physiology lead to possible differences in $\delta^{18}O$ values of up to 8-9‰ between contemporary species (Kohn et al. 1996, Sponheimer and Lee-Thorp 1999a). Plant leaf evapotranspiration leads to higher oxygen values in plant leaves, and therefore in mammals ingesting water mainly from green food. Browsers, which do not drink regularly, can then be distinguished from regular drinkers because of the extra enrichment (Sponheimer and Lee-Thorp 1999a). Regular drinkers are most large grazers, although exceptions exist. *A. bondi* for example is a grazer that specialises on green shoots, and is therefore more independent of water sources. Other species, e.g. Tragelaphini, can sustain themselves for some time without drinking, but will only do so if necessary. This subchapter explores how those differences are reflected in the Wonderwerk assemblage. The following Chapter 7 explores the significance of general trends in the $\delta^{18}O$ record through time for the climate record of the region.

The small browsers in Wonderwerk, *R. campestris*, *P. capreolus* and *O. oreotragus,* feed on leaves which is their main source of water. Compared to the larger browsers and the grazers, their $\delta^{18}O$ mean values are higher in most strata, but also not statistically significant. The $\delta^{18}O$ values in *R. campestris* span a large range in most Holocene Strata (up to 9‰), maybe reflecting the influence of several seasons with different evapotranspiration regimes. A non-significant trend is visible in the grazers, with Equids having lower $\delta^{18}O$ values than Tragelaphini. Equids drink regularly, whereas some of the Alcelaphini species, e.g. *Alcelaphus buselaphus*, can sustain themselves for a limited time without drinking. The lowest $\delta^{18}O$ value is for a single *Ceratotherium simum*, and the

highest is for a single *Procavia capensis* specimen. The potential isotopic variation possible within their species is therefore unknown. There are no physiological reasons known why Rhinocerotidae should have lower oxygen values than other Perissodactyla, and the few studies with *C. simum* $\delta^{18}O$ values (Zazzo et al. 2000, Kingston 2011) show no especially low values. They drink regularly and wallow in water to cool down, and this particularly low value could point to an isotopically light lake or a climatic cold period. *Procavia capensis* $\delta^{18}O$ values are possibly high because of its selective feeding on evapotranspirated leaves, its baking in the full sun and its water-concentrating body. It is often among the highest $\delta^{18}O$ values in an assemblage (e.g. Hare and Sealy 2013).

P. capensis and *H. africaeaustralis* both have consistently lower $\delta^{18}O$ values compared to the other species. This is most likely due to both being nocturnal animals that feed on the underground organs of plants. This difference is significant, with both being statistically significant different to Alcelaphini, Tragelaphini, *R. campestris* and *R. fulvorufula* in the Holocene (Appendix 6.2). They are not significantly different to each other. The lower $\delta^{18}O$ values are also visible in the Pleistocene, but are not significant. This could be an artefact of small sample sizes in the Pleistocene strata. Another explanation could be that plants were less water-stressed, and less evapotranspiration took place. The Wonderwerk sample from the Holocene is large enough to explore physiological and dietary influences in the $\delta^{18}O$ values, whereas sample sizes in the Pleistocene are too small and time-averaged to distinguish confidently between physiology and climate. Inter-species trends in $\delta^{18}O$ over time are explored in Chapter 7.

Aridity index

Levin et al. (2006) published an index to calculate past aridity, which became popular among stable isotope researchers working in East Africa (e.g. Kingston 2011, Bedaso et al. 2010, 2012, Garrett et al. 2014). It is based on the principle of evaporation sensitive taxa

(ES), which obtain their water mainly from leaf water (e.g. Giraffids, Alcelaphini, Antilopini, Tragelaphini) and evaporation insensitive taxa (EI), which obtain their main water intake from drinking meteoric water (e.g. Reduncini, Suidae, Equidae, Rhinocerotidae). The enrichment factor (Ɛ) between both is calculated from $\delta^{18}O$ enamel, and the water deficit (WD) can then be inferred using modern weather data for a regression line. This method has not been used in southern Africa. This, so far since there are not enough published sites from different biomes in South Africa with modern enamel $\delta^{18}O$ data to calculate $\varepsilon_{Es\text{-}Ei}$, which is an essential parameter or water deficit values from modern weather data to calculate a regression model. Only then could archaeological data be plotted onto the regression line. Another problem for the Wonderwerk data is the uneven sample sizes, since the index needs at least ten ES and EI samples per unit to be reliable. The Wonderwerk faunal assemblage furthermore is dominated by bovids and lacks typical environmental sensitive fauna like hippopotamus or giraffids. It was therefore not possible to use the Levin et al. (2006) aridity index or develop a similar index for the Wonderwerk Cave data.

6.7 Conclusions

Oxygen isotope values show significant differences between nocturnal and diurnal species in the Holocene Strata. Other small, but not significant, trends in $\delta^{18}O$ values in the Holocene Strata can be explained by physiological differences, especially drinking behaviour. Strata 10-12 show differences in $\delta^{13}C$ values compared to the rest of the Pleistocene Strata and to the Holocene. This certainly is evident in the grazer species (Alcelaphini, Equids, *P. capensis*). A threshold seems to be reached around one million years ago, when those species started to show a shift to more C_4 dietary values. The dating for the archaeological Strata is too coarse to allow speculations about how abrupt or gradual these changes happened. There are no modern analogues in southern Africa today for the

Early and Middle Pleistocene assemblage from Wonderwerk with its high percentage of mixed-feeders. A trend is evident in the Middle and Late Pleistocene that peaks in the Holocene with the modern separation in African savannah ecosystems into grazers, browsers and few mixed-feeding species.

Chapter 7 - Implications of the results for palaeoclimate, past environment and archaeology in Wonderwerk Cave

The principal aim of this chapter is to compare the Wonderwerk Cave stable isotope results with the other proxy records for palaeoclimate and past environment from Wonderwerk Cave and from the wider region. The chapter begins by comparing the OES and the herbivore enamel data and discusses the conclusions which can be drawn from combining these two independent proxies. Comparison to faunal abundances and other environmental proxies from Wonderwerk Cave follows, providing a coherent picture of vegetation and humidity changes at the site. Thereafter possible drivers of the observed changes are discussed, and the isotope records are set in the context of existing palaeoenvironmental records from the region. Part 7.5 explores the hypothesis of environmental changes triggering cultural changes visible in the archaeological record. The chapter concludes by summarizing the implications of this study for the wider region and the field of African palaeoenvironmental research.

7.1 Comparison of results from OES and enamel stable isotope analyses

The reasoning behind using two different materials in this study, ostrich eggshell and enamel, was to explore different aspects of the environment and create two independent sequences complementing each other. Though both $\delta^{18}O$ and $\delta^{13}C$ values were obtained for OES and herbivore tooth enamel, the OES $\delta^{18}O$ record is mainly used as an index of aridity since eggshell reflects the moisture conditions under which it was formed while the $\delta^{13}C$ values of OES reflect the diet of the ostrich, which is known to be selective. In contrast, the large set of herbivore enamel $\delta^{13}C$ reflects vegetation changes. Despite these differences,

the herbivore enamel and OES[1] $\delta^{13}C$ and $\delta^{18}O$ records for the Wonderwerk Pleistocene and Holocene sequence generally follow the same pattern, with a few notable exceptions noted below. The enamel $\delta^{13}C$ and $\delta^{18}O$ values in Strata 12-10, especially in Alcelaphini and Equids, are lower than those for the rest of the sequence, with Stratum 11 having the lowest $\delta^{18}O$ values of all (Fig. 6.1). For Stratum 11 (but n=1), both the OES $\delta^{18}O$ and $\delta^{13}C$ values are lower than those obtained for the rest of the sequence. Together with the enamel $\delta^{18}O$ only in Stratum 11 (but n=1), this provides conclusive evidence from both proxy data sets for reduced humidity in this Stratum. (Figure 7.1).

In Stratum 10 the OES $\delta^{18}O$ value is lower than that of the other Pleistocene layers and $\delta^{13}C$ higher than any of the other Pleistocene or Holocene strata in the entire sequence. Thus Stratum 10 is showing variable signals with both highest and lowest values for the entire sequence indicative of a fluctuating climate. The changes in humidity denoted by shifts in the $\delta^{18}O$ values in the early Pleistocene samples may indicate that proportions of C_3 and C_4 vegetation did not change significantly, but sample sizes are low and the Strata represent long time spans.

In Strata 9 to 6 the OES $\delta^{18}O$ and $\delta^{13}C$ values are respectively indistinguishable between layers, with a small but not significant trend to more dry spells (Figure 7.1). While the $\delta^{18}O$ values for herbivore enamel do not fluctuate much in Alcelaphini, Equids and Cape porcupine, the $\delta^{13}C$ isotope values are more variable, especially in the grazers. However, comparisons are limited in those Strata due to the low numbers of enamel samples and the Strata are highly time-averaged. The OES samples appear to track the moisture fluctuations in the early Pleistocene Strata well, and the herbivore enamel is closely reflecting C_3 and

[1] This discussion includes Holocene OES data from Lee-Thorp and Ecker (2015) (see Chapter 6).

C_4 vegetation changes, with the ostrich carbon values reflecting a similar percentage of C_4 intake in all levels (about 20%).

In Excavation 2 stratum 2, OES $\delta^{18}O$ values hint at the existence of a wet spell. Compared to the Excavation 1 OES sequence, the $\delta^{18}O$ values are similar, but not as low as, those for Excavation 1 Stratum 5. In the enamel results, Excavation 2 Stratum 2 does not show lower $\delta^{18}O$ values (except for *R. campestris*), but the presence of *K. leche* indicates standing water. Low $\delta^{13}C$ values suggest the influence of a well-watered and more mixed vegetation. Excavation 1 Stratum 5 has lower $\delta^{13}C$ and $\delta^{18}O$ OES values only in spit 5I. In Stratum 5 as a whole, the enamel $\delta^{13}C$ values for grazers - Alcelaphini and Equids - are lower compared to the Holocene Strata, but no difference is evident in the browsers. The enamel $\delta^{18}O$ is similar to the early Holocene and does not show lower $\delta^{18}O$ as in the OES samples. This could be an artefact of the fact that, unlike the OES samples, the enamel samples were not divided into spits (5I, 5II), with their values averaged out over the whole stratum.

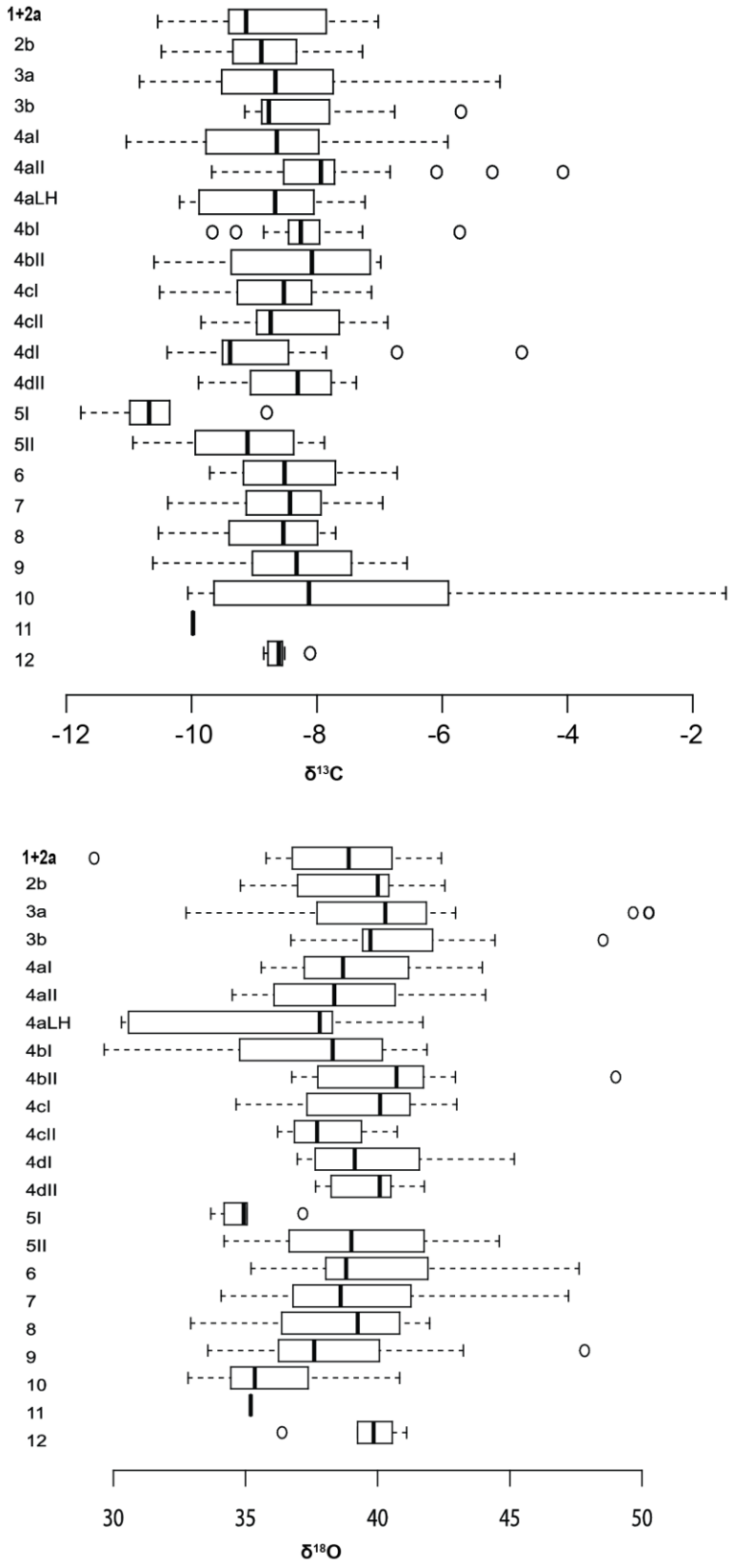

Figure 7.1: Ostrich eggshell $\delta^{13}C$ and $\delta^{18}O$ boxplots from Excavation 1 (data in Appendix 5.1). Includes Holocene data from the supplement in Lee-Thorp and Ecker (2015).

In the Holocene, $\delta^{13}C$ values in OES are rather similar throughout all Strata, with a somewhat lower median at the start of the Holocene and the highest values in the mid-Holocene (Figure 7.1). Enamel values show similar trends (Chapter 6). The $\delta^{18}O$ OES values fluctuate, with highest medians in Strata 4d and 3, and lowest in Stratum 4aLH and 4bI (Figure 1.1). In contrast, in enamel, the highest $\delta^{18}O$ values are in Stratum 4aLH and 4bI, (except for *A. marsupialis* and *R. campestris,* which are highest in Stratum 3). This is the largest discrepancy between both proxy records. As OES is formed during a few days at the start of the rainy season, the low values might reflect a change in rainfall season. As enamel is formed over months or years, a single rainy season cannot stand out and so a more significant change in rainfall intensity, season, source and/or amount of rainfall is indicated. Another explanation, indicated by the pollen record (Chapter 3), would be a change in vegetation composition, with increasing proportions of grasses. As ostriches concentrate on tender plants (Chapter 5), this could reflect an increase in these types of plants after a wet spell, whereas overall the vegetation became more open with an increase in grass. Likewise, seasonal hunting of herbivores and/ or carnivore accumulation must also be considered as a possible factor. The following part explores these questions further by combining the isotope results with the other Wonderwerk Cave proxy records.

7.2 The Pleistocene and Holocene environmental record of Wonderwerk Cave

The record of environmental proxies from Wonderwerk Cave is described in detail in Chapter 3. In this part, the different proxies are discussed in connection to the OES and enamel isotope results. The summary of all evidence shows a coherent picture of vegetation and rainfall changes over time, although small discrepancies remain due to the nature of the different proxy records.

Faunal abundances

In principle, the abundance of grazers versus browsers in an assemblage reflects the local environment. In particular the percentages of Alcelaphini and Antilopini compared to the whole bovid or faunal assemblage have been used as indicators of open or closed landscapes (Vrba 1985, Bobe et al. 2007, Cerling 2015). The faunal abundance per Stratum in Wonderwerk is shown in figures 7.2, 7.3 (Excavation 1 Holocene) and 7.4 (Excavation 1 Pleistocene and Excavation 2 Stratum 2). These graphs show all the identified dental samples, including the samples used for stable isotope analysis. These dental records are not necessarily a complete reflection of the relative abundances of the various taxa, but are used as full species lists for all strata are not published yet. It was noted elsewhere that in the Holocene faunal assemblages, Equids and Alcelaphini rise from 35% of the total assemblage in the early Holocene to 45% in the Late Holocene (Thackeray 2015). The same author notes the rise of springbok from 0% to 16% in the same time frame, and argues this further reflects an increase in grazing ungulates. Although the dental faunal abundances are consistent with Thackeray's estimation of an increase in grazing species and springbok in the mid and late Holocene, the stable isotope data show that *A. marsupialis* is a browser to mixed-feeder. Its increase might therefore reflect increasing aridity rather than increasing grassland. The latest specimen of the definite grazing springbok species *A. bondi* (Brink and Lee-Thorp 1992) is from the early Holocene Stratum 4c.

Faunal abundances in Stratum 4d might be skewed due to the high percentage of *Hystrix* and the small number of large herbivores, which might be a taphonomic problem. Comparing the large grazer bovids (Alcelaphini) with the large browser bovids (Tragelaphini), both tribes are found in low numbers in Strata 4d and 4b, with more Tragelaphini than Alcelaphini specimen in Stratum 4c and 3b. Strata 4aLH, 4a and 3a show increased numbers of Alcelaphini (Fig. 7.2), which could reflect more open grassland in

those Strata, however since sample sizes are generally small these conclusions must be considered as only tentative. Equids are low in numbers until the mid-Holocene Stratum 4a when their numbers rise (Fig. 7.2), further pointing to an expansion of grassland. The possible appearance of *A. hofmeyri*, the Kalahari springbok, in Strata 4aLH, 4a and 3b could point to a biome shift to more arid environments, but the dental samples are not complete enough for a definite identification of species.

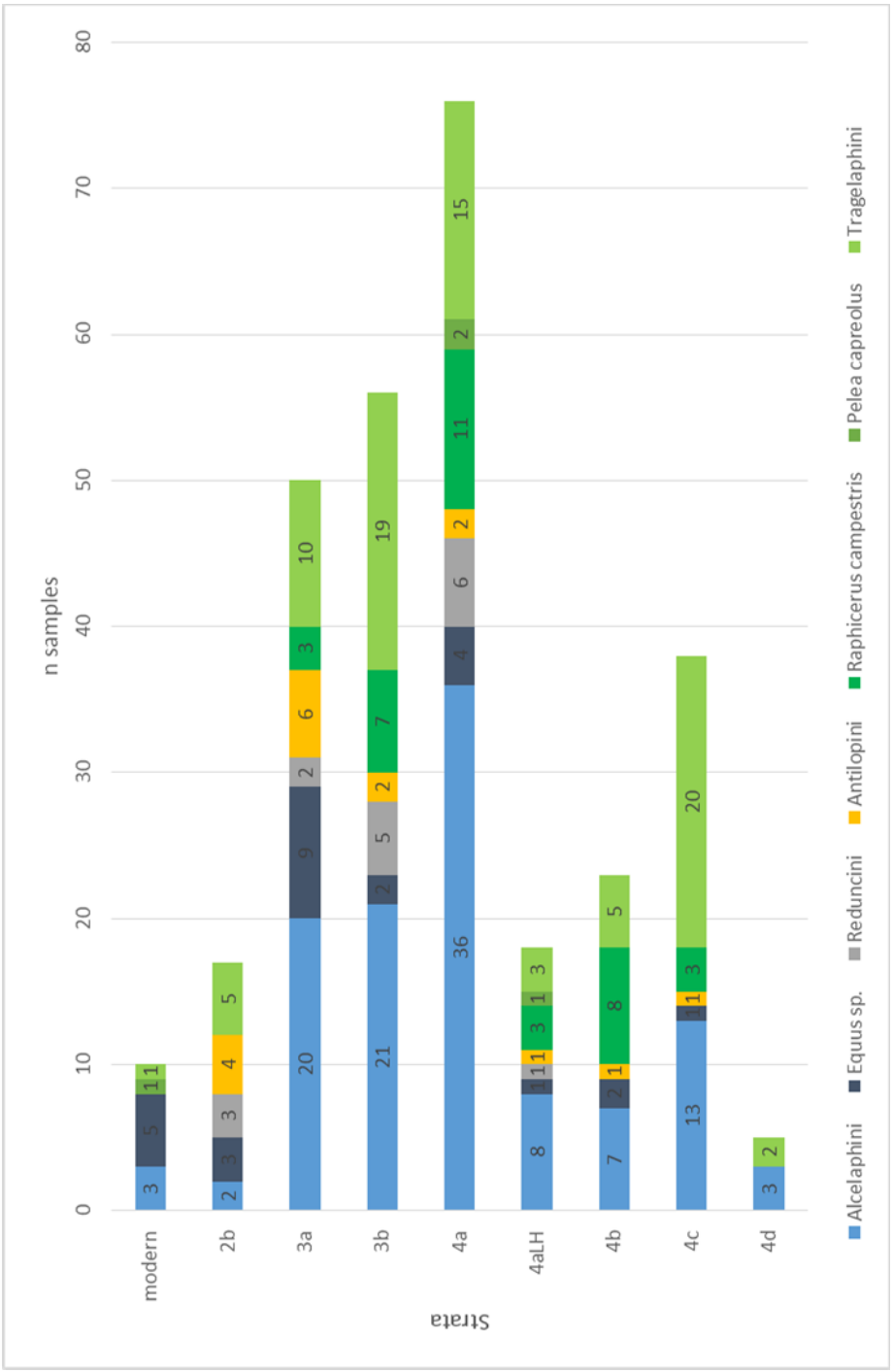

Figure 7.2: Faunal abundance stack chart of Holocene Bovidae and Equidae. The vertical axis represents the number of identified teeth, as are the numbers inside the bars for each species respectively. Excludes Hyracoidae, *O. oreotragus* and *P. africanus* because of small sample sizes, and Rodentia.

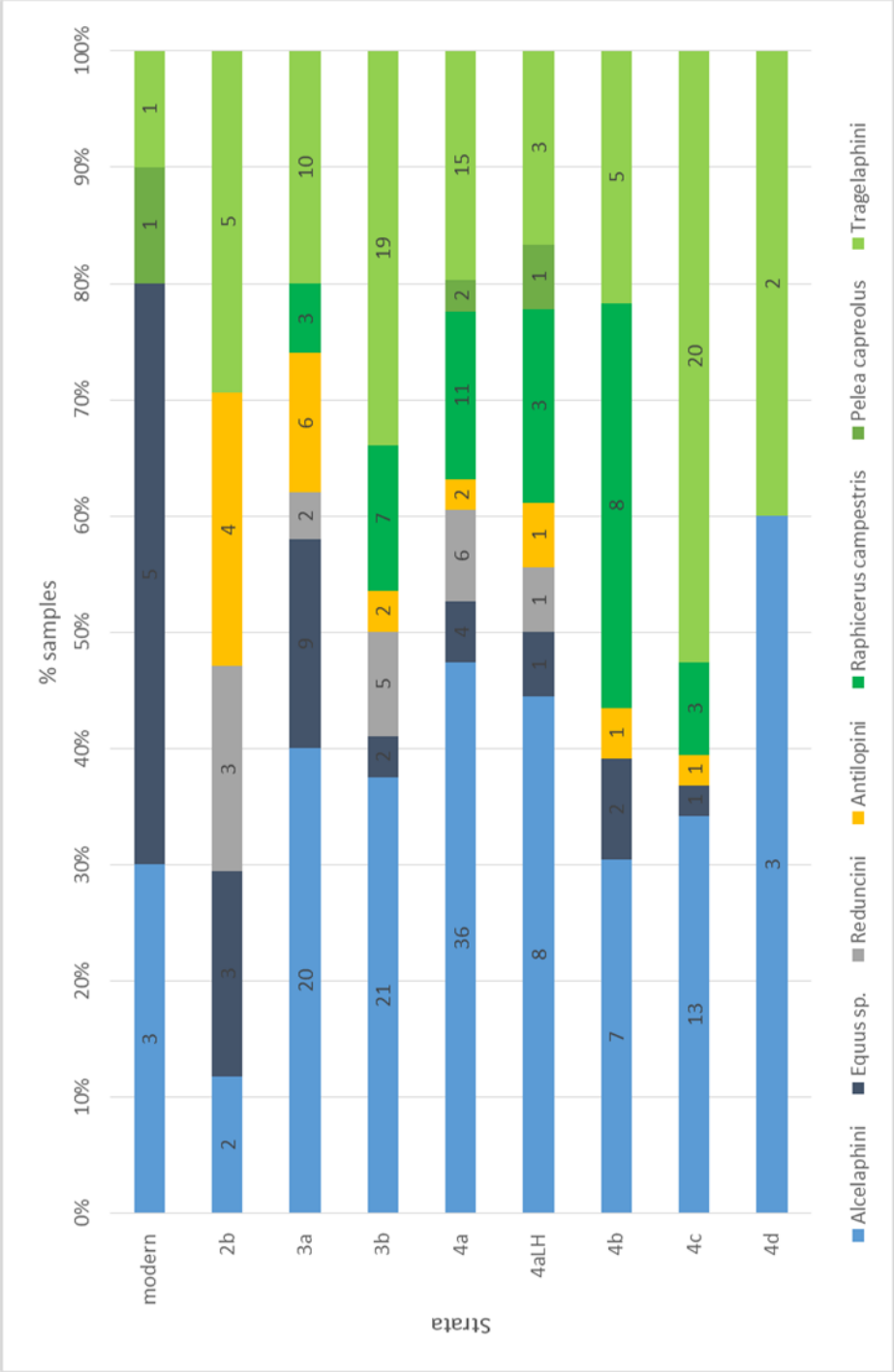

Figure 7.3: Faunal abundance stack chart of Holocene Bovidae and Equidae, showing the percentage of each species per stratum, and the number of samples written in the respectable column. Excludes Hyracoidae, *O. oreotragus* and *P. africanus* because of small sample sizes, and Rodentia.

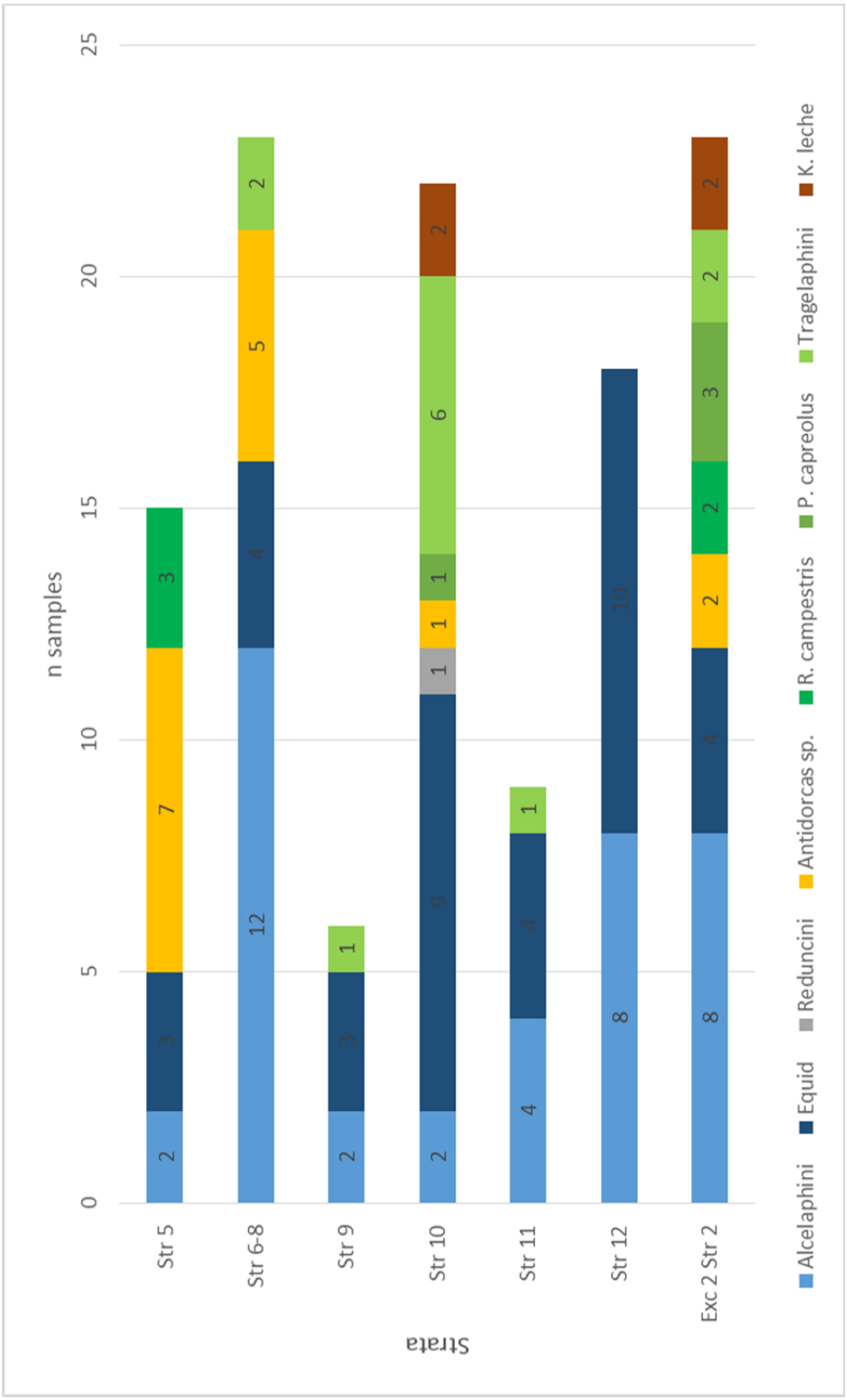

Figure 7.4: Faunal abundance stack chart of Excavation 1 and 2 Pleistocene Strata Bovidae and Equidae species. The vertical axis represents the number of identified teeth, as are the numbers inside the bars for each species respectively. Because of the scattered nature of the samples, the possibility of counting the same individual cannot be completely excluded. Excludes Rodentia.

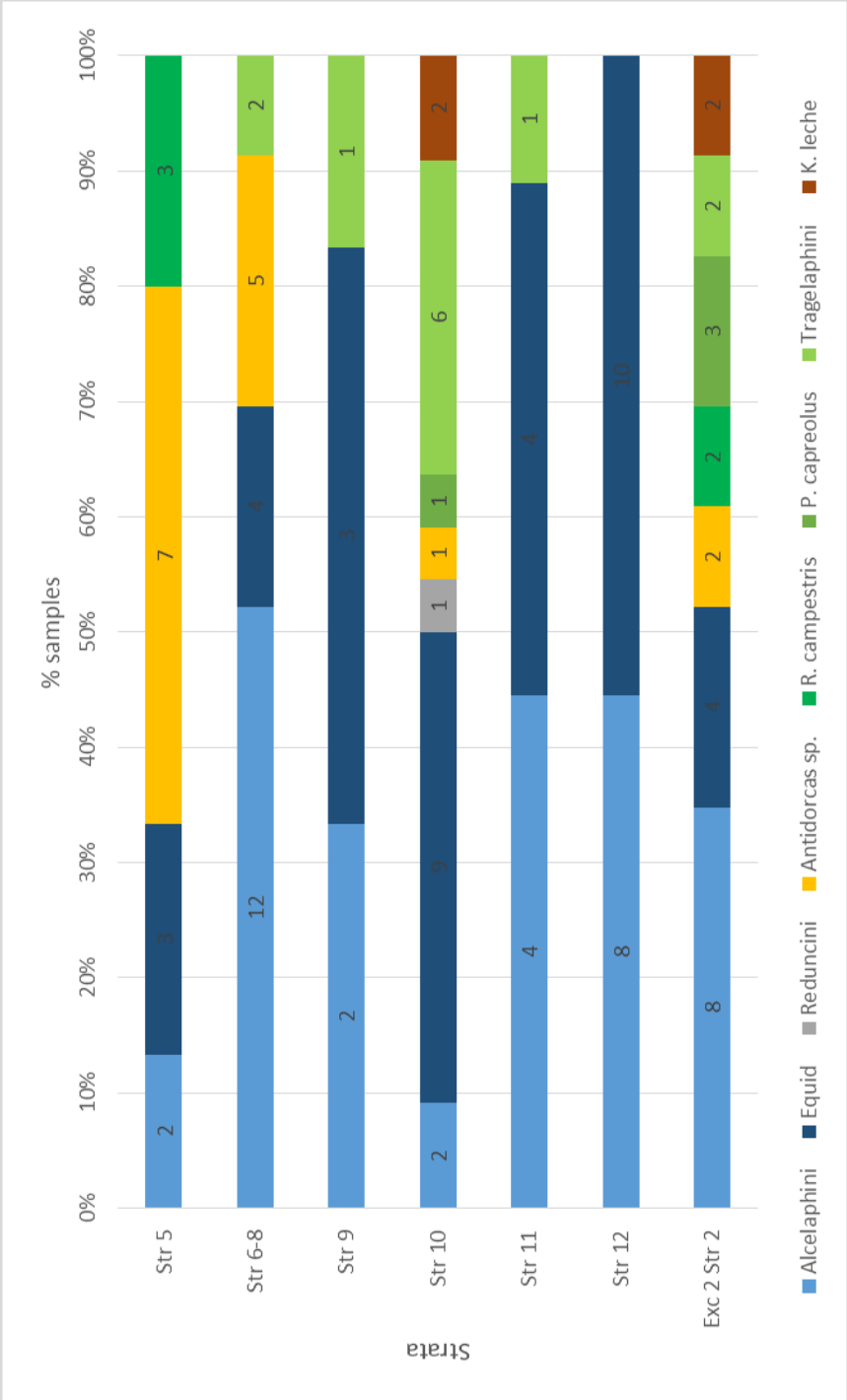

Figure 7.5: Faunal abundance stack chart of Pleistocene Bovidae and Equidae, showing the percentage of each species per stratum, and the number of samples written in the respectable column. Excludes Rodentia.

The Pleistocene Strata in Wonderwerk are dominated by high percentages of Equids and Alcelaphini, with Alcelaphines especially abundant in Stratum 11 (Brink et al. 2015). Reduncini, Hippotragini, Suids or Antelopines are missing. This has been interpreted as

reflecting a semi-arid environment (Brink et al. 2015). Although only grazers were analysed in Stratum 12, it has to be taken into account that the enamel isotope analysis revealed C_3 to mixed feeding values for these specimens. Tragelaphini numbers are low with two or fewer samples per stratum, except for Stratum 10, which also has the highest numbers of browsers and mixed feeders in the Pleistocene. Together with the *K. leche* in Stratum 10, these observations hint at a wetter and wooded C_3 environment at this time. *Antidorcas* sp. numbers are increasing in the middle to late Pleistocene Strata 8 to 5, which might indicate an arid environment. The faunal abundances in the Pleistocene strata are in agreement with the OES and enamel stable isotope results.

Table 7.1 shows the percentage of Alcelaphini and Antilopini, as well as Alcelaphini and Equids from the Wonderwerk assemblage. It includes the percentage of grazers, browsers and mixed feeders as categorized by the enamel stable isotope values. These are used in Figure 7.6 to show an index of the percentage of Alcelaphini and Antilopini versus the percentage of dominant C_4 grazers in several modern African National Parks and in the Wonderwerk Strata. This index has been used by several researchers to compare archaeological sites to the most similar modern biome (e.g. Sponheimer and Lee-Thorp 2003, Garett et al. 2014). In Figure 7.6, all Wonderwerk Strata fall in the gap between the more closed habitats in eastern South Africa (e.g. Kruger, Hluhluwe) and the more open habitats in north-western South Africa and Namibia (e.g. Kalahari, Etosha Pan). This analysis indicates that Strata 10 and 9 are relatively more closed, and Strata 5, 4a and 4aLH more relatively open. Although this could reflect a more mixed environment than presently found at Wonderwerk Cave, the picture is skewed because it combines the grazer *A. bondi* and the variable mixed-feeder *A. marsupialis* in the same category. Equids and Alcelaphini abundances might be a better representation (Table 7.1). Chapter 6 has furthermore shown that in the Pleistocene the vegetation around Wonderwerk was unlike any modern analogue

anywhere in sub-Saharan Africa. As the index only calculates open/closed percentages, it does not show other vegetation dynamics. It is therefore not surprising that the Wonderwerk data do not overlap with any modern National Park in Figure 7.6.

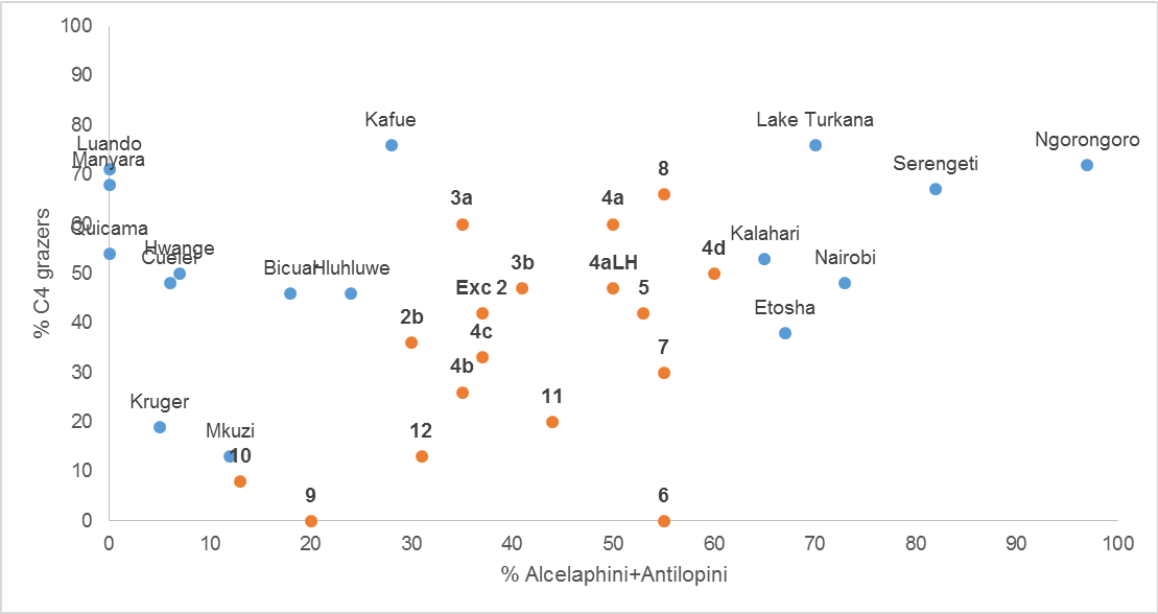

Fig. 7.6: The percentage of Alcelaphini and Antilopini as well as the percentage of C_4 grazers from modern African National Parks (after Sponheimer and Lee-Thorp 2003, Table 1) and for the Strata in Wonderwerk Cave. The left side of the graph reflects more closed, wooded habitats and the right-hand side more open and arid habitats.

Stratum	%Alcelaphini+Antilopini	%Alcelaphini+Equids	G:M:B
2b	30	17	36:29:36
3a	35	50	60:18:23
3b	41	56	47:20:33
4a	50	76	60:25:15
4aLH	50	18	47:16:37
4b	35	23	26:42:32
4c	37	38	33:39:27
4d	60	5	50:0:50
5	53	17	42:42:17
6	55	31	0:33:66
7	55	31	30:50:30

8	55	31	66:0:33
9	20	10	0:50:50
10	13	24	8:46:46
11	44	9	20:40:40
12	31	26	13:63:25
Exc2 Str 2	37	27	42:16:42

Table 7.1: The percentage of Alcelaphini and Antilopini from all identified teeth in Wonderwerk Cave, as well as the percentage of Alcelaphini and Equids from the same assemblage. Row four shows the percentage of grazers (G), mixed feeders (M) and browsers (B) per Stratum after stable isotope analysis (B>-9‰ $\delta^{13}C$; G<-3‰ $\delta^{13}C$).

Comparisons to other proxy records from Wonderwerk Cave and summary through time

The analyses and results to date for the environmental proxy records in Wonderwerk Cave are described in Chapter 3. They are now compared with the OES and enamel stable isotope data. It has to be considered that various proxies differ in resolution, partly due to differences in sampling methods. The Holocene Excavation1 Strata 1-5 samples (pollen, microfauna, macrobotanical remains and fauna) were acquired from different excavators in different years. Their only connections are the radiocarbon dated Strata, although they do not always come from the same profile, section and/or square. In Excavation 1 Strata 6 to 12, the phytolith data was sampled in concert with the lithostratigraphy and provides a far finer resolution than the micromammal, faunal and stable isotope data. There are no environmental proxies available for comparison from Excavation 2 to date.

Eleven Equid apatite samples from Strata 2a to 4d at Excavation 1 were measured for $\delta^{13}C$ in a previous study (Thackeray and Lee-Thorp 1992). The results (from -0.7‰ to 1.3‰) are consistent with the results in this study. Two samples from Stratum 4d complement the record, as there has been no Equid samples run from Stratum 4d in this study. The largest discrepancy between the two studies is in Stratum 4aLH, but since it is based on small sample sizes the difference is probably not significant.

The Holocene pollen record, like the oxygen and carbon isotope data, indicates a semi-arid climate (Scott and Thackeray 2015). Strata 4a and 3b have the largest proportion of grasses. This is further evident in the high proportions of C_4 feeders and grazing fauna in these Strata (Table 7.1). The reconstruction of a mesic climate in Stratum 4d indicates a wetter start of the Holocene, as also indicated from nitrogen isotopes in Equid dentine (Thackeray and Lee-Thorp 1992) and is not challenged by this study. In contrast, the micromammal abundances are argued to reflect a dry and open scrub landscape in Stratum 4d, which then slowly changed into a woodland savannah (Avery 1981, Thackeray 1984). This is also reflected in lower $\delta^{13}C$ values in the grazer and browser enamel in the early Holocene compared to the later Holocene. Pollen, micromammals and enamel isotopes show a grassland expansion from Stratum 4aLH onwards. There is variation in the composition of the grassland, with a suggestion of arid grassland in Stratum 4a. This is strengthened by the low OES $\delta^{18}O$ values in Stratum 4aLH (Lee-Thorp and Ecker 2015). Nitrogen isotopes in dentine have been argued to show a drier mid and late Holocene (Thackeray and Lee-Thorp 1992). A dry and open late Holocene agrees with the OES and enamel stable isotope values from this study, as well as with data from the speleothem next to Excavation 1 (Brook et al. 2010). Pollen and micromammals indicate a wetter Stratum 3b, and in contrast an arid Stratum 3a (Avery 1981, Thackeray 1984, Scott and Thackeray 2015).

The botanical remains in Stratum 5 and the OES and enamel $\delta^{18}O$ results show a wetter and/or cooler event (Bamford 2015). In the lower ESA Strata, micromammal abundances indicate a closed and humid environment followed by drier and more open conditions, but finer resolution is lacking (Avery 2007, Fernandez-Yalvo and Avery 2015). Phytolith data is the best complement for stable isotopes, as they can distinguish finer differences between plant types. Results of phytolith analysis shows Stratum 12 as arid summer rainfall Nama-Karoo grassland, much like in the $\delta^{18}O$ OES results. A shift to cooler conditions and C_3

vegetation dominance occurs in Stratum 11 (Chazan et al. 2015, Horwitz et al. in press), also visible in both the OES and enamel isotopes. In general, all the different proxies agree well with each other, despite small differences which are mainly due to different seasonal and temporal resolution that a proxy represents. Table 7.2 summarizes the emerging picture from combining all available independent records.

In summary, moving from earlier to later periods, in Stratum 12 a semi-arid, open environment with predominantly C_3 vegetation and a small component of C_4 plants existed at Wonderwerk Cave. From 1.78Ma through to 1.07Ma (base of Stratum 10), wetter and cooler conditions prevailed, with a shift to Succulent Karoo vegetation, possibly due to some winter rainfall influence. Within the Jaramillo subchron (Stratum 10), environmental conditions appear to have been unstable and fluctuated greatly. There are extremes of mesic and xeric conditions, associated with swings from a C_3 environment to one dominated by C_4 grasses. Oscillating climatic conditions are also reflected in the geomorphology of Stratum 10 due to the presence of silty clay aggregates. The end of Stratum 10 and start of Stratum 9 show a return to increasingly more arid conditions or more frequent dry spells, resulting in the most arid and open Pleistocene environment in Strata 8-6. Stratum 5 includes evidence of a cold event with more C_3 vegetation. This could be during the Younger Dryas, but the Stratum is not dated well enough to be certain. The early Holocene was semi-arid to arid with more C_3 plant cover than the following mid to late Holocene, where grassland expansion reached a maximum in Strata 4aLH and 4a. The later Holocene until modern times shows an aridification trend with fluctuations, and a dominance of grazers, and the slow increase of the C_3 thornveld of today.

Time period	**Strata and Age**	**Lithic technology**	**Environment**	**Climate**	**Proxy evidence**
Late Holocene	2b, 3a 553-1598 cal. BP	Ceramic LSA	Mostly open C_4 savannah	Aridification trend	Microfauna, macrofauna, OES $\delta^{18}O$, pollen, enamel $\delta^{18}O$ and $\delta^{13}C$
Mid Holocene	4a, 3b, 3a 1598-4416 cal. BP	Wilton (backed bladelets/ chert)	Mostly open C_4 savannah	Aridification trend	Microfauna, macrofauna, enamel $\delta^{18}O$ and $\delta^{13}C$, OES $\delta^{18}O$, pollen
	4aLH, 4a 4362-6075 cal. BP	Wilton (backed bladelets/ chert)	Expansion of C_4 grasses	Fluctuating: Wet-spell, Arid-spells	Microfauna, macrofauna, enamel $\delta^{18}O$ and $\delta^{13}C$, OES $\delta^{18}O$, pollen
Early Holocene	4b, 4c 5786-9336 Cal BP	Wilton (scrapers/ ironstone)	Mostly savannah woodland	Semi-arid	Microfauna, macrofauna, enamel $\delta^{18}O$ and $\delta^{13}C$, pollen
	4d 10416-11844 cal. BP	Oakhurst	Mostly shrubland	Semi-arid to arid	Microfauna, macrofauna, OES $\delta^{18}O$, botanical remains, enamel $\delta^{18}O$ and $\delta^{13}C$
Late Pleistocene	5 <11436 BP	LSA indet./mixed	Shrubland/ woodland	Cold and/or humid	Botanical remains, pollen, OES $\delta^{18}O$, enamel $\delta^{18}O$ and $\delta^{13}C$, macrofauna, geomorphology
Exc. 2 Str. 2	97-220 ka	Early MSA	Savannah with C_4 grasses	Humid conditions	OES and enamel $\delta^{18}O$ and $\delta^{13}C$, macrofauna
Mid Pleistocene	6-8 ?	Late Acheulean	Spread of C_4 grass, open savannah	Semi-arid, summer rainfall, more frequent dry spells	OES $\delta^{18}O$, enamel $\delta^{18}O$ and $\delta^{13}C$, microfauna, macrofauna, eggshell biometry
Early Pleistocene	9 0.99-0.78 Ma	Late Acheulean	Mixed C_3-C_4 savanna	Semi-arid, summer rainfall	enamel $\delta^{18}O$ and $\delta^{13}C$, OES $\delta^{18}O$, phytoliths

	10 0.99-1.07 Ma	Acheulean	Mixed C_3-C_4 savanna, First extreme C_4 values	Fluctuating warm/cold and humid/dry phases; overall more mesic	enamel $\delta^{18}O$ and $\delta^{13}C$, OES $\delta^{18}O$, micromorphology, macrofauna, microfauna, phytoliths, eggshell biometry, sedimentology
	11 1.07-1.78 Ma	Acheulean	Shrubland/ Woodland/succulent Karoo	Cold and/or humid	enamel $\delta^{18}O$ and $\delta^{13}C$, OES $\delta^{18}O$ and $\delta^{13}C$, phytoliths, microfauna
	12 1.78-1.96 Ma	Oldowan	open savanna, small C_4 component	Semi-arid, warm	OES $\delta^{18}O$ and $\delta^{13}C$, enamel $\delta^{18}O$ and $\delta^{13}C$, phytoliths, microfauna, macrofauna

Table 7.2: Summary of changes in climate and vegetation through time inferred from proxy records at Wonderwerk Cave. Dates for Strata 2b to 5 from Table 4.1; for discussion of Pleistocene Strata dates see Chapter 3.

The drivers behind the local changes are most likely a complex mix of the quantity of rainfall and its seasonality, CO_2 of the atmosphere, glacial-interglacial changes and local developments in vegetation composition and animal ecology. It is clear that Wonderwerk Cave was located in a relatively arid and open environment over most of the last two million years, with some mesic phases where the vegetation was more closed and where standing water could persist. Although a summer rainfall regime similar to today (and most of the Holocene) dominated large parts of the sequence, there is more inter-seasonal rainfall influence visible in the Pleistocene. In the Holocene, the strength of the summer rainfall regime varied. This would clearly have influenced the resources available for hominins in the Wonderwerk area, as will be explored in the next section.

7.3 Vegetation change over time

How does the palaeoenvironmental record at Wonderwerk compare with other vegetation records from the summer rainfall zone in southern Africa, and what are possible the drivers

of the observed changes? Aridity is often cited as a driver of C_4 expansion (e.g. Schefuß et al. 2003, Edwards et al. 2010), but there are also records, mainly from pedogenic carbonate isotopes, showing wet phases at the same time as C_4 expansions (Levin et al. 2011, Levin 2015). In the Wonderwerk stable isotope record, there is a general, long-term trend of increasing aridity and increasing C_4 grasses through the Pleistocene and into the Holocene, but there are clear exceptions, where wet phases coincide with increased C_4 (Chapter 7.1). Another driver of variation in C_4 vegetation, besides aridity, has been argued to be timing and amount of rainfall, in particular increasing seasonality (Chapter 7.4; Pagini et al. 1999). Bush fires and disturbance of the vegetation layer by herbivores have also been proven to have a substantial effect on C_4 plant distribution (Bond et al. 2005). This evidence is currently limited to simulation models and charcoal from marine sediment cores. Atmospheric pCO_2, as a direct influence on photosynthesis, is another important factor to consider (Sage 2004, Levin 2015).High-resolution pCO_2 records are available from ice cores, but only reach back to 800ka. New proxies like boron isotopes and alkenones in phytoplankton from marine sediment cores have significantly extended the pCO_2 record to 4Ma recently (e.g. Hönisch et al. 2009, Seki et al. 2010, Bartoli et al. 2011, Zhang et al. 2013). Ségalen et al. (2006) ruled out low pCO_2 as cause for C_4 expansion in the Namib, but this related to periods prior to the Pleistocene. An increased consumption of C_4 grasses over time is visible in the Wonderwerk animals but does not mark the first appearance of C_4 grasses in the region (which was 4-5Ma in South Africa [Osborne and Beerling 2006, Hopley et al. 2007a, Ségalen et al. 2007]). There is some evidence to indicate that there have been times before the Pleistocene when a C_4 grass savannah dominated the southern Kalahari (Ségalen et al. 2006, Kuhn et al. 2015).

C_4 plants are favored when pCO_2 is under 350ppm and growing season temperature is above 25°C (Ehleringer et al. 1997). Ice core pCO_2 records from Antarctica (Fig. 7.7) show

means of 180-300 parts per million by volume (ppmv) for the last four glacial cycles, and 170-260 ppmv from 800ka to 450ka, which are lower mean values than in the late Pleistocene ice core records (Petit et al. 1999, Siegenthaler et al. 2005, Lüthi et al. 2008). A boron isotope record examined by Hönisch et al. (2009) shows pre-MPT (Mid Pleistocene Transition) pCO_2 interglacial values similar to the most recent ones, but pre-MPT glacial values higher than post MPT. According to that study, pCO_2 was relatively stable prior to the mid-Pleistocene transition and was higher afterwards (Hönisch et al. 2009). This could explain the differences in the $\delta^{13}C$ values pre (Strata 10-12) and post MPT (Strata 9 and above) in Wonderwerk (Fig. 7.7). The conditions might not have been ideal for C_4 grasses yet, and C_3 grasses could have existed, especially in glacial times.

With average grazer $\delta^{13}C$ values in Strata 9-12 is below -2‰ and in the rest of the Pleistocene below +2‰, there is little evidence of a dominant C_4 grass component in the local vegetation that would be comparable to today. The Buffalo Cave speleothem record in South Africa shows phases of C_4 expansion at 1.78 to 1.69 Ma (Hopley et al. 2007a). Lee-Thorp et al. (2007) also place the largest shift to open grassy conditions at Sterkfontein and Swartkrans shortly after 2 Ma, possibly in connection with the onset of the Walker circulation. The faunal record reflects remnants of woodland and closed habitat fauna (Cornelian Land Mammal Age [LMA], at 1Ma to 700ka) (Hendey 1974), seemingly confirming this interpretation but shows more wooded grassland components after 700ka in the Florisian LMA (Brink 2005). The sparse South African environmental records between 2Ma and 1Ma therefore agree on a more closed habitat in the early to mid-Pleistocene than in the Holocene with a spread of C_4 grasses happening during the mid-Pleistocene. The Wonderwerk data points to a rather late start at ~800ka for the spread of C_4 grasses, whereas some of the other records place it earlier.

The Middle Pleistocene Strata 6-8 $\delta^{13}C$ values are similar to Excavation 2 Stratum 2 and Excavation 1 Stratum 5 grazer values, which are higher than in the Early Pleistocene, but lower than in the Holocene Strata. The $\delta^{13}C$ data imply an overall continued spread of C_4 grasses. The poor dating of the Middle Pleistocene Wonderwerk Strata does not allows us to create a clear picture of biome changes, or if there were fluctuations back and forth in this trend. Comparable Middle Pleistocene vegetation records from the interior are rare. Gladysvale Cave, situated at the interface of the grassland and savannah biomes, has an episodic dated sequence from 570ka to 7ka. Fluctuations without a clear trend are visible in the $\delta^{13}C$ flowstone record, and C_4 grasses were present in varying parts throughout the sequence. As $\delta^{13}C$ does not appear to be connected to the $\delta^{18}O$ flowstone record, the authors suggested that more than glacial-interglacial differences must have driven vegetation changes (Pickering et al. 2007). Wonderwerk Stratum 5 is supposedly of Late Pleistocene age, and documents a cold shrub/woodland, a significantly different vegetation than found in the region today (Chapter 7.2). Pollen from nearby Equus Cave also indicate dry woodland and lower temperatures before 17ka (Scott et al. 2012). Stratum 5 could fall within the Younger Dryas, where pollen records indicate dry conditions in the Northern Cape (Scott et al. 2012).

The early Holocene pollen and enamel $\delta^{13}C$ record in Wonderwerk indicates more C_4 grasses in the local vegetation than were found in the Pleistocene Strata, but more C_3 plants compared to the mid-late Holocene. Rose Cottage Cave, in the Free State, is another site in the grassland biome with lower $\delta^{13}C$ values for large herbivore enamel in the early Holocene (Smith et al. 2002). Pollen from east of Wonderwerk at Wonderkrater, Rietvlei, Tata Vonde and Tswaing Crater indicates a spread of Kalahari thornveld at this time (Scott 1993, 1999). Blydefontein rockshelter shows an abundance of C_3 Asteraceae charcoal to

8.7kyr and at 7.1kyr (Bousman 1991), further indicating variation but overall a persistence of a significant C_3 component in the vegetation.

Only in the mid-Holocene (Stratum 4aLH and higher) do $\delta^{13}C$ values in Wonderwerk reach up to 4‰ and support at the same time both hypergrazers ($\delta^{13}C$ >2‰), as well as hyperbrowsers ($\delta^{13}C$ <-12‰). With CO_2 values in the mid-Holocene reaching a low of <260 ppm (Monnin et al. 2001), C_4 grasses had a greater advantage and could spread (Fig. 7.8). In the mid-Holocene, from Stratum 4aLH upwards, there is also the re-appearance of the specialized grazer *R. fulvorufula* as well as *A. marsupialis*. Further evidence for an increased mid-Holocene spread of C_4 grasses comes from grassland pollen in records in the central Namib (Scott et al. 1991) and is also corroborated by high $\delta^{13}C$ in grazers from Rose Cottage Cave (Smith et al. 2002). A spread of savannah into the grassland biome is interpreted in the Rietvlei Dam pollen sequence (Scott and Vogel 1983), indicating biome shifts for a limited time period in the mid-Holocene.

In the later Holocene (Strata 3a, 3b), carbon isotope values for browsers like *R. campestris*, Tragelaphini and *A. marsupialis* shift even further into the pure C_3 range with lower carbon values than in the early to mid-Holocene. At the same time, grazers and pollen records indicate an abundance of C_4 in the environment. The Holocene was therefore not a stagnant period in the interior of southern Africa, but fostered the development of the modern niches of grazers and browsers. Rising CO_2 levels would further explain the retreat to more woody cover during recent times. The connection of rising CO_2 in the atmosphere and tree cover in South Africa has been demonstrated in the laboratory (Kgope et al. 2010) and in long-term outdoor experiments (Buitenwerf et al. 2012). C_3 plants showed increased stem growth and re-sprouting with higher CO_2 levels, whereas C_4 grasses showed no reaction in productivity (Kgope et al. 2010). It was also noted that semi-arid and mesic savannahs did not react in the same way (Buitenwerf et al. 2012), showing that different conditions need

to coincide to reach a threshold. The third possible driver of the stable light isotope values, rainfall amount and seasonality, can be explored by looking at the trends in both $\delta^{13}C$ and $\delta^{18}O$ isotope values, which is the topic of the next subchapter.

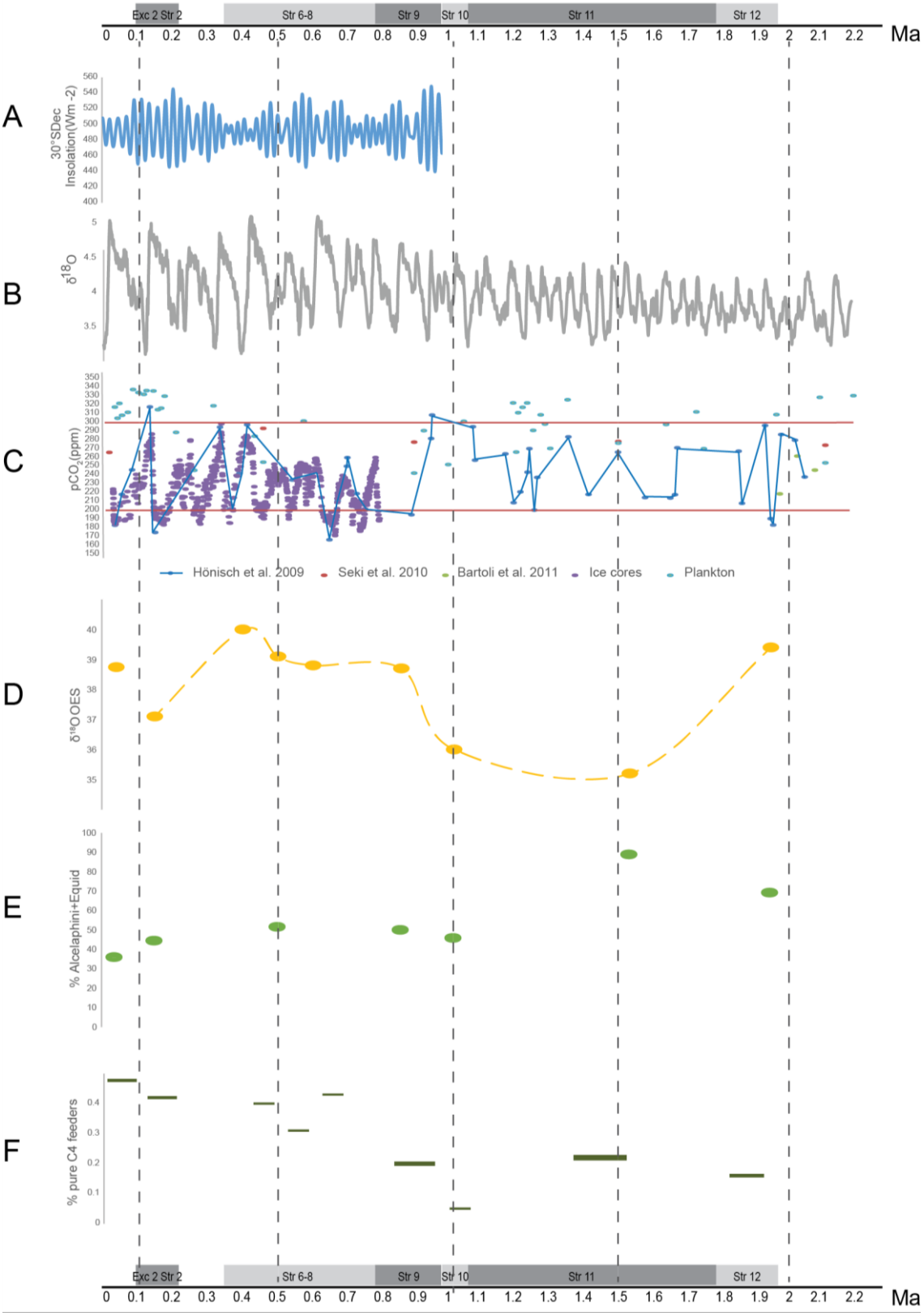

Figure 7.7: Climate parameters of the last 2.2Ma and Wonderwerk Cave data for Excavation 2 Stratum 2, Excavation 1 Strata 6-12 and a mean value of the Holocene Strata. A: December insolation at 30°S (Berger 1992); B: $\delta^{18}O$ (‰) from the LR04 stack of benthic

foraminifera (Lisiecki and Raymo 2005); C: pCO_2 records including boron isotope data (from Hönisch et al. 2009, Seki et al. 2010 and Bartolli et al. 2011), ice core data from Antarctica (from Monnin et al. 2001, Lüthi et al. 2008, Siegenthaler et al. 2005, Petit et al. 1999) and plankton data (from Seki et al. 2010, Zhang et al. 2013), red lines at 300ppm and 200ppm to visualise extreme high and low values; D: $\delta^{18}O$ (‰) in OES from Wonderwerk Cave (this thesis, Ecker et al. 2015); E: percentage of Alcelaphini and Equids compared to all herbivores per stratum; F: percentage of specimens with a predominantly C_4 diet per Stratum (this thesis).

7.4 The climate record over time: aridity and wet phases

$\delta^{13}C$ and $\delta^{18}O$ values are influenced by different sets of parameters, but linked as both are influenced by hydrological conditions. For example, atmospheric pressure CO_2 drives marine $\delta^{18}O$ variations (Hopley et al. 2007b). This effects tropical vegetation as well as precipitation, whereas precipitation in turn effects vegetation again (Huang et al. 2001, Schefuß et al. 2003). In the tropics, rainfall amount is dominated by the precessional cycle, and $\delta^{18}O$ values in speleothems have been linked to insolation as a proxy of monsoon intensity. Insolation maxima reflect more humid periods compared to dry insolation minima (Hopley et al. 2007a,b, Levin 2015).

Another factor to consider in the Wonderwerk region is the influence of winter rainfall. Today the region is 450km from the border of the winter rainfall region in the west, but several researchers proposed expansions of the winter rainfall region during the glacials (van Zinderen Bakker 1976, Cockcroft et al. 1987, Chase and Meadows 2007). The amplitude and geographical extent of the proposed expansions and contractions is still debated (e.g. Chase et al. 2010). One proposed driver for such a shift is sea surface temperatures (SSTs) in the Indian Ocean, as the modern control of summer rainfall, opposing ideas of direct orbital forcing as the main influence. Singarayer and Burrough

(2015) reviewed all studies for this region, however, the picture seems complex without one particular forcing mechanism standing out.

In the Pleistocene (including Excavation 1 Stratum 5 and Excavation 2 Stratum 2), no $\delta^{18}O$ mean values are above 36‰ (except for *Antidorcas* sp. in Stratum 6). The lowest $\delta^{18}O$ mean values in all species are in Strata 9-12 (25.7‰ to 31.7‰), with the values for Alcelaphini and Equids in Stratum 11 significantly different compared to the same taxa in the Holocene Strata ($p<0.05$; Appendix 7.6). As noted above, reasons for the low $\delta^{18}O$ values can be glacial conditions, increased humidity or changes in the rainfall season and source. For the Pleistocene, the LR04 stack (Fig. 7.7) interglacial $\delta^{18}O$ are comparable over the last 2Ma, but glacial values are around 4.3‰ pre-MPT and around 5.1‰ after. This is linked to the pCO_2 record from Hönisch et al. (2009). The less extreme glacial periods could reflect less sea ice extent and/or warmer SSTs. This is another explanation for the visible difference in isotopes between Strata 12-10 and later periods. Stratum 12 does not have lower $\delta^{18}O$ values in the OES record. It falls within the Olduvai subchron, which over its timespan has not as extreme glacial-interglacial maxima and minima, compared to the rest of the Pleistocene. This could be one reason for the rather arid signal, although high eccentricity cycles in this time period are possibly linked to intensification of the Walker circulation. Geomorphological evidence for aridity ~2.5-1.7Ma comes for example from the Makgadikgadi palaeo-lake in the northern Kalahari (Moore et al. 2012).

Stratum 11 on the other hand is almost certainly cooler, and possibly influenced by winter rainfall. MIS 25 at 950ka shows especially high pCO_2 from boron isotope (Hönisch et al. 2009), as well as extremely warm interglacial SSTs (Medina-Elizalde et al. 2005), and falls into the period of Stratum 10 and early Stratum 9, where the Wonderwerk record shows extreme variability in both $\delta^{13}C$ and $\delta^{18}O$ values, including some high C_4 values. The resolution of the archaeological Strata in Wonderwerk is not fine enough to test the orbital

parameters of eccentricity, obliquity and precession against the enamel isotope data, as has been done for example in the Makapansgat speleothem (Hopley et al. 2007a). The $\delta^{18}O$ in this speleothem have been linked to the precession cycle, while $\delta^{13}C$ followed a obliquity signal. In general, this speleothem record shows a gradual increase in $\delta^{18}O$ from the Plio-Pleistocene to the middle Pleistocene and an increase to the Holocene record at Cold Air Cave (Hopley et al. 2007a+b). This result resembles those from a study on tufas on the Ghaap Escarpment (Doran et al. 2015) and the OES and enamel $\delta^{18}O$ record from Wonderwerk Cave. Further evidence for a change in hydrological regimes over southern Africa at the MPT is provided by a core from Lake Malawi (Lyons et al. 2015). In this study, high lake levels are associated with high eccentricity. After the MPT, there is evidence for higher variability, wetter climate than before, but also for prolonged dry episodes at Lake Malawi (Lyons et al. 2015). Although there is a substantial distance between Wonderwerk Cave and Lake Malawi, both studies propose a change in larger atmospheric circulation patterns around 800ka.

Excavation 2 Stratum 2 is only roughly constrained to 220-97ka, therefore potentially spanning the glacial MIS6 and/or the last interglacial MIS5e, which had warmer conditions than today. The $\delta^{18}O$ mean values for all species are above 30‰ (except *H. africaeaustralis* and *C. simum)* which might suggest interglacial conditions. The species *Antidorcas* sp., *H. africaeaustralis* and *K. leche* show high variability in $\delta^{18}O$, possibly an indication of mixed signals or palimpsests (Hopley and Maslin 2010). *K. leche* in itself is an indicator for a significantly wetter environment than today. The Tswaing Crater record to the east of Wonderwerk indicates wetter conditions at the MIS6/7 interface and higher rainfall than today in MIS5e. The Florisbad fauna and pollen too suggest a wet initial occupation of the glacial MIS6 and a rainfall maximum at 157ka, but also modern sub-arid conditions in later MIS6 (Brink 1988, van Zinderen Bakker 1989). Pollen from marine core GeoB1711-4 off

Namibia shows cool and moist conditions, interpreted as an extension of the winter rainfall zone at this time (Shi et al. 2001). Therefore, there is evidence elsewhere of more humid conditions in the Excavation 2 Stratum 2 timeframe, but as the dating is rather broad the evidence might also indicate fluctuations. Excavation 1 Stratum 5 shows high $\delta^{18}O$ mean values in Alcelaphini (mean 35.3‰, n=2), Equids (mean 31.2‰, n=3), *H. africaeaustralis* (mean 28.7‰, n=2) and *R. campestris* (mean 34.4‰, n=3), whereas the Stratum 5I OES $\delta^{18}O$ values are low. As absolute dates for this Stratum are so broad, and the archaeological material shows no clear affiliations to any industry, one explanation might be mixing of sediment from a late Pleistocene short cold phase with a late Pleistocene/early Holocene warming phase (Hopley and Maslin 2010).

All the Pleistocene Strata span glacial and interglacial periods, and the oxygen isotope values are therefore most likely an averaged value. In the Holocene Strata the $\delta^{18}O$ means of all species are higher than in the Pleistocene Strata and are always above 30‰, with only *P. capensis* and *H. africaeaustralis* under 30‰. The highest values are in Stratum 4aLH, where mean oxygen isotope values are above 36‰ and in *P. capensis* and *H. africaeaustralis* above 30‰ respectively. This shows the Holocene, judging by comparison of $\delta^{18}O$ values of herbivore enamel, as drier than the previous Pleistocene periods at Wonderwerk. Higher mean $\delta^{18}O$ in the EDML Antarctic ice core in the first half of the Holocene and equally higher SSTs in the marine core GeoB9307-3 (Zambezi basin) (Fig. 7.8) might point to the Indian Ocean SSTs as a driver to explain the high $\delta^{18}O$ enamel isotope values in the Wonderwerk Holocene record. In general, the Holocene climate conditions seem highly variable, and it is unknown in which ways the Holocene represents or does not represent a typical interglacial.

A systematic review of the Holocene climate in the interior finds that conditions were general warm and/or arid at the start of the Holocene; with warmer and wetter conditions

7-5ka and an aridification trend after 5ka (Scott and Lee-Thorp 2004). This matches with the Wonderwerk OES $\delta^{18}O$ record. Another review of pollen records proposes signs of increased moisture at 7-8ka at several sites (Scott et al. 2012). The duration of increased mid-Holocene moisture is impossible to constrain from the published records, but the signal also shows up in Wonderwerk in pollen and OES $\delta^{18}O$. At Wonderwerk, fluctuations seem especially high in Strata 4b/4aLH (~5.4-7ka cal BP), including a wet spell (OES $\delta^{18}O$), high enamel $\delta^{18}O$ and increased C_4 consumption in grazers as well as browsers (enamel $\delta^{13}C$). At the same time, the summer insolation at 30°S (Wonderwerk is at 27°S) is on the threshold changing from minimum to maximum (Fig. 7.8), possibly further helping the manifestation of the strong summer rainfall regime today, which might not have been fully established until the mid-Holocene. Around 2-3ka most interior records show a dry event with reduced summer rainfall (reviews in Nicholson et al. 2001, Scott et al. 2012). In Wonderwerk, the browser *R. campestris* and the Tragelaphini have significantly higher $\delta^{18}O$ isotope values in Strata 3a and 3b compared to the early and mid-Holocene, possibly reflecting increased evapotranspiration ($p<0.05$; Appendix 7.6). The OES $\delta^{18}O$ values suggest maximum aridity around 2ka. Climate records for the last two millennia are available in high resolution, and show a large amount of temporal and spatial variability, which most certainly existed earlier but is not visible due to the nature of the proxy records.

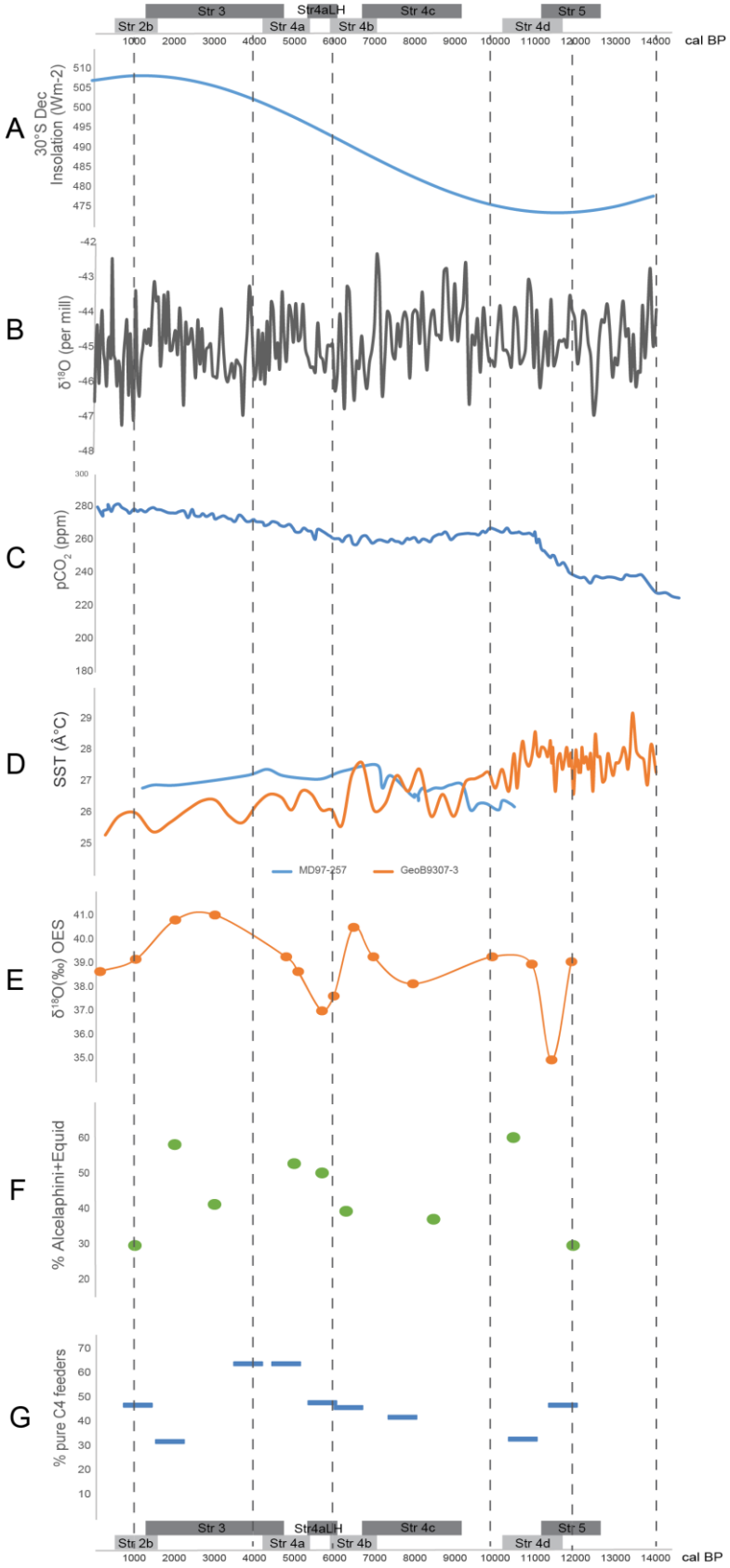

Figure 7.8: Climate parameters of the last 14,000 years and Wonderwerk data for Strata 2b to 5. From top to bottom: A: December insolation at 30°S (Berger 1992); B: calculated

$\delta^{18}O$ (‰) from the EDML ice core (EPICA community members 2010); C: pCO_2 from EPICA Dome C ice core (Monnin et al. 2006); D: sea surface temperatures calculated from alkenones from cores MD79-257 (Leduc et al. 2010) and lipids from core GeoB9307-3 (Schefuß et al. 2011); E: $\delta^{18}O$ (‰) in OES from Wonderwerk Cave (Lee-Thorp and Ecker 2015, this thesis); F: percentage of Alcelaphini and Equids compared to all herbivores per Stratum (this thesis); G: percentage of specimen with predominantly a C_4 diet in each Strata (this thesis).

7.5 Evaluation of the archaeological record of Wonderwerk Cave against the environmental record

The connection of environmental changes and human evolution has been debated for decades (Chapter 1). Potts (2013) argues for major events in lithic technology and behaviour of hominins being linked to phases of increased habitat instability. Most importantly, he notes that it is that not one aspect but the impact of a whole range of parameters that triggered changes. He makes his argument for East Africa, but his hypothesis will be tested here for the Wonderwerk region in South Africa. The null hypothesis is that environmental change does not affect human evolution and can take place independently (Potts 2012a).

Early Stone Age sites in South Africa are extremely difficult to date since the majority are open air sites, and often lack associated fauna and other organic remains. Moreover, many assemblages are from little documented contexts. Therefore, little is known about the spatial and temporal variability of sites in the Oldowan and Acheulean. Recent research focussed on two areas: the Kuruman hills around Wonderwerk Cave, and the 'Cradle of Humankind' sites near Pretoria, including Sterkfontein and Swartkrans. The Oldowan in Wonderwerk Stratum 12 shows technological similarities to Swartkrans Members 1-3 and Sterkfontein Member 5. Wonderwerk Stratum 11 is contemporaneous with the onset of the Acheulean in East Africa as well as with the flake-based Early Acheulean industry of

Sterkfontein (Chazan et al. 2008), although the dating for the onset of many lithic industries is currently being reconsidered (e.g. Granger et al. 2015). The Wonderwerk ESA Strata in Excavation 1 have a low artefact density (Chazan et al. 2008), with little anthropogenic material in the geological matrix (Goldberg et al. 2015). All raw material is local banded ironstone, with some evidence of stone tool production on site (Chazan 2015). This points to the use of Wonderwerk Cave not as a main camp site, but rather as an opportunistically used shelter or location used for special purposes by small groups of hominins. This is in marked contrast to the nearby ESA sites of the Kathu complex on the western side of the Kuruman hills. Kathu Townlands for example is a production site featuring hundreds of thousands of handaxes in all stages of production next to raw material outcrops (Walker et al. 2014). This could reflect the use of the same landscape by hominins for diverse purposes.

Stratum 11 shows marked climatic and environmental differences to Stratum 12, but the resolution of the two is too coarse to allow testing as to whether those changes are related to the technological change from Oldowan to Acheulean in the area. This globally occurring shift in technology has many suggested drivers, including climate instability, competition with new hominin forms and independent development in several places. Climatically, this time period (~1.7Ma) marks the onset of the Walker circulation (Chapter 2). An expansion of C_4 grasses in South Africa has been linked to this phenomenon (Hopley et al. 2007a, Lee-Thorp et al. 2007), an argument strengthened by the increase of grazing bovids in East and South Africa (Vrba 1995, Bobe and Behrensmeyer 2004). In East Africa, this has been identified as one period of climatic instability, including evidence of aridity from dust records (deMenocal 2004) and soil isotopes (Wynn 2004), and evidence for wet conditions from high lake levels (Trauth et al. 2005). The evidence for highly fluctuating climate in the Wonderwerk area is stronger at the time of the Mid Pleistocene Transition, ~1Ma, in Stratum 10. This includes stable isotope proxy evidence, ostrich eggshell biometry, faunal

abundances, phytoliths, and the Mamatwan mine sedimentary record. The first clear Acheulean industry is present in this stratum. Evidence for the intentional use of fire in Stratum 10 (Berna et al. 2012) shows another innovation. Further evidence for fire is argued for the Cradle site of Swartkrans Member 3 (Brain and Sillen 1988). Again much more research into the timing, origin, use and spread of fire is needed to find the driver behind this major step in human evolution. Unfortunately, the poor archaeological and environmental record for this time period in southern Africa further hinders testing of this hypothesis. One of the sparse environmental evidence from this time period are sea level fluctuations (Compton 2011). In East Africa, this time period shows variability with dust records denoting arid conditions (deMenocal 2004, Donges et al. 2011) and high lake levels (Trauth et al. 2005, 2015). Extinction of robust Australopithecines around 1.2Ma (Potts 2013) and increasing brain size in *Homo* species (Shultz et al. 2012) have been linked to this phase, but there is no substantial review of the cultural records of this time period to indicate significant changes in technology.

Archaeologically, the time period ~780-350ka marks the introduction of blade production, the appearance of prepared core reduction strategies and possibly the proliferation of regional traditions (Wilkins and Chazan 2012). It is proposed that increased climate variability at the Mid Pleistocene transition increased selective pressures for behavioural adaptability (Potts 1998). These technological changes are not visible in the lithic record from Excavation 1 Strata 9 to 6 which features a handaxe-dominated Acheulean technology, and in general low find density. One explanation might be that deposits younger than 500ka are missing in Excavation 1 (Matmon et al. 2012). Possible lithic innovations come from Excavation 6, Excavation 2 Strata 3-4 and from the site of Kathu Pan 1, which have levels younger than 500ka, but these assemblages are not fully analysed

as yet. Another aspect are the large number of juvenile specimens in the Wonderwerk Pleistocene Strata, which might suggest seasonal activities.

The lithic MSA assemblage in Wonderwerk is not published as yet, but is tentatively described as early MSA. Its preliminary dating does not allow speculation as to its start and end. Although there is a wet phase within this time period, as evident from the faunal record, further analysis of the archaeology and dating of this section is needed before comparing the archaeological and environmental record. The same applies to Excavation 1 Stratum 5, the cultural assemblage of which is currently undescribed but appears to represent a lag deposit resulting from an erosional event (Chazan and Horwitz 2015).

The first Holocene lithic industry appears in Stratum 4d, the Oakhurst, and is significantly different in technology compared to the overlying Wilton. While the Oakhurst has large scrapers of local banded ironstone, small microlithic scrapers and bladelets dominate the Wilton assemblage (Thackeray 1981). Environmental proxies tentatively indicate more arid bush and scrub in Stratum 4d and more semi-arid savannah woodland in Stratum 4c. The low artefact and faunal density in Stratum 4d and the possible hiatus identified through the tighter chronology using new radiocarbon dates and Bayesian modelling (Chapter 4) point to the possibility that new groups of hunter-gatherers came into the region, connected or unconnected to the environmental change.

A shift in the percentage of the dominant raw material and tool types appears in the mid-Holocene, where more bladelets on chert are found from Stratum 4aLH onwards, together with a higher artefact density (Thackeray 1981). This change has been noted at other Wilton sites in South Africa, and attributed to the adoption of different hunting strategies during the mid-Holocene climatic optimum. At Wonderwerk, a wet episode followed marked by increasing grassland and an increase in grazing species, such as it might be connected to a

change in hunting strategy or seasonal use of the cave. Strata 4aLH and 4a have the highest densities of cultural artefacts in any deposit at Wonderwerk Cave (Thackeray 1981). The wet spell and expansion of grassland must have improved the resource availability for hunter-gatherers at this time, such that they made more intensive use of the cave and/or increased their population numbers. Another development is the introduction of ceramics during the Wilton in Strata 3a and 2b (Thackeray 1981), showing that the hunter-gatherers might have been in contact with herders, who spread from Central to southern Africa during this time. Proxies from Wonderwerk Cave and other records show high aridity around 2000BP, which would have influenced the resources available for hunter-gatherers as well as the herders and their livestock.

In conclusion, periods of changing (Stratum 12 to 11) or highly variable climate and environment (Stratum 10) in Wonderwerk fall within periods of climatic instability as identified by Potts (2013). Still, the Wonderwerk lithic assemblage is currently too small to pinpoint developments to a specific point in time. Forthcoming excavation, analysis and publication of the Wonderwerk cultural record might enable us to re-think this question in the near future. The time period between 800ka and 100ka currently lacks a corpus of well dated archaeological assemblages as well as good proxy environmental records for South as well as East Africa and should be a focus of future research. In the Holocene, higher temporal resolution indicates phases of environmental change coinciding with changes in the cultural record at several times.

7.6 Conclusion

In combining the two independently created stable isotope records on OES and herbivore enamel, it has been possible to show different aspects of the changes occurring in Wonderwerk Cave over time. As both materials have strengths and weaknesses for certain

parameters, the combination of both enhances the study. Combining the results with other researchers' findings from Wonderwerk, a coherent record of Holocene and Pleistocene changes emerges. The Pleistocene shows a general trend of increasing aridity and increasing C_4 plants in the diet of grazer species, but with phases of increased humidity (Excavation 1 Stratum 10 and Excavation 2 Stratum 2), and phases with a shift to cooler, C_3 conditions and/or increased year-round rainfall (Strata 11 and 5). Other regional records agree with biome and rainfall shifts in the Pleistocene, and especially with increased moisture in the southern Kalahari at the Mid Pleistocene transition.

The Holocene shows conditions unlike any documented for the Pleistocene Strata, with the modern savannah ecosystem and strong niche separation of species in its final stages of development. Overall, records show the Holocene as a dynamic period, with wetter mid-Holocene conditions and increasing C_4 grass cover, as well as a clear trend to aridification at about 2ka. Major influence on climate and environmental change over the last 2Ma are most likely a combination of pCO_2 and amount of rainfall and its seasonality. The data also demonstrate that regional developments are important, and inter-region comparisons are only possible on the scale of general trends.

A finer chronology is needed to explore what impact those environmental changes had on local hominin populations. Nearby sites with evidence for standing water at times might have served as more attractive habitats for humans and mammals than Wonderwerk Cave, which in comparison has a low find density in Excavation 1. As the only big cave site in the Kuruman hills, Wonderwerk offers shelter and an excellent viewing point over the Ghaap Plateau. Evidence for standing water around Wonderwerk is also starting to emerge (Goldberg et al. 2015). Wonderwerk Cave is therefore a unique site and has been of changing significance in the past.

Chapter 8 - Comparison to other relevant studies

The aim of this chapter is to bring the Wonderwerk data into a wider regional context and especially to compare them to other relevant stable isotope studies (Table 8.1). There is a growing amount of contemporaneous enamel isotope data from South Africa as well as East Africa. Fewer studies exist using OES stable isotopes as a proxy in the Pleistocene; these are discussed in Chapter 5.

Comparative records			
Time	Wonderwerk Cave	South Africa	East Africa
Holocene	Exc. 1 Str. 1-4d	Kareepan, Equus Cave; Caledon River sites; Blydefontein Rock Shelter	
>12ka and <30ka	Exc. 1 Str. 5	Equus Cave; Caledon River sites, Erfkroon	
30-100ka			Lake Victoria MSA sites, Kenya
200-100ka	Exc. 2 Str. 2	Florisbad Spring	
200-300ka		Bundu Farm; Florisbad Spring	
>350ka	Exc. 1 Str. 6-8	Kathu Pan 1	Asbole, Ethiopia
0.99-0.78Ma	Exc. 1 Str. 9	Kathu Pan 1; Cornelia-Uitzhoek	
1.07-0.99Ma	Exc. 1 Str. 10	Mamatwan mine lake; Kathu Pan 1; Ghaap Escarpment tufa, Cornelia-Uitzhoek	Turkana Basin, Kenya
1.78-1.07Ma	Exc. 1 Str. 11	Mamatwan mine lake; Kathu Pan 1; Swartkrans Member 2; Sterkfontein member 5C	Turkana Basin, Kenya
1.96-1.78Ma	Exc. 1 Str. 12	Gondolin Caves; Swartkrans Member 1, Sterkfontein member 5B	Turkana Basin, Kenya; Kanjera South, Kenya; Olduvai Bed II, Tanzania
2.5-2.0Ma		Sterkfontein Member 4	Turkana Basin, Kenya
3.0-2.5Ma		Makapansgat Member 3	Turkana Basin, Kenya; Laetoli, Tanzania
>3.0Ma			Turkana Basin, Kenya; Dikika, Ethiopia; Laetoli, Tanzania

Table 8.1: Table of sites mentioned in this chapter, whose stable isotope or relevant environmental data are compared to Wonderwerk Cave. Sites are listed broadly chronologically, as are the Wonderwerk Strata.

8.1 The Northern Cape

There are no long-sequence sites like Wonderwerk Cave in the Northern Cape Province. There are numerous ESA assemblages but most are from surface scatters with no associated organic remains that can serve as palaeoenvironmental proxies. There are even fewer MSA sites. Equus Cave, a karstic infill site, is an exception. It has several environmental proxy records (Scott 1987, Lee-Thorp and Beaumont 1995, Johnson et al. 1997), but its sequence is short and poorly dated and much of the material may not be anthropogenic in origin. Later Stone Age research has traditionally focussed on exploring case studies, but has not benefitted from the same level of ongoing research, dating and interdisciplinary approaches used in Wonderwerk Cave, although new research has commenced in the region, for instance at Kathu Pan and other places (Chazan et al. 2012, Walker et al. 2014, Doran et al. 2015). The following discusses Northern Cape sites in chronological order from older to more recent and explores how their assemblages can be compared to, and combined with, the Wonderwerk data to create an environmental record for the broader region.

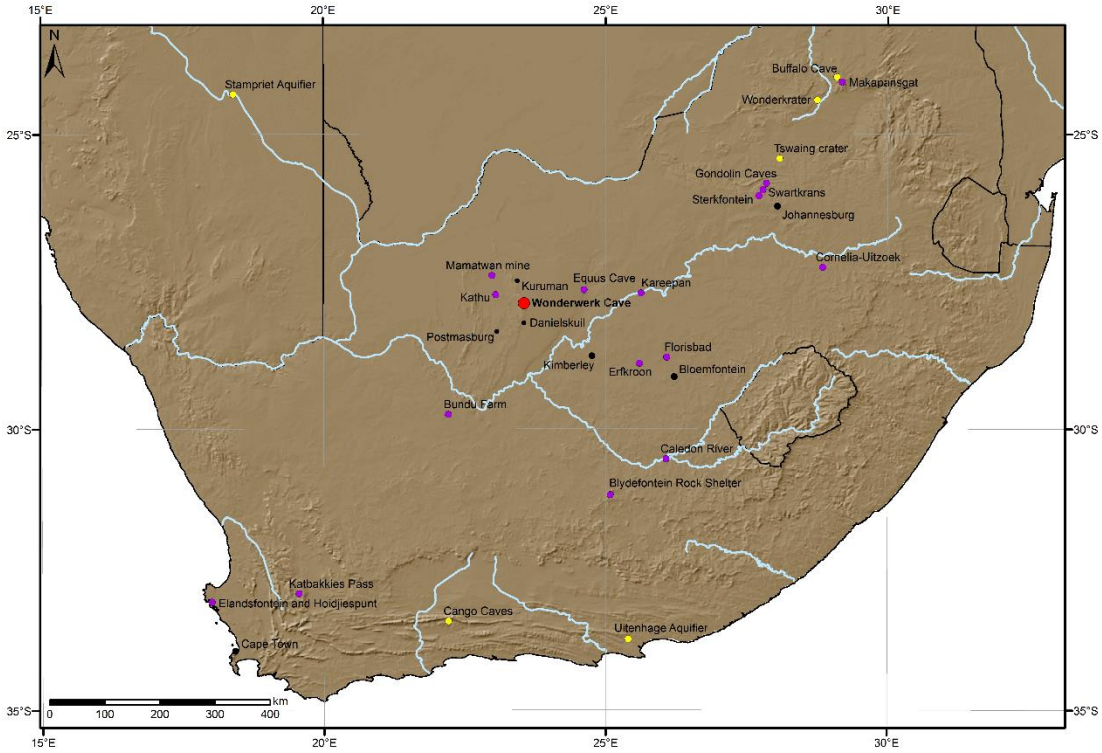

Figure 8.1: Location of comparison sites mentioned in the text (purple) in relationship to Wonderwerk Cave (red), modern towns and cities (black) and selected sites with major environmental archives in southern Africa (yellow).

The modern Mamatwan mine is located 80km north of Wonderwerk Cave (Fig. 8.1) between the Kuruman and the Langeberg hills. The profile opened by modern mining activity was used for cosmogenic ^{10}Be and ^{26}Al dating and analysis of the Kalahari group sediments (Matmon et al. 2015). The study found that a large shallow water body had existed for at least 450 thousand years in the area, before the basin rapidly filled with sand at 1.0-1.2Ma. Similar cycles might have taken place earlier, but most evidence has been eroded, with only remnants of earlier basins and deposition events archived in the sediments of Stratum 12 in Wonderwerk (Matmon et al. 2015). Suspected drivers for the rapid change around 1 Ma are speculative and include increased erosion and sediment transport triggered by the Mid Pleistocene Transition. Similar processes are known in the Kalahari, for example from Palaeolake Etosha in Namibia (Miller et al. 2010). The presence

of the Mamatwan mine water body is contemporaneous with the Kathu and Wonderwerk Acheulean industries (Matmon et al. 2015). This freshwater lake might have been an important habitat for early *Homo*, as may have also been the case for the East African lakes in the rift system (Trauth et al. 2007, Maslin et al. 2014). The area west of the Kuruman hills was, similarly, attractive for hominins and mammals through the pans and springs around the modern town of Kathu. Wonderwerk, on the other side of the Kuruman hills, might have had less large fresh water sources available. Exceptions are Boesmansgat, a sinkhole 15km to the south, and a freshwater seep some 5km to the south in the Kuruman hills (Beaumont and Vogel 2006).

The Kathu complex is located about 50km from Wonderwerk (Fig. 8.1) as the crow flies, west of the Kuruman hills. The main site, Kathu Pan (KP), consists of eleven localities, excavated between 1978 and 1990 by P. Beaumont (Beaumont 1990b, 2004) and since 2004 by M. Chazan. KP1 main site is a former spring vent with ESA, MSA and LSA Strata (Table 8.2).

Stratum	Technology	Age	Dating method	Reference
1	Wilton and Albany	10±0.6ka	Radiocarbon	Beaumont 1990b, 2004
2	Undefined LSA	16.5±1ka	Radiocarbon	Beaumont 1990b, 2004
3	MSA	291±45ka	OSL	Porat et al. 2010
4a	Fauresmith	~ 500ka	OSL and ESR	Porat et al. 2010
4b	Acheulean	?	Undated	Beaumont 1990b, 2004

Table 8.2: Stratigraphy, age and lithic technology of Kathu Pan 1.

The faunal MSA assemblage is small and dominated by grazers. Grazer and hippo remains indicate a grassy savannah and permanent water in the Fauresmith Stratum 4a. In contrast,

the Acheulean Stratum 4b is dominated by dental remains of *Elephas recki* (Klein 1988). The faunal assemblage has a different structure to Wonderwerk with water-dependent *Hippopotamus amphibius*, as well as *C. simum*, *Giraffa* sp., *Hippotragus* sp., *Syncerus caffer* and *Pelorovis antiquus*. The perennial presence of water in the pans and a general water table just 2-3m under the surface in the past provided seasonal water sources in the region, and supported herds of large animals, possibly making it a core area of hominins whereas Wonderwerk Cave remained on the periphery. This idea is further consistent with evidence from the site of Kathu Townlands, a massive surface of more than hundred thousand scattered Acheulean artefacts (Walker et al. 2014), compared to low find density in the Wonderwerk ESA strata.

Holocene pollen was analysed from site KP2, about 100m from KP1. The non-stratified test pit was divided into pollen zones by van Zinderen Bakker. Zone III is attributed to the time range 2.7ka to present and has a grassland spectra which implies locally wet conditions. Pollen from Zone II (~ 2.7 - 4.5ka) indicates a drier climate with no trees and wet habitat species. Zone I (~ 4.5 - 8.0ka) indicates grassland with varied tree cover, and warm and wet climate (Morris and Beaumont 2004). The sparse documentation and the presence of only four radiocarbon dates on peat samples (Beaumont 1990) restrict the usefulness of this pollen record. The other KP sites, as well as the newly discovered ESA site of Bestwood (Chazan et al. 2012), have not revealed environmental data to date.

New investigations into tufas in the nearby Ghaap Escarpment found Strata dating to the Jaramillo event ~1.05-0.8Ma. The level is therefore contemporaneous with Wonderwerk Stratum 10, and also contains the wetland species *K. leche* (Doran et al. 2015). The Ghaap Escarpment rockshelters were also surveyed by Humphrey and Thackeray (1983), who found several LSA sites. These sequences are shorter than Wonderwerk and no comprehensive environmental reconstructions have been undertaken. The site of Bundu

Farm (Fig. 8.4) in the nearby Nama-Karoo biome is a pan site, with faunal remains and lithics roughly dated to 200 - 300ka. The mix of faunal species is similar to the grassland site of Florisbad and includes the extinct *E. capensis* and *M. priscus*, as well as *A. bondi*. The fauna is mainly associated with grassland, which would mean increased or more regular rainfall than today and cooler temperatures (Kiberd 2006). This could also have affected Wonderwerk Cave, but the time period 200-300ka is only marginally represented by lower Excavation 2 Stratum 2.

One of the geographically closest comparable sites to Wonderwerk Cave is Equus Cave, a collapsed cave and former hyena den located east of Wonderwerk on the Ghaap Escarpment (Fig. 8.1) near Taung. Environmental information is available from stable light isotope analysis in OES (Johnson et al. 1997, also Chapter 6) as well as equid enamel (Lee-Thorp and Beaumont 1995), and a pollen record (Scott 1987). The sequence spans the last >30,000 years, but the stratigraphy is problematic because of movement of material (Johnson et al. 1997). Artificial subunits 1a, 1b, 2a and 2b make up the 2.5m of deposit. Radiocarbon dates suggest a Holocene age for Stratum 1a, and a late Pleistocene/early Holocene age for 1b. A pilot study with equid enamel (Lee-Thorp and Beaumont 1990), followed by a larger study on four grazer (*A. bondi, M. priscus, E. capensis, E. quagga*) and two mixed-feeding to browsing species (*A. marsupialis, S. grimmia*) revealed the expected niche separation of browsers and grazers (Lee-Thorp and Beaumont 1995). Grazers never switched to a C_3 diet, which the authors used as proof that the winter rainfall zone never extended that far inland. Possible phases of more regular year round rainfall influence were identified in levels 1b, 2a/2b interface and lower 2b (Lee-Thorp and Beaumont 1995).

It is clear from the records reviewed that there were substantially more mesic phases in the southern Kalahari region in the past compared to today. The occurrence, at various points in time, of standing water bodies that could persist stands out, as they would attract herds

of large mammals as well as hominins (Chapter 7.5). One driver could be a change in rainfall seasonality, with more year-round rainfall supporting a C_3-C_4 mixed savannah, an ecosystem not found anywhere in Africa today. Another possibility is less evaporation in the dry season, which could also be achieved by multiple rainy seasons throughout the year. The following section will explore if this is a regional trend, or mirrored in other regions of southern Africa's interior, by comparison to other stable isotope studies.

8.2 South Africa's interior

Stable isotope studies of Pleistocene environments in the summer rainfall region have focussed on two different landscapes, the Cradle of Humankind sites in Gauteng, and the grassland biome sites of the Free State. Both areas are today somewhat more humid than the Wonderwerk region. This subchapter will also briefly review Holocene interior studies and if there is any evidence from within the winter rainfall region itself for its expansion or contraction in the past.

Cradle of Humankind sites

One dominant region of research on isotopic values and the ecology of southern African faunas has been the sites located in the dolomitic cave sites in the Cradle of Humankind. Today, these sites are located in markedly different biomes to Wonderwerk Cave. Like the Pleistocene strata of Wonderwerk Cave, the infills lack fine chronological detail, meaning that deposits represent time-averaged complexes. This is compounded by the lack of consensus on the chronology of sites (e.g. Reed 1997, Berger et al. 2002, de Ruiter 2003, Partridge et al. 2003, Herries et al 2010, Granger et al. 2015), making it difficult to establish contemporaneity between assemblages. Therefore, while a comparison with Wonderwerk is useful to explore regional trends spanning the period 2-1Ma, differences are expected due to the nature of the sites and the different existing vegetation zones they are located in.

The Gondolin Caves are located on the northwestern edge of the Cradle area (Fig. 8.1), and were excavated in 1979 by E. Vrba. The GD2 assemblage, has been analysed for enamel $\delta^{13}C$ on 22 specimens. The results show that at 1.8Ma the environment was an open-to-wooded highland grassland (Herries et al. 2006), with *O. oreotragus* and *Redunca* sp. being the most abundant species. The stable isotope results for the species are similar to extant animals in southern Africa, with *Redunca* sp. a pure grazer (1.0‰ to 3.5‰) and *O. oreotragus* a browser (-7.6‰ to -9.9‰) (Adams 2012). Other animals comparable to Wonderwerk also show expected values (*T. oryx* and *T. strepsiceros* with means of -9.3‰ and -8.4‰ respectively, and grazing values for *C. simum* and the Suid *M. andrewsi*). The extinct Antilopini *A. recki* has mixed-feeder values (Adams 2012), much like *A. marsupialis* at Wonderwerk. Although GD2 is of similar age to Stratum 12 in Wonderwerk Cave, the grazing species in GD2 show higher $\delta^{13}C$ values, besides the assemblage featuring no large grazers like Alcelaphini or Equids.

Swartkrans (Fig. 8.1) is one of the best researched sites in the Cradle in terms of stable isotope analyses. The developed Oldowan Members 1 and 2 were suggested to be between 1 and 2Ma (Brain 1993), but new cosmogenic burial dating puts Member 1 at ~2.19Ma and 1.8Ma respectively (Gibbon et al. 2014). Primates make up 50% of the faunal assemblage in Member 1 (Brain 1981), a significant difference to Wonderwerk Cave. There are isotope enamel data from *A. robustus* and early *Homo*, as well as large numbers of carnivores (Lee-Thorp et al. 2000). In Member 1, the grazers and browsers show niche separation, although grazers are somewhat lower in $\delta^{13}C$ values (0.7‰ to 1.1‰) compared to modern grassland specimens (Lee-Thorp et al. 2000). $\delta^{13}C$ values are lower in Member 2, especially the Equid values with -6.4‰ to 0.0‰ (Lee-Thorp et al. 1994), although overall sample sizes are small. As at Wonderwerk, *A. bondi* has a grazing signal and *A. marsupialis* mixed-feeding values, whereas the extinct *A. recki* and *A. australis* are browsers (Lee-Thorp et al. 1994).

Homo ergaster and *A. robustus* values overlap, with both having higher $\delta^{13}C$ values than the browsers. The suggested habitat reconstruction is of closed vegetation with some woodland/thicket and possible remnants of C_3 grasses in Member 2, and a more open environment in Member 1; a C_4 grassland component is present throughout (Avery 1995, Lee-Thorp et al. 2000). The site is comparable to Strata 12 and 11 in Wonderwerk Cave, and, although existing in a more closed environment, the grazer-browser niche partitioning was much more developed in the Cradle (Fig. 8.2).

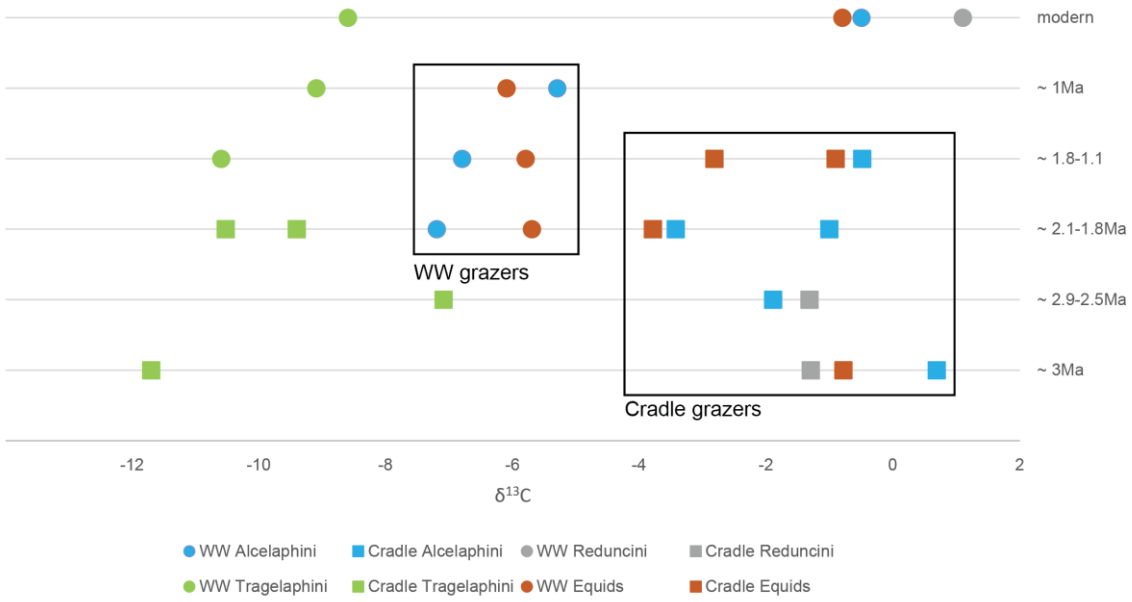

Figure 8.2: Wonderwerk (Excavation 1 Strata 10-12) and Cradle sites (Makapansgat Member 3, Swartkrans Member 1 and 2, Sterkfontein Member 4 and 5; Lee-Thorp et al. 2007) $\delta^{13}C$ mean values for Alcelaphini, Tagelaphini, Reduncini and Equids per time interval between 3Ma and 1Ma. The modern interval includes mean values from Wonderwerk Strata 1-2b for comparison.

Stable isotope studies on the nearby site of Sterkfontein (Fig. 8.1) were carried out on samples from Member 4 and Member 5. Member 4 pre-dates Wonderwerk Cave, with suggested dates of 2.9-2.0Ma (Herries et al. 2003, van der Merwe et al. 2003, Partridge et al. 2005), but possibly older as the overlying Member 5B has been re-dated to ~2.18 Ma

(Oldowan infill, Granger et al. 2015). The Member 5C Acheulean assemblage is dated between 1.4 and 1.1 Ma (Herries and Shaw 2011). As at Swartkrans, the focus has been on the isotopic composition of enamel, not only of herbivores, but also of hominins (*A. africanus*, Member 4, flexible mixed feeder) and carnivores. The isotope results are similar to Swartkrans with clear C_3 (*T. strepsiceros, A. recki*) and C_4 endmembers (*A. bondi, Damaliscus, H. equinus, C. taurinus*), leading both sites to be reconstructed as mosaic habitats of riverine woodland and grassland (van der Merwe et al. 2003). Figure 8.2 shows the comparison to similar dated Strata at Wonderwerk Cave, showing the generally higher $\delta^{13}C$ values in the Cradle sites.

Makapansgat (Fig.8.1) represents the oldest isotopically analysed assemblage from the Cradle sites. Its Pliocene Member 3 (2.9-2.6Ma; Herries 2003, Hopley et al. 2007b) includes fauna extinct in the younger sites. In general, it is a more wooded environment than the other Cradle sites, but most grazers and browsers are already in the expected feeding niches. The extinct *Hipparion* has a mean $\delta^{13}C$ of -0.8±0.9‰. *C. simum* is a mixed-feeder (Sponheimer et al. 2001b) as in Wonderwerk Excavation 2 Stratum 2. Alcelaphini and Reduncini have $\delta^{13}C$ means of 0.7±0.7‰ and -1.4±2.4‰ respectively, with Tragelaphini having values of -11.7±0.5‰ (Sponheimer et al. 1999). This site is one million years older than Wonderwerk Cave Stratum12. Its higher $\delta^{13}C$ values in grazers (Fig. 8.2) shows that there were more C_4 grasses in the environment in this part of the country, which possibly persisted and expanded earlier than in the Wonderwerk region.

Summarizing Makapansgat Member 3, Sterkfontein Member 4, 5 (Unit B and C) and Swartkrans Member 1 and 2 there is a general decline in browser proportions over time, and a rise in grazers (Vrba 1980, 1985). Makapansgat Member 3 has the most C_3 herbivores, and some mixed feeders. The younger sites have higher portions of C_4 species, although with $\delta^{13}C$ values slightly lower than modern open grassland mammals. There is

some intra-site variation, especially between Sterkfontein Member 5B (more mixed feeders) and 5C (higher proportion of grazers) (Lee-Thorp et al. 2007). It has been suggested that the lower values and greater proportions of browsers in the older Members demonstrates less dietary specialization or else the survival of C_3 grasses in the local vegetation. Compared to Wonderwerk Cave, the grazers in the Cradle sites have higher $\delta^{13}C$ values throughout their sequences (Fig. 8.5), possibly showing that specialization or full replacement of C_3 by C_4 grasses took place at a different time scale in both regions. The differences between Wonderwerk Cave and the Cradle sites are significant for the time period 2-1Ma in Alcelaphini (p-value 0.01) and Equids (p-value 0.01), but not for Tragelaphini (p-value 0.99; all tests ANOVA with Tukey HSD test). This confirms differences in the diet of large grazers between both areas.

Open grassy environments are dominant in the Cradle region after 1.7Ma (Lee-Thorp et al. 2007).This is also evident from the Buffalo Cave speleothem record (Hopley et al. 2007a). This record shows that fluctuations in vegetation are related to the obliquity periodicity (40 ka), crucial information that cannot be obtained from the episodic occurring faunal remains. However, obliquity (Fig. 7.6) alone is not enough to explain the excursions in the proportions of C_3 plants at Wonderwerk. The grazer $\delta^{13}C$ data show that in some periods at least C_3 grasses were a component of the local environment.

Grassland biome sites

The grassland biome, east of Wonderwerk Cave, spans most of the eastern part of South Africa. Herbivores from several sites, spanning 1Ma to modern times, have been analysed isotopically to explore if competition between animals or environmental turnover is responsible for the evolution of the feeding niches in African ungulates today (Codron et al. 2008). The results are similar to the Wonderwerk results; more so than the Cradle sites' results (Fig. 8.3). The oldest analysed assemblage is from Cornelia Uitzhoek in the Free

State (Fig. 8.1), 115km south of Johannesburg, and dated to 1.0-0.8Ma (Jaramillo event) by biostratigraphy and palaeomagnetism. New excavations into the Acheulean level discovered a bone bed, including an upper first molar of early *Homo* (Brink et al. 2012). The Middle Pleistocene is represented by the site of Florisbad Spring in the Free State near Bloemfontein (Fig. 8.1). The MSA artefacts and faunal remains roughly span 400-100ka (Grün et al. 1996, Kuman et al. 1999). The site is the typesite for the Florisian Land Mammal Age, showing wetland components in the faunal assemblage. Palynological investigations indicate wet phases associated with open grassland landscapes, while dry phases have pollen from salt-hardy plants that characterise brackish habitats (van Zinderen Bakker 1989, 1995). The Holocene is represented by the mid-Holocene site of Kareepan in the North West Province dated to 4ka (Fig. 8.1) and by modern comparison samples from grassland biomes in the Free State, eastern Kwazulu-Natal and Mpumalanga province (Codron et al. 2008).

The results of the stable isotope study by Codron et al. (2008) show differences within related taxa, e.g. between *A. marsupialis* and *A. bondi* as in Wonderwerk Cave. A shift from C_3/C_4 mixed feeding in Cornelia Uitzhoek to more C_4 feeding in Florisbad and even higher C_4 values in modern times is observed in several grazer taxa, e.g. Equids, Alcelaphini and Bovini (Fig. 8.3). Although a similar trend is evident over time in Wonderwerk and the interior sites noted here, the grazers overall show higher $\delta^{13}C$ values in the interior sites compared to Wonderwerk. This is confirmed statistically for the time period 2-1Ma in Alcelaphini (p-value >0.00) and Equids (p-value 0.01), but not for Tragelaphini (p-value 0.30; all tests ANOVA with Tukey HSD test). Comparable to Wonderwerk, browsers become more C_3 specialised in the Holocene. The authors conclude that diet in the ancient species seem more flexible than in their modern counterparts. All taxa shift at the same times, inferred as an environmental shift that drives speciation

(Codron et al. 2008). This is also one of the few stable enamel isotope studies which reported oxygen isotope results. $\delta^{18}O$ values generally show an increasing trend, interpreted as reflecting increasing aridity (Codron et al. 2008).

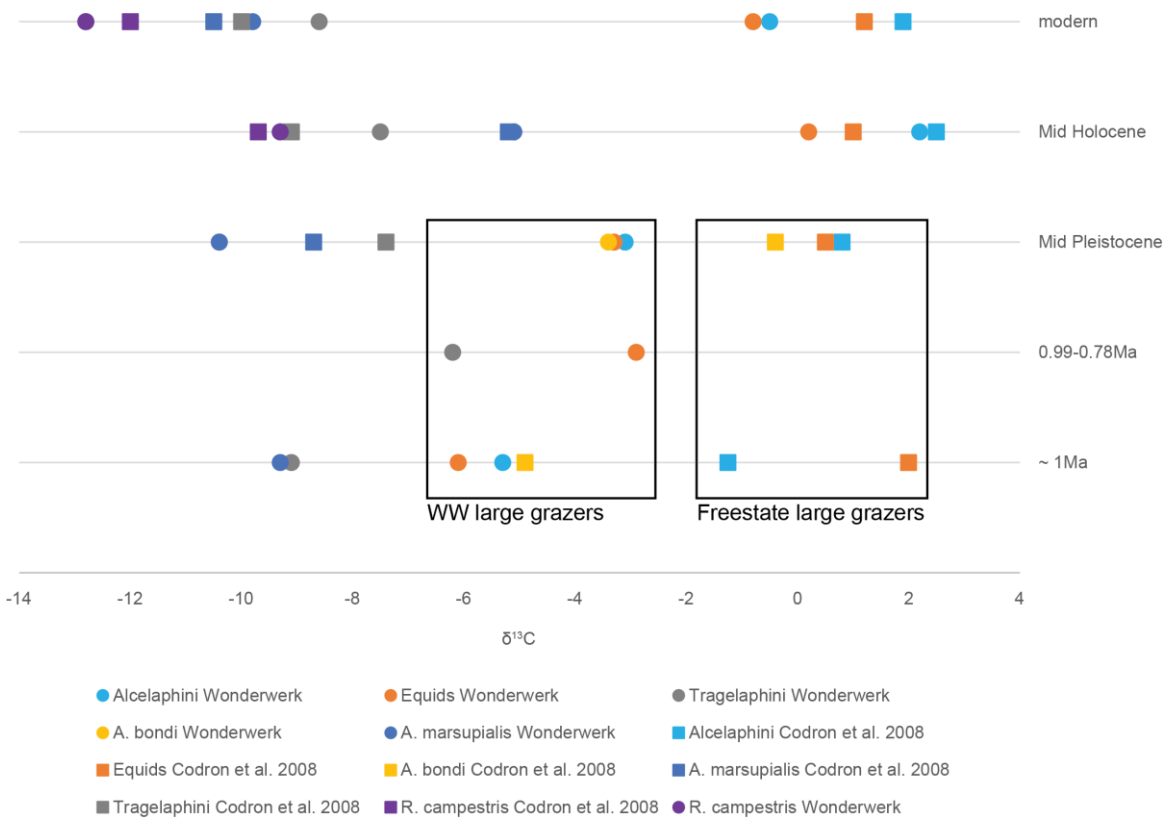

Fig. 8.3: Wonderwerk (Stratum 10, 9-6, 4a) and grassland biome sites (Cornelia Uitzhoek, Florisbad spring, Kareepan, modern assemblages; all Codron et al. 2008) $\delta^{13}C$ mean values for several species in time intervals between 1Ma and today. The modern interval includes mean values from Wonderwerk Strata 1-2b.

Erkfroon is a site in the Free State with several environmental proxy records, including fauna abundance records, phytolith and pollen analysis as well as herbivore enamel stable isotopes (Churchill et al. 2000, Bateman et al. 2012, Lyons et al. 2014). For the time period 120-10ka, preliminary stable isotope and phytolith results show the presence of C_3 grasses around the time of the Last Glacial Maximum (Bateman et al. 2012). This possible evidence of winter rainfall influence is supported by new analysis of the river terrace palaeosols

(Lyons et al. 2014). The Erfkroon record, east of Wonderwerk Cave, is therefore important to reveal rainfall seasonality in time periods not covered by the Wonderwerk Cave record.

Holocene sites in the interior

Compared to the amount of enamel stable isotope data from Early Stone Age and Hominid sites in South Africa's interior, no MSA site has been analysed with the same methods so far, and few Holocene sites. Smith et al. (2002) analysed $\delta^{13}C$ and $\delta^{18}O$ in fauna from four sites along the Caledon River (Fig. 8.1) in South Africa and Lesotho (Rose Cottage Cave, Tloutle, Ntloana Tsoana and Ha Makotoko), spanning together 16 to 6 cal. BP. These grassland biome sites lie on a gradient from 1500m to 2000m above sea level, whereas the modern boundary for C_3 grasses is about 2300m above sea level, depending on aspect (Livingstone and Clayton 1980). C_3 grasses were identified in Smith et al. (2002) at 16-14 cal. BP, 10.2-9.6 cal. BP and 8.4-8ka cal. BP, indicating cool growing seasons during these time spans. The study also inferred centennial changes and intense summer rainfall in the mid-Holocene from their dataset (Smith et al. 2002). This fits especially with the Wonderwerk $\delta^{18}O$ OES record, which shows fluctuations between spits throughout the Holocene, and a change in rainfall seasonality and/or amount in the mid-Holocene.

Blydefontein Rock Shelter is located south of Wonderwerk in the Eastern Cape Karoo (Fig. 8.1). The Karroid Mountain Veld has a mixture of C_3 and C_4 grasses today (Bousman 2005), due to shifting seasonality of rainfall. Pollen from various Blydefontein Basin sites from 11.8ka onwards indicate a dry start of the Holocene (till 5.4ka). A phase with increased grass in the environment is evident in the pollen record from 5.4ka onwards, possibly because of increased summer rain. Cool and varying moisture conditions existed 3-4ka, with general variability in rainfall and millennial or short shifts between grassland and drier karroid veld (Scott et al. 2005). In general, the results show similar trends to the OES stable isotope record at the same site (see Chapter 6) (Bousman 2005, Scott et al. 2005).

Western Cape isotope studies

Besides the Cradle of Humankind area, the Western Cape is another region in South Africa with a concentration of stable isotope studies (e.g. Luyt et al. 2000, Hare and Sealy 2013). As those sites are located in the fynbos biome, characterised by the winter rainfall zone, they will not be discussed in any detail in this thesis due to their different climatic influences (Chapter 2). Studies of Middle and Late Pleistocene sites, for example Elandsfontein (Luyt et al. 2000) or Hoidjiespunt (Hare and Sealy 2013) (Fig. 8.1) have shown that the winter rainfall regime persisted throughout the Pleistocene in this area, as reflected in C_3 values for all mammals. At Elandsfontein, increasing C_4 values of bovid enamel isotopes are read as showing an influence of the summer rainfall zone in the mid-Holocene (Stowe and Sealy 2015). Interestingly, the same suggestion has been made for a hyrax isotope record from the Cederberg region (Chase et al. 2015), which has currently both summer and winter rainfall influence. The South African Katbakkies Pass midden (Fig. 8.1) mentioned above has a stable isotope, microcharcoal and pollen record from 700 to 7000 cal. BP. The results of the various proxies together are presented as showing increased humidity 6900-5600 cal. BP and 4700-3200 cal. BP and a long arid episode 3200 to 2700 cal. BP. The authors conclude that increased easterly flow of humidity from the Indian Ocean increased the influence of the summer rainfall zone and brought more humidity to the site, before increasing winter rain prevailed again afterwards (Chase et al. 2015). Increased summer rainfall intensity in the mid-Holocene might also explain the humid phase and vegetation changes at Wonderwerk around 6000 cal. BP, as well as the high proportions of C_4 plants in the browser species diet, compared to before and after. There is therefore not only evidence for the influence of increased winter rainfall in the past, but also for an expansion of the summer rainfall zone at other times.

8.3 East Africa

Significantly more stable isotope studies exploring Plio-Pleistocene environments have been undertaken in Eastern Africa compared to southern Africa. This is partly due to the dating of the East African sequences containing volcanic tuff deposits, which can be correlated across regions. A comparison to the Wonderwerk data set is useful in order to test major hypotheses in a South African savannah setting. Compared to carbon isotope results, oxygen isotope data are rarely reported, and are mostly discussed in connection to the Levin (2006) aridity index (see Chapter 6.6.2). Pedogenic oxygen isotope records as measures of moisture availability generally exhibit trends of increasing $\delta^{18}O$ values, which are consistent with an aridification from the early Pliocene to today (Levin et al. 2004). One difficulty in comparing $\delta^{13}C$ enamel isotopes could be endemic species that only exist in one region of the continent and that animal communities differ, however, Alcelaphini and Equids also dominate the savannah environments of East Africa. OES stable isotope studies in East Africa are rare (exceptions are e.g. van der Merwe et al. 1999, Plummer et al. 2009a, Kingston 2011). Rather, stable carbon isotopes in carbonates have been extensively applied as a tool for estimating proportions of C_3 and C_4 plants in palaeolandscapes (Levin et al. 2004).

In general, it is agreed that open environments increased and woody cover decreased over the last 10Ma (Levin 2015). Although increasing aridity has been one hypothesis for influencing hominin and animal evolution in Africa (e.g. deMenocal 2004), the transition between wet and arid phases has been another recent point of discussion (Trauth et al. 2007, Potts 2013, Maslin et al. 2014). While some papers identified, for example, the occurrence of lakes in East Africa with major evolutionary transitions (Trauth et al. 2007), others point to the appearance of Acheulean stone tools and the appearance of *H. erectus* after the start of the lakes, decoupling it from climate as a driver (Lepre et al. 2014). In East Africa, equids

are the first animals to show a dominant C_4 diet by 7Ma (Uno et al. 2011). Other grazer species followed and show much more C_4 intake by 2Ma than the Wonderwerk specimens (Fig. 8.4).There is considerably less environmental information from East Africa for the MSA, with only one published palaeosol study (Yellen et al. 2005) and two published enamel isotope studies (see below; Faith et al. 2014, Garrett et al. 2014) to date. Even fewer stable isotope studies exist on Later Stone Age assemblages in East Africa, but modern mammals from national parks have been extensively analysed to provide comparisons to the ancient data. Relevant studies from Kenya, Ethiopia and Tanzania are discussed below.

ESA

The largest stable isotope enamel study so far is on the Turkana basin fossil assemblage (Cerling et al. 2015). Over 900 Artiodactyla, Perissodactyla and Proboscidae specimen have been analysed and compared to a dataset of extant mammals from east and central Africa. The samples from the Koobi Fora, Kanapoi and Nachukui Formations are analysed in time intervals from >4Ma to 1.0Ma. Changes of less than 2‰ have been observed over the whole time period in Alcelaphini (means -0.2‰ to 2.0‰) (Fig. 8.4). *Bovini*, *Reduncini*, *Ceratotherium*, *Metriochoerus-Phacochoerus* and *Equus* also show pure C_4 grazer values. This contrasts to Wonderwerk, and reflects for the time period 2-1Ma a significant difference in $\delta^{13}C$ values for Alcelaphini (p-value >0.00) and Equids (p-value >0.00, all tests ANOVA with Tukey HSD test). There is also a difference in the Tragelaphini (p-value 0.02; ANOVA with Tukey HSD test), which are higher in $\delta^{13}C$ in Turkana compared to Wonderwerk. In general, the period 4.1-2.35Ma has many mixed feeding taxa, while 2.35-1.0Ma shows more C_4 grazers. Diets that differ from their modern descendants are shown for several taxa, another example against simple inference of modern diets into the past (Cerling et al. 2015). The authors note that if C_3 grasses were present in these formations, there must have been strong selectivity for one or the other. Still, this fossil record is unlike

any modern African ecosystem (Cerling et al. 2015), as also shown at Wonderwerk Cave (Chapter 6).

The open grassland site of Kanjera South in Kenya is dated to ~2.3 to 1.95Ma and contains fauna and Oldowan lithics (Plummer et al. 2009a). Pedogenic carbonates over a 130km transect show over 75% C_4 vegetation in the sequence. The small enamel sample has Equid $\delta^{13}C$ values above 1‰, Tragelaphini at -2.4‰ and -1.7‰ and Alcelaphini as well as Reduncini between 2‰ to 4‰. These are highly enriched enamel values, especially for the Tragelaphini. Compared to other Oldowan sites, which are reconstructed on the basis of palaleosol measurements as mosaic habitats (e.g. Gona Ethiopia [Quade et al. 2004]; Koobi Fora, Kenya [Quinn et al. 2007]), Kanjera South shows no woodland component (Plummer et al. 2009a). This is also in marked contrast to the Oldowan Stratum 12 at Wonderwerk, and furthermore shows higher $\delta^{13}C$ values than the Turkana Basin (Fig. 8.4), highlighting regional differences within Kenya.

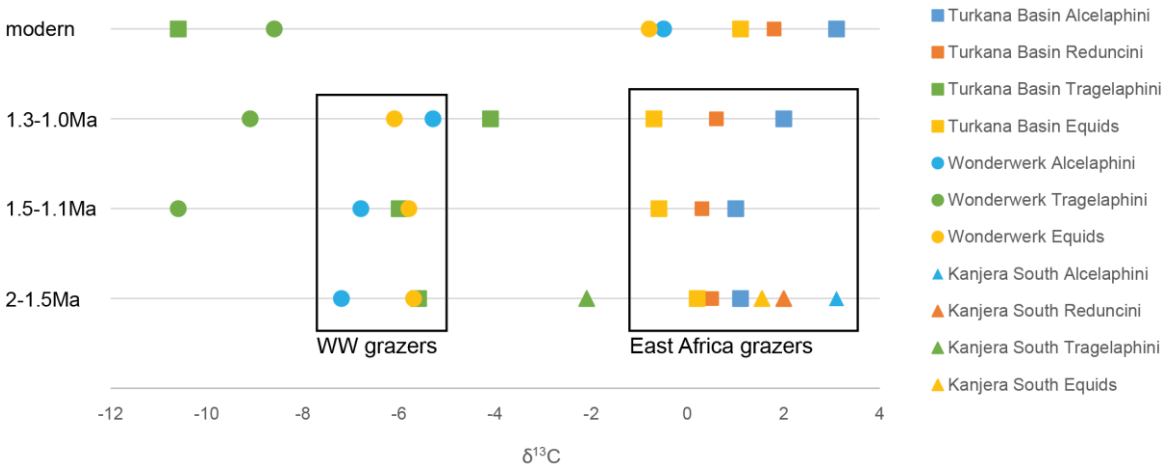

Fig. 8.4: Wonderwerk Cave (Stratum 10-12, and 1-2b for modern values) $\delta^{13}C$ mean values compared to Kenyan fossil site values (Turkana Basin, Cerling et al. 2015; Kanjera South, Plummer et al. 2009a) for several Alcelaphini, Reduncini, Tragelaphini and Equids in time intervals between 2-1Ma and for today.

Another large enamel stable isotope dataset of 210 samples from 15 taxa comes from the Basal Member (~3.8-3.2Ma) of the middle Pliocene Hadar Formation site Dikika, which is associated with *Australopithecus afarensis* remains (Bedaso et al. 2012). The full range from C_3 to C_4 values is present and no significant changes appear through time, though slight shifts occur within taxa. Tragelaphini are mixed feeders, averaging around -5‰ in SHM, while Alcelaphini are C_4 dominated, with individual specimens showing up as mixed feeders (Bedaso et al. 2012). This shows early adaptations to "pure" C_4 diets in Ethiopia, comparable to the Kenyan sites. The younger Asbole assemblage in the Busidima Formation (0.8Ma to 0.64Ma) has 80 enamel samples from 15 taxa analysed, and shows similar results (Bedaso et al. 2010). Equidae and Alcelaphini have $\delta^{13}C$ values above 0‰, while Bovini, Reduncini, Hippotragini and Suidae are all predominantly grazers. Tragelaphini and Antilopini (*Gazella* sp.) have mixed-feeding values. Faunal abundance data confirms the reconstruction of an open environment, with gallery forest or a wooded element comprising about 14% of local biomass nearby, this as five primate species are present at the site (Bedaso et al. 2010).

In Laetoli, Tanzania, herbivore enamel and OES were analysed from the Lower Laetoli Bed (LLB; 4.36-3.85Ma), the Upper Laetoli Bed (ULB; 3.85-3.63 Ma) and the Upper Ndolanya Bed (UNB; 2.66Ma) (Kingston 2011). OES $\delta^{13}C$ values show predominantly C_3 intake with a little C_4 influence at times, similar to the Wonderwerk Cave OES data. OES $\delta^{18}O$ values show more mesic conditions in the Upper Ndolanya Bed, which is the opposite of what the enamel values indicate, another phenomenon discussed for Wonderwerk (Chapter 7.1). Over 500 specimens of herbivore enamel from 23 species show a general increase in grazers in the Upper Ndolanya beds, but with no statistically significant shifts between beds. This could also be an artefact of small sample sizes and time-averaged surface collections. The $\delta^{13}C$ results show Tragelaphini to have mixed to browse values in

UPB and C_4 grazing in UNB, which is unknown for Tragelaphini today. Alcelaphini have values characteristic of mixed-feeders in the ULB but with a greater grazing component before and after, in the LLB and UNB, respectively. Equids have $\delta^{13}C$ values of -4.1‰ to 1.9‰ in LLB and ULB, which indicates some C_3 intake. Phytolith analysis shows evidence for C_3 grasses, especially in the lower beds, which could explain the mixed-feeding values (Kingston 2011). $\delta^{18}O$ values are low compared to modern samples, which is a phenomenon also noted at Wonderwerk (Chapter 7).

Enamel from palaeolake Olduvai, Tanzania, Bed II (after 1.78Ma) and Bed I (after 1.83Ma) of similar age to Wonderwerk Stratum 12 show Alcelaphines slowly increasing their C_4 intake through time from 0.2‰ to 2.2‰ to 3.2‰ today (van der Merwe et al. 1999). The Hippopotami, Equids and Suids are already pure grazers, while Tragelaphini have mixed-feeding values around -5‰ (van der Merwe et al. 1999).

Although there are slight regional differences and a slow increase of C_4 over time in the grazer diet in the East African ESA stable isotope studies, they show a clear dissimilar diet to the Wonderwerk ESA grazers. This is reflected in significantly different $\delta^{13}C$ values for Alcelaphini and Equids in Wonderwerk compared to sites in the Turkana Basin, which had the largest comparable dataset. While the mixed C_3-C_4 plant diet of the Wonderwerk grazers suggests the presence of C_3 and C_4 grasses in the Early Pleistocene, C_3 grasses must not have been a substantial part of the East African ecosystem at this time. The East African sites have no significant different $\delta^{13}C$ values to the Cradle and grassland biome sites in South Africa, east of Wonderwerk Cave.

MSA

Mfangano and Rusinga are islands in modern Lake Victoria, with MSA assemblages estimated to date to 100-45ka (Garrett et al. 2014). For environmental reconstruction,

pedogenic carbonates, bulk sediment organic matter and enamel isotopes were analysed. The sediment results suggest high cover of woodland and a low percentage of C_4 grasses. In contrast, the enamel results show most animals had over 70% C_4 consumption, and grazers dominate the assemblage. The authors conclude that the samples are from a woodland setting with a large C_4 grassland nearby, with a climate that was drier than today, making the modern islands possible highpoints in an ancient grassland landscape (Garrett et al. 2014).

Pollen cores (Kendall 1969), geochemical proxies for vegetation cover (Talbot et al. 2006) and faunal analysis (Tyron et al. 2012, 2014) from Karungu at the modern shore of Lake Victoria (45-94ka) confirm low lake levels with grassland compared to bushland thicket and forest in the present day. Faunal abundances also show high percentages of Alcelaphini and Antilopini, interpreted as reflecting decreased precipitation and more open environments compared to today (Faith et al. 2015). Twenty grazer enamel and 17 rodent enamel samples from surface collections were analysed with stable isotopes. They show diets dominated by C_4 grasses. (Faith et al. 2015). Both studies from Lake Victoria show slightly higher C_4 intake in the grazer diet than the Wonderwerk MSA stratum, similar to modern values from East Africa, but both are on assemblages younger than the MSA stratum at Wonderwerk Cave.

8.4 Conclusion

Compared to similar studies of herbivore enamel $\delta^{13}C$ in South Africa and East Africa, where grazers have a C_4 dominant diet from before 2Ma, the Wonderwerk Cave herbivores survived for a longer time on a mixed grass diet. The presence of C_4 grasses alone was a more recent development after 800ka. This is reflected in significantly different $\delta^{13}C$ values for Alcelaphini and Equids in Wonderwerk compared to sites in the Turkana Basin, the

Cradle sites and the grassland biome sites, all of which had enough material for a statistical comparison. Isotopic values for those three regions do not differ from each other in the time range 2-1Ma, but are dissimilar to coeval values from Wonderwerk. The closest match to Wonderwerk are the nearby grassland biome sites. Reasons for the seemingly disparate and regional timing for the development of the C_4 grazing niche at Wonderwerk are not fully understood. The most likely explanation is an expansion of the winter rainfall zone, leading to more year-round water availability. Archaeological and geological sites in the Kuruman Hills area and along the Ghaap Escarpment confirm the evidence from Wonderwerk Cave for phases of increased humidity in the southern Kalahari, especially around 1Ma. This would imply a different atmospheric circulation system than today over southern Africa. The southern African flora and fauna, and every region within, clearly followed its own evolutionary path. This result can, however, be a caution that one should not generalise between different biomes, rainfall zones and over large distances. Much more research, especially in the time period 1Ma to mid-Holocene, is needed to create a coherent picture.

Chapter 9 - Conclusion

This chapter summarises the main results and conclusions of this study. The hypotheses and research aims set out at the start of the thesis are assessed in the light of new information gained from stable isotope analyses in ostrich eggshell (OES) and enamel from Wonderwerk Cave. Finally, directions for future research are provided.

9.1 The main results

In this thesis, bulk isotopic analysis, both on herbivore enamel and OES from Excavations 1 and 2 in Wonderwerk Cave, was used to create two long-term proxy records. Additionally, the Holocene sequence in Wonderwerk Cave was strengthened with nine new radiocarbon dates (Chapter 4). The Bayesian modelling of these new dates, together with those that had already been published, allowed us all the better to constrain the Holocene Strata 4d to 2b in Excavation 1. Stratum 4aLH in particular could be narrowed to 5.3-6.2ka cal. BP, in which the OES isotope data indicate a wet spell occurred (Chapter 5). The OES isotope record revealed arid but variable conditions for Wonderwerk, with distinct phases of increased humidity. The enamel isotope study confirmed these results (Chapter 6), while providing a more detailed picture of vegetation changes in the area. The Holocene was used as a baseline for exploring the Pleistocene strata, due to the possibility of much better chronological control. This approach delivered some surprises because the Holocene stable isotope data are strikingly different to the Pleistocene ones. Together these substantially increase our knowledge of climatic and environmental changes over the last two million years in the arid interior of southern Africa.

The lowest Strata at Wonderwerk Cave point to the presence of an open savannah, comprised mainly of C_3 vegetation with small amount of C_4 grasses. Stratum 11 shows evidence of wetter and colder climate with a dominance of C_3 vegetation. In the

Wonderwerk region, Matmon et al. (2015) have documented moist conditions in the southern Kalahari 1.5-1Ma based on the presence of a stable though shallow water body in the region. Archaeological sites are associated with lakes and pans at Kathu, at the eastern site of the Kuruman hills (Beaumont 2004b, Walker et al. 2014). In the following, Wonderwerk attests to the expansion of C_4 grasses after ~800ka. This can be associated with the Mid Pleistocene transition (MPT) (1.2 to 0.7Ma). It has been proposed that ca. 1Ma was a phase of climate instability in Africa (deMenocal 1995; Maslin and Christensen 2007; Trauth et al. 2009, Potts 2013, Maslin et al. 2014), associated in East Africa with evidence of wet phases (Trauth et al. 2005, 2010) as well as aridity (deMenocal 2004, Donges et al. 2011). The OES and enamel stable isotope data in this thesis suggest fluctuating conditions in Stratum 10 (ca. 1Ma) with C_3 dominance, as well as extreme C_4 spells in the vegetation, in an overall humid setting (Chapter 5, Ecker et al. 2015). The following Middle Pleistocene Strata in Wonderwerk Cave show increasing aridity from the OES isotope record, as well as more C_4 consumption by grazer species from the enamel isotope record. A significant change in eggshell thickness and pore density between Strata 10 and 9 (Ecker et al. 2015) and the micromammal record support the assertion of increasing aridity (Chapter 7).

Aridity was not the main driver behind the increase in C_4 grasses, but pCO_2 was identified a possible key factor (Chapter 7). This is strengthened by Maslin and Brierly (2015), who suggest atmospheric CO_2 as a driving force of the 100ka cycles dominating after the MPT. Another explanation could be increased competition for resources, rather than an increase in C_4 vegetation. This is unlikely to be the main explanation for the diet changes visible in this study, for the following reasons. First, several species show similar diet changes, and it is unlikely that Equids, Alcelaphines and *Pedetes capensis* switched at the same rate. Second, the phytolith and pollen records from Wonderwerk correspond with the stable

isotope data, confirming vegetation changes (Chapter 7). This points to faunal turnover being driven by environmental turnover as opposed to competition, as suggested by Codron et al. (2008).

The MSA Stratum (Excavation 2 Stratum 2) indicates a wetter environment from faunal abundances and OES $\delta^{18}O$ values, but is in need of more temporal constrains. Stratum 5 in Excavation 1 is perhaps the most enigmatic Stratum in the Wonderwerk record. Its radiocarbon dating and the lithic record indicate mixing of Pleistocene sediment with the overlaying LSA Strata. Botanical remains and pollen indicate a cool environment (Bamford 2015, Scott and Thackeray 2015), as do the OES $\delta^{18}O$ values, although microfaunal remains are absent.

One reason for examining the proxies in the Holocene, which is relatively well-understood, was to provide a basis for understanding those archives further back in the past. However, the Holocene is dissimilar to any Pleistocene Stratum. The manifestation of the modern savannah ecosystem and the niche separation of species is evident from the proxy records. It is, however, a dynamic period, whose changing nature is an important result for interpreting earlier records. In the early part, there was a semi-arid, mixed wooded savannah. The mid-Holocene saw an expansion of C_4 grass cover, probably due to a strengthening of summer rainfall. The later Holocene is variable with an overall trend of increasing aridity, reaching a peak around 2ka cal. BP.

$\delta^{18}O$ values in Wonderwerk are mainly influenced by rainfall patterns. Wonderwerk Cave is currently 450km from the border with the winter rainfall zone. One reason the winter storms do not come inland is because of the Great Escarpment. On the upper west coast, the escarpment has a lower profile, so diminished high pressure and high clouds might have been able to penetrate inland. Winter storms are more depleted in $\delta^{18}O$ than is summer rain,

and this could explain the low OES $\delta^{18}O$ values in Strata 11, 10 and 5. C_3 grasses need a cool growing season (Ehleringer et al. 1997) - conditions that could be created by winter rainfall. Especially strong evidence for this scenario is in Stratum 11, where the phytolith record shows a Nama-Karoo type vegetation (Chazan et al. 2012). The existence of C_3 grasses would explain the mixed-feeding values in the grazers. In other parts of South Africa at this time (e.g. the Cradle sites), C_4 grasses are already dominant, as is evident in higher $\delta^{13}C$ grazer values than in the Wonderwerk specimens (Chapter 8). The Wonderwerk region seems to have been influenced by both summer and winter rain, as the consistent presence of C_3 and C_4 in the grazer enamel clearly shows. The increased influence of winter rainfall, and more rainfall year-round, are likely. This scenario provides a setting for the persistence of lakes and pans in the area. It is unknown how fluctuations in rainfall occurred, and how often a strong summer rainfall regime, like that of today, prevailed. If the enamel $\delta^{13}C$ results are taken as evidence, this would not have been established before 800ka, and only fully set in during the Holocene.

From the $\delta^{13}C$ results, it can be concluded that the dietary ecology of the sampled species changed significantly over time. The earlier samples contained more mixed-diet species than today's low diversity ecosystem. Not all lineages shift their diet over time, but the enamel isotope results clearly record a shift to a "pure" C_4 diet in Equids, Alcelaphini and springhares. From the results for grazers it can be concluded that in those periods of the Pleistocene represented in the Wonderwerk Cave deposits, vegetation structure differed from today.

The Wonderwerk faunal abundances reflect the ecozones around the Cave: the plains of the Ghaap plateau to the east and the mountainous area to the west (Brink 2015). Equids, Alcelaphini and, in some Strata, Antilopini, dominate the faunal assemblage, reflecting the open plain. The mammals living in the hills (e.g. *Redunca fulvorufula, Oreotragus*

oreotragus) are smaller and identified less often in the very fragmentary Pleistocene faunal sample (Brink 2015). In the Holocene, their numbers in the faunal record increase (Thackeray 1984). The diversity of available habitats in the Kuruman hills means that the area was probably suitable as an ecological refugium. Furthermore, the evidence for fresh water in the early Pleistocene on the eastern site of the Kuruman hills (Matmon et al. 2015), as well as on the western site close to Wonderwerk Cave (Goldberg et al. 2015) support this hypothesis. Following the principle from Lister and Stuart (2008), species become extinct within long-term refugia. The last appearance – to date - of *Antidorcas bondi* and *Megalotragus priscus* can be found in the Wonderwerk Holocene Stratum 4c (Chapter 4), which would agree with this hypothesis. The faunal assemblage also shows that *Damaliscus pygargus* inhabited in this region longer than previously thought. Genetic studies provide further evidence for the idea of a refugium in the Kuruman hills area. One study shows that two baboon lineages emerged in southern Africa at 1.9-1.6Ma, and have been isolated since (Sithaldeen et al. 2015). The Kuruman Hills area has been suggested as a refugium for dispersal of those primates in favourable wet conditions, later the hills were favourable in dry glacials (Sithaldeen et al. 2015). A similar hypothesis, from genetic studies, has been proposed for *Pedetes capensis* (Prinsloo and Robinson 1992), which is present in Wonderwerk throughout the sequence. The Wonderwerk Cave environmental record revealed that environmental changes in this region do not follow a simple glacial-interglacial dichotomy, as assumed in the genetic studies. Therefore, more interdisciplinary research is needed to test this hypothesis.

9.2 Review of the research aims and hypotheses

Going back to the initial aims of this doctoral thesis, the results from this study are used to review the hypotheses formulated in Chapter 1.

- Climate and vegetation shifts do appear with phase changes in global climate variability, e.g. with the onset of the Walker circulation 1.9-1.7 Ma (Maslin and Christensen 2007) in Stratum 11 and the Mid Pleistocene Transition (Trauth et al. 2015) in Stratum 10. Climatic and environmental instability has no direct influence on species evolution, but it is clear that hominins and fauna had to deal with changing food resources, probably leading to changes in population density and vegetation communities (e.g. presence or absence of C_3 grasses).
- The evolutionary shift in African ungulates towards dietary speciation due to constant exposure to C_4 grasses (Codron et al. 2008) has been confirmed through increasing proportions of C_4 in the Wonderwerk grazing species diet after 800ka. The highest $\delta^{13}C$ enamel values in the entire sequence are in the mid-Holocene. Variations within the general trend are hidden due to the coarse dating of the Middle and Late Pleistocene Strata. Despite this clear trend, regional independent developments have to be considered, as other regions in South and East Africa show C_4 dominated diets in herbivores at earlier times than at Wonderwerk (Chapter 8).
- The Wonderwerk OES and enamel isotope data confirm an overall arid setting as expected. Humid phases are identified in Excavation 1 Strata 11, 10, 4aLH and Excavation 2 Stratum 2. The drivers behind the humid phases differ significantly. Whereas the influence of winter rainfall was identified as a cause of increased water availability in Stratum 11, the opposite, increased summer rainfall, is suggested as the cause for a humid episode of C_4 expansion in Stratum 4aLH. Excavation 1 Stratum 10 and Excavation 2 Stratum 2 are both identified as wet episodes by the presence of *K. leche*, besides others. Both Strata show variable isotope results, and their time span includes at least one prominent interglacial (MIS 29 and MIS 5e, respectively). Higher $\delta^{18}O$ values in the Holocene compared to the Pleistocene

Strata are confirmed in the enamel isotope record. The OES $\delta^{18}O$ record is mainly used as an index of aridity, whereas the large set of herbivore enamel $\delta^{13}C$ is better reflecting vegetation changes. As a result, the enamel and OES $\delta^{13}C$ and $\delta^{18}O$ records often follow each other, but with few notable exceptions (Chapter 7.1).This is especially evident in the well-dated Holocene record, e.g. the short mid-Holocene humid episode at Stratum 4aLH.

- No significant differences exists between obligate and non-obligate drinkers in the Wonderwerk enamel $\delta^{18}O$ results, with exception of the Neotragini (*Raphicerus campestris, Oreotragus oreotragus*). This species provides the clearest evidence for high $\delta^{18}O$ values due to the strong influence of leafwater subject to strong evapotranspiration. Comparisons are limited by the low number of samples from non-obligate drinkers in the Pleistocene strata. This also limits correlations with arid episodes determined from the ostrich eggshell data. One result of the enamel isotope analysis is that there are significant differences between nocturnal and diurnal species, as visible in significant lower $\delta^{18}O$ values for *Hystrix africaeaustralis* and *Pedetes capensis*, compared to the other analysed species (Chapter 6).
- Periods of changing (Stratum 12 to 11) or highly variable climate and environment (Stratum 10) in Wonderwerk fall within periods of climatic instability as identified by Potts (2013). Still, the Wonderwerk ESA and MSA lithic assemblage is currently too small to pinpoint developments to a specific time. In the Holocene, higher temporal resolution indicates phases of environmental change coinciding with changes in the cultural record at several times (e.g. Stratum 4aLH, Chapter 7.5). Other drivers, independent of the environment, cannot be excluded. The variability selection hypothesis (Potts 2013) is therefore a valid possibility to explain

evolutionary and cultural changes visible in southern Africa, but many more well-dated sites are needed confirm it.

9.3 Directions for future research

The potential of Wonderwerk Cave for recovering archaeological and environmental information is large and still only partially explored (Horwitz and Chazan 2015). Currently, more proxies are being analysed and new excavations are being planned. Better dating is one issue to be solved to achieve the full potential of the new analyses. Although Wonderwerk Cave is a more stratigraphically controlled site than e.g. Sterkfontein or the other dolomitic infill sites, the chronological resolution of the various layers is frequently poor and the time 'slices' large. Therefore it is possible that the materials are palimpsests (Hopley and Maslin 2010). This makes it impossible to distinguish finer time slices. Precise dating is also crucial to match up environmental data and cultural changes in a meaningful way, a problem that is widespread in South African Palaeolithic archaeology. A current collaboration using Amino Acid Racemization dating on Wonderwerk OES is a promising step in this direction. Preliminary results also reveal how cautiously the whole stratigraphy needs to be re-examined. Wonderwerk Cave has currently the longest archaeological and environmental proxy record in the interior of southern Africa, making it a key reference site. More terrestrial environmental records and more interior archaeological sites with good dating and stratigraphy are needed to link to this record. Only a comparison can show the full range of variability and regional developments, and provide information on time periods missing in the Wonderwerk record.

The presence of C_3 grasses in the Early Pleistocene at Wonderwerk implies a cooler growing season than possible with the current summer rainfall regime. Using climate models would be one way to explore drivers and responses creating such a scenario. The

largescale shifts in isotope ecology and faunal abundances need to be set into the broader context of South African vegetation patterning. Not only climate drivers need to be explored, but also how biomes change and expand or contract.

More research is required in the time period from 1Ma to today in East Africa (Cerling et al. 2015, Behrensmeyer 2015) as well as South Africa. Especially the Mid Pleistocene (~800-100ka) should be focus of future research, as not enough records exist for this timeframe from both archaeology and environment, and therefore a gap exists in connecting the late Pleistocene with the early Pleistocene. Following Potts' (2013) variability selection hypothesis, there must be more phases of climatic instability, e.g. 500-300ka at the transition to the MSA. There are almost no environmental records from this time period in South Africa, but ongoing work (archaeological and environmental) in Wonderwerk Excavation 6 and 2, and at Kathu Pan, might help to test this hypothesis.

A larger number of southern African mammals need to be analysed with stable isotopes to explore species variation, especially of extinct animals, as it becomes apparent that species had different proportions of C_3 and C_4 plants their diet over time. The diet of modern taxa cannot simply be projected into the past or to ancestral species, even over the short time span of the Holocene. Morphological data alone do not provide all the information, as discrepancies between diet and dental morphology have shown. The southern Kalahari had a significantly different fauna and flora in the Pleistocene compared to today. The drivers and conditions behind this ecology and its changes need to be explored before changing cultural sequences can be evaluated.

Bibliography

Adams, J.W. 2012. Stable carbon isotope analysis of fauna from the Gondolin GD 2 fossil assemblage, South Africa. *Annals of the Ditsong National Museum of Natural History*, 2, 1-5.

Ambrose, S.H., Norr, L. 1993. Experimental evidence for the relationship of the carbon isotope ratios of whole diet and dietary protein to those of bone collagen and carbonate. In: Lambert, J.B., Grupe, G. (eds.), *Prehistoric human bone*, 1-37. Berlin Heidelberg: Springer.

Anderson, C. 1991. The Birds and Mammals of the Wonderwerk Cave Area. Unpublished Report, McGregor Museum Archive.

Anderson, T. 1991. Wonderwerk Cave as a Botanical Reserve. Unpublished Report, McGregor Museum Archive.

Apps, P. 2012. *Smither's Mammals of Southern Africa. A field guide*. Cape Town: Struik Nature.

Araguás-Araguás, L., Froehlich, K., Rozanski, K. 2000. Deuterium and oxygen-18 isotope composition of precipitation and atmospheric moisture. *Hydrological Processes*, 14(8), 1341-1355.

Attwell, C.A.M., Jeffery, R.C.V. 1981. Aspects of molariform tooth attrition in eland and wildebeest. *South African Journal of Wildlife research,* 11(1), 31-34.

Avery, D.M. 1981. Holocene microfaunal faunas from the northern Cape Province, South Africa. *South African Journal of Science*, 77, 265-273.

Avery, D.M. 1998. An assessment of the Lower Pleistocene micromammalian fauna from Swartkrans Members 1-3, Gauteng, South Africa. *Geobios*, 31(3), 393-414.

Avery, D.M. 2007. Pleistocene micromammals from Wonderwerk Cave, South Africa: practical issues. *Journal of Archaeological Science*, 10, 1-13.

Backwell, L.R., McCarthy, T.S., Wadley, L., Henderson, Z., Steininger, C.M., Barré, M., Lamothe, M., Chase, B.M., Woodborne, S., Susino, G.J., Bamford, M.K., Sievers, C., Brink, J.S., Rossouw, L., Pollarolo, L., Trower, G., Scott, S., d'Errico, F. 2014. Multiproxy

record of late Quaternary climate change and Middle Stone Age human occupation at Wonderkrater, South Africa. Quaternary Science Reviews, 99, 42-59.

Bamford, M.K. 2014. *Pre-Holocene charcoals from Stratum Five of Wonderwek Cave, Northern Cape*. Abstract, 'From Past to Present - Changing Climates, Ecosystems and Environments of Arid Southern Africa' Conference, Bloemfontein.

Bamford, M.K. 2015. Macrobotanical remains from Wonderwerk Cave (Excavation 1), Oldowan to Late Pleistocene (2 Ma to 14 ka BP), South Africa. *African Archaeological Review*, DOI 10.1007/s10437-015-9200-0.

Barbour, M.M., McDowell, N.G., Tcherkez, G., Bickford, C.P., Hanson, D.T. 2007. A new measurement technique reveals rapid post-illumination changes in the carbon isotope composition of leaf-respired CO_2. *Plant, Cell & Environment*, 30(4), 469-482.

Barham, L., Mitchell, P. 2008. *The first Africans. African Archaeology from the earliest toolmakers to the most recent foragers*. Cambridge: Cambridge University Press.

Barry, R., Bloomer, P., Hoeck, H., Shoshani, H. (IUCN SSC Afrotheria Specialist Group) 2008. Procavia capensis. The IUCN Red List of Threatened Species. Version 2014.3. <www.iucnredlist.org>. Downloaded on 01 May 2015.

Bartoli, G., Hönisch, B., Zeebe, R.E. 2011. Atmospheric CO_2 decline during the Pliocene intensification of Northern Hemisphere glaciations. *Paleoceanography*, 26(4), 1-14.

Bateman, M.D., Bousman, B., Brink, J., Meier, H., Trower, G., Grün, R., Codron, D.I., Rossouw, L. Bronk Ramsey, C., Thornton-Barnett, S., Scott, L. 2012. The Middle and Late Pleistocene Palaeoenvironment of the Modder River Valley, South Africa. In: *Southern African Association of Geomorphologists - Celebrating 50 Years of Namib Desert Research at Gobabeb*, 37. Conference proceedings.

Beaumont, P.B. 1990a. Wonderwerk Cave. In: Beaumont, P.B., Morris, D. (eds.), *Guide to the Archaeological Sites in the Northern Cape,* 1-70. Kimberley: McGregor Museum.

Beaumont, P.B. 1990b. Kathu Pan. In: Beaumont, P.B., Morris, D. (eds.), *Guide to the Archaeological Sites in the Northern Cape*, 71-109. Kimberley: McGregor Museum.

Beaumont, P.B. 2004a. Wonderwerk Cave. In: Morris, D., Beaumont, P.B. (eds.), *Archaeology in the Northern Cape: Some Key Sites*, 31-36. Kimberley: McGregor Museum.

Beaumont, P.B. 2004b. Kathu. In: Morris, D., Beaumont, P.B. (eds.), *Archaeology in the Northern Cape: Some Key Sites*, 31-36. Kimberley: McGregor Museum.

Beaumont, P.B. 2011. The edge: more on fire-making by about 1.7 million years ago at Wonderwerk Cave in South Africa. *Current Anthropology*, 52(4), 585-595.

Beaumont, P.B., Vogel, J.C. 2006. On a timescale for the past million years of human history in central South Africa. *South African Journal of Science*, 102, 217-228.

Bedaso, Z.K., Wynn, J.G., Alemseged, Z., Geraads, D. 2010. Paleoenvironmental reconstruction of the Asbole fauna (Busidima Formation, Afar, Ethiopia) using stable isotopes. *Geobios*, 43(2), 165-177.

Bedaso, Z.K., Wynn, J.G., Alemseged, Z., Geraads, D. 2013. Dietary and paleoenvironmental reconstruction using stable isotopes of herbivore tooth enamel from middle Pliocene Dikika, Ethiopia: Implication for *Australopithecus afarensis* habitat and food resources. *Journal of human evolution*, 64(1), 21-38.

Behrensmeyer, A.K. 2015. Four million years of African herbivory. *Proceedings of the National Academy of Sciences*, 112(37), 11428-11429.

Berger, A. 1992. Orbital variations and insolation database. *IGBP PAGES/World Data Center-A for Paleoclimatology Data Contribution Series*, 92(007).

Berger, A., Loutre, M.F. 1991. Insolation values for the climate of the last 10 million years. *Quaternary Science Reviews*, 10(4), 297-317.

Berger, L.R., Lacruz, R., De Ruiter, D.J. 2002. Revised age estimates of *Australopithecus*-bearing deposits at Sterkfontein, South Africa. *American Journal of Physical Anthropology*, 119(2), 192-197.

Berger, L.R., de Ruiter, D.J., Churchill, S.E., Schmid, P., Carlson, K.J., Dirks, P.H.G.M., Kibii, J.M. 2010. *Australopithecus sediba*: A New species of Homo-like Australopith from South Africa. *Science*, 328, 195-204.

Berna, F., Goldberg, P., Kolska, L., Brink, J., Holt, S., Bamford, M. 2012. Microstratigraphic evidence of in situ fire in the Acheulean strata of Wonderwerk Cave, Northern Cape province, South Africa. *Proceedings of the National Academy of Sciences*, 109, 7593–7594.

Birkenfeld, M., Avery, M.D., Horwitz, L.K. 2015. GIS Virtual Reconstructions of the Temporal and Spatial Relations of Fossil Deposits at Wonderwerk Cave (South Africa). *African Archaeological Review*, *in press*.

Bobe, R., Behrensmeyer, A.K. 2004. The expansion of grassland ecosystems in Africa in relation to mammalian evolution and the origin of the genus Homo. *Palaeogeography, Palaeoclimatology, Palaeoecology*, 207, 399-420.

Bobe, R., Behrensmeyer, A.K., Eck, G.G., Harris, J.M. 2007. Patterns of abundance and diversity in late Cenozoic bovids from the Turkana and Hadar Basins, Kenya and Ethiopia. In: Bobe, R., Alemseged, Z., Behrensmeyer, A.K. (eds.), *Hominin environments in the East African Pliocene: An assessment of the faunal evidence*, 129-157. Netherlands: Springer.

Bond, W.J., Woodward, F.I., Midgley, G.F. 2005. The global distribution of ecosystems in a world without fire. *New Phytologist*, 165(2), 525-538.

Bousman, C.B. 1991. *Holocene paleoecology and Later Stone Age hunter-gatherer adaptations in the South African interior plateau*. PhD Thesis, Texas State University.

Bousman, C.B. 2005. Coping with risk: Later Stone Age technological strategies at Blydefontein Rock Shelter, South Africa. *Journal of Anthropological Archaeology*, 24(3), 193-226.

Brain, C.K. 1981. *The Hunters or the Hunted? An Introduction to African Cave Taphonomy*. Chicago: University of Chicago Press.

Brain, C.K. (ed.) 1993. *Swartkrans: A cave's chronicle of early man*. Transvaal Museum (No. 8).

Brain, C.K., Sillent, A. 1988. Evidence from the Swartkrans cave for the earliest use of fire. *Nature*, 336(6198), 464-466.

Brink, J.S. 1988. The taphonomy and palaeoecology of the Florisbad spring fauna. *Palaeoecology of Africa*, 19(16), 179.

Brink, J.S. 2005. The evolution of the black wildebeest, *Connochaetes gnou*, and modern large mammal faunas in central Southern Africa. Doctoral dissertation, University of Stellenbosch.

Brink, J.S., Lee-Thorp, J. 1992. The feeding niche of an extinct springbok, *Antidorcas bondi* (Antilopini, Bovidae), and its palaeoenvironmental meaning. *South African Journal of Science*, 88(4), 227-229.

Brink, J.S., Herries, A.I.R., Moggi-Cecchi, J., Gowlett, J.A.J., Bousman, C.B., Hancox, J.P., Grün, R., Eisenmann, V., Adams, J.W., Rossouw, L. 2012. First hominine remains from a~ 1.0 million year old bone bed at Cornelia-Uitzoek, Free State Province, South Africa. *Journal of human evolution*, 63(3), 527-535.

Brink, J., Holt, S., Horwitz, L.K. 2015. The Oldowan and early Acheulean Mammalian Fauna of Wonderwerk Cave (Northern Cape Province, South Africa). *African Archaeological Review, in press*.

Brock, F., Higham, T., Ditchfield, P., Ramsey, C.B. 2010. Current pretreatment methods for AMS radiocarbon dating at the Oxford Radiocarbon Accelerator Unit (ORAU). *Radiocarbon*, 52(1), 103-112.

Bronk Ramsey, C. 2008. Radiocarbon dating: Revolutions in Understanding. *Archaeometry*, 50(2), 249-275.

Bronk Ramsey, C. 2009. Bayesian analysis of radiocarbon dates. *Radiocarbon*, 51, 337-360.

Bronk Ramsey, C. 2013. OxCal 4.2. URL http://c14.arch.ox.ac.uk.

Bronk Ramsey, C., Higham, T., Leach, P. 2004. Towards high-precision AMS: Progress and limitations. *Radiocarbon*, 46(1), 17-24.

Brook, G.A., Cowart, J.B., Brandt, S.A. 1998. Comparison of Quaternary environmental change in eastern and southern Africa using cave speleothem, tufa and rock shelter sediment data. In: Alsharhan, G., Whittle, K. (eds.), *Quaternary deserts and climate change*. Rotterdam: Balkema.

Brook, G.A., Srivastava, P., Marais, E. 2006. Characteristics and OSL minimum ages of relict fluvial deposits near Sossus Vlei, Tsauchab River, Namibia, and a regional climate record for the last 30 ka. *Journal of Quaternary Science*, 21(4), 347-362.

Brook, G.A., Scott, L., Railsback, L.B., Goddard, E.A. 2010. A 35ka pollen and isotope record of environmental change along the southern margin of the Kalahari from a

stalagmite and animal dung deposits in Wonderwerk Cave, South Africa. *Journal of Arid Environments*, 74, 870–884.

Brook, G.A, Railsback, L.B., Scott, L., Voarintsoa, N.R.G., Liang, F. 2015. Late Holocene stalagmite and tufa climate records for Wonderwerk Cave: Relationships between archaeology and climate in southern Africa. *African Archaeological Review,* 32, 669-700.

Brooks, A.S., Hare, P.E., Kokis, J.E., Miller, G.H., Ernst, R.D., Wendorf, F. 1990. Dating Pleistocene archaeological sites by protein diagenesis in ostrich eggshell. *Science*, 248(4951), 60-64.

Brown L.H., Urban E.K., Newman K. 1982. *The Birds of Africa, Vol. 1*. Academic Press.

Bryant, J.D., Luz, B., Froelich, P.N. 1994. Oxygen isotopic composition of fossil horse tooth phosphate as a record of continental paleoclimate. *Palaeogeography, Palaeoclimatology, Palaeoecology*, 107(3), 303-316.

Bryant, J.D., Koch, P.L., Froelich, P.N., Showers, W.J., Genna, B.J. 1996. Oxygen isotope partitioning between phosphate and carbonate in mammalian apatite. *Geochimica et Cosmochimica Acta*, 60(24), 5145-5148.

Buitenwerf, R., Bond, W.J., Stevens, N., Trollope, W.S.W. 2012. Increased tree densities in South African savannas: >50 years of data suggests CO_2 as a driver. *Global Change Biology*, 18(2), 675-684.

Burney, D.A., Brook, G.A., Cowart, J.B. 1994. A Holocene pollen record for the Kalahari Desert of Botswana from a U-series dated speleothem. *Holocene*, 4, 225-232.

Burrough, S.L., Thomas, D.S., Shaw, P.A., Bailey, R.M. 2007. Multiphase quaternary highstands at lake Ngami, Kalahari, northern Botswana. *Palaeogeography, Palaeoclimatology, Palaeoecology*, 253(3), 280-299.

Burrough, S.L., Thomas, D.S., Singarayer, J.S. 2009. Late Quaternary hydrological dynamics in the Middle Kalahari: forcing and feedbacks. *Earth-Science Reviews*, 96(4), 313-326.

Butynski, T.M.M., De Jong, Y. 2008. Pedetes capensis. The IUCN Red List of Threatened Species. Version 2014.3. <www.iucnredlist.org>. Downloaded on 28 April 2015.

Butzer, K.W. 1984a. Late Quaternary environments in South Africa. In: Vogel, J.C. (ed.), *Late Cainozoic Palaeoclimates of the Southern Hemisphere*, 235-264. Rotterdam: Balkema.

Butzer, K.W. 1984b. Archeology and quaternary environment in the interior of southern Africa. In: Klein, R.G. (ed.), *Southern African Prehistory and Paleoenvironments*, 1-64. Rotterdam and Boston: Balkema.

Butzer, K.W., Stuckenrath, R., Bruzewicz, A.J., Helgren, D.M. 1978. Late Cenozoic paleoclimates of the Ghaap Escarpment, Kalahari margin, South Africa. *Quaternary Research*, 10, 310-339.

Butzer K.W., Fock G.J., Scott L., Stuckenrath R. 1979a. Dating and context of rock engravings in Southern Africa. *Science*, 203, 1201–1214.

Butzer K.W., Stuckenrath R., Vogel J.C. 1979b. The geo-archaeological sequence of Wonderwerk Cave, South Africa. Abstract, Society of Africanist Archaeologists Meeting, Calgary.

Camin, F., Perini, M., Colombari, G., Bontempo, L., Versini, G. 2008. Influence of dietary composition on the carbon, nitrogen, oxygen and hydrogen stable isotope ratios of milk. *Rapid Communications in Mass Spectrometry*, 22(11), 1690–1696.

Camp, C.L. 1948. University of California Expedition – Southern Section. *Science*, 108, 550-552.

Cerling T.E., Harris J.M. 1999. Carbon isotope fractionation between diet and bioapatite in ungulate mammals and implications for ecological and paleoecological studies. *Oecologia*, 120, 347–363.

Cerling, T.E., Harris, J.M., MacFadden, B.J., Leakey, M.G., Quade, J., Eisenmann, V., Ehleringer, J.R. 1997. Global vegetation change through the Miocene/Pliocene boundary. *Nature*, 389(6647), 153-158.

Cerling, T.E., Andanje, S.A., Blumenthal, S.A., Brown, F.H., Chritz, K.L., Harris, J.M., Hart, J.A., Kirera, F.M., Kaleme, P., Leakey, L.N., Leakey, M.G., Levon, N.E., Kyalo Manthi, F., Passey, B.H., Uno, K.T. 2015. Dietary changes of large herbivores in the Turkana Basin, Kenya from 4 to 1 Ma. *Proceedings of the National Academy of Sciences*, 112(37), 11467-11472.

Chase, B.M., Meadows, M.E. 2007. Late Quaternary dynamics of southern Africa's winter rainfall zone. *Earth-Science Reviews*, 84(3), 103-138.

Chase, B.M., Meadows, M.E., Scott, L., Thomas, D.S.G., Marais, E., Sealy, J., Reimer, P.J. 2009. A record of rapid Holocene climate change preserved in hyrax middens from southwestern Africa. *Geology*, 37(8), 703-706.

Chase, B.M., Meadows, M.E., Carr, A.S., Reimer, P.J. 2010. Evidence for progressive holocene aridification in southern Africa recorded in Namibian hyrax middens: implications for African Monsoon dynamics and the 'African Humid Period'. *Quaternary Research*, 74, 36-45.

Chase, B.M., Quick, L.J., Meadows, M.E., Scott, L., Thomas, D.S., Reimer, P.J. 2011. Late glacial interhemispheric climate dynamics revealed in South African hyrax middens. *Geology*, 39(1), 19-22.

Chase, B.M., Lim, S., Chevalier, M., Boom, A., Carr, A.S., Meadows, M.E., Reimer, P.J. 2015. Influence of tropical easterlies in southern Africa's winter rainfall zone during the Holocene. *Quaternary Science Reviews*, 107, 138-148.

Chazan, M. 2015. Technological trends in the Acheulean of Wonderwerk Cave, South Africa. *African Archaeological Review*, 32(4), 701-728.

Chazan, M., Horwitz, L.K. 2009. Milestones in the development of symbolic behaviour: a case study from Wonderwerk Cave, South Africa. *World Archaeology*, 41(4), 521-539.

Chazan,M., Horwitz, L.K. 2015. An overview of recent research atWonderwerk Cave, South Africa. In: Thiaw, I., Bocoum H. (Eds.), *Preserving African cultural heritage*, 253–261. Proceedings of the 13th Congress of the Panafrican Archaeological Association for Prehistory and Related Studies – PAA, and of the 20th Meeting of the Society of Africanist Archaeologists – SAfA, Dakar. Mémoires de l'IFAN - C. A. DIOP, n° 93.

Chazan, M., Horwitz, L.K., Ron, H., Matmon, A., Porat, N., Avery, M., Yates, R., Sumner, A., Goldberg. P. 2008. The Earlier Stone Age sequence in the Northern Cape Province, South Africa: new research. In: de Lumley, H. (ed.), *Les Culture á Biface du Pleistocene Inferieur et Moyen dans le Monde*. Tautavel conference proceedings: in press.

Chazan, M., Avery, D.M., Bamford, M.K., Berna, F., Brink, J., Fernandez-Jalvo, Y., Goldberg, P., Holt, S., Matmon, A., Porat, N., Ron, H., Rossouw, L., Scott, L., Horwitz,

L.K. 2012. The Oldowan horizon in Wonderwerk Cave (South Africa): archaeological, geological, paleontological and paleoclimatic evidence. *Journal of Human Evolution*, 63, 859–866.

Chazan, M., Wilkins, J., Morris, D., Berna, F. 2012. Bestwood 1: a newly discovered Earlier Stone Age living surface near Kathu, Northern Cape Province, South Africa. *Antiquity*, 86(331).

Chevalier, M., Chase, B.M. 2015. Southeast African records reveal a coherent shift from high-to low-latitude forcing mechanisms along the east African margin across last glacial–interglacial transition. *Quaternary Science Reviews*, 125, 117-130.

Churchill, S.E., Brink, J.S., Berger, L.R., Hutchison, R.A., Rossouw, L., Stynder, D., Hahncox, P.J., Brandt, D., Woodborne, S., Loock, J.C., Scott, L., Ungar, P. 2000. Erfkroon: a new Florisian fossil locality from fluvial contexts in the western Free State, South Africa. *South African Journal of Science*, 96, 161-163.

Clayton, F., Sealy, J., Pfeiffer, S. 2006. Weaning age among foragers at Matjes River Rock Shelter, South Africa, from stable nitrogen and carbon isotope analyses. *American Journal of Physical Anthropology*, 129(2), 311-317.

Cockcroft, M.J., Wilkinson, M.J., Tyson, P.D. 1987. The application of a present-day climatic model to the late Quaternary in southern Africa. *Climate Change*, 161-181.

Codron, D., Brink, J.S., Rossouw, L., Clauss, M. 2008. The evolution of ecological specialization in southern African ungulates: competition- or physical environmental turnover? *Oikos*, 117, 344-353.

Collins, J.A., Schefuß, E., Heslop, D., Mulitza, S., Prange, M., Zabel, M., Tjallingii, R., Dokken, T.M., Huang, E., MacKensen, A., Schulz, M., Tian, J., Zarriess, M., Wefer, G., 2011. Interhemispheric symmetry of the tropical African rainbelt over the past 23,000 years. *Nature Geoscience*, 4, 42-45.

Collins, J.A., Schefuß, E., Govin, A., Mulitza, S., Tiedemann, R. 2014. Insolation and glacial–interglacial control on southwestern African hydroclimate over the past 140 000 years. *Earth and Planetary Science Letters*, 398, 1-10.

Compton, J.S. 2011. Pleistocene sea-level fluctuations and human evolution on the southern coastal plain of South Africa. *Quaternary Science Reviews*, 30(5), 506-527.

Crisp, M.K. 2013. *Amino acid racemization dating: Method development using African ostrich (Struthio camelus) eggshell*. PhD thesis, University of York.

Cruz-Uribe, K., Klein, R.G., Avery, G., Avery, M., Halkett, D., Hart, T., Milo, R.G., Garth Sampson, C., Volman, T.P. 2003. Excavation of buried Late Acheulean (Mid-Quaternary) land surfaces at Duinefontein 2, Western Cape Province, South Africa. *Journal of Archaeological Science*, 30, 559–575.

Cueno, F. 1965. Observations of the breeding of the klipspringer antelope, *Oreotragus oreotragus*, and the behaviour of their young born at the Naples zoo. *International Zoo Yearbook*, 5(1), 45-48.

Cumming, D.H.M. 2008. Phacochoerus africanus. The IUCN Red List of Threatened Species. Version 2014.3. <www.iucnredlist.org>. Downloaded on 01 May 2015.

D'Errico, F., Henshilwood, C., Vanharen, M., van Niekerk, K. 2005. *Nassarius kraussianus* shell beads from Blombos Cave: evidence for symbolic behaviour in the Middle Stone Age. *Journal of human evolution*, 48, 3-24

D'Errrico, F., Vanhaeren, M., Wadley, L. 2008. Possible shell beads from the Middle Stone Age layers of Sibudu Cave, South Africa. *Journal of Archaeological Science*, 35, 2675-2685.

D'Errico, F., Backwell, L., Villa, P., Degano, I., Lucejko, J.J., Bamford, M.K., Higham, T.F.G., Colombini, M.P. Beaumont, P.B. 2012. Early evidence of San material culture represented by organic artifacts from Border Cave, South Africa. *Proceedings of the National Academy of Sciences*, 109(33), 13214-13219.

D'Errico, F., Backwell, L.R., Wadley, L. 2012. Identifying regional variability in Middle Stone Age bone technology. The case of Sibudu Cave. *Journal of Archaeological Science*, 39(7), 2479-2495.

Dansgaard, W. 1964. Stable isotopes in precipitation. *Tellus A*, 16(4).

Dart, R.A. 1925. *Australopithecus africanus*: The man-ape of South Africa. *Nature*, 115, 195-199.

Dart, R.A. 1953. *The predatory transition from ape to man*. Brill.

Dawson, T.E., Ehleringer, J.R. 1991. Streamside trees that do not use stream water. *Nature*, 350(6316), 335-337.

Dawson, T.E., Mambelli, S., Plamboeck, A.H., Templer, P.H., Tu, K.P. 2002. Stable isotopes in plant ecology. *Annual review of ecology and systematics*, 507-559.

De Ruiter, D.J. 2003. Revised faunal lists for members 1–3 of Swartkrans, South Africa. *Annals of the Transvaal Museum*, 40, 29-41.

Deacon, J.C.G. 1982. *The Later Stone Age in the Southern Cape South Africa*. Doctoral dissertation, University of Cape Town.

Deacon, J. 1984. Later Stone Age people and their descendants in southern Africa. In: Klein, R.G. (ed.), *Southern African Prehistory and Palaeoenvironments*, 221-328. Rotterdam: Balkema.

Deacon, J. 1990. Weaving the fabric of Stone Age research in Southern Africa. In: Robertshaw, P.T. (ed.), *A History of African Archaeology*, 39-58. London: James Curry.

Deacon, H.J. 1995. Two Late Pleistocene-Holocene Archaeological depositories from the southern Cape, South Africa. *South African Archaeological Bulletin*, 50, 121-131.

Deacon, H.J., Lancaster, N. 1988. *Late Quaternary palaeoenvironments of southern Africa*. Oxford: Clarendon Press.

Deacon, H.J., Deacon, J. 1999. *Human beginnings in South Africa: Uncovering the secrets of the Stone Age*. Cape Town: David Philip.

Dee, M., Bronk Ramsey, C. 2000. Refinement of graphite target production at ORAU. *Nuclear Instruments and Methods in Physics Research B*, 172, 449-453.

DeMenocal, P.B. 1995. Plio-Pleistocene African climate. *Science*, 270(5233), 53-59.

DeMenocal, P.B. 2004. African climate change and faunal evolution during the Pliocene–Pleistocene. *Earth and Planetary Science Letters*, 220(1-2), 3-24.

DeNiro, M.J., Epstein, S. 1978. Influence of diet on the distribution of carbon isotopes in animals. *Geochimica et cosmochimica acta*, 42(5), 495-506.

Dewar, G., Stewart, B.A. 2012. Preliminary results of excavations at Spitzkloof rockshelter, Richtersveld, South Africa. *Quaternary International*, 270, 30-39.

Donges, J.F., Donner, R.V., Trauth, M.H., Marwan, N., Schellnhuber, H.J., Kurths, J. 2011. Nonlinear detection of paleoclimate-variability transitions possibly related to human evolution. *Proceedings of the National Academy of Sciences*, 108(51), 20422-20427.

Doran, T.L., Herries, A.I., Hopley, P.J., Sombroek, H., Hellstrom, J., Hodge, E., Kuhn, B.F. 2015. Assessing the paleoenvironmental potential of Pliocene to Holocene tufa deposits along the Ghaap Plateau escarpment (South Africa) using stable isotopes. *Quaternary Research*, 84, 133-143.

Du Toit, J.T. 1993. The feeding ecology of a very small ruminant, the steenbok (*Raphicerus campestris*). *African Journal of Ecology*, 31, 35–48.

Dupont, L.M., Caley, T., Kim, J.H., Castaneda, I., Malaize, B., Giraudeau, J. 2011. Glacial-interglacial vegetation dynamics in South Eastern Africa coupled to sea surface temperature variations in the Western Indian Ocean. *Climate Past,* 7, 1209-1224.

Dupont, L.M., Rommerskirchen, F., Mollenhauer, G., Schefuß, E. 2013. Miocene to Pliocene changes in South African hydrology and vegetation in relation to the expansion of C_4 plants. *Earth and Planetary Science Letters*, 375, 408-417.

Ecker, M., Botha-Brink, J., Lee-Thorp, J.A., Piuz, A., Horwitz, L.K. 2015. Ostrich eggshell as a source of palaeoenvironmental information in the arid interior of South Africa: A case study from Wonderwerk Cave. In: Runge, J. (ed.), *Changing Climates, Ecosystems and Environments within Arid Southern Africa and Adjoining Regions: Palaeoecology of Africa*, 33, 95-115.

Edwards, E.J., Osborne, C.P., Strömberg, C.A., Smith, S.A. 2010. The origins of C_4 grasslands: integrating evolutionary and ecosystem science. *Science*, 328(5978), 587-591.

Ehleringer, J.R., Cerling, T.E., Helliker, B.R. 1997. C_4 photosynthesis, atmospheric CO_2, and climate. *Oecologia*, 112(3), 285-299.

Elliot, J.C. 1997. Structure, crystal chemistry and desnity of enamel apatites. In: Chadwick, D.J., Cardew, G. (eds.), *Dental Enamel,* 54-84. Ciba Foundation Symposium 205. Chichester: Wiley.

EPICA Community Members 2010. Stable oxygen isotopes of ice core EDML. doi:10.1594/PANGAEA.754444.

Estes, R. 1991. *The behaviour guide to African mammals* (Vol. 64). Berkeley: University of California Press.

Faith, J.T. 2014. Late Pleistocene and Holocene mammal extinctions on continental Africa. *Earth-Science Reviews*, 128, 105-121.

Faith, J.T., Tryon, C.A., Peppe, D.J., Beverly, E.J., Blegen, N., Blumenthal, S., Chritz, K.L., Driese, S.G., Patterson, D. 2015. Paleoenvironmental context of the Middle Stone Age record from Karungu, Lake Victoria Basin, Kenya, and its implications for human and faunal dispersals in East Africa. *Journal of Human Evolution*, 83, 28-45.

Farquhar, G.D., Ehleringer, J.R., Hubick, K.T. 1989. Carbon isotope discrimination and photosynthesis. *Annual review of plant biology*, 40(1), 503-537.

Fernandez-Jalvo, Y., Avery, M.D. 2015. Pleistocene Micromammals and Their Predators at Wonderwerk Cave, South Africa. *African Archaeological Review, in press*.

Franz-Odendaal, T.A., Lee-Thorp, J.A., Chinsamy, A. 2003. Insights from stable light isotopes on enamel defects and weaning in Pliocene herbivores. *Journal of biosciences*, 28(6), 765-773.

Gagnon, M., Chew, A.E. 2000. Dietary preferences in extant African Bovidae. *Journal of Mammalogy*, 81(2), 490-511.

Garrett, N.D., Fox, D.L., Mcnulty, K.P., Tryon, C.A., Faith, J.T., Peppe, D.J. 2014. Stable isotopic paleoenvironmental reconstruction of the late Pleistocene Middle Stone Age sites on Rusinga and Mfangano Islands, Lake Victoria, Kenya. *American Journal of Physical Anthropology*, 153(S58), 124-124.

Gasse, F., Chalie, F., Vincens, A., Williams, M.A.J., Williamson, D. 2008. Climatic patterns in equatorial and southern Africa from 30,000 to 10,000 years ago reconstructed from terrestrial and near-shore proxy data. *Quaternary Science Reviews*, 27, 2316-2340.

Gatesy, J., Amato, G., Vrba, E., Schaller, G., DeSalle, R. 1997. A cladistic analysis of mitochondrial ribosomal DNA from the Bovidae. *Molecular phylogenetics and evolution*, 7(3), 303-319.

Gibbon, R.J., Pickering, T.P., Sutton, M.B., Heaton, J.L., Kuman, K., Clarke, R.J. Brain, C.K., Granger, D.E. 2014. Cosmogenic nuclide burial dating of hominin-bearing

Pleistocene cave deposits at Swartkrans, South Africa. *Quaternary Geochronology*, 24, 10-15.

Godwin, H. 1962. Half-life of radiocarbon. *Nature*, 195, 984.

Goldberg, P., Berna, F., Chazan, M. 2015. Deposition and Diagenesis in the Earlier Stone Age of Wonderwerk Cave, Excavation 1, South Africa. *African Archaeological Review*, 32, 613-643.

Gonfiantini, R., Gratziu, S., Tongiorgi, E. 1965. Oxygen isotopic composition of water in leaves. *Isotopes and Radiation in Soil-Plant Nutrition Studies*, 405-410.

Goodwin, A.J.H., van Riet Lowe, C. 1929. The Stone Age Cultures of South Africa. *Annals of the South African Museum*, 27, 1-289.

Granger, D.E., Gibbon, R.J., Kuman, K., Clarke, R.J., Bruxelles, L., Caffee, M.W. 2015. New cosmogenic burial ages for Sterkfontein Member 2 Australopithecus and Member 5 Oldowan. *Nature*, doi:10.1038/nature14268.

Green, H., Pickering, R., Drysdale, R., Johnson, B.C., Hellstrom, J., Wallace, M. 2015. Evidence for global teleconnections in a late Pleistocene speleothem record of water balance and vegetation change at Sudwala Cave, South Africa. *Quaternary Science Reviews*, 110, 114-130.

Gröcke, D.R., Bocherens, H., Mariotti, A. 1997. Annual rainfall and nitrogen-isotope correlation in Macropod collagen: Application as a paleoprecipitation indicator. *Earth and Planetary Science Letters*, 153, 279–285.

Grubb, P. 2008. Hystrix africaeaustralis. The IUCN Red List of Threatened Species. Version 2014.3. <www.iucnredlist.org>. Downloaded on 29 April 2015.

Grün, R., Brink, J.S., Spooner, N.A., Taylor, L. Stringer, C.B., Franciscus, R.G., Murray, A.S. 1996. Direct dating of Florisbad hominid. *Nature*, 382, 500-501.

Hare, V., Sealy, J. 2013. Middle Pleistocene dynamics of southern Africa's winter rainfall zone from $\delta^{13}C$ and $\delta^{18}O$ values of Hoedjiespunt faunal enamel. *Palaeogeography, Palaeoclimatology, Palaeoecology*, 374, 72-80.

Hatch, M.D. 1971. The C_4-pathway of photosynthesis. Evidence for an intermediate pool of carbon dioxide and the identity of the donor C_4-dicarboxylic acid. *Biochemical Journal*, 125, 425-432.

Hattersley, P.W. 1992. C_4 photosynthetic pathway variation in grasses (Poaceae): its significance for arid and semi-arid lands. In: Chapman, G.P. (ed.), *Desertified grasslands: their biology and management*, 181-212. Linnaeus Society Symposium series 13. London: Academic Press.

Hattersley P.W. 1982. ^{13}C values of C_4 types in grasses. *Functional Plant Biology*, 9, 139–154.

Heaton, T.H.E., Talma, A.S., Vogel, J.C. 1986. Dissolved gas paleotemperatures and ^{18}O variations derived from groundwater near Uitenhage, South Africa. *Quaternary Research*, 25(1), 79-88.

Helliker, B.R., Ehleringer, J.R. 2000. Establishing a grassland signature in veins: ^{18}O in the leaf water of C_3 and C_4 grasses. *Proceedings of the National Academy of Sciences*, 97(14), 7894-7898.

Hendey, Q.B. 1974. Faunal dating of the late Cenozoic of Southern Africa, with special reference to the Carnivora. *Quaternary Research*, 4(2), 149-161.

Henshilwood, C.S., F. D'Errico, C. Marean, R. Milo, R. Yates. 2001. An early bone tool industry from the Middle Stone Age at Blombos Cave, South Africa: implications for the origins of modern human behaviour, symbolism and language. *Journal of human evolution*, 41, 631–678.

Henshilwood, C.S., d'Errico, F., Yates, R., Jacobs, Z., Tribolo, C., Duller, G., T., Mercier, N., Sealy, J.C., Valladas, H., Watts, I., Wintle, A.G. 2002. Emergence of modern human behavior: Middle Stone Age engravings from South Africa. *Science*, 295, 1278–1280.

Henshilwood, C.S., d'Errico, F., van Niekerk, K.L., Coquinot, Y., Jacobs, Z., Lauritzen, S.-E., Menu, M., García-Moreno, R. 2011. A 100,000-year-old ochre-processing workshop at Blombos Cave, South Africa. *Science*, 334, 219–222.

Herries, A.I.R 2003. Magnetostratigraphy of the South African hominid palaeocaves. *American Journal of Physical Anthropology*, 113-113.

Herries, A.I.R., Shaw, J. 2011. Palaeomagnetic analysis of the Sterkfontein palaeocave deposits : Implications for the age of the hominin fossils and stone tool industries. *Journal of human evolution*, 60, 523–539.

Herries, A.I.R., Adams, J.W., Kuykendall, K.L., Shaw, J. 2006. Speleology and magnetobiostratigraphic chronology of the GD 2 locality of the Gondolin hominin-bearing paleocave deposits, North West Province, South Africa. *Journal of Human Evolution*, 51(6), 617-631.

Herries, A.I.R., Hopley, P.J., Adams, J.W., Curnoe, D., Maslin, M.A. 2010. Geochronology and Palaeoenvironments of Southern African Hominin-Bearing Localities-A Reply to Wrangham et al., 2009, 'Shallow-Water Habitats as Sources of Fallback Foods for Hominins'. *American Journal of Physical Anthropology*, 143(4), 640-646.

Hillman-Smith, A.K.K., Owen-Smith, N., Anderson, J.L., Hall-Martin, A.J., Selaladi, J.P. 1986. Age estimation of the white rhinoceros (*Ceratotherium simum*). *Journal of Zoology*, 210(3), 355-377.

Hillson, S. 2005. *Teeth*. Cambridge University Press.

Hilton-Barber, B., Berger, L.R. 2004. *Field Guide to the Cradle of Humankind. Sterkfontein, Swartkrans, Kromdraai & Environs World Heritage Site*. Cape Town: Struik Nature.

Hobson, K.A. 1995. Reconstructing avian diets using stable-carbon and nitrogen isotope analysis of egg components: patterns of isotopic fractionation and turnover. *Condor*, 752-762.

Hofmann, R.R. 1968. Comparisons of the rumen and omasum structure in East African game ruminants in relation to their feeding habits. *Symposium Zoological Society London*, 21, 179-194.

Hogg, A.G., Hua, Q., Blackwell, P.G., Niu, M., Buck, C.E., Guilderson, T.P., Heaton, T.J., Palmer, J.G., Reimer, P.J., Reimer, R.W., Turney, C.S.M., Zimmerman, S.R.H. 2013. SHCal13 Southern Hemisphere Calibration, 0-50,000 Years cal BP. *Radiocarbon*, 55(4), 1889-1903.

Holmgren, K., Karlen, W., Shaw, P.A. 1995. Paleoclimatic significance of the stable isotopic composition and petrology of a Late Pleistocene stalagmite from Botswana. *Quaternary Research*, 43(3), 320–328.

Holmgren, K., Lee-Thorp, J.A., Cooper, G.R.J., Lundblad, K., Partridge, T.C., Scott, L., Sithaldeen, R., Talma, A.S., Tyson, P.D. 2003. Persistent millennial-scale climatic variability over the past 25,000 years in Southern Africa. *Quaternary Science Reviews*, 22(21-22), 2311–2326.

Holzkämper, S., Holmgren, K., Lee-Thorp, J.A., Talma, S., Mangini, A., Partridge, T. 2009. Late pleistocene stalagmite growth in Wolkberg cave, South Africa. *Earth and Planetary Science Letters*, 282(1), 212-221.

Hönisch, B., Hemming, N.G., Archer, D., Siddall, M., McManus, J.F. 2009. Atmospheric carbon dioxide concentration across the mid-Pleistocene transition. *Science*, 324(5934), 1551-1554.

Hopley, P.J., Maslin, M.A. 2010. Climate-averaging of terrestrial faunas: an example from the Plio-Pleistocene of South Africa. *Journal Information*, 36(1).

Hopley, P.J., Weedon, G.P., Marshall, J.D., Herries, A.I.R., Latham, A.G., Kuykendall, K.L. 2007a. High-and low-latitude orbital forcing of early hominin habitats in South Africa. *Earth and Planetary Science Letters*, 256(3), 419-432.

Hopley, P.J., Marshall, J.D., Weedon, G.P., Latham, A.G., Herries, A.I.R., Kuykendall, K.L. 2007b. Orbital forcing and the spread of C_4 grasses in the late Neogene: Stable isotope evidence from South African speleothems. *Journal of human evolution*, 53(5), 620-634.

Hoppe, K.A., Stover, S.M., Pascoe, J.R., Amundson, R. 2004. Tooth enamel biomineralization in extant horses: implications for isotopic microsampling. *Palaeogeography, Palaeoclimatology, Palaeoecology*, 206(3), 355-365.

Horwitz, L.K., Chazan, M. 2015. Past and present at Wonderwerk Cave (Northern Cape Province, South Africa). *African Archaeological Review*, 32(4), 595-612.

Horwitz, L.K., Avery, M.D., Bamford, M., Berna, F., Brink, J., Ecker, M., Fernandez-Jalvo, Y., Goldberg, P., Holt, S., Lee-Thorp, J.A., Matmon, A., Pickering, R., Porat, N., Rossouw, L., Scott, S., Chazan, M. *in press*. Wonderwerk Cave, Northern Cape Province: An Early Pleistocene Palaeo-environmental Sequence for the Interior of South Africa. In: Reynolds,

S.C., Bobe, R. (ed.), *African Palaeoenvironments*. Cambridge: Cambridge University Press.

Huang, Y.A., Street-Perrott, F.A., Metcalfe, S.E., Brenner, M., Moreland, M., Freeman, K.H. 2001. Climate change as the dominant control on glacial-interglacial variations in C_3 and C_4 plant abundance. *Science*, 293(5535), 1647-1651.

Humphreys, A.J.B., Thackeray, A.I. 1983. *Ghaap and Gariep. Later Stone Age Studies in the Northern Cape*. Cape Town: South African Archaeological Society Monograph No. 2.

Huntsman-Mapila, P., Ringrose, S., Mackay, A.W., Downey, W.S., Modisi, M., Coetzee, S.H., Tiercelin, J.-J., Kampunzu, A.B., Vanderpost, C. 2006. Use of the geochemical and biological sedimentary record in establishing palaeo-environments and climate change in the Lake Ngami basin, NW Botswana. *Quaternary International*, 148(1), 51–64.

IUCN SSC Antelope Specialist Group 2008a. Tragelaphus strepsiceros. The IUCN Red List of Threatened Species. Version 2014.3. <www.iucnredlist.org>. Downloaded on 28 April 2015.

IUCN SSC Antelope Specialist Group 2008b. Antidorcas marsupialis. The IUCN Red List of Threatened Species. Version 2014.3. <www.iucnredlist.org>. Downloaded on 28 April 2015.

IUCN SSC Antelope Specialist Group 2008c. Raphicerus campestris. The IUCN Red List of Threatened Species. Version 2014.3. <www.iucnredlist.org>. Downloaded on 01 May 2015.

IUCN SSC Antelope Specialist Group 2008d. Redunca fulvorufula. The IUCN Red List of Threatened Species. Version 2014.3. <www.iucnredlist.org>. Downloaded on 28 April 2015.

IUCN SSC Antelope Specialist Group 2008e. Kobus leche. The IUCN Red List of Threatened Species. Version 2014.3. <www.iucnredlist.org>. Downloaded on 01 May 2015.

Jacobson, L., De Beer, F.C., Nshimirimana, R. 2011. Tomography imaging of South African archaeological and heritage stone and pottery objects. *Nuclear Instruments and Methods in Physics Research Section A: Accelerators, Spectrometers, Detectors and Associated Equipment*, 651(1), 240-243.

Jacobson, L., De Beer, F.C., Nshimirimana, R., Horwitz, L.K., Chazan, M. 2013. Neutron tomographic assessment of incisions on prehistoric stone slabs: a case study from Wonderwerk Cave, South Africa. *Archaeometry*, 55(1), 1-13.

Johnson B.J., Miller G.H., Beaumont P.B., Fogel M.L. 1997. The determination of late Quaternary paleoenvironments at Equus Cave, South Africa, using stable isotopes and amino acid racemization in ostrich eggshell. *Palaeogeography, Palaeoclimatology Palaeoecology*, 136, 121–137.

Johnson, B.J., Fogel, M.L., Miller, G.H. 1998. Stable isotopes in modern ostrich eggshell: A calibration for paleoenvironmental applications in semi-arid regions of southern Africa. *Geochimica et Cosmochimica Acta*, 62(14), 2451–2461.

Jouzel, J., Masson-Delmotte, V., Cattani, O., Dreyfus, G., Falourd, S., Hoffmann, G., Minster, B., Nouet, J., Barnola, J.M., Chappellaz, J., Fischer, H., Gallet, J.C., Johnson, S., Leuenberger, M., Loulergue, L., Lüthi, D., Oerter, H., Parrenin, F., Raisbeck, G., Raynaud, D., Schilt, A., Schwander, J., Selmo, E., Souchez, R., Spahni, R., Stauffer, B., Steffensen, J.P., Stenni, B., Stocker, T.F., Tison, J.L., Werner, M., Wolff, E.W. 2007. Orbital and millennial Antarctic climate variability over the past 800,000 years. *Science*, 317(5839), 793-796.

Kaplan, J. 1990. The Umhlatuzana Rock Shelter sequence: 100 000 years of Stone Age history. *Natal Museum Journal of Humanities*, 2, 1–94.

Keeling, C.D., Bacastow, R.B., Bainbridge, A.E., Ekdahl, C.A., Guenther, P.R., Waterman, L.S., Chin, J.F. 1976. Atmospheric carbon dioxide variations at Mauna Loa observatory, Hawaii. *Tellus*, 28(6), 538-551.

Keeling, C.D., Piper, S.C., Bacastow, R.B., Wahlen, M., Whorf, T.P., Heimann, M., Meijer, H.A. 2005. Atmospheric CO_2 and $^{13}CO_2$ exchange with the terrestrial biosphere and oceans from 1978 to 2000: observations and carbon cycle implications. In: Cerling, T.E., Dearing, M.D., Ehleringer, J.R. (eds.), *A history of atmospheric CO_2 and its effects on plants, animals, and ecosystems*, 83-113. New York: Springer.

Kendall, R.L. 1969. An ecological history of the Lake Victoria basin. *Ecological Monographs*, 121-176.

Kgope, B.S., Bond, W.J., Midgley, G.F. 2010. Growth responses of African savanna trees implicate atmospheric CO_2 as a driver of past and current changes in savanna tree cover. *Austral Ecology*, 35(4), 451-463.

Kiberd, P. 2006. Bundu Farm: a report on archaeological and palaeoenvironmental assemblages from a pan site in Bushmanland, Northern Cape, South Africa. *The South African Archaeological Bulletin*, 189-201.

Kingdon, J. 1979. *Proboscids (Proboscidea): Elephantids (Elephantidae). East African mammals: an atlas of evolution in Africa*. New York: Academic Press.

Kingdon, J. 1982. *East African Mammals. An Atlas of Evolution in East Africa, Vol. 3*. New York: Academic Press.

Kingdon, J., Happold, D., Butynski, T., Hoffmann, M., Happold, M., Kalina, J. 2013. *Mammals of Africa* (Vol. 1-6). A&C Black.

Kingston, J.D. 2011. Stable isotopic analyses of Laetoli fossil herbivores. In: Harrison, T. (ed.), *Paleontology and geology of Laetoli: Human evolution in context*, 293-328. Netherlands: Springer.

Klein, R.G. 1988. The archaeological significance of animal bones from Acheulean sites in southern Africa. *African Archaeological Review*, 6(1), 3-25

Klein, R.G., 2009. *The human career. Human biological and cultural origins*. Chicago: The University of Chicago press.

Klein, R.G., Cruz-Uribe, K. 1987. Large mammal and tortoise bones from Elands Bay Cave and nearby sites, Western Cape Province, South Africa. In: Parkington, J.E., Hall, M. (ed.), *Papers in the Prehistory of the Western Cape, South Africa,* 132–163. Oxford: British Archaeological Reports International Series 332.

Koch, P.L., Tuross, N., Fogel, M.L. 1997. The effects of sample treatment and diagenesis on the isotopic integrity of carbonate in biogenic hydroxylapatite. *Journal of Archaeological Science*, 24(5), 417-429.

Kohfeld, K.E., Graham, R.M., De Boer, A.M., Sime, L.C., Wolff, E.W., Le Quéré, C., Bopp, L. 2013. Southern Hemisphere westerly wind changes during the Last Glacial Maximum: paleo-data synthesis. *Quaternary Science Reviews*, 68, 76-95.

Kohn, M.J., Schoeninger, M.J., Valley, J.W. 1996. Herbivore tooth oxygen isotope compositions: effects of diet and physiology. *Geochimica et Cosmochimica Acta*, 60(20), 3889-3896.

Kohn, M.J., Schoeninger, M.J., Valley, J.W. 1998. Variability in oxygen isotope compositions of herbivore teeth: reflections of seasonality or developmental physiology? *Chemical Geology*, 152, 97–112.

Kroopnick, P., Craig, H. 1972. Atmospheric oxygen: isotopic composition and solubility fractionation. *Science*, 175(4017), 54-55.

Kuhn, B.F., Carlson, K.J., Hopley, P.J., Zipfel, B., Berger, L.R. 2015. Identification of fossilized eggshells from the Taung hominin locality, Taung, Northwest Province, South Africa. *Palaeontologia Electronica*, 18(1), 1-16.

Kulongoski, J.T., Hilton, D.R. 2004. Climate variability in the Botswana Kalahari from the late Pleistocene to the present day. *Geophysical Research Letters*, 31, 1-5.

Kuman, K.A., Field, A.S., Thackeray, J.F. 1997. Dicovery of new artefacts at Kromdraii. *South African Journal of Science*, 93, 187-193.

Kuman, K., Inbar, M., Clarke, R.J. 1999. Palaeoenvironments and cultural sequence of the Florisbad Middle Stone Age hominid site, South Africa. *Journal of Archaeological Science*, 26(12), 1409-1425.

Leduc, G., Schneider, R., Kim, J.H., Lohmann, G. 2010. Holocene and Eemian sea surface temperature trends as revealed by alkenone and Mg/Ca paleothermometry. *Quaternary Science Reviews*, 29(7), 989-1004.

Lee-Thorp, J.A., Beaumont, P.B. 1990. Environmental shifts in the last 20 000 years. *South African Journal of Science*, 86(7-10), 452-453

Lee-Thorp, J.A., van der Merwe, N.J. 1991. Aspects of the chemistry of modern and fossil biological apatites. *Journal of Archaeological Science*, 18(3), 343-354.

Lee-Thorp, J.A., Beaumont, P.B. 1995. Vegetation and seasonality shifts during the late Quaternary deduced from $^{13}C/^{12}C$ ratios of grazers at Equus Cave, South Africa. *Quaternary Research*, 43, 426–432.

Lee-Thorp, J.A., Talma, A.S. 2000. Stable light isotopes and environments in the southern African Quaternary and Late Pliocene. *Oxford Monographs on Geology and Geophysics*, 40, 236-251.

Lee-Thorp, J.A., Ecker, M. 2015. Holocene climate and environmental changes from stable isotopes in ostrich egg shell at Wonderwerk Cave, South Africa. *African Archaeological Review*, DOI 10.1007/s10437-015-9202-y.

Lee-Thorp, J.A., van der Merwe, N.J., Brain, C.K. 1994. Diet of *Australopithecus robustus* at Swartkrans from stable carbon isotopic analysis. *Journal of human evolution*, 27(4), 361-372.

Lee-Thorp, J.A., Thackeray, J.F., van der Merwe, N. 2000. The hunters and the hunted revisited. *Journal of human evolution*, 39(6), 565-576.

Lee-Thorp, J.A., Sponheimer, M., Luyt, J. 2007. Tracking changing environments using stable carbon isotopes in fossil tooth enamel: an example from the South African hominin sites. *Journal of human evolution*, 53(5), 595-601.

Lee-Thorp, J.A., Sponheimer, M., Passey, B.H., de Ruiter, D.J., Cerling, T.E. 2010. Stable isotopes in fossil hominin tooth enamel suggest a fundamental dietary shift in the Pliocene. *Philosophical Transactions of the Royal Society B: Biological Sciences*, 365(1556), 3389-3396.

Lee-Thorp, J.A., Likius, A., Mackaye, H.T., Vignaud, P., Sponheimer, M., Brunet, M. 2012. Isotopic evidence for an early shift to C_4 resources by Pliocene hominins in Chad. *Proceedings of the National Academy of Sciences*, 109(50), 20369-20372.

LeGeros, R.Z. 1981. Apatites in biological systems. *Progress in crystal growth and characterization*, 4(1), 1-45.

LeGeros, R.Z., Bonel, G., Legros, R. 1978. Types of "H2O" in human enamel and in precipitated apatites. *Calcified Tissue Research*, 26(1), 111-118.

LeGeros, R.Z., Trautz, O.R., LeGeros, J.P., Klein, E., Shirra, W.P. 1967. Apatite crystallites: effects of carbonate on morphology. *Science*, 155(3768), 1409-1411.

Leonard, J.A., Rohland, N., Glaberman, S., Fleischer, R.C., Caccone, A., Hofreiter, M. 2005. A rapid loss of stripes: the evolutionary history of the extinct quagga. *Biology Letters*, 1(3), 291-295.

Lepre, C.J. 2014. Early Pleistocene lake formation and hominin origins in the Turkana–Omo rift. *Quaternary Science Reviews*, 102, 181-191.

Levin, N.E., Quade, J., Simpson, S.W., Semaw, S., Rogers, M. 2004. Isotopic evidence for Plio–Pleistocene environmental change at Gona, Ethiopia. *Earth and Planetary Science Letters*, 219(1), 93-110.

Levin, N.E., Cerling, T.E., Passey, B.H., Harris, J.M., Ehleringer, J.R. 2006. A stable isotope aridity index for terrestrial environments. *Proceedings of the National Academy of Sciences*, 103(30), 11201-11205.

Levin, N.E., Brown, F.H., Behrensmeyer, A.K., Bobe, R., Cerling, T.E. 2011. Paleosol carbonates from the Omo Group: Isotopic records of local and regional environmental change in East Africa. *Palaeogeography, Palaeoclimatology, Palaeoecology*, 307(1), 75-89.

Levin, N.E. 2015. Environment and Climate of Early Human Evolution. *Annual Review of Earth and Planetary Sciences*, 43(1).

Lisiecki, L.E., Raymo, M.E. 2005. A Pliocene-Pleistocene stack of 57 globally distributed benthic $\delta^{18}O$ records. *Paleoceanography*, 20(1).

Lister, A.M. 2013. The role of behaviour in adaptive morphological evolution of African proboscideans. *Nature,* 500(7462), 331-334.

Lister, A.M., Stuart, A.J. 2008. The impact of climate change on large mammal distribution and extinction: evidence from the last glacial/interglacial transition. *Comptes Rendus Geoscience*, 340(9), 615-620.

Livingstone, D.A., Clayton, W.D. 1980. An altitudinal cline in tropical African grass floras and its paleoecological significance. *Quaternary Research*, 13(3), 392-402.

Lombard, M., Haidle, M.N. 2012. Thinking a Bow-and-arrow Set: Cognitive Implications of Middle Stone Age Bow and Stone-tipped Arrow Technology. *Cambridge Archaeological Journal*, 22, 237–264.

Lombard, M., Wadley, L., Deacon, J., Wurz, S., Parsons, I., Mohapi, M., Swart, J., Mitchell, P. 2012. South African and Lesotho Stone Age Sequence updated (I). *South African Archaeological bulletin*, 67(195), 1-22.

Long, A., Hendershott, R., Martin, P. 1983. Radiocarbon dating of fossil eggshell. *Radiocarbon*, 25(2), 533-539.

Longinelli, A. 1984. *Oxygen isotopic composition of mammal bones as a new tool for studying ratios of paleoenvironmental water and paleoclimates*. Vienna: International Atomic Energy Agency.

López-Polín, L. 2012. Possible interferences of some conservation treatments with subsequent studies on fossil bones: A conservator's overview. *Quaternary International*, 275, 120-127.

Lorenzen, E.D., Arctander, P., Siegismund, H.R. 2008. High variation and very low differentiation in wide ranging plains zebra (*Equus quagga*): insights from mtDNA and microsatellites. *Molecular ecology*, 17(12), 2812-2824.

Lüthi, D., Le Floch, M., Bereiter, B., Blunier, T., Barnola, J.-M., Siegenthaler, U., Raynaud, D., Jouzel, J., Fischer, H., Kawamura, K., Stocker, T.F. 2008. High-resolution carbon dioxide concentration record 650,000–800,000 years before present. *Nature*, 453(7193), 379-382.

Luyt, J., Lee-Thorp, J.A., Avery, G. 2000. New light on Middle Pleistocene west coast environments from Elandsfontein, Western Cape Province, South Africa. *South African Journal of Science*, 96, 399-403.

Lyons, R.P., Scholz, C.A., Cohen, A.S., King, J.W., Brown, E.T., Ivory, S.J., Johnson, T.C., Deino, A.L., Reinthal, P.N., McGlue, M.M,. Blome, M.W. 2015. Continuous 1.3-million-year record of East African hydroclimate, and implications for patterns of evolution and biodiversity. *Proceedings of the National Academy of Sciences*, 112(51), 15568-15573.

Lyons, R., Tooth, S., Duller, G.A. 2014. Late Quaternary climatic changes revealed by luminescence dating, mineral magnetism and diffuse reflectance spectroscopy of river terrace palaeosols: a new form of geoproxy data for the southern African interior. *Quaternary Science Reviews*, 95, 43-59.

Mackay, A. 2006. A characterization of the MSA stone artefact assemblages from the 1984 excavations at Klein Kliphuis, Western Cape. *South African Archaeological Bulletin*, 61, 181–188.

Mackay, A. 2010. The late Pleistocene archaeology of Klein Kliphuis Rock Shelter, Western Cape: 2006 excavations. *South African Archaeological Bulletin*, 65, 132–147.

Mackay, A., Welz, A. 2008. Engraved ochre from a Middle Stone Age context at Klein Kliphuis in the Western Cape of South Africa. *Journal of Archaeological Science,* 35, 1521-1532.

Malan, B.D., Cooke, H.B.S. 1941. A preliminary account of the Wonderwerk Cave, Kuruman. *South African Journal of Science*, 37, 300-312.

Malan, B.D., Wells, L.H. 1943. A further report on the Wonderwerk Cave, Kuruman. *South African Journal of Science*, 40, 258-270.

Maslin, M.A., Christensen, B. 2007. Tectonics, orbital forcing, global climate change, and human evolution in Africa: introduction to the African paleoclimate special volume. *Journal of Human Evolution*, 53(5), 443-464.

Maslin, M.A., Trauth, M.H. 2009. Plio-Pleistocene East African pulsed climate variability and its influence on early human evolution. In: Grine, F.E., Fleagle, J.G., Leakey, R.E. (eds.), *The First Humans–Origin and Early Evolution of the Genus Homo*, 151-158. Netherlands: Springer.

Maslin, M.A., Brierley, C.M. 2015. The role of orbital forcing in the Early Middle Pleistocene Transition. *Quaternary International*, http://dx.doi.org/10.1016/j.quaint.2015.01.047.

Maslin, M.A., Brierley, C.M., Milner, A.M., Shultz, S., Trauth, M.H., Wilson, K.E. 2014. East African climate pulses and early human evolution. *Quaternary Science Reviews*, 101, 1-17.

Matmon, A., Ron, H., Chazan, M., Porat, N., Horwitz, L.K. 2012. Reconstructing the history of sediment deposition in caves : A case study from Wonderwerk Cave. South Africa. *Geological Society of America Bulletin*, 124 (3-4), 611-625.

Matmon, A., Hidy, A.J., Vainer, S., Crouvi, O., Fink, D., Erel, Y., Horwitz, L.K., Chazan, M., ASTER Team 2015. New chronology for the southern Kalahari Group sediments with implications for sediment-cycle dynamics and early hominin occupation. *Quaternary Research*, http://dx.doi.org/10.1016/j.yqres.2015.04.009.

Matthee, C.A., Robinson, T.J. 1997. Mitochondrial DNA phylogeography and comparative cytogenetics of the springhare, *Pedetes capensis* (Mammalia: Rodentia). *Journal of Mammalian Evolution*, 4(1), 53-73.

McBrearty, S., Brooks, A.S. 2000. The revolution that wasn't: a new interpretation of the origin of modern human behavior. *Journal of human evolution*, 39, 453–563.

McCormac, F.G., Hogg, A.G., Blackwell, P.G., Buck, C.E., Higham, T.F., Reimer, P.J. 2004. SHCal04 Southern Hemisphere calibration, 0–11.0 cal kyr BP. *Radiocarbon*, 46(3), 1087-1092.

McCarroll, D., Loader, N.J. 2004. Stable isotopes in tree rings. *Quaternary Science Reviews*, 23(7), 771-801.

McNabb, J., Sinclair, A. 2009. *The Cave of Hearths: Makapan Middle Pleistocene Research Project: Field Research by Anthony Sinclair and Patrick Quinney, 1996-2001*. Oxford: Archaeopress.

Meadows, M.E., Baxter, A.J. 1999. Late Quaternary palaeoenvironments of the southwestern Cape, South Africa: a regional synthesis. *Quaternary International*, 57-8, 193–206.

Medina-Elizalde, M., Lea, D.W. 2005. The mid-Pleistocene transition in the Tropical Pacific. *Science*, 310(5750), 1009-1012.

Metcalfe, J.Z., Longstaffe, F.J., Zazula, G.D. 2010. Nursing, weaning, and tooth development in woolly mammoths from Old Crow, Yukon, Canada: implications for Pleistocene extinctions. *Palaeogeography, Palaeoclimatology, Palaeoecology*, 298(3), 257-270.

Methuen, H.H. 1846. *Life in the Wilderness*. London: Richard Bentley.

Michels, J.W. 1973. *Dating methods in archaeology*. Seminar Press.

Miller, J.M., Willoughby, P.R. 2014. Radiometrically dated ostrich eggshell beads from the Middle and Later Stone Age of Magubike Rockshelter, southern Tanzania. *Journal of Human Evolution*, 74, 118-122.

Miller, G.H., Beaumont, P.B., Jull, A.J.T., Johnson, B. 1992. Pleistocene geochronology and palaeothermometry from protein diagenesis in ostrich eggshells: implications for the

evolution of modern humans. *Philosophical Transactions of the Royal Society B: Biological Sciences*, 337(1280), 149-157.

Miller, R.M., Pickford, M., Senut, B. 2010. The geology, palaeontology and evolution of the Etosha Pan, Namibia: Implications for terminal Kalahari deposition. *South African Journal of Geology,* 113(3), 307-334.

Milton, S.J., Dean, W.R.J., Siegfried, W.R. 1994. Food Selection by Ostrich in Southern Africa. *The Journal of Wildlife Management*, 58(2), 234-248.

Mitchell, P. 2000. The Organization of Later Stone Age Lithic Technology in the Caledon Valley, Southern Africa. *African Archaeological Review*, 17(3), 141-176.

Mitchell, P. 2005. Modelling Later Stone Age Societies in Southern Africa. In: Stahl, A.B. (ed.), *African Archaeology*, 150-173. Blackwell Studies in Global Archaeology.

Mitchell, P. 2008. Developing the archaeology of marine isotope stage 3. *South African Archaeological Society Goodwin Series*, 10, 52-65.

Mitchell, P. 2014. Southern African Hunter-Gatherers of the Last 25,000 Years, In: Mitchell, P., Lane, P.J. (eds.), *The Oxford Handbook of African Archaeology*. Oxford: Oxford University Press.

Monnin, E. 2006. EPICA Dome C high resolution carbon dioxide concentrations. doi:10,1594/PANGAEA,472488.

Monnin, E., Indermühle, A., Dällenbach, A., Flückiger, J., Stauffer, B., Stocker, T.F., Raynaud, D., Barnola, J.-M. 2001. Atmospheric CO_2 concentrations over the last glacial termination. *Science*, 291(5501), 112-114.

Mooney, H.A., Troughton, J.H., Berry, J.A. 1977. Carbon isotope ratio measurements of succulent plants in southern Africa. *Oecologia*, 30(4), 295-305.

Moore, A.E., Eckardt, F. 2012. The evolution and ages of Makgadikgadi palaeo-lakes: Consilient evidence from Kalahari drainage evolution south-central Africa. *South African Journal of Geology*, 115(3), 385-413.

Mucina, L., Rutherford, M.C. 2006. *The vegetation of South Africa, Lesotho and Swaziland*. Pretoria: South African National Biodiversity Institute.

Neumann, F.H., Scott, L., Bousman, C.B., Van As, L. 2010. A Holocene sequence of vegetation change at Lake Eteza, coastal KwaZulu-Natal, South Africa. *Review of Palaeobotany and Palynology*, 162(1), 39-53.

Nicholson, S.E. 2000. The nature of rainfall variability over Africa on time scales of decades to millennia. *Global and Planetary Change*, 26(1–3), 137-158.

Nicholson, S.E. 2001. Climatic and environmental change in Africa during the last two centuries. *Climate Research*, 17(2), 123-144.

Nicholson, S.E. 2011. *Dryland climatology*. Cambridge: Cambridge University Press.

Nicholson, S.E., Flohn, H. 1980. African environmental and climatic changes and the general atmospheric circulation in late Pleistocene and Holocene. *Climatic change*, 2(4), 313-348.

Norström, E., Scott, L., Partridge, T.C., Risberg, J., Holmgren, K. 2009. Reconstruction of environmental and climate changes at Braamhoek wetland, eastern escarpment South Africa, during the last 16,000 years with emphasis on the Pleistocene–Holocene transition. *Palaeogeography, Palaeoclimatology, Palaeoecology*, 271(3), 240-258.

Orlando, L., Metcalf, J.L., Alberdi, M.T., Telles-Antunes, M., Bonjean, D., Otte, M., Martin, F., Eisenmann, V., Mashkour, M., Morello, F., Prado, J.L., Salas-Gismondi, R., Shockey, B.J., Wrinn, P.J., Vasilev, S.K., Ovodov, N.D., Cherry, M.I., Hopwood, B., Male, D., Austin, J.J., Hänni, C., Cooper, A. 2009. Revising the recent evolutionary history of equids using ancient DNA. *Proceedings of the National Academy of Sciences*, 106(51), 21754-21759.

Orton, J. 2012. *Late Holocene archaeology in Namaqualand, South Africa: hunter-gatherers and herders in a semi-arid environment*. DPhil thesis, University of Oxford

Orton, J. 2014. SALSA: The Holocene technocomplexes, a reply to Lombard and colleagues. *South African Archaeological Bulletin*, 69(199), 110-112.

Osborne, C.P., Beerling, D.J. 2006. Nature's green revolution: the remarkable evolutionary rise of C_4 plants. *Philosophical Transactions of the Royal Society B: Biological Sciences*, 361(1465), 173-194.

Osmond, C.B., Harris, B. 1971. Photorespiration during C_4 photosynthesis. *Biochimica et Biophysica Acta (BBA)-Bioenergetics*, 234(2), 270-282.

Pagani, M., Freeman, K.H., Arthur, M.A. 1999. Late Miocene atmospheric CO_2 concentrations and the expansion of C_4 grasses. *Science*, 285, 876-878.

Parkington, J., Cartwright, C., Cowling, R.M., Baxter, A., Meadows, M. 2000. Palaeovegetation at the Last Glacial Maximum in the Western Cape, South Africa: wood charcoal and pollen evidence from Elands Bay Cave. *South African Journal of Science,* 96(11-12), 543–546.

Partridge, T.C. 2005. Dating of the Sterkfontein hominids: progress and possibilities: aspects of hominid evolution. *Transactions of the Royal Society of South Africa*: A Festschrift to PV Tobias FRS, Hon. FRSSAf, 60(2), 107-109.

Partridge, T.C., deMenocal, P.B., Lorentz, S.A., Paiker, M.J., Vogel, J.C. 1997. Orbital forcing of climate over South Africa: a 200,000-year rainfall record from the Pretoria Saltpan. *Quaternary Science Review*, 16, 1125-1133.

Partridge, T.C., Scott, L., Hamilton, J.E. 1999. Synthetic reconstructions of southern African environments during the Last Glacial Maximum (21–18kyr) and the Holocene Altithermal (8–6kyr). *Quaternary International*, 57, 207-214.

Partridge, T.C., Granger, D.E., Caffee, M.W., Clarke, R.J. 2003. Lower Pliocene hominid remains from Sterkfontein. *Science*, 300(5619), 607-612.

Passey, B.H., Robinson, T.F., Ayliffe, L.K., Cerling, T.E., Sponheimer, M., Dearing, M.D., Roeder, B.L., Ehleringer, J.R. 2005. Carbon isotope fractionation between diet, breath CO_2, and bioapatite in different mammals. *Journal of Archaeological Science*, 32(10), 1459-1470.

Petit, J.R., Jouzel, J., Raynaud, D., Barkov, N.I., Barnola, J.M., Basile, I., Bender, M., Chappellaz, J., Davis, M., Delaygue, G., Delmotte, M., Kotlyakov, V.M., Legrand, M., Lipenkov, V.Y., Lorius, C., Pépin, L., Ritz, C., Saltzman, E., Stievenard, M. 1999. Climate and atmospheric history of the past 420,000 years from the Vostok ice core, Antarctica. *Nature*, 399(6735), 429-436.

Pickering, R. 2015. U–Pb Dating Small Buried Stalagmites from Wonderwerk Cave, South Africa: a New Chronometer for Earlier Stone Age Cave Deposits. *African Archaeological Review*, 32, 645-668.

Pickering, R., Hancox, P.J., Lee-Thorp, J.A., Grün, R., Mortimer, G.E., McCulloch, M., Berger, L.R. 2007. Stratigraphy, U-Th chronology, and paleoenvironments at Gladysvale Cave: insights into the climatic control of South African hominin-bearing cave deposits. *Journal of human evolution*, 53(5), 602-619.

Plug, I. 1982. Bone tools and shell, bone and ostrich eggshell beads from Bushman Rock Shelter (BRS), Eastern Transvaal. *The South African Archaeological Bulletin*, 57-62.

Plug, I., Engela, R. 1992. The Macrofaunal Remains from Recent Excavations at Rose Cottage Cave, Orange Free State. *The South African Archaeological Bulletin*, 47(155), 16-25.

Plummer, T.W., Bishop, L.C., Ditchfield, P.W., Ferraro, J.V., Kingston, J.D., Hertel, F., Braun, D.R. 2009. The environmental context of Oldowan hominin activities at Kanjera South, Kenya. In: Hovers, E., Braun, D.R. (eds.), *Interdisciplinary approaches to the Oldowan*, 149-160. Netherlands: Springer.

Porat, N., Chazan, M., Grün, R., Aubert, M., Eisenmann, V., Horwitz, L.K. 2010. New radiometric ages for the Fauresmith industry from Kathu Pan, southern Africa: Implications for the Earlier to Middle Stone Age transition. *Journal of Archaeological Science*, 37(2), 269-283.

Potts, R. 1998. Variability selection in hominid evolution. *Evolutionary Anthropology: Issues, News, and Reviews*, 7(3), 81-96.

Potts, R. 2012. Evolution and Environmental Change in Early Human Prehistory 1. *Annual Review of Anthropology*, 41, 151-167.

Potts, R. 2013. Hominin evolution in settings of strong environmental variability. *Quaternary Science Reviews*, 73, 1-13.

Poyart, C.F., Freminet, A., Bursaux, E. 1975. The bone CO_2 compartment: evidence for a bicarbonate pool. *Respiration Physiology*, 25, 89-99.

Prinsloo, P., Robinson, T.J. 1992. Geographic mitochondrial DNA variation in the rock hyrax, *Procavia capensis*. *Molecular Biology and Evolution*, 9(3), 447-456.

Quade, J., Levin, N., Semaw, S., Stout, D., Renne, P., Rogers, M., Simpson, S. 2004. Paleoenvironments of the earliest stone toolmakers, Gona, Ethiopia. *Geological Society of America Bulletin*, 116(11-12), 1529-1544.

Quick, L.J., Chase, B.M., Meadows, M.E., Scott, L., Reimer, P.J. 2011. A 19.5 kyr vegetation history from the central Cederberg Mountains, South Africa: palynological evidence from rock hyrax middens. *Palaeogeography, Palaeoclimatology, Palaeoecology*, 309(3), 253-270.

Quinn, R.L., Lepre, C.J., Wright, J.D., Feibel, C.S. 2007. Paleogeographic variations of pedogenic carbonate $\delta^{13}C$ values from Koobi Fora, Kenya: implications for floral compositions of Plio-Pleistocene hominin environments. *Journal of human evolution*, 53(5), 560-573.

R Core Team 2013. R: A language and environment for statistical computing. R Foundation for Statistical Computing, Vienna, Austria. URL http://www.R-project.org/.

Rasmussen, S.O., Andersen, K.K., Svensson, A.M., Steffensen, J.P., Vinther, B.M., Clausen, H.B., Siggaard-Andersen, M.-L., Johnson, S.J., Larsen, L.B., Dahl-Jensen, D., Bigler, M., Röthlisberger, R., Fischer, H., Goto-Azuma, K., Hansson, M.E., Ruth, U. 2006. A new Greenland ice core chronology for the last glacial termination. *Journal of Geophysical Research-Part D-Atmospheres*, 111(6).

Rautenbach, I.L. 1971. Ageing criteria in the springbok, *Antidorcas marsupialis* (Zimmermann, 1780) (Artiodactyla: Bovidae). *Annals of the Transvaal Museum*, 27(6), 83-133.

Reimer, P.J., Baillie, M.G., Bard, E., Bayliss, A., Beck, J.W., Bertrand, C.J., Blackwell, P.J., Buck, C.E., Burr, G.S., Cutler, K.B., Damon, P.E., Edwards, R.L., Fairbanks, R.G., Friedrich, M., Guilderson, T.P., Hogg, A.G., Hughen, K.A., Kromer, B., McCormac, G., Manning, S., Ramsey, C.B., Reimer, R.W., Remmele, S., Southon, J.R., Stuiver, M., Talamo, S., Taylor, F.W., Van der Plicht, J., Weyhenmeyer, C.E. 2004. IntCal04 terrestrial radiocarbon age calibration, 0-26 cal kyr BP. *Radiocarbon*, 46(3), 1029-1058.

Roberts, P. 2013. Stable carbon and oxygen isotope analysis of ostrich eggshell (OES) samples from LSA and MSA levels at Blombos Cave, Klipdrift Shelter, and Klipdrift Cave (South Africa). MSc dissertation, University of Oxford.

Rossouw, L., Scott, L. 2016. Phytolith analysis in Wonderwerk Cave. *African Archaeological Review, in press.*

Rozanski, K., Araguás-Araguás, L., Gonfiantini, R. 1993. Isotopic patterns in modern global precipitation. *Climate change in continental isotopic records*, 1-36.

Rüther, H., Chazan, M., Schroeder, R., Neeser, R., Held, C., Walker, S.J., Horwitz, L.K. 2009. Laser scanning for conservation and research of African cultural heritage sites: the case study of Wonderwerk Cave, South Africa. *Journal of Archaeological Science*, 36(9), 1847-1856.

Sadr, K. 2013. *A short history of early herding in southern Africa. Pastoralism in Africa: Past, Present and Future,* 171-197. New York and Oxford: Berghahn Books.

Sage, R.F. 2004. The evolution of C4 photosynthesis. *New phytologist*, 161(2), 341-370.

Sakae, T., Hirai, G. 1982. Calcification and crystallization in bovine enamel. *Journal of dental research*, 61(1), 57-59.

Sampson, C.G. 1974. *The Stone Age Archaeology of South Africa*. New York: Academic Press.

Sauer, E.G.F., Sauer, E.M. 1967. Yawning and other maintenance activities in the South African Ostrich. *The Auk,* 571-587.

Sauer, E.G.F., Sauer, E.M. 1966. Social behaviour of the South African ostrich *Struthio camelus australis*. *Ostrich: Journal of African Ornithology*, 37, 183-191.

Schefuß, E., Schouten, S., Jansen, J.F., Damsté, J.S.S. 2003. African vegetation controlled by tropical sea surface temperatures in the mid-Pleistocene period. *Nature*, 422(6930), 418-421.

Schefuß, E. et al. 2011: Lipids of sediment core GeoB9307-3. doi:10.1594/PANGAEA.771395. In Supplement to: Schefuß, E., Kuhlmann, H., Mollenhauer, G., Prange, M., Pätzold, J. 2011. Forcing of south-east African wet phases during the last 17,000 years. *Nature*, 480(7378), 509-512.

Schmidt, C.W. 2008. *The recovery and study of burned human teeth. In The analysis of burned human remains*. London: Elsevier.

Schmidt, F., Oberhänsli, H., Wilkes, H. 2014. Biocoenosis response to hydrological variability in Southern Africa during the last 84 ka BP: A study of lipid biomarkers and

compound-specific stable carbon and hydrogen isotopes from the hypersaline Lake Tswaing. *Global and Planetary Change*, 112, 92-104.

Scott, L. 1987. Pollen analysis of hyena coprolites and sediments from Equus Cave, Taung, southern Kalahari (South Africa). *Quaternary Research*, 28(1), 144-156.

Scott, L. 1993. Palynological evidence for Late Quaternary warming episodes in southern Africa. *Palaeogeography, Palaeoclimatology, Palaeoecology*, 101(3), 229-235.

Scott, L. 1999. Vegetation history and climate in the Savanna biome South Africa since 190,000 ka: a comparison of pollen data from the Tswaing Crater (the Pretoria Saltpan) and Wonderkrater. *Quaternary International*, 57-8, 215–223.

Scott, L., Vogel, J.C. 1983. Late Quaternary Pollen Profile from the Transvaal Highveld. *South African Journal of Science*, 79, 266-272.

Scott, L., Lee-Thorp, J.A. 2004. Holocene climatic trends and rhythms in southern Africa. In: Batterbee, R., Gasse, F. (eds), *Past Climatic Variability through Europe and Africa*, 691-699. Netherlands: Springer.

Scott, L., Woodborne, S. 2007. Pollen analysis and dating of late Quaternary faecal deposits (hyraceum) in the Cederberg, Western Cape, South Africa. *Review of Palaeobotany and Palynology*, 144 (3-4), 123–134.

Scott, L. Thackeray, J.F. 2015. Palynology of Holocene Deposits in Excavation 1 at Wonderwerk Cave, Northern Cape (South Africa). *African Archaeological Review*, DOI10.1007/s10437-015-9204-9.

Scott, L., Cooremans, B., De Wet, J.S., Vogel, J.C. 1991. Holocene environmental changes in Namibia inferred from pollen analysis of swamp and lake deposits. *The Holocene*, 1(1), 8-13.

Scott, L., Holmgren, K., Talma, A.S., Woodborne, S., Vogel, J.C. 2003. Age interpretation of the Wonderkrater spring sediments and vegetation change in the Savanna Biome, Limpopo province, South Africa: research letter. *South African Journal of Science*, 99(9-10), 484-488.

Scott, L., Bousman, C.B., Nyakale, M. 2005. Holocene pollen from swamp, cave and hyrax dung deposits at Blydefontein (Kikvorsberge), Karoo, South Africa. *Quaternary International*, 129(1), 49-59.

Scott, L., Neumann, F.H., Brook, G.A., Bousman, C.B., Norström, E., Metwally, A.A. 2012. Terrestrial fossil-pollen evidence of climate change during the last 26 thousand years in Southern Africa. *Quaternary Science Reviews*, 32, 100-118.

Ségalen, L. 2003. *Evolution environnementale du Désert du Namib depuis le Miocène. Apports de la sédimentologie et des rapports isotopiques (^{13}C, ^{18}O) mesurés sur des coquilles de ratites*. PhD thesis, University Pierre and Marie Curie Paris.

Ségalen, L., Renard, M., Lee-Thorp, J.A., Emmanuel, L., Le Callonnec, L., De Rafélis, M., Senut, B., Pickford, M., Melice, J.-L. 2006. Neogene climate change and emergence of C_4 grasses in the Namib, southwestern Africa, as reflected in ratite ^{13}C and ^{18}O. *Earth and Planetary Science Letters*, 244(3), 725-734.

Ségalen, L., Lee-Thorp, J.A., Cerling, T. 2007. Timing of C4 grass expansion across sub-Saharan Africa. *Journal of Human Evolution*, 53(5), 549-559.

Seki, O., Foster, G.L., Schmidt, D.N., Mackensen, A., Kawamura, K., Pancost, R.D. 2010. Alkenone and boron-based Pliocene pCO_2 records. *Earth and Planetary Science Letters*, 292(1–2), 201–211.

Sharp, Z. 2007. *Principles of stable isotope geochemistry*. Upper Saddle River, NJ: Pearson Education.

Shi, N., Schneider, R., Beug, H.-J., Dupont, L.M. 2001. Southeast trade wind variations during the last 135 kyr: evidence from pollen spectra in eastern South Atlantic sediments. *Earth and Planetary Science Letters,* 187, 311-321.

Shipman, P., Foster, G., Schoeninger, M. 1984. Burnt bones and teeth: an experimental study of color, morphology, crystal structure and shrinkage. *Journal of archaeological science*, 11(4), 307-325.

Shorrocks, B., Bates, W. 2014. *The Biology of African Savannahs.* Second Edition. Oxford: Oxford University Press.

Siegenthaler, U., Stocker, T.F., Monnin, E., Lüthi, D., Schwander, J., Stauffer, B., Raynaud, D., Barnola, J.-M., Fischer, H., Masson-Delmotte, V., Jouzel, J. 2005. Stable carbon cycle–climate relationship during the late Pleistocene. *Science*, 310(5752), 1313-1317.

Singarayer, J.S., Burrough, S.L. 2015. Interhemispheric dynamics of the African rainbelt during the late Quaternary. *Quaternary Science Reviews*, 124, 48-67.

Singer, R., Wymer, J.J. 1982. *The Middle Stone Age at Klasies River Mouth in South Africa*. Chicago: University of Chicago Press.

Sithaldeen, R., Ackermann, R.R., Bishop, J.M. 2015. Pleistocene Aridification Cycles Shaped the Contemporary Genetic Architecture of Southern African Baboons. *PLoS ONE*, 10(5): e0123207.

Skinner, J.D., Chimimba, C.T. 2005. *The Mammals of the Southern African Subregion*. Cambridge: Cambridge University Press.

Smith, J.M., Lee-Thorp, J.A., Sealy, J.C. 2002. Stable carbon and oxygen isotopic evidence for late Pleistocene to middle Holocene climatic fluctuations in the interior of southern Africa. *Journal of Quaternary Science*, 17(7), 683-695.

Smuts, G.L. 1974. Age determination in Burchell's zebra (*Equus burchelli antiquorum*) from the Kruger National Park. *Journal of the South African Wildlife Management Association*, 4, 103-115.

Sponheimer, M. 1999. *Isotopic ecology of the Makapansgat Limeworks fauna*. PhD thesis, Rutgers University NJ.

Sponheimer, M., Lee-Thorp, J.A. 1999a. Oxygen isotopes in enamel carbonate and their ecological significance. *Journal of Archaeological Science*, 26(6), 723-728.

Sponheimer, M., Lee-Thorp, J.A. 1999b. Alteration of enamel carbonate environments during fossilization. *Journal of Archaeological Science*, 26(2), 143-150.

Sponheimer, M., Lee-Thorp, J.A. 2003. Using carbon isotope data of fossil bovid communities for palaeoenvironmental reconstruction: research articles: human origins research in South Africa. *South African Journal of Science*, 99(5-6), 273-275.

Sponheimer, M., Reed, K.E., Lee-Thorp, J.A. 1999. Combining isotopic and ecomorphological data to refine bovid paleodietary reconstruction: a case study from the Makapansgat Limeworks hominin locality. *Journal of human evolution*, 36(6), 705-718.

Sponheimer, M., Reed, K., Lee-Thorp, J.A. 2001. Isotopic palaeoecology of Makapansgat Limeworks Perissodactyla: research letter. *South African Journal of Science*, 97(7-8), 327-329.

Sponheimer, M., Lee-Thorp, J.A., DeRuiter, D.J., Smith, J.M., van der Merwe, N.J., Reed, K., Grant, C.C., Ayliffe, L.K., Robinson, T.F., Heidelberger, C., Marcus, W. 2003. Diets of Southern African Bovidae: Stable isotope evidence. *Journal of Mammalogy*, 84(2), 471-479.

Stager, J.C., Ryves, D.B., King, C., Madson, J., Hazzard, M., Neumann, F.H., Maud, R. 2013. Late Holocene precipitation variability in the summer rainfall region of South Africa. *Quaternary Science Reviews*, 67, 105-120.

Stern, L.A., Johnson, G.D., Chamberlain, C.P. 1994. Carbon isotope signature of environmental change found in fossil ratite eggshells from a South Asian Neogene sequence. *Geology*, 22(5), 419-422.

Steyn, D., Hanks, J. 1983. Age determination and growth in the hyrax *Procavia capensis* (Mammalia: Procaviidae). *Journal of Zoology*, 201, 247-257.

Stone, A.E.C., Thomas, D.S.G. 2008. Linear dune accumulation chronologies from the southwest Kalahari, Namibia: challenges of reconstructing late Quaternary palaeoenvironments from aeolian landforms. *Quaternary Science Reviews*, 27(17), 1667-1681.

Stowe, M-J., Sealy, J. 2015. Terminal Pleistocene and Holocene dynamics of southern Africa's winter rainfall zone based on carbon and oxygen analysis of bovid tooth enamel from Elands Bay Cave. *Quaternary International*, http://dx.doi.org/10.1016/j.quaint.2015.09.055.

Stute, M., Talma, A.S. 1998. Glacial temperatures and moisture transport regimes reconstructed from noble gases and $\delta^{18}O$, Stampriet aquifer, Namibia. In: *Isotope techniques in the study of environmental change*. Vienna: International Atomic Energy Agency.

Stuut, J.B.W., Prins, M.A., Schneider, R.R., Weltje, G.J., Jansen, J.F., Postma, G. 2002. A 300-kyr record of aridity and wind strength in southwestern Africa: inferences from grain-

size distributions of sediments on Walvis Ridge, SE Atlantic. *Marine Geology*, 180(1), 221-233.

Stuut, J.B.W., Crosta, X., van der Borg, K., Schneider, R. 2004. Relationship between Antarctic sea ice and southwest African climate during the late Quaternary. *Geology*, 32(10), 909-912.

Swart, D. 1988. Studies on the hatching, growth and energy metabolism of ostrich chicks: Struthio Camelus var. Domesticus. Doctoral dissertation, University of Stellenbosch.

Talbot, M.R., Jensen, N.B., Lærdal, T., Filippi, M.L. 2006. Geochemical responses to a major transgression in giant African lakes. *Journal of Paleolimnology*, 35(3), 467-489.

Texier, P.-J., Porraz, G., Parkington, J., Rigaud, J.-P., Poggenpoel, C., Miller, C., Tribolo, C., Cartwright, C., Coudenneau, A., Klein, R., Steele, T., Verna, C. 2010. A Howiesons Poort tradition of engraving ostrich eggshell containers dated to 60,000 years ago at Diepkloof Rock Shelter, South Africa. *Proceedings of the National Academy of Sciences*, 107, 6180–6185.

Thackeray, A.I. 1981. *The Holocene cultural sequence in the northern Cape Province, South Africa*. Ph.D. thesis, Yale University.

Thackeray, A.I. 1981. *Dating the rock art of southern Africa*. Goodwin Series, 21-26.

Thackeray, A.I., Thackeray, J.F., Beaumont, P.B., Vogel, J.C. 1981. Dated rock engravings from Wonderwerk Cave, South Africa. *Science*, 214, 64-67.

Thackeray, J.F. 1984. *Man, animals and extinctions: the analysis of Holocene faunal remains from Wonderwerk Cave, South Africa*. Ph.D. thesis, Yale University.

Thackeray, J.F. 1987. Late Quaternary environmental changes inferred from small mammalian fauna, southern Africa. *Climatic Change*, 10, 285-305.

Thackeray, J.F. 1990. More on *Damaliscus niro* from Wonderwerk Cave. *Pal News*, 6(4), 3-4.

Thackeray, J.F. 2013. The Principle of "Sympathetic Magic" in the Context of Hunting, Trance and Southern African Rock Art. *The Digging Stick*, 30(1), 1-4.

Thackeray, J.F. 2015. Faunal remains from Holocene deposits, Excavation 1, Wonderwerk Cave, South Africa. *African Archaeological Review, in press*.

Thackeray, J.F., Lee-Thorp, J.A. 1992. Isotopic analysis of equid teeth from Wonderwerk Cave, northern Cape Province, South Africa. *Palaeogeography, Palaeoclimatology, Palaeoecology*, 99, 141-150.

Thackeray, J.F., Brink, J.S. 2004. *Damaliscus niro* horn from Wonderwerk Cave and other Pleistocene sites: morphological and chronological considerations. *Palaeontologia Africana*, 40, 89-93.

Thackeray, J.F., de Ruiter, D.J., Berger, L.R., van der Merwe, N.J. 2001. Hominid fossils from Kromdraai: a revised list of specimens discovered since 1938. *Annals of the Transvaal Museum*, 38, 43-56.

Thomas, D.S.G., Burrough, S.L. 2012. Interpreting geoproxies of late Quaternary climate change in African drylands: implications for understanding environmental change and early human behaviour. *Quaternary International*, 253, 5-17.

Thomas, D.S.G., Brook, G., Shaw, P., Bateman, M., Haberyan, K., Appleton, C., Nash, D., McLaren, S., Davies, F. 2003. Late Pleistocene wetting and drying in the NW Kalahari: an integrated study from the Tsodilo Hills, Botswana. *Quaternary International*, 104(1), 53–67.

Tierney, J.E., DeMenocal, P.B. 2013. Abrupt shifts in Horn of Africa hydroclimate since the last glacial maximum. *Science*, 342, 843-846.

Tierney, J.E., Russell, J.M., Damsté, J.S.S., Huang, Y., Verschuren, D. 2011. Late Quaternary behavior of the East African monsoon and the importance of the Congo Air Boundary. *Quaternary Science Reviews*, 30(7), 798-807.

Tieszen, L.L. 1994. Stable isotopes on the plains: vegetation analyses and diet determinations. *Skeletal Biology in the Great Plains*, 261-82.

Trauth, M.H., Maslin, M.A., Deino, A., Strecker, M.R. 2005. Late cenozoic moisture history of East Africa. *Science*, 309(5743), 2051-2053.

Trauth, M.H., Maslin, M.A., Deino, A.L., Strecker, M.R., Bergner, A.G., Dühnforth, M. 2007. High-and low-latitude forcing of Plio-Pleistocene East African climate and human evolution. *Journal of human evolution*, 53(5), 475-486.

Trauth, M.H., Larrasoaña, J.C., Mudelsee, M. 2009. Trends, rhythms and events in Plio-Pleistocene African climate. *Quaternary Science Reviews*, 28(5), 399-411.

Trauth, M.H., Maslin, M.A., Deino, A.L., Junginger, A., Lesoloyia, M., Odada, E.O., Olago, D.O., Olaka, L.A., Strecker, M.R., Tiedemann, R. 2010. Human evolution in a variable environment: the amplifier lakes of Eastern Africa. *Quaternary Science Reviews*, 29(23), 2981-2988.

Trauth, M.H., Bergner, A.G., Foerster, V., Junginger, A., Maslin, M.A., Schaebitz, F. 2015. Episodes of environmental stability versus instability in Late Cenozoic lake records of Eastern Africa. *Journal of human evolution* 87, 21-31.

Truc, L., Chevalier, M., Favier, C., Cheddadi, R., Meadows, M.E., Scott, L., Carr, A.S., Smith, G.F., Chase, B.M. 2013. Quantification of climate change for the last 20,000 years from Wonderkrater, South Africa: implications for the long-term dynamics of the Intertropical Convergence Zone. *Palaeogeography, Palaeoclimatology, Palaeoecology*, 386, 575-587.

Tryon, C.A., Peppe, D.J., Faith, J.T., Van Plantinga, A., Nightingale, S., Ogondo, J., Fox, D.L. 2012. Late Pleistocene artefacts and fauna from Rusinga and Mfangano islands, Lake Victoria, Kenya. *Azania: Archaeological Research in Africa*, 47(1), 14-38.

Tryon, C.A., Faith, J.T., Peppe, D.J., Keegan, W.F., Keegan, K.N., Jenkins, K.H., Nithingale, S., Patterson, D., Van Plantinga, A., Driese, S., Johnson, C.R., Beverly, E.J. 2014. Sites on the landscape: Paleoenvironmental context of late Pleistocene archaeological sites from the Lake Victoria basin, equatorial East Africa. *Quaternary International*, 331, 20-30.

Tyson, P.D. 1986. *Climatic Change and Variability in Southern Africa*. Cape Town: Oxford University Press.

Tyson, P.D., Preston-Whyte, R.A. 2000. *Weather and climate of southern Africa*. Oxford: Oxford University Press.

Underhill, D. 2011. A history of Stone Age archaeological study in South Africa. *South African Archaeological Bulletin*, 66, 3–14.

Ungar, P.S., Scott, R.S., Grine, F.E., Teaford, M.F. 2010. Molar microwear textures and the diets of *Australopithecus anamensis* and *Australopithecus afarensis*. *Philosophical Transactions of the Royal Society B: Biological Sciences*, 365(1556), 3345-3354.

Uno K.T., Cerling, T.E., Harris, J.M., Kanimatsu, Y., Leakey, M.G., Nakatsukasa, M., Nakaya, H. 2011. Late Miocene to Pliocene carbon isotope record of differential diet change among East African herbivores. *Proceedings of the National Academy of Sciences*, 108(16), 6509–6514.

van der Merwe, N.J., Cushing, A., Blumenschine, R. 1999. Stable isotope ratios of fauna and the environment of palaeolake Olduvai. *Journal of human evolution*, 36(4), 24-25.

van der Merwe, N.J., Thackeray, J.F., Lee-Thorp, J.A., Luyt, J. 2003. The carbon isotope ecology and diet of *Australopithecus africanus* at Sterkfontein, South Africa. *Journal of human evolution*, 44, 581–597.

Van Langevelde, F., Van De Vijver, C.A., Kumar, L., Van De Koppel, J., De Ridder, N., Van Andel, J., Skidmore, A.K., Hearne, J.W., Stroosnijder, L., Bond, W.J., Prins, H.H. 2003. Effects of fire and herbivory on the stability of savanna ecosystems. *Ecology*, 84(2), 337-350.

van Zinderen Bakker, E.M. 1976. The evolution of late Quaternary paleoclimates of Southern Africa. *Palaeoecology of Africa*, 9, 160–202.

van Zinderen Bakker, E.M. 1982. Pollen analytical studies of the Wonderwerk Cave, South Africa. *Pollen et Spores*, 24, 235-250.

van Zinderen Bakker, E.M. 1989. Middle Stone Age palaeoenvironments at Florisbad (South Africa). *Palaeoecology of Africa*, 20, 133-154.

van Zinderen Bakker, E.M. 1995. Archaeology and palynology. *The South African Archaeological Bulletin*, 98-105.

Vogel, J.C., Fuls, A., Visser, E. 1986. Pretoria radiocarbon dates III. *Radiocarbon*, 28(3), 1133-1172.

Volman, T.P. 1981. *The Middle Stone Age in the southern Cape*. PhD dissertation, University of Chicago.

von Schirnding, Y., van der Merwe, N.J., Vogel, J.C. 1982. Influence of diet and age on carbon isotope ratios in ostrich eggshell. *Archaeometry*, 24, 3-20.

Vrba, E.S. 1985. Ecological and adaptive changes associated with early hominid evolution. In: Delson, E., (ed.), *Ancestors: The hard evidence*, 63-71. New York: Alan R. Liss.

Vrba, E.S. 1993. The pulse that produced us. *Natural History*, 102(5), 47-51.

Vrba, E.S. 1995. The fossil record of African antelopes (Mammalia, Bovidae) in relation to human evolution and paleoclimate. In: Vrba, E.S., Denton, G., Partridge, T., Burckle, L. (eds.), *Paleoclimate and Evolution*, 385–424. New Haven: Yale University Press.

Vrba, E.S., Schaller, G.B. 2000. *Phylogeny of Bovidae (Mammalia) based on behavior, glands and skull morphology. Antelopes, deer, and relatives: fossil record, behavioral ecology, systematics, and conservation*, 203-222. New Haven Connecticut: Yale University Press.

Vrba, E.S., Vaisnys, J.R., Gatesy, J.E., Desalle, R., Wei, K.Y. 1994. Analysis of paedomorphosis using allometric characters: the example of Reduncini antelopes (Bovidae, Mammalia). *Systematic Biology*, 43(1), 92-116.

Wadley, L. 1993. The Pleistocene Later Stone Age south of the Limpopo River. *Journal of World Prehistory*, 7, 243–296.

Wadley, L. 2005. A typological study of the final Middle Stone Age stone tools from Sibudu Cave, KwaZulu-Natal. *South African Archaeological Bulletin*, 60, 1–13.

Wadley, L., Sievers, C., Bamford, M., Goldberg, P., Berna, F., Miller, C. 2011. Middle Stone Age bedding construction and settlement patterns at Sibudu, South Africa. *Science*, 334, 1388–1391.

Walker, S.J., Lukich, V., Chazan, M. 2014. Kathu Townlands: a high density Earlier Stone Age locality in the interior of South Africa. *PLoS ONE,* 9(7): e103436.

Wang, Y., Kromhout, E., Zhang, C., Xu, Y., Parker, W., Deng, T., Qiu, Z. 2008. Stable isotopic variations in modern herbivore tooth enamel, plants and water on the Tibetan Plateau: Implications for paleoclimate and paleoelevation reconstructions. *Palaeogeography, Palaeoclimatology, Palaeoecology*, 260(3), 359-374.

Watson, V. 1993. Composition of the Swartkrans bone accumulations, in terms of skeletal parts and animals represented. In: Brain, C.K. (ed.), *Swartkrans: A Cave's Chronicle of Early Man*, 35–73. Pretoria: Transvaal Museum.

Weinmann, J.P., Wessinger, G.D., Reed, G. 1942. Correlation of chemical and histological investigations on developing enamel. *Journal of Dental Research*, 21(2), 171-182.

Werger, M.J.A. 1978. *Biogeographical division of southern Africa*, 145-170. Netherlands: Springer.

West, A.G., February, E.C., Bowen, G.J. 2014. Spatial analysis of hydrogen and oxygen stable isotopes ("isoscapes") in ground water and tap water across South Africa. *Journal of Geochemical Exploration*, 145, 213-222.

White, T.D., Asfaw, B., Beyene, Y., Haile-Selassie, Y., Lovejoy, C.O., Suwa, G., WoldeGabriel, G. 2009. *Ardipithecus ramidus* and the paleobiology of early hominids. *Science*, 326(5949), 64-86.

Wilkins, J., Chazan, M. 2012. Blade production~ 500 thousand years ago at Kathu Pan 1, South Africa: support for a multiple origins hypothesis for early Middle Pleistocene blade technologies. *Journal of Archaeological Science*, 39(6), 1883-1900.

Williams, J.B., Siegfried, W.R., Milton, S.J., Adams, N.J., Dean, W.R.J., du Plessis, M.A., Jackson, S., Nagy, K.A. 1993. Field metabolism, water requirements, and foraging behavior of wild ostriches in the Namib. *Ecology*, 74, 390-404.

Wurz, S. 2002. Variability in the Middle Stone Age lithic sequence, 115,000-60,000 years ago at Klasies River, South Africa. *Journal of Archaeological Science,* 29, 1001-1012.

Wynn, J.G. 2004. Influence of Plio-Pleistocene aridification on human evolution: Evidence from paleosols of the Turkana Basin, Kenya. *American Journal of Physical Anthropology*, 123(2), 106-118.

Yakir, D. 1992. Variations in the natural abundances of oxygen-18 and deuterium in plant carbohydrates. *Plant, Cell and Environment*, 15, 1005-1020.

Yellen, J., Brooks, A., Helgren, D., Tappen, M., Ambrose, S., Bonnefille, R., Feathers, J., Goodfirend, G., Ludwig, K., Renne, P., Stewart, K. 2005. The archaeology of Aduma Middle Stone Age sites in the Awash Valley, Ethiopia. *PaleoAnthropology*, 10(2).

Zazzo, A., Bocherens, H., Brunet, M., Beauvilain, A., Billiou, D., Mackaye, H.T., Vignaud, P., Mariotti, A. 2000. Herbivore paleodiet and paleoenvironmental changes in Chad during the Pliocene using stable isotope ratios of tooth enamel carbonate. *Paleobiology*, 26(2), 294-309.

Zazzo, A., Lécuyer, C., Mariotti, A. 2004. Experimentally-controlled carbon and oxygen isotope exchange between bioapatites and water under inorganic and microbially-mediated conditions. *Geochimica et Cosmochimica Acta*, 68(1), 1-12.

Zazzo, A., Balasse, M., Patterson, W.P. 2005. High-resolution $\delta^{13}C$ intratooth profiles in bovine enamel: Implications for mineralization pattern and isotopic attenuation. *Geochimica et Cosmochimica Acta*, 69(14), 3631-3642.

Zhang, Y.G., Pagani, M., Liu, Z., Bohaty, S.M., DeConto, R. 2013. A 40-million-year history of atmospheric CO_2. *Philosophical Transactions of the Royal Society of London A: Mathematical, Physical and Engineering Sciences*, 371, 20130096.

Appendices

Appendix 1 - Terrestrial climate proxy records in southern Africa's summer rainfall zone and neighbouring regions consulted for this thesis.

Site	**Proxies**	**References**	**Latitude/ Longitude**
Austerlitz	$\delta^{13}C$ and $\delta^{15}N$ hyrax midden	Chase et al. 2010	-20.47/14.45
Braamhoek wetland	pollen	Norstöm et al. 2009	-28.23/29.35
Buffalo Cave	$\delta^{13}C$ and $\delta^{18}O$ speleothem	Hopley et al. 2007a	-24.13/29.18
Cango Caves	$\delta^{18}O$ speleothem	Talma and Vogel 1992	-33.39/22.21
De Rif	pollen, $\delta^{13}C$ and $\delta^{15}N$ hyrax midden	Chase et al. 2011, Quick et al. 2011	-32.45/19.22
Drotsky's Cave	pollen and speleothem growth	Brook et al. 1998, Burney et al. 1994	-20.02/21.35
Erfkroon	Pollen, phytolith, enamel $\delta^{13}C$, fauna, river terrace palaeosols	Churchill et al. 2000, Bateman et al. 2012, Lyons et al. 2014	-28.87/25.6
Equus Cave	OES and enamel $\delta^{13}C$ and $\delta^{15}N$, pollen	Scott 1987, Lee-Thorp and Beaumont 1995, Johnson et al. 1997	-27.62/24.62
Florisbad	fauna, pollen, pan sediment	van Zinderen Bakker 1989, Kuman et al. 1997	-28.76/26.08
Ghaap escarpment	tufas	Doran et al. 2015	e.g. -28.57/24.3
Lake Eteza	pollen	Neumann et al. 2010	-28.52/32.15
Lake Ngami	geochemistry, shoreline OSL	Huntsman-Mapila et al. 2006, Burrough et al. 2007	-20.46/22.42
Lake Sibaya	diatoms	Stager et al. 2013	-27.3/32.6
Lethakeng Aquifier	noble gas, $\delta^{18}O$ in groundwater	Kulongoski and Hilton 2004	-24.00/25.00
Lobatse Cave	$\delta^{13}C$ and $\delta^{18}O$ speleothem	Holmgren et al. 1995	-25.33/25.92
Makapansgat (Cold Air Cave)	speleothem $\delta^{13}C$ and $\delta^{18}O$	Lee-Thorp and Talma 2000, Holmgren et al. 2003	-24.02/29.18
Makgadikgadi basin	shoreline OSL	Burrough et al. 2009	-20.62/25.36
Mamatwan mine	sedimentology	Matmon et al. 2015	-27.39/57.67
Pakhuis Pass	pollen, $\delta^{13}C$ hyrax midden	Scott and Woodborne 2007	-32.10/19.07
Sossus Vlei	fluvial OSL	Brook et al. 2006	-24.73/15.37
Southwest Kalahari dunefield	dune OSL	Stone and Thomas 2008	n/a
Spitzkoppe	$\delta^{13}C$ and $\delta^{15}N$ hyrax midden	Chase et al. 2009	-21.82/15.18
Stampriet Aquifier	Excess air concentration	Stute and Talma 1998	-24.34/18.40
Sudwala Cave	speleothem	Green et al. 2015	-25.61/21.18
Tsodilo Hills	Lacustrine and aeolian sediment	Thomas et al. 2003	-18.50/22.00
Tswaing crater (=Pretoria Salt Pan)	geochemistry, pollen, lipid biomarkers, $\delta^{13}C$ and δH	Partridge et al. 1997, Kristen et al. 2007, Schmidt et al. 2014	-25.58/28.75

Uitenhage Aquifier	δH, $\delta^{18}O$, gas composition	Heaton et al. 1986	-33.71/25.40
Wolkberg Cave	Speleothem $\delta^{13}C$ and $\delta^{18}O$	Holzkämper et al. 2009	-24.16/29.95
Wonderkrater	Pollen, phytolith, charcoal	Scott et al. 2003, Blackwell et al. 2014	-24.43/28.75

Appendix 2 - Radiocarbon model.

2.1 Model code of OxCal radiocarbon model of Excavation 1.

```
Plot()
 {
  Outlier_Model("General",T(5),U(0,4),"t");
  Curve="ShCal13.14c";
  Sequence()
  {
   Boundary("Start 5a");
   Phase("5a")
   {
    R_Date("6884", 10080, 100)
    {
     Outlier(0.05);
    };
    R_Date("2852", 9760, 120)
    {
     Outlier(0.05);
    };
   };
   Boundary("End 5a");
   Boundary("Start 4d");
   Phase("Phase 4d")
   {
    Sequence("4dI Sequence")
    {
     Boundary("Start 4dI");
     Phase("4dI")
     {
      R_Date("2546", 9130, 90)
      {
       Outlier(0.05);
      };
      R_Date("2786", 10200, 90)
      {
       Outlier(0.05);
      };
     };
     Boundary("End 4dI");
    };
    Sequence("4dII Sequence")
    {
     Boundary("Start 4dII");
     Phase("4dII")
     {
      R_Date("2790", 10000, 70)
      {
       Outlier(0.05);
      };
      R_Date("6872", 10120, 120)
      {
       Outlier(0.05);
      };
      R_Date("6871", 10120, 100)
      {
       Outlier(0.05);
      };
     };
     Boundary("End 4dII");
    };
```

```
};
Boundary("End 4d");
Boundary("Start 4c");
Phase("4c")
{
 R_Date("2545", 5970, 70)
 {
  Outlier(0.05);
 };
 R_Date("2798", 7430, 60)
 {
  Outlier(0.05);
 };
 R_Date("31897", 5063, 30)
 {
  Outlier(0.05);
 };
};
Boundary("End 4c");
Boundary("Start 4b");
Phase("Phase 4b")
{
 Sequence("4bI Sequence")
 {
  Boundary("Start 4bI");
  Phase("4bI")
  {
   R_Date("30640", 5627, 33)
   {
    Outlier(0.05);
   };
   R_Date("30641", 5771, 34)
   {
    Outlier(0.05);
   };
   R_Date("30642", 5915, 34)
   {
    Outlier(0.05);
   };
  };
  Boundary("End 4bI");
 };
 R_Date("2544", 5180, 70)
 {
  Outlier(0.05);
 };
};
Boundary("End 4b");
Boundary("Start 4aLH");
Phase("4aLH")
{
 R_Date("2797", 4890, 70)
 {
  Outlier(0.05);
 };
 R_Date("30638", 5340, 33)
 {
  Outlier(0.05);
 };
 R_Date("30639", 4887, 33)
 {
  Outlier(0.05);
 };
};
Boundary("End 4aLH");
Boundary("Start 4a");
Phase("Phase 4a")
{
 Sequence("4aI Sequence")
 {
  Boundary("Start 4aI");
  Phase("4aI")
```

```
 {
  R_Date("2541", 4240, 60)
  {
   Outlier(0.05);
  };
 };
 Boundary("End 4aI");
};
Sequence("4aII Sequence")
{
 Boundary("Start 4aII");
 Phase("4aII")
 {
  R_Date("30566", 4459, 30)
  {
   Outlier(0.05);
  };
  R_Date("30567", 4427, 29)
  {
   Outlier(0.05);
  };
  R_Date("30568", 4207, 30)
  {
   Outlier(0.05);
  };
 };
 Boundary("End 4aII");
};
};
Boundary("End 4a");
Boundary("Start 3");
Phase("Phase 3")
{
 R_Date("6873", 2120, 80)
 {
  Outlier(0.05);
 };
 R_Date("2542", 1890, 50)
 {
  Outlier(0.05);
 };
 R_Date("2543", 2910, 60)
 {
  Outlier(0.05);
 };
 R_Date("2785", 3990, 60)
 {
  Outlier(0.05);
 };
};
Boundary("End 3");
Boundary("Start 2b");
Phase("2b")
{
 R_Date("2779", 1210, 50)
 {
  Outlier(0.05);
 };
};
Boundary("End 2b");
};
Difference("Hiatus 2b/3", "Start 2b", "End 3");
Difference("Hiatus 4a/3", "Start 3", "End 4a");
Difference("Hiatus 4aLH/4a", "Start 4a", "End 4aLH");
Difference("Hiatus 4aLH/4b", "Start 4aLH", "End 4b");
Difference("Hiatus 4c/4b", "Start 4b", "End 4c");
Difference("Hiatus 4c/4d", "Start 4c", "End 4d");
Difference("Hiatus 4d/5a", "Start 4d", "End 5a");
Difference("Phase 5a Duration", "End 5a", "Start 5a");
```

```
Difference("Phase 4d Duration", "End 4d", "Start 4d");

Difference("Phase 4c Duration", "End 4c", "Start 4c");

Difference("Phase 4b Duration", "End 4b", "Start 4b");

Difference("Phase 4aLH Duration", "End 4aLH", "Start 4aLH");

}.

Difference("Phase 4a Duration", "End 4a", "Start 4a");

Difference("Phase 3 Duration", "End 3", "Start 3");

Difference("Phase 2b Duration", "End 2b", "Start 2b");
```

2.2 Graphical OxCal output of all dates, boundaries and difference functions of radiocarbon model of Excavation 1.

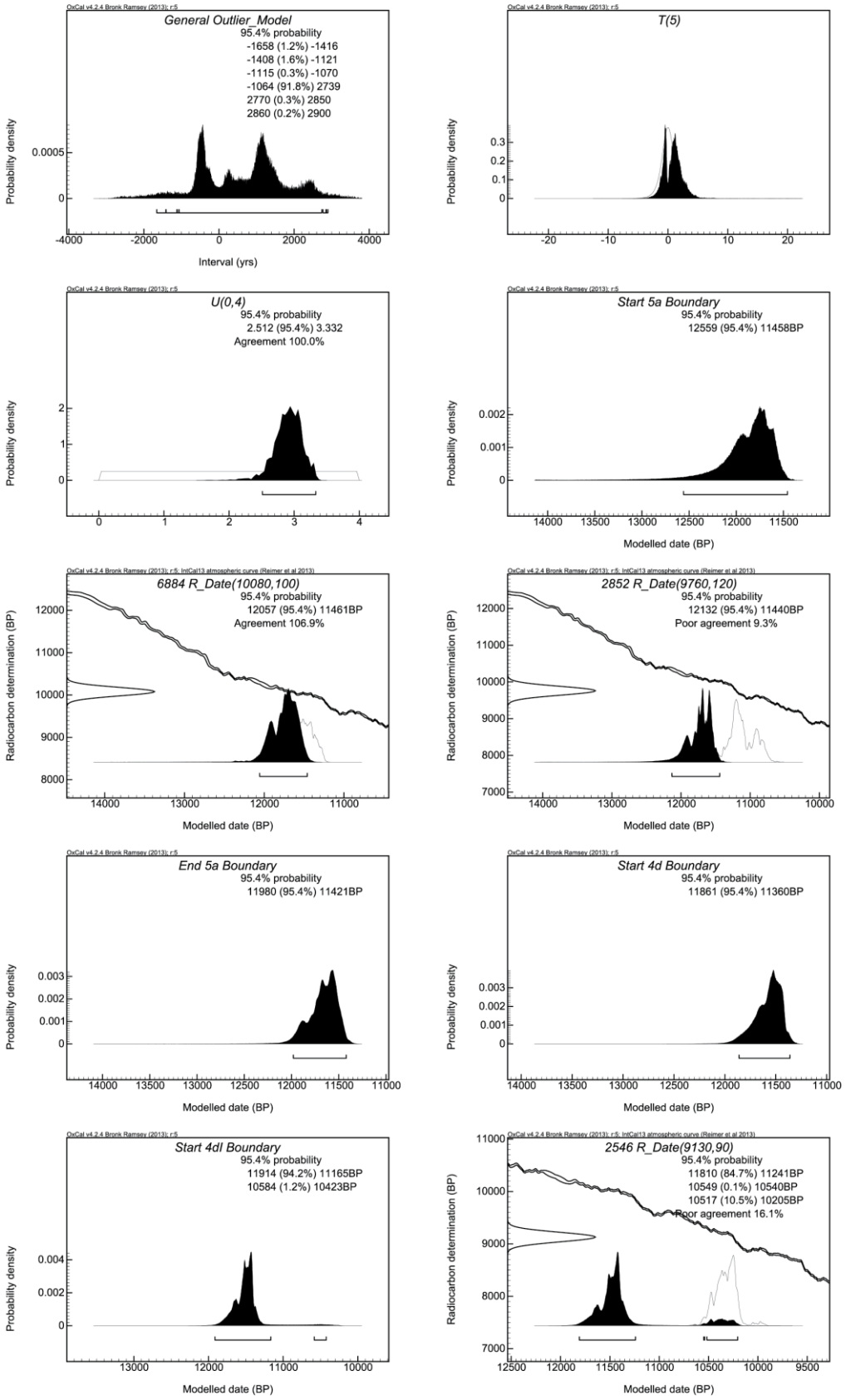

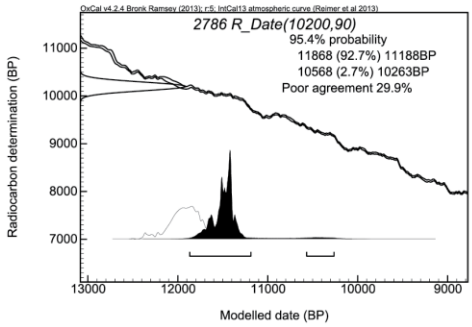
OxCal v4.2.4 Bronk Ramsey (2013); r:5; IntCal13 atmospheric curve (Reimer et al 2013)
2786 R_Date(10200,90)
95.4% probability
11868 (92.7%) 11188BP
10568 (2.7%) 10263BP
Poor agreement 29.9%
Radiocarbon determination (BP)
Modelled date (BP)

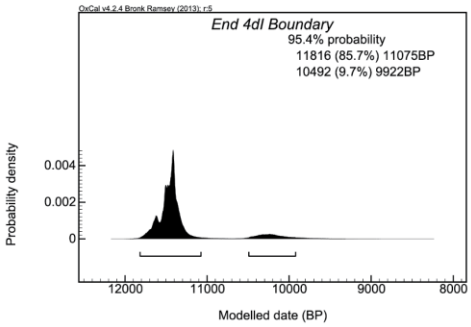
OxCal v4.2.4 Bronk Ramsey (2013); r:5
End 4dI Boundary
95.4% probability
11816 (85.7%) 11075BP
10492 (9.7%) 9922BP
Probability density
Modelled date (BP)

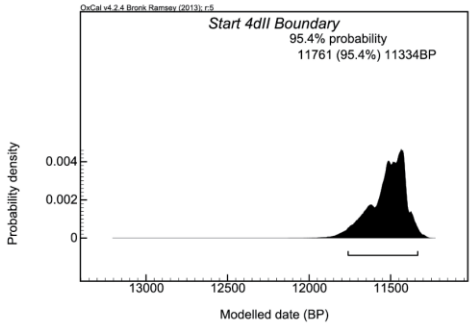
OxCal v4.2.4 Bronk Ramsey (2013); r:5
Start 4dII Boundary
95.4% probability
11761 (95.4%) 11334BP
Probability density
Modelled date (BP)

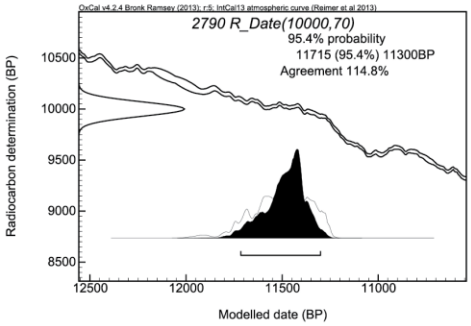
OxCal v4.2.4 Bronk Ramsey (2013); r:5; IntCal13 atmospheric curve (Reimer et al 2013)
2790 R_Date(10000,70)
95.4% probability
11715 (95.4%) 11300BP
Agreement 114.8%
Radiocarbon determination (BP)
Modelled date (BP)

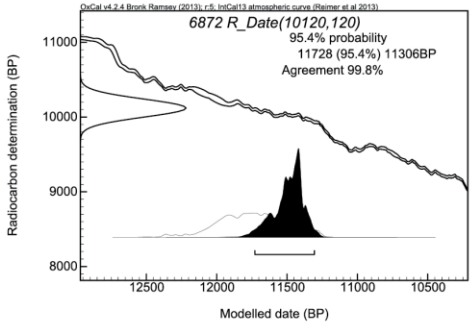
OxCal v4.2.4 Bronk Ramsey (2013); r:5; IntCal13 atmospheric curve (Reimer et al 2013)
6872 R_Date(10120,120)
95.4% probability
11728 (95.4%) 11306BP
Agreement 99.8%
Radiocarbon determination (BP)
Modelled date (BP)

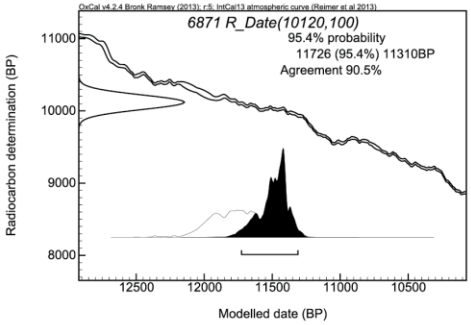
OxCal v4.2.4 Bronk Ramsey (2013); r:5; IntCal13 atmospheric curve (Reimer et al 2013)
6871 R_Date(10120,100)
95.4% probability
11726 (95.4%) 11310BP
Agreement 90.5%
Radiocarbon determination (BP)
Modelled date (BP)

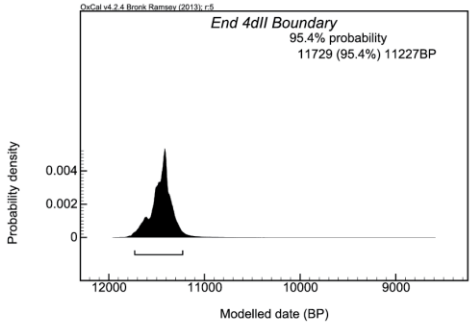
OxCal v4.2.4 Bronk Ramsey (2013); r:5
End 4dII Boundary
95.4% probability
11729 (95.4%) 11227BP
Probability density
Modelled date (BP)

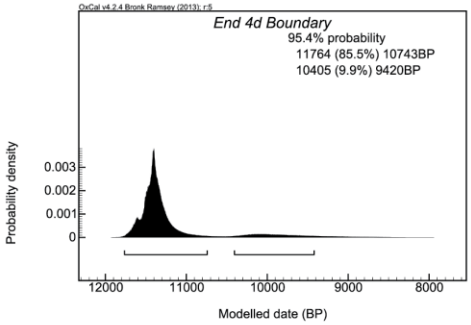
OxCal v4.2.4 Bronk Ramsey (2013); r:5
End 4d Boundary
95.4% probability
11764 (85.5%) 10743BP
10405 (9.9%) 9420BP
Probability density
Modelled date (BP)

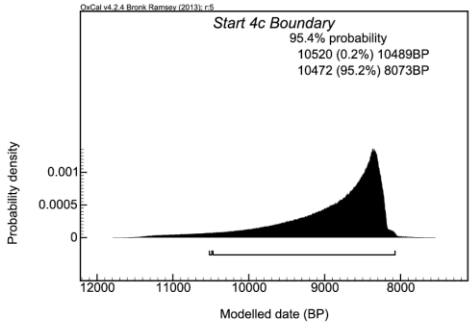
OxCal v4.2.4 Bronk Ramsey (2013); r:5
Start 4c Boundary
95.4% probability
10520 (0.2%) 10489BP
10472 (95.2%) 8073BP
Probability density
Modelled date (BP)

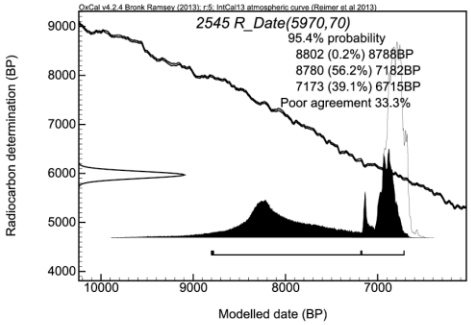
OxCal v4.2.4 Bronk Ramsey (2013); r:5; IntCal13 atmospheric curve (Reimer et al 2013)
2545 R_Date(5970,70)
95.4% probability
8802 (0.2%) 8788BP
8780 (56.2%) 7182BP
7173 (39.1%) 6715BP
Poor agreement 33.3%
Radiocarbon determination (BP)
Modelled date (BP)

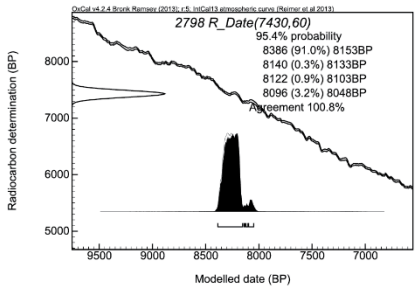
2798 R_Date(7430,60)
95.4% probability
8386 (91.0%) 8153BP
8140 (0.3%) 8133BP
8122 (0.9%) 8103BP
8096 (3.2%) 8048BP
Agreement 100.8%
Radiocarbon determination (BP)
Modelled date (BP)

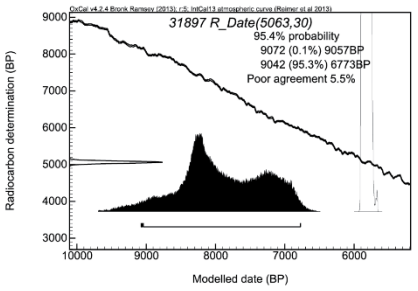
31897 R_Date(5063,30)
95.4% probability
9072 (0.1%) 9057BP
9042 (95.3%) 6773BP
Poor agreement 5.5%
Radiocarbon determination (BP)
Modelled date (BP)

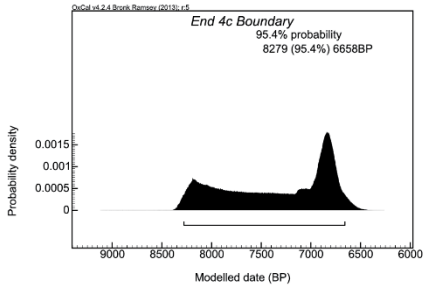
End 4c Boundary
95.4% probability
8279 (95.4%) 6658BP
Probability density
Modelled date (BP)

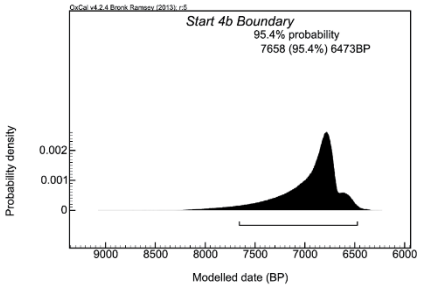
Start 4b Boundary
95.4% probability
7658 (95.4%) 6473BP
Probability density
Modelled date (BP)

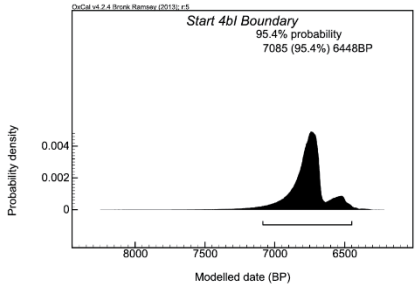
Start 4bl Boundary
95.4% probability
7085 (95.4%) 6448BP
Probability density
Modelled date (BP)

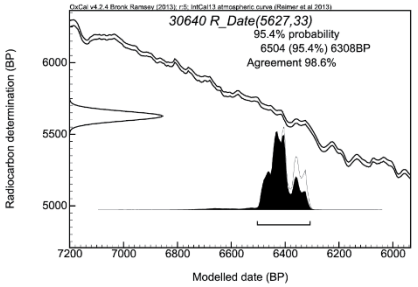
30640 R_Date(5627,33)
95.4% probability
6504 (95.4%) 6308BP
Agreement 98.6%
Radiocarbon determination (BP)
Modelled date (BP)

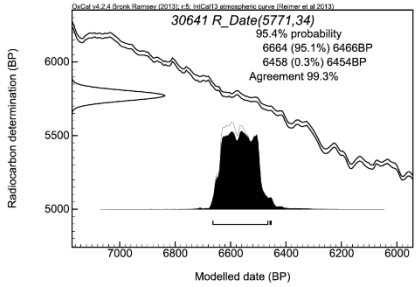
30641 R_Date(5771,34)
95.4% probability
6664 (95.1%) 6466BP
6458 (0.3%) 6454BP
Agreement 99.3%
Radiocarbon determination (BP)
Modelled date (BP)

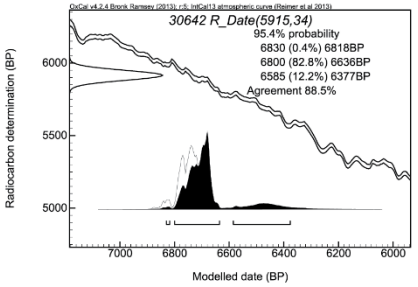
30642 R_Date(5915,34)
95.4% probability
6830 (0.4%) 6818BP
6800 (82.8%) 6636BP
6585 (12.2%) 6377BP
Agreement 88.5%
Radiocarbon determination (BP)
Modelled date (BP)

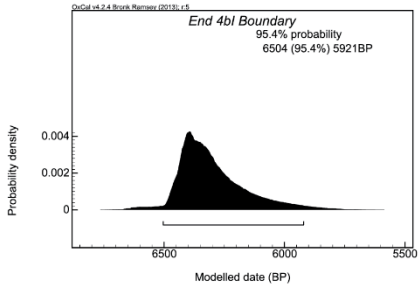
End 4bl Boundary
95.4% probability
6504 (95.4%) 5921BP
Probability density
Modelled date (BP)

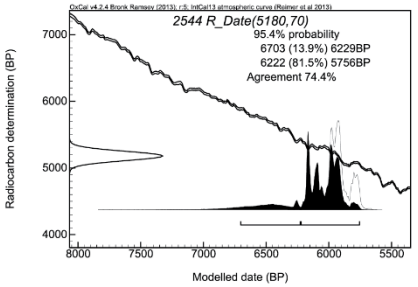
2544 R_Date(5180,70)
95.4% probability
6703 (13.9%) 6229BP
6222 (81.5%) 5756BP
Agreement 74.4%
Radiocarbon determination (BP)
Modelled date (BP)

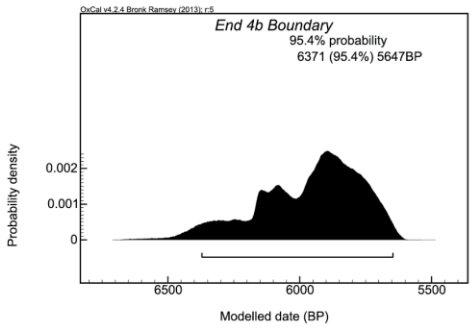
OxCal v4.2.4 Bronk Ramsey (2013); r:5
End 4b Boundary
95.4% probability
6371 (95.4%) 5647BP
Probability density
0.002
0.001
0
6500
6000
5500
Modelled date (BP)

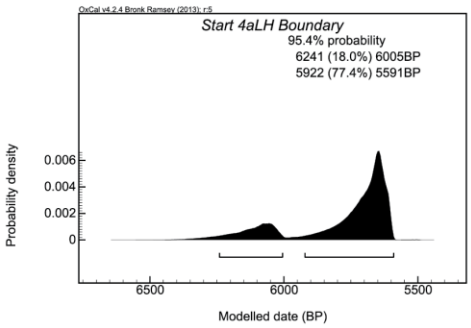
OxCal v4.2.4 Bronk Ramsey (2013); r:5
Start 4aLH Boundary
95.4% probability
6241 (18.0%) 6005BP
5922 (77.4%) 5591BP
Probability density
0.006
0.004
0.002
0
6500
6000
5500
Modelled date (BP)

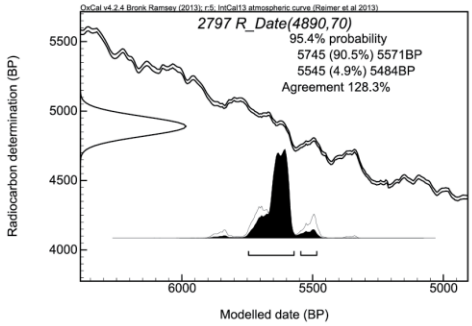
OxCal v4.2.4 Bronk Ramsey (2013); r:5; IntCal13 atmospheric curve (Reimer et al 2013)
2797 R_Date(4890,70)
95.4% probability
5745 (90.5%) 5571BP
5545 (4.9%) 5484BP
Agreement 128.3%
Radiocarbon determination (BP)
5500
5000
4500
4000
6000
5500
5000
Modelled date (BP)

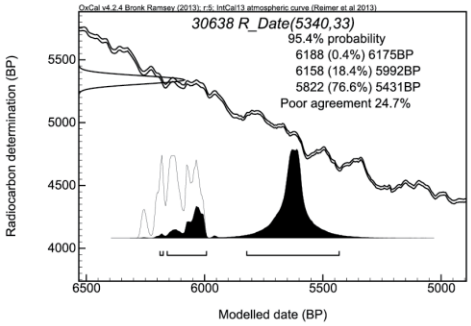
OxCal v4.2.4 Bronk Ramsey (2013); r:5; IntCal13 atmospheric curve (Reimer et al 2013)
30638 R_Date(5340,33)
95.4% probability
6188 (0.4%) 6175BP
6158 (18.4%) 5992BP
5822 (76.6%) 5431BP
Poor agreement 24.7%
Radiocarbon determination (BP)
5500
5000
4500
4000
6500
6000
5500
5000
Modelled date (BP)

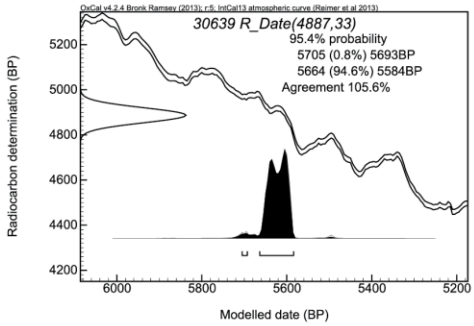
OxCal v4.2.4 Bronk Ramsey (2013); r:5; IntCal13 atmospheric curve (Reimer et al 2013)
30639 R_Date(4887,33)
95.4% probability
5705 (0.8%) 5693BP
5664 (94.6%) 5584BP
Agreement 105.6%
Radiocarbon determination (BP)
5200
5000
4800
4600
4400
4200
6000
5800
5600
5400
5200
Modelled date (BP)

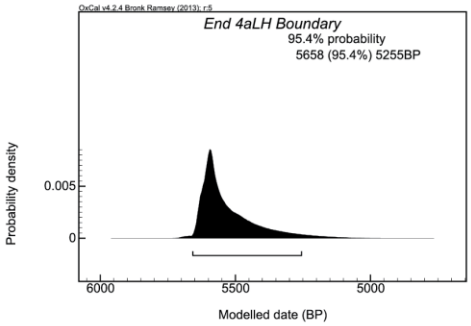
OxCal v4.2.4 Bronk Ramsey (2013); r:5
End 4aLH Boundary
95.4% probability
5658 (95.4%) 5255BP
Probability density
0.005
0
6000
5500
5000
Modelled date (BP)

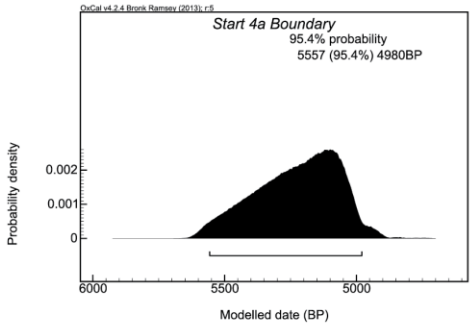
OxCal v4.2.4 Bronk Ramsey (2013); r:5
Start 4a Boundary
95.4% probability
5557 (95.4%) 4980BP
Probability density
0.002
0.001
0
6000
5500
5000
Modelled date (BP)

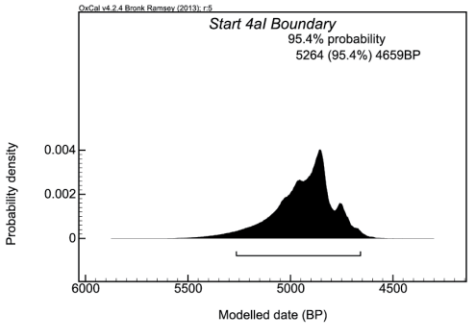
OxCal v4.2.4 Bronk Ramsey (2013); r:5
Start 4al Boundary
95.4% probability
5264 (95.4%) 4659BP
Probability density
0.004
0.002
0
6000
5500
5000
4500
Modelled date (BP)

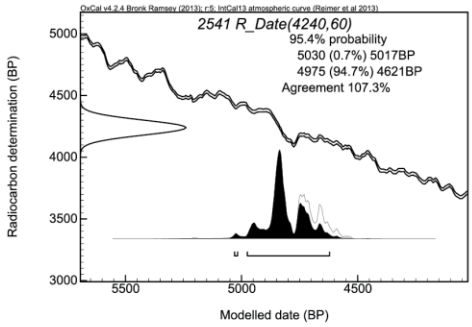
OxCal v4.2.4 Bronk Ramsey (2013); r:5; IntCal13 atmospheric curve (Reimer et al 2013)
2541 R_Date(4240,60)
95.4% probability
5030 (0.7%) 5017BP
4975 (94.7%) 4621BP
Agreement 107.3%
Radiocarbon determination (BP)
5000
4500
4000
3500
3000
5500
5000
4500
Modelled date (BP)

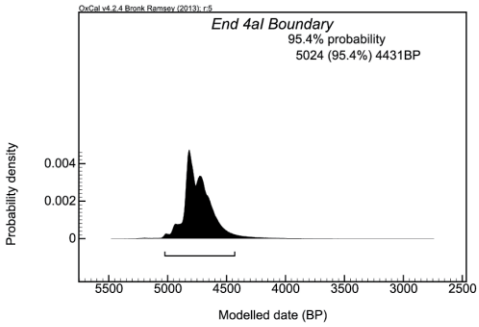
OxCal v4.2.4 Bronk Ramsey (2013); r:5
End 4al Boundary
95.4% probability
5024 (95.4%) 4431BP
Probability density
0.004
0.002
0
5500
5000
4500
4000
3500
3000
2500
Modelled date (BP)

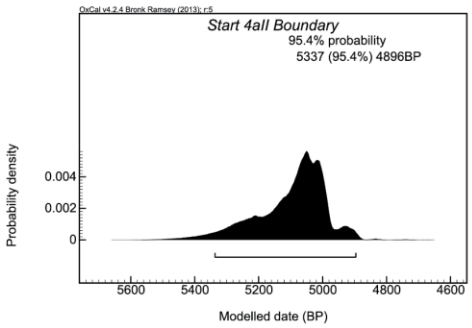
OxCal v4.2.4 Bronk Ramsey (2013); r:5
Start 4all Boundary
95.4% probability
5337 (95.4%) 4896BP
Probability density
Modelled date (BP)

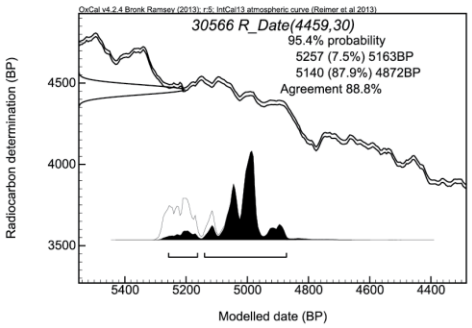
OxCal v4.2.4 Bronk Ramsey (2013); r:5; IntCal13 atmospheric curve (Reimer et al 2013)
30566 R_Date(4459,30)
95.4% probability
5257 (7.5%) 5163BP
5140 (87.9%) 4872BP
Agreement 88.8%
Radiocarbon determination (BP)
Modelled date (BP)

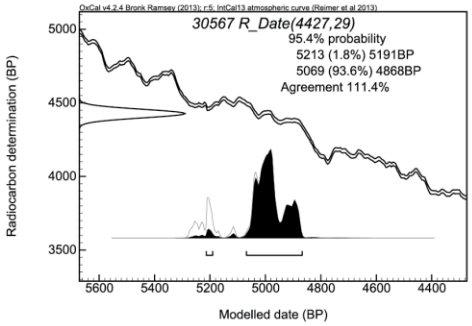
OxCal v4.2.4 Bronk Ramsey (2013); r:5; IntCal13 atmospheric curve (Reimer et al 2013)
30567 R_Date(4427,29)
95.4% probability
5213 (1.8%) 5191BP
5069 (93.6%) 4868BP
Agreement 111.4%
Radiocarbon determination (BP)
Modelled date (BP)

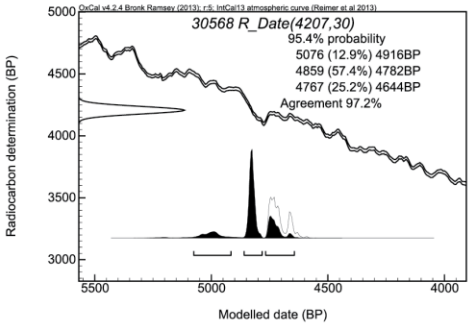
OxCal v4.2.4 Bronk Ramsey (2013); r:5; IntCal13 atmospheric curve (Reimer et al 2013)
30568 R_Date(4207,30)
95.4% probability
5076 (12.9%) 4916BP
4859 (57.4%) 4782BP
4767 (25.2%) 4644BP
Agreement 97.2%
Radiocarbon determination (BP)
Modelled date (BP)

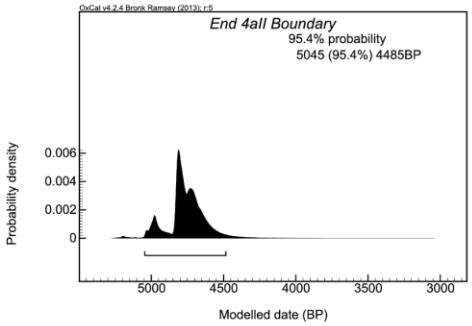
OxCal v4.2.4 Bronk Ramsey (2013); r:5
End 4all Boundary
95.4% probability
5045 (95.4%) 4485BP
Probability density
Modelled date (BP)

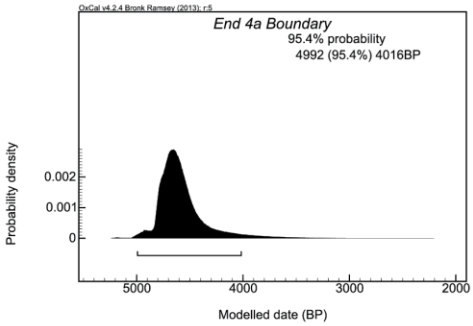
OxCal v4.2.4 Bronk Ramsey (2013); r:5
End 4a Boundary
95.4% probability
4992 (95.4%) 4016BP
Probability density
Modelled date (BP)

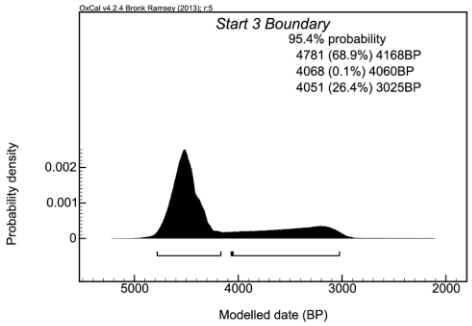
OxCal v4.2.4 Bronk Ramsey (2013); r:5
Start 3 Boundary
95.4% probability
4781 (68.9%) 4168BP
4068 (0.1%) 4060BP
4051 (26.4%) 3025BP
Probability density
Modelled date (BP)

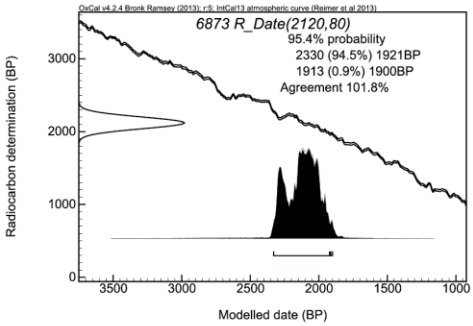
OxCal v4.2.4 Bronk Ramsey (2013); r:5; IntCal13 atmospheric curve (Reimer et al 2013)
6873 R_Date(2120,80)
95.4% probability
2330 (94.5%) 1921BP
1913 (0.9%) 1900BP
Agreement 101.8%
Radiocarbon determination (BP)
Modelled date (BP)

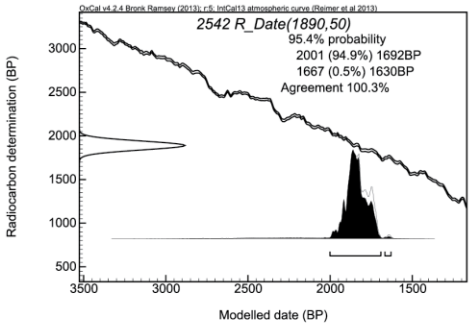
OxCal v4.2.4 Bronk Ramsey (2013); r:5; IntCal13 atmospheric curve (Reimer et al 2013)
2542 R_Date(1890,50)
95.4% probability
2001 (94.9%) 1692BP
1667 (0.5%) 1630BP
Agreement 100.3%
Radiocarbon determination (BP)
Modelled date (BP)

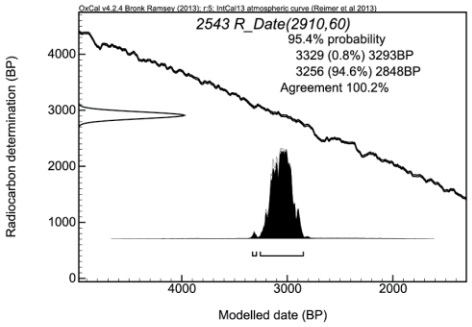
OxCal v4.2.4 Bronk Ramsey (2013); r:5; IntCal13 atmospheric curve (Reimer et al 2013)
2543 R_Date(2910,60)
95.4% probability
3329 (0.8%) 3293BP
3256 (94.6%) 2848BP
Agreement 100.2%
Radiocarbon determination (BP)
Modelled date (BP)

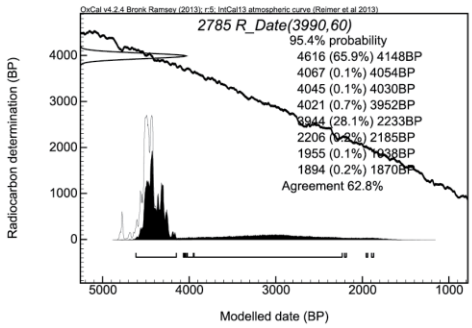
OxCal v4.2.4 Bronk Ramsey (2013); r:5; IntCal13 atmospheric curve (Reimer et al 2013)
2785 R_Date(3990,60)
95.4% probability
4616 (65.9%) 4148BP
4067 (0.1%) 4054BP
4045 (0.1%) 4030BP
4021 (0.7%) 3952BP
3944 (28.1%) 2233BP
2206 (0.2%) 2185BP
1955 (0.1%) 1938BP
1894 (0.2%) 1870BP
Agreement 62.8%
Radiocarbon determination (BP)
Modelled date (BP)

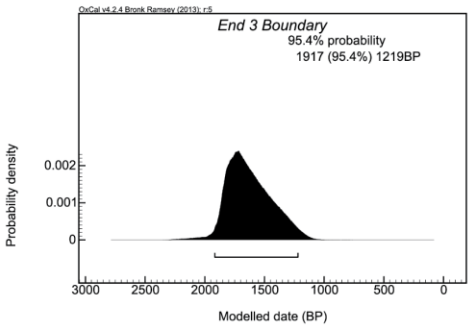
OxCal v4.2.4 Bronk Ramsey (2013); r:5
End 3 Boundary
95.4% probability
1917 (95.4%) 1219BP
Probability density
Modelled date (BP)

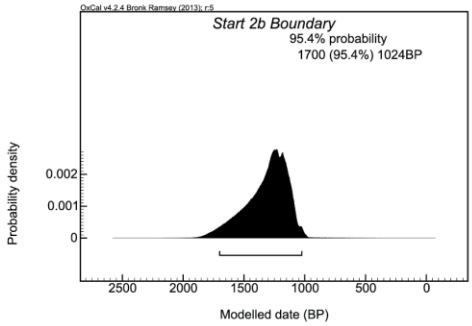
OxCal v4.2.4 Bronk Ramsey (2013); r:5
Start 2b Boundary
95.4% probability
1700 (95.4%) 1024BP
Probability density
Modelled date (BP)

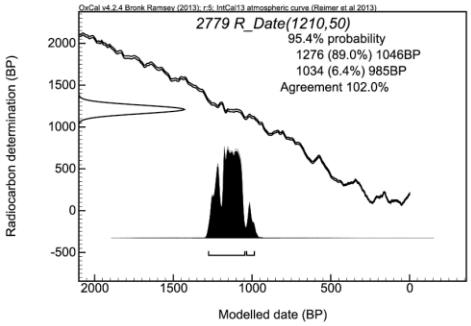
OxCal v4.2.4 Bronk Ramsey (2013); r:5; IntCal13 atmospheric curve (Reimer et al 2013)
2779 R_Date(1210,50)
95.4% probability
1276 (89.0%) 1046BP
1034 (6.4%) 985BP
Agreement 102.0%
Radiocarbon determination (BP)
Modelled date (BP)

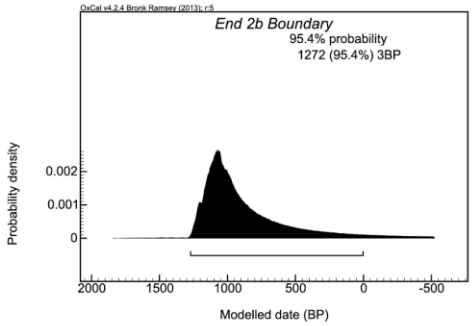
OxCal v4.2.4 Bronk Ramsey (2013); r:5
End 2b Boundary
95.4% probability
1272 (95.4%) 3BP
Probability density
Modelled date (BP)

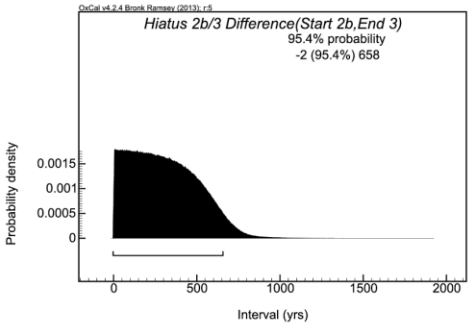
OxCal v4.2.4 Bronk Ramsey (2013); r:5
Hiatus 2b/3 Difference(Start 2b,End 3)
95.4% probability
-2 (95.4%) 658
Probability density
Interval (yrs)

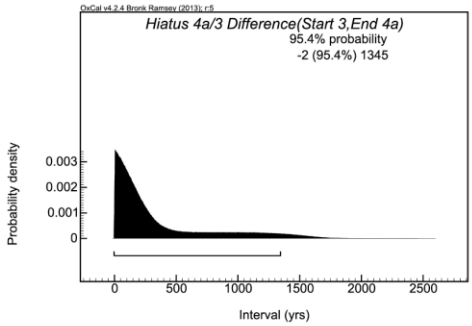
OxCal v4.2.4 Bronk Ramsey (2013); r:5
Hiatus 4a/3 Difference(Start 3,End 4a)
95.4% probability
-2 (95.4%) 1345
Probability density
Interval (yrs)

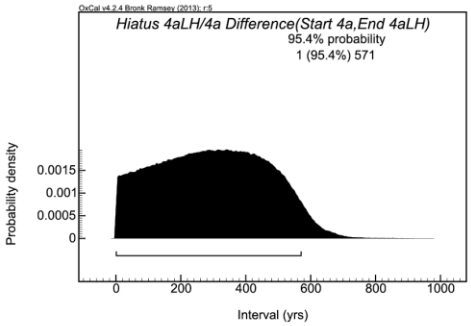
OxCal v4.2.4 Bronk Ramsey (2013); r:5
Hiatus 4aLH/4a Difference(Start 4a,End 4aLH)
95.4% probability
1 (95.4%) 571
Probability density
Interval (yrs)

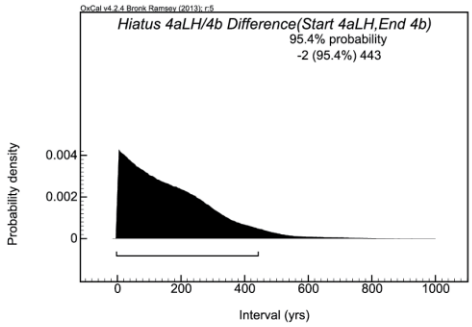
OxCal v4.2.4 Bronk Ramsey (2013); r:5
Hiatus 4aLH/4b Difference(Start 4aLH,End 4b)
95.4% probability
-2 (95.4%) 443
Probability density
Interval (yrs)

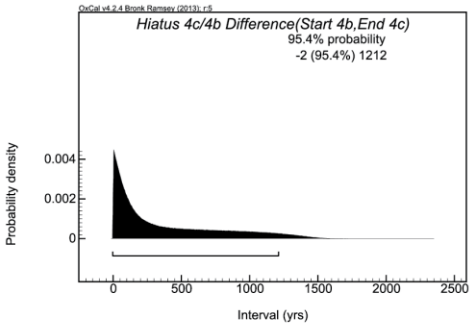
OxCal v4.2.4 Bronk Ramsey (2013); r:5
Hiatus 4c/4b Difference(Start 4b,End 4c)
95.4% probability
-2 (95.4%) 1212
Probability density
Interval (yrs)

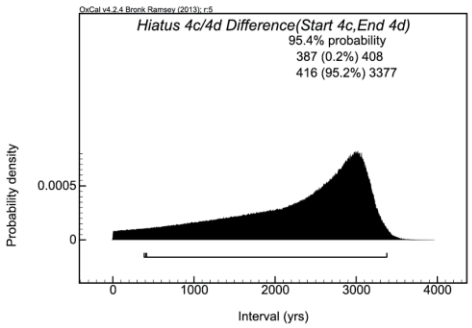
OxCal v4.2.4 Bronk Ramsey (2013); r:5
Hiatus 4c/4d Difference(Start 4c,End 4d)
95.4% probability
387 (0.2%) 408
416 (95.2%) 3377
Probability density
0.0005
0
0
1000
2000
3000
4000
Interval (yrs)

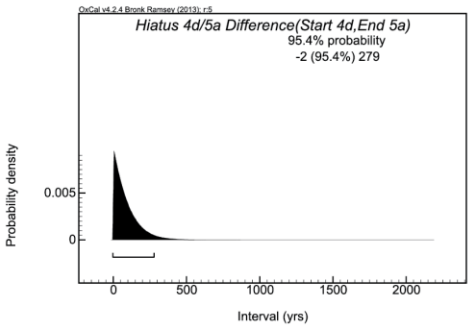
OxCal v4.2.4 Bronk Ramsey (2013); r:5
Hiatus 4d/5a Difference(Start 4d,End 5a)
95.4% probability
-2 (95.4%) 279
Probability density
0.005
0
0
500
1000
1500
2000
Interval (yrs)

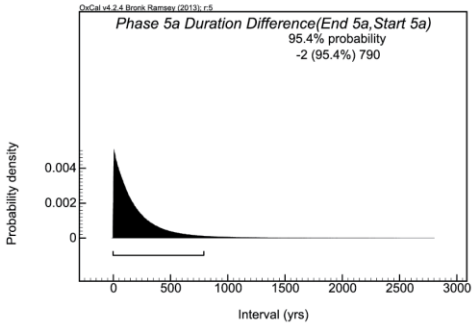
OxCal v4.2.4 Bronk Ramsey (2013); r:5
Phase 5a Duration Difference(End 5a,Start 5a)
95.4% probability
-2 (95.4%) 790
Probability density
0.004
0.002
0
0
500
1000
1500
2000
2500
3000
Interval (yrs)

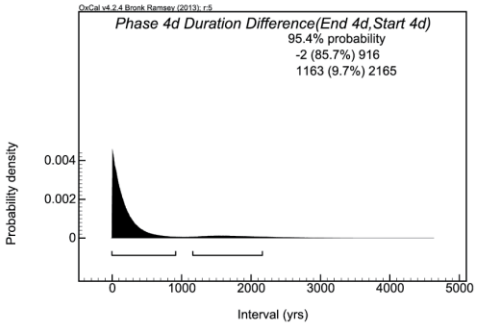
OxCal v4.2.4 Bronk Ramsey (2013); r:5
Phase 4d Duration Difference(End 4d,Start 4d)
95.4% probability
-2 (85.7%) 916
1163 (9.7%) 2165
Probability density
0.004
0.002
0
0
1000
2000
3000
4000
5000
Interval (yrs)

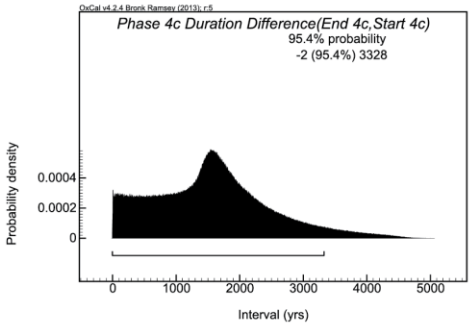
OxCal v4.2.4 Bronk Ramsey (2013); r:5
Phase 4c Duration Difference(End 4c,Start 4c)
95.4% probability
-2 (95.4%) 3328
Probability density
0.0004
0.0002
0
0
1000
2000
3000
4000
5000
Interval (yrs)

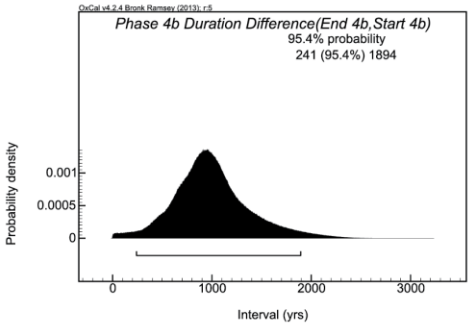
OxCal v4.2.4 Bronk Ramsey (2013); r:5
Phase 4b Duration Difference(End 4b,Start 4b)
95.4% probability
241 (95.4%) 1894
Probability density
0.001
0.0005
0
0
1000
2000
3000
Interval (yrs)

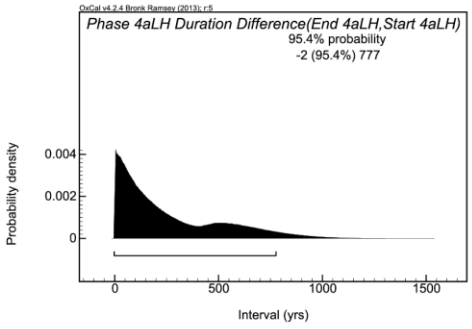
OxCal v4.2.4 Bronk Ramsey (2013); r:5
Phase 4aLH Duration Difference(End 4aLH,Start 4aLH)
95.4% probability
-2 (95.4%) 777
Probability density
0.004
0.002
0
0
500
1000
1500
Interval (yrs)

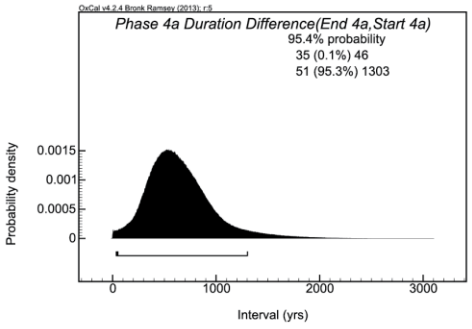
OxCal v4.2.4 Bronk Ramsey (2013); r:5
Phase 4a Duration Difference(End 4a,Start 4a)
95.4% probability
35 (0.1%) 46
51 (95.3%) 1303
Probability density
0.0015
0.001
0.0005
0
0
1000
2000
3000
Interval (yrs)

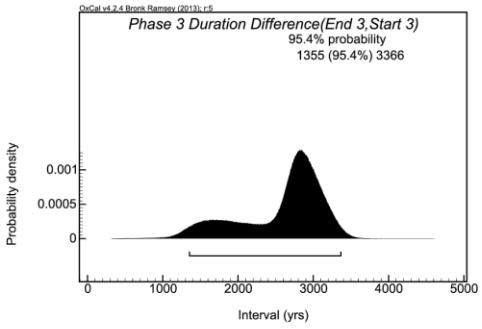
OxCal v4.2.4 Bronk Ramsey (2013); r:5
Phase 3 Duration Difference(End 3,Start 3)
95.4% probability
1355 (95.4%) 3366
Probability density
0.001
0.0005
0
0
1000
2000
3000
4000
5000
Interval (yrs)

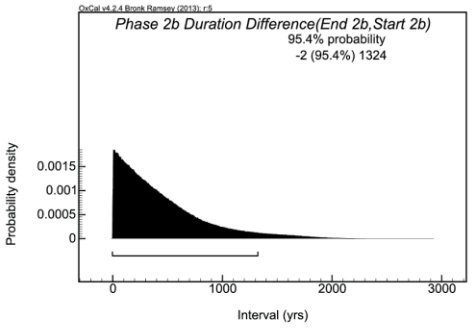
OxCal v4.2.4 Bronk Ramsey (2013); r:5
Phase 2b Duration Difference(End 2b,Start 2b)
95.4% probability
-2 (95.4%) 1324
Probability density
0.0015
0.001
0.0005
0
0
1000
2000
3000
Interval (yrs)

Appendix 3

Diet, habitat requirements and water dependency summarized from modern studies on species sampled at Wonderwerk Cave. (References: [1]Apps 2012, [2]Sponheimer et al. 2003, [3]Gagnon & Chew 2000, [4]Hilton-Barber & Berger 2004, [5]Kingdon 1982, [6]Codron et al. 2008, [7]IUCN SSC Antelope Specialist Group 2008, [8]Skinner and Chimimba 2005, [9]Kingdon et al. 2013, [10]Du Toit 1993, [11]Kingdon 1979, [12]Grubb, P. 2008, [13]Butynski and De Jong 2008, [14]Cumming 2008, [15]Barry et al. 2008).

Species	Diet	Water dependency	Habitat	Comment	Refe-rences
Bovidae					
Alcelaphini					
Alcelaphus buselaphus (Hartebeest)	Variable mixed, selective, coarse diet, mainly grazer, some browse;	Not entirely independent.	Moist or dry open grassland, bush savanna, some open woodland.		1, 2, 3, 4, 5, 8, 9
Connochaetes sp. (Wildebeest), incl. *C. taurinus* (Blue Wildebeest), *C. gnou* (Black Wildebeest)	Variable grazer, prefers fresh short growth, non-selective;	Dependent.	Dry open woodland, scrub and grassland; homogenous habitats.	Diurnal; will migrate in drought seasons.	1, 3, 5, 6
Damaliscus sp. incl. *D. pygargus* (Blesbok)	Variable grazer, selective, occasionally browse;	Needs water.	Grassland and low scrubland, needs shelter.	Highly mobile; Diurnal.	1, 2, 3, 4, 6
Tragelaphini					
Tragelaphus strepsiceros (Greater Kudu)	Browse, forbs, leaves, favours acacia, eats grass only fresh green; concentrate selector (higher quality than Eland)	No water if enough green food.	Dry savanna woodland, slopes and rocky areas, needs cover; no desert, forest, open grassland.	Diurnal.	1, 2, 3, 4, 5, 7a
Taurotragus oryx (Eland)	Mainly browser, eat some fresh (10%) grass in summer. Leaves, twigs, fruit berries. Eats dry leaves and burned grass; mixed-feeder.	Independent of water (if enough succulent forage).	Very flexible: arid scrub and grassland, savanna woodland, montane grassland, flats/gentle slopes.	Move long distances for food and seasonal migrations in some areas; feed at night.	1, 2, 3, 4, 5, 6, 8
Antilopini					
Antidorcas marsupialis (Springbok)	Versatile, graze more in summer, browse more in winter. Grass, forbs, bushes, seeds,	Completely independent from water. But will	Arid scrub and grassland.	Highly mobile.	1, 2, 3, 6, 7b, 8

	pods, fruit, flowers, roots, bulbs, melons, shoots, leafs, cucumbers;	drink if water is present.			
Antidorcas bondi (Bond's Springbok)	Fresh green grass, grazer	n/a	Grasslands, savanna	extinct	6
Neotragini					
Raphicerus campestris (Steenbok)	Browser, selective feeders, grass only few %; roots, tubers and bulbs, young grass, eats near ground level	No drink if enough green food and melons.	Grassland with cover, open woodland, no rocky areas/forest, open plains, dry Kalahari climate	Active day and night.	1, 2, 3, 6, 7c, 10
Oreotragus oreotragus (Klipspringer)	Generalist; predominantly browser, leaves, berries, fruit, seed pods, flowers; herbs, shrubs, bushes, creepers and lichen, twigs, seeds, pods; selective	Independent. Drink if water is available.	Rocky areas, can feed on flatter areas, valley grassland specialist, thickets, dry savannah and woodland, needs ground cover.	Partly nocturnal.	1, 3, 4, 5
Reduncini					
Redunca fulvorufula (Mountain Reedbuck)	Obligate grazer, coarse grazing, soft green parts, leaves, selective;	Dependent.	Slopes, mountains, tree or bush cover, grassland, dry soils.	Diurnal.	1, 2, 3, 4, 5, 7d
Kobus leche (Lechwe)	Obligate Grazer, 99% grasses and sedges;	Dependent.	Near permanent standing water.		1, 2, 3, 6, 7e
Pelea capreolus (Grey Rhebok)	Browse, forbs, broad-leaf plants;	Independent of water.	Hills, slopes, mountains, plateaus with grass cover, grassland.		1, 3, 5
Perissodactyla					
Equids, incl. *Equus burchelli* (Burchell's zebra), *Equus quagga* (extinct), *Hipparion* sp. (extinct)	Grazer (>95-99%), occ. Browse shrubs, leaves, stems and herbs.	Dependent on water daily.	Open woodland, scrub and grassland.		1, 4, 6, 11
Ceratotherium simum (White Rhinoceros)	Grazer 99%, non-selective, occasionally small shrubs.	Dependent.	Grassland, flat areas; no thicket or dense woodland.	Wallow in water to cool down.	1, 11
Rodentia					
Hystrix africaeaustralis (Cape Porcupine)	Generalist herbivore: Fruit, bulb, root, bark, seed. Gnaw bones for calcium.		Wide-Spread, not in forests.	Nocturnal.	1, 4, 8, 12
Pedetes capensis (Springhare)	Predominantly Grazer: Grass, seeds, underground stems, selective.	Independent.	Widespread, sandy/soft soil, no heavy vegetation cover.	Nocturnal.	1, 4, 8, 13
Suidae					

Phacochoerus africanus (Common warthog)	Mainly grazer, selective, and rootles. Grass, sedges, shrubs, herbs, roots, rhizomes, leafs. Also sometimes fruit bark, invertebrates, small animals. Bones and stones for minerals.	Daily.	Open woodland and shrubland, grassland, floodplains, wooded grassland, open and mosaic habitats.	Diurnal.	1, 4, 5, 6, 8, 14
Procaviidae					
Procavia capensis (Cape Hyrax)	Opportunistic feeder, proportions browse/graze change seasonally: Grass, forbs, shrubs, trees, fruits, berries, buds.	Independent if green food.	Need shelter, otherwise a wide range of habitats.	Basking in sun to save energy, diurnal.	1, 4, 8, 9, 15

Appendix 4 - Methods

4.1 Loss calculations from enamel isotope pretreatment.

Sample ME	empty weight	with sample	Sample weight	weight (g) after pretreatment	Loss (g)	Loss (%)	Sample weight (g) after pretreatment
449	0.945	0.983	0.038	0.978	0.005	13.2	0.033
232	0.938	0.955	0.017	0.952	0.003	17.6	0.014
512	0.945	1.027	0.082	1.021	0.006	7.3	0.076
322	0.935	0.976	0.041	0.971	0.005	12.2	0.036
339	0.946	0.99	0.044	0.986	0.004	9.1	0.040
397	0.942	0.974	0.032	0.97	0.004	12.5	0.028
207	0.934	0.948	0.014	0.946	0.002	14.3	0.012
316	0.945	0.983	0.038	0.979	0.004	10.5	0.034
213	0.929	0.942	0.013	0.939	0.003	23.1	0.010
317	0.938	0.962	0.024	0.959	0.003	12.5	0.021
212	0.931	0.948	0.017	0.946	0.002	11.8	0.015
313	0.945	0.979	0.034	0.974	0.005	14.7	0.029
233	0.945	0.957	0.012	0.952	0.005	41.7	0.007
458	0.935	1.004	0.069	1.001	0.003	4.3	0.066
408	0.938	0.961	0.023	0.955	0.006	26.1	0.017
487	0.945	0.995	0.05	0.986	0.009	18.0	0.041
247	0.942	0.955	0.013	0.952	0.003	23.1	0.010
222	0.937	0.954	0.017	0.95	0.004	23.5	0.013
490	0.945	0.987	0.042	0.976	0.011	26.2	0.031
383	0.935	0.992	0.057	0.985	0.007	12.3	0.050
251	0.945	0.975	0.03	0.97	0.005	16.7	0.025
407	0.945	0.96	0.015	0.957	0.003	20.0	0.012
550	0.939	0.999	0.06	0.993	0.006	10.0	0.054
211	0.945	0.967	0.022	0.964	0.003	13.6	0.019
275	0.941	0.96	0.019	0.956	0.004	21.1	0.015
507	0.945	0.987	0.042	0.982	0.005	11.9	0.037
521	0.937	1.01	0.073	0.999	0.011	15.1	0.062
202	0.942	0.987	0.045	0.982	0.005	11.1	0.040
484	0.944	1.009	0.065	0.998	0.011	16.9	0.054

359	0.945	1	0.055	0.992	0.008	14.5	0.047
494	0.937	0.987	0.05	0.978	0.009	18.0	0.041
216	0.942	1.005	0.063	0.995	0.01	15.9	0.053
437	0.935	0.967	0.032	0.96	0.007	21.9	0.025
551	0.935	1.037	0.102	1.029	0.008	7.8	0.094
554	0.944	1.001	0.057	0.995	0.006	10.5	0.051
215	0.942	0.956	0.014	0.952	0.004	28.6	0.010
223	0.943	0.989	0.046	0.983	0.006	13.0	0.040
546	0.945	1.007	0.062	0.999	0.008	12.9	0.054
430	0.946	0.987	0.041	0.98	0.007	17.1	0.034
224	0.945	0.962	0.017	0.958	0.004	23.5	0.013
547	0.945	0.958	0.013	0.954	0.004	30.8	0.009
542	0.935	0.964	0.029	0.959	0.005	17.2	0.024
267	0.941	0.975	0.034	0.97	0.005	14.7	0.029
392	0.937	0.967	0.03	0.962	0.005	16.7	0.025
374	0.94	0.945	0.005	0.943	0.002	40.0	0.003
511	0.944	0.983	0.039	0.976	0.007	17.9	0.032
433	0.943	0.969	0.026	0.964	0.005	19.2	0.021
217	0.945	0.964	0.019	0.959	0.005	26.3	0.014
386	0.944	0.983	0.039	0.976	0.007	17.9	0.032
337	0.945	0.986	0.041	0.981	0.005	12.2	0.036
495	0.93	0.966	0.036	0.96	0.006	16.7	0.030
201	0.943	0.969	0.026	0.965	0.004	15.4	0.022
401	0.941	0.965	0.024	0.96	0.005	20.8	0.019
549	0.94	0.982	0.042	0.978	0.004	9.5	0.038
367	0.945	1.006	0.061	1	0.006	9.8	0.055

4.2 Carbon and oxygen isotope values of standards interspersed in the OES and enamel isotope measurement runs.

Standard	**$\delta^{13}C$ value**	**$\delta^{18}O$ value**
NBS 19	1.95	28.65
CO-1	2.49±0.03	28.41±0.07
CO-8	-5.76±0.03	7.55±0.19
Merck $CaCO_3$	-35.45	13.35
BES	-11.1	25.0
OES	-10.72	25.45
MAM*	-12.12±0.15	24.01±0.32
WILD*	0.59±0.13	32.92±0.21

*MAM and WILD were developed in Oxford and tested in Bradford during this time, values as of December 2014.

All standard values measured in the OES runs.

Standard sample	$\delta^{13}C_{VPDB}$ ‰	sd	$\delta^{18}O_{VSMOW}$ ‰	sd	Run
BES	-11.1	0.0	25.0	0.1	COL431
CO-1	2.3	0.1	28.6	0.1	COL429
CO-1	2.5	0.0	28.6	0.1	COL429
CO-1	2.4	0.0	28.5	0.0	COL430
CO-1	2.5	0.1	28.5	0.1	COL430
CO-8	-5.8	0.0	7.4	0.1	COL431
MERCK	-35.6	0.1	13.3	0.1	COL429
MERCK	-35.4	0.1	13.4	0.1	COL430
MERCK	-35.3	0.1	13.4	0.1	COL431
Merck CaCO3	-35.7	0.1	13.7	0.0	COL429
Merck CaCO3	-35.6	0.1	13.4	0.1	COL429
Merck CaCO3	-35.3	0.1	13.4	0.1	COL430
Merck CaCO3	-35.4	0.0	13.4	0.1	COL431
NBS19	2.0	0.2	28.8	0.1	COL429
NBS19	2.1	0.0	28.8	0.1	COL430
NBS19	2.0	0.1	28.6	0.1	COL431
NBS19	1.9	0.0	28.7	0.1	COL431
OES	-10.6	0.0	25.7	0.1	COL429
OES	-10.5	0.1	25.6	0.1	COL429
OES	-10.9	0.0	25.6	0.0	COL429
OES	-10.7	0.1	25.6	0.1	COL430
OES	-10.5	0.0	25.5	0.1	COL430
OES	-10.8	0.0	25.6	0.1	COL430
OES	-10.4	0.1	25.7	0.1	COL431

All standard values measured in the enamel runs:

Standard sample	$\delta^{13}C_{VPDB}$ ‰	sd	$\delta^{18}O_{VSMOW}$ ‰	sd	Run
BES	-10.8	0.1	25.3	0.2	COL468B
BES	-11.1	0.1	24.8	0.2	COL468B
BES	-11.2	0.1	25.4	0.2	COL468B
BES	-11.5	0.2	24.8	0.3	COL468B
BES	-10.9	0.1	24.7	0.1	COL498
BES	-11.0	0.1	24.9	0.2	COL499
BES	-11.3	0.1	24.4	0.2	COL504
CO-1	2.5	0.2	28.6	0.2	COL468B
CO-1	2.6	0.1	28.7	0.1	COL468B
CO-1	2.1	0.2	28.2	0.3	COL468B
CO-1	2.5	0.1	28.6	0.1	COL498
CO-1	2.4	0.1	28.8	0.1	COL499
CO-1	2.3	0.1	28.5	0.3	COL500
CO-1	2.4	0.2	28.2	0.2	COL501
CO-1	2.4	0.1	28.6	0.2	COL501
CO-1	2.3	0.1	28.4	0.2	COL503
CO-1	2.4	0.2	28.5	0.1	COL504
CO-1	2.7	0.2	29.2	0.2	COL504
CO-1	2.3	0.1	28.4	0.1	COL505b
CO-8	-5.5	0.1	7.4	0.1	COL468B
CO-8	-5.6	0.2	7.7	0.2	COL500
CO-8	-5.8	0.1	7.6	0.1	COL503
CO-8	-5.7	0.1	7.3	0.1	COL504
CO-8	-5.9	0.4	8.9	0.8	COL505b
MAM	-12.5	0.2	24.0	0.3	COL468B

MAM	-12.4	0.2	24.2	0.3	COL468B
MAM	-12.1	0.1	24.6	0.3	COL468B
MAM	-12.1	0.1	23.9	0.1	COL498
MAM	-12.1	0.1	23.8	0.1	COL498
MAM	-11.9	0.1	24.5	0.1	COL499
MAM	-12.0	0.1	23.9	0.1	COL499
MAM	-12.2	0.1	24.1	0.1	COL500
MAM	-12.1	0.1	23.8	0.3	COL500
MAM	-12.0	0.1	23.8	0.1	COL501
MAM	-12.2	0.1	24.2	0.1	COL503
MAM	-12.2	0.1	23.9	0.1	COL503
MAM	-12.1	0.1	23.9	0.2	COL504
MERCK	-35.6	0.1	13.3	0.1	COL468B
MERCK	-35.7	0.1	13.2	0.1	COL498
MERCK	-35.6	0.1	13.4	0.2	COL499
MERCK	-35.4	0.1	13.4	0.1	COL500
MERCK	-35.4	0.1	13.0	0.2	COL501
MERCK	-35.6	0.1	13.3	0.1	COL503
MERCK	-35.6	0.2	13.2	0.4	COL504
Merck CaCO3	-35.7	0.1	12.2	0.4	COL468B
Merck CaCO3	-35.7	0.1	13.6	0.2	COL468B
Merck CaCO3	-35.7	0.2	13.2	0.4	COL468B
Merck CaCO3	-35.5	0.1	13.1	0.2	COL498
Merck CaCO3	-35.2	0.1	13.3	0.1	COL499
Merck CaCO3	-35.5	0.1	13.2	0.1	COL500
Merck CaCO3	-35.4	0.1	12.9	0.2	COL501
Merck CaCO3	-35.3	0.1	13.4	0.1	COL503
Merck CaCO3	-35.1	0.1	13.5	0.2	COL504
Merck CaCO3	-35.0	0.1	13.2	0.1	COL505b
NBS19	1.6	0.2	28.4	0.4	COL468B
NBS19	2.0	0.1	28.8	0.1	COL468B
NBS19	2.2	0.1	29.0	0.1	COL498
NBS19	2.1	0.1	29.0	0.1	COL499
NBS19	2.0	0.1	28.5	0.2	COL501
NBS19	1.9	0.1	28.6	0.2	COL504
NBS19	2.1	0.1	28.8	0.1	COL505b
OES	-10.7	0.1	25.4	0.1	COL500
OES	-10.9	0.1	25.9	0.1	COL501
OES	-10.7	0.1	25.1	0.1	COL501
OES	-10.8	0.1	25.4	0.2	COL505b
WILD	0.4	0.1	33.0	0.2	COL468B
WILD	0.6	0.1	33.3	0.1	COL468B
WILD	0.4	0.1	32.9	0.2	COL468B
WILD	0.4	0.1	32.8	0.1	COL498
WILD	0.7	0.1	33.3	0.1	COL498
WILD	0.7	0.1	33.0	0.1	COL499
WILD	0.7	0.1	33.0	0.1	COL499
WILD	0.6	0.1	33.2	0.1	COL500
WILD	0.6	0.1	33.1	0.3	COL500
WILD	0.9	0.1	33.2	0.2	COL501
WILD	0.7	0.1	33.1	0.1	COL503
WILD	0.7	0.1	33.2	0.1	COL503
WILD	0.5	0.1	32.7	0.2	COL504
WILD	0.5	0.1	32.8	0.2	COL505b

4.3 Examples of quality control tests for enamel samples. A: Pleistocene Equid teeth, marked as possibly burnt or unburnt during sampling. B: *Alcelaphus buselaphus* samples from Holocene Strata by tooth type. C: *Alcelaphus buselaphus* samples (Holocene Strata) plotted by Square (Squares were given a numerical code).

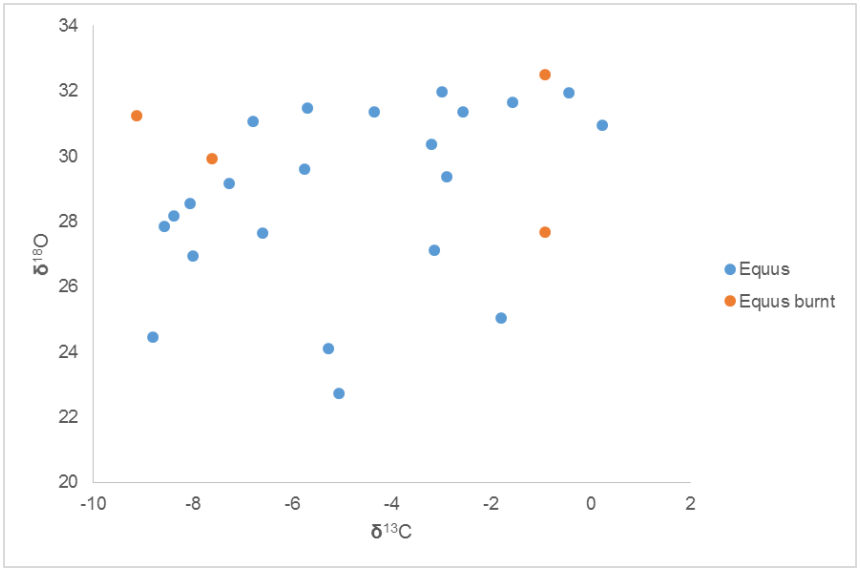

A

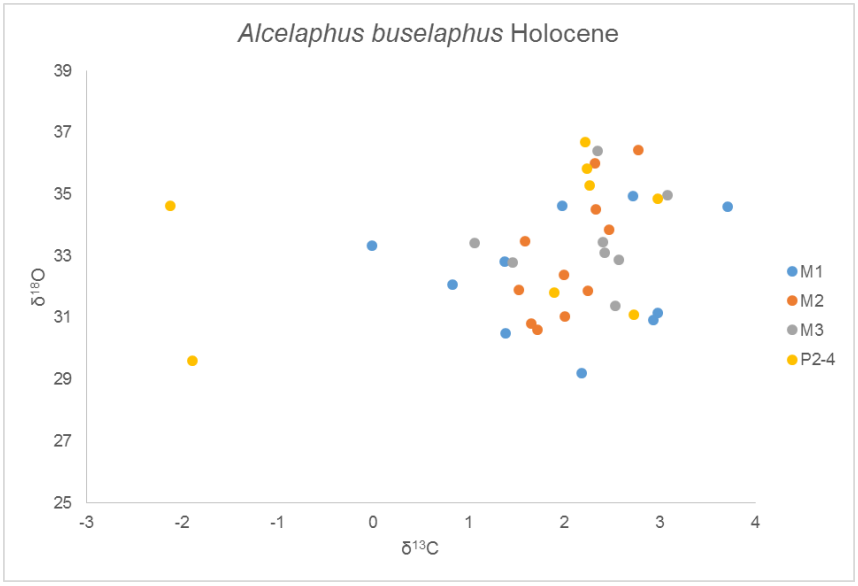

B

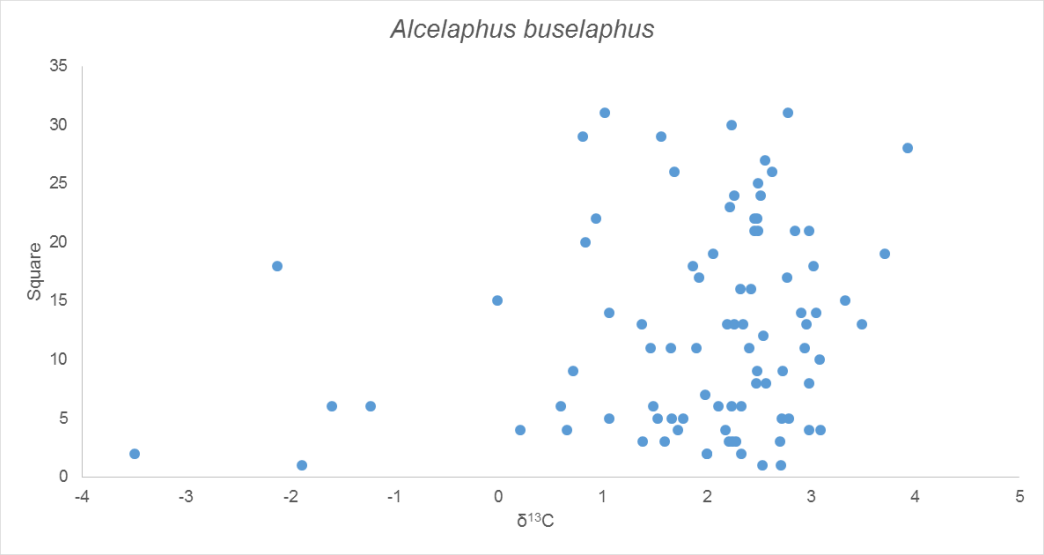

C

4.4 Samples measured twice and a comparison of the results from both runs.

Sample	**^{13}C run 1**	**δ^{13}C run 2**	**difference**	**Mean of run 1+2**	**δ^{18}O run 1**	**δ^{18}O run 2**	**difference**	**Mean of run 1+2**	**Species**	**Stratum**
ME 247	-8.7	-8.8	0.1	**-8.8**	40.1	40.3	0.2	**40.2**	*Raphicerus campestris*	4c
ME 317	-11.9	-11.7	0.2	**-11.8**	42.0	42.6	0.6	**42.3**	*Raphicerus campestris*	4aLH
ME 532	-4.3	-4.3	0.1	**-4.3**	41.4	41.4	0.1	**41.4**	*Procavia capensis*	2b
ME 576	-1.5	-1.5	0.01	**-1.5**	28.2	28.4	0.2	**28.3**	*Hystrix africaeaustralis*	12
ME 619	-8.4	-8.4	0.1	**-8.4**	40.9	41.2	0.2	**41.1**	*Antidorcas marsupialis?*	Exc 2 Str 2
ME 294	-0.8	-3.7	2.9	**-2.2**	29.1	28.2	0.9	**28.2**	*Hystrix africaeaustralis*	4bI
ME 406	-0.2	-3.2	3.1	**-1.7**	31.8	42.3	10.6	**37.1**	*Hsystrix africaeaustralis*	4aII
ME 687	-7.8	-5.3	2.5	**-6.6**	20.0	21.3	1.4	**20.6**	*Ceratotherium simum*	Exc 2 Str 2
ME 481	-10.4	-10.2	0.2	**-10.3**	28.1	28.5	0.4	**28.5**	*Tragelaphini*	3a

Appendix 5: Raw data

5.1 All stable isotope data for OES samples, indicating origin and colour, as well as smell while sampling.

Sample	**SPF#**	**$\delta^{13}C_{VPDB}$ ‰**	**$\delta^{18}O_{VSMOW}$ ‰**	**Exc.**	**Stratum**	**sublevel**	**Square**	**depth 1**	**depth 2**	**colour**	**smell**
ME 112	4593	**-8.5**	**38.8**	1	6	I	T33			brown	yes
ME 109	4590	**-9.2**	**42.9**	1	6	I	S34			no	no
ME 108	4592	**-7.7**	**43.5**	1	6	I	S30			brown	no
ME 111	4591	**-9.2**	**38.8**	1	6	I	T31			no	no
ME 110	4594	**-9.5**	**41.0**	1	6	II	S34			black	yes
ME113	4595	**-9.1**	**37.7**	1	6	II	T34			black	yes
ME 31		**-7.1**	**47.6**	1	6		Q30	10	15	no	no
ME 33		**-9.7**	**35.2**	1	6		R29	5	15	no	no
ME 32		**-8.2**	**38.1**	1	6		Q34	25	30	brown	yes
ME 34		**-6.7**	**38.1**	1	6		P34	15	20	black	yes
ME 107	4596	**-7.7**	**38.0**	1	6		R31	5	10	brown	yes
ME 127	4497	**-7.8**	**43.2**	1	7	b	T30	0	5	brown	no
ME 123	4577	**-9.1**	**36.5**	1	7	b	Q29	0	5	brown	yes
ME 116	4490	**-8.4**	**38.6**	1	7	b	M29	0	5	no	no
ME 126	4500	**-8.4**	**40.7**	1	7	b	T29	0	5	no	no
ME 128	4535	**-9.1**	**37.0**	1	7	b	T32	0	5	no	no
ME 36	4532	**-7.6**	**39.1**	1	7	b	T32	0	5	no	no
ME 114	4552	**-9.5**	**39.0**	1	7		O34	25	30	no	no
ME 121	4539	**-9.2**	**37.4**	1	7		O29	0	5	brown	yes
ME 118	4526	**-7.6**	**36.0**	1	7		M34	15	20	no	no
ME 124	4564	**-8.2**	**38.2**	1	7		R31	0	5	no	yes
ME 37	4485	**-8.5**	**42.0**	1	7		M32	n.a.	n.a.	no	no
ME 120	4488	**-7.0**	**41.8**	1	7		M34	20	25	no	no
ME 125	4502	**-8.9**	**38.7**	1	7		S30	0	5	no	no
ME 35	4511+4512	**-9.1**	**37.8**	1	7		N33	n.a.	n.a.	brown	no

ME 119	4525	**-8.1**	**42.7**	1	7		M34	15	20	no	no
ME 129	4544	**-9.7**	**36.6**	1	7		T31	20	25	brown	yes
ME 115	4489	**-10.4**	**35.8**	1	7		L29	5	10	no	no
ME 117	4529	**-7.1**	**47.2**	1	7		M34	15	20	no	no
ME 122	4521	**-8.4**	**34.1**	1	7		P34	20	25	no	yes
ME 153	4448	**-9.4**	**39.2**	1	8	a	R30	30	35	black	yes
ME 168	4447	**-10.5**	**37.1**	1	8	a	R28	0	5	black	no
ME 141	4470	**-8.9**	**35.9**	1	8	a	O28	0	5	no	no
ME 137	4469	**-9.8**	**35.9**	1	8	a	O28	0	5	brown	yes
ME 160	4449	**-8.5**	**39.3**	1	8	a	R29	0	5	no	no
ME 151	4479	**-9.6**	**40.0**	1	8	a?	O28	0	5	no	yes
ME 140	4459	**-8.0**	**40.4**	1	8	b	O29	10	15	no	no
ME 40	4458	**-9.1**	**37.5**	1	8	b	O29	10	15	brown	no
ME 144	4456	**-8.6**	**41.3**	1	8	b	O28	5	10	no	no
ME 158	4468	**-7.8**	**41.1**	1	8	b-c	N29	10	15	brown	yes
ME 161	4466	**-8.1**	**36.4**	1	8	c	Q25	0	5	no	no
ME 38	4465	**-8.1**	**36.2**	1	8	c	Q25	0	5	no	no
ME 148	4467	**-7.7**	**42.0**	1	8	c-d	T26	0	5	no	no
ME 156	4453	**-9.9**	**32.9**	1	8	d	T24	0	5	brown	yes
ME 157	4452	**-8.0**	**39.6**	1	8	d	T24	0	5	brown	no
ME 133	4472	**-8.0**	**40.8**	1	8	d	O28	15/20	20/25	no	no
ME 163	4482	**-8.7**	**41.6**	1	8	e	T24	15	20	no	no
ME 150	4471	**-7.9**	**37.6**	1	8	e	Q22	25	30	no	no
ME 41	4450	**-8.2**	**35.4**	1	8		T27	15	20	brown	no
ME 39	4463	**-8.8**	**45.5**	1	8		T28	20	25	no	no
ME 134	4414	**-10.3**	**35.3**	1	9	a	Q31	0	5	brown	no
ME 149	4442	**-7.9**	**40.1**	1	9	a	R33	0	5	no	no
ME 130	4434	**-7.9**	**37.6**	1	9	a	R29	0	5	no	no
ME 146	4440	**-8.4**	**43.2**	1	9	a	R33	0	5	brown	no
ME 44	4439	**-6.6**	**39.6**	1	9	a	R33	0	5	no	no
ME 165	4441	**-6.8**	**47.8**	1	9	a	R33	0	5	no	no

ME 154	4435	**-10.6**	**35.4**	1	9	a	R29	0	5	brown	yes
ME 142	4406	**-8.4**	**43.1**	1	9	b	S25	5	10	no	no
ME 131	4407	**-8.7**	**37.1**	1	9	b	S27	15	20	no	no
ME 138	4413	**-8.1**	**39.8**	1	9	b	S24	15	20	no	no
ME 152	4411	**-6.6**	**37.6**	1	9	b	R26	35	40	no	no
ME 162	4424	**-8.3**	**40.1**	1	9	b	S23	0	5	no	no
ME 164	4417	**-7.1**	**37.2**	1	9	c	R34	0	5	red	no
ME 139	4420	**-9.1**	**33.9**	1	9	d	R30	25	30	black	yes
ME 43	4419	**-9.0**	**33.6**	1	9	d	R30	25	30	black	no
ME 155	4418	**-9.1**	**37.6**	1	9	e	T31	5	10	no	no
ME 170	4396	**-7.5**	**36.3**	1	10	a	R25	10	15	black	yes
ME 191	4384	**-9.4**	**33.7**	1	10	a	R23	10	15	black	yes
ME 174	4385	**-6.6**	**35.1**	1	10	a	R23	10	15	black	yes
ME 182	4383	**-9.7**	**32.8**	1	10	a	T30	20	25	grey	yes
ME 173	4393	**-1.5**	**34.1**	1	10	a	R25	15	20	no	no
ME 180	4398	**-9.6**	**35.7**	1	10	a	Q29	5	10	black	yes
ME 47	4394	**-5.1**	**35.0**	1	10	a	R23	10	15	black	no
ME 175	4395	**-10.0**	**36.6**	1	10	a	S29	15	20	black	yes
ME 181	4401	**-5.7**	**34.9**	1	10	a	R27	5	10	black	no
ME 185	4387	**-4.1**	**34.2**	1	10	a	R23	5	10	black	no
ME187	4399	**-9.2**	**38.2**	1	10	a	Q29	5	10	black	yes
ME 184	4397	**-7.6**	**40.8**	1	10		Q34	40	50	no	no
ME 46	4390	**-8.6**	**39.3**	1	10		Q33	15	20	brown	no
ME 169	4391	**-10.1**	**34.7**	1	10		Q33	15	20	black	no
ME 147	4382	**-6.1**	**38.9**	1	10		R33	15	20	black	no
ME 171	4389	**-9.8**	**35.6**	1	10		Q33	15	20	black	yes
ME 48	4380	**-10.0**	**35.2**	1	11		R29	0	5	black	yes
ME 159	903	**-8.8**	**39.2**	1	12		Q33	10	15	no	no
ME 145	77	**-8.9**	**36.4**	1	12		T31	30	35	black	yes
ME 188	23A	**-8.6**	**39.8**	1	12		Q32	60	65	no	no
ME 186	874	**-8.6**	**40.6**	1	12		R25	15	20	no	no

ME 172	95	**-8.1**	**41.1**	1	12		T31	20	25	no	no
ME 176		**-9.4**	**37.4**	1	4d	I	Q24			brown	yes
ME 166		**-7.9**	**41.4**	1	4d	I	P25			brown	no
ME 190		**-9.8**	**41.8**	1	4d	I	R24			no	yes
ME 167		**-9.5**	**37.0**	1	4d	I	Q23			brown	yes
ME 132		**-4.7**	**45.2**	1	4d	I	T28			no	no
ME 189		**-9.1**	**37.9**	1	4d	I	T22			no	no
ME 135		**-6.7**	**41.8**	1	4d	I	S22			brown	yes
ME 23		**-9.5**	**37.0**	1	4d	I	P26			no	no
ME 183		**-9.3**	**39.1**	1	4d	I	S23			brown	yes
ME 177		**-8.2**	**41.8**	1	4d	II	P25			brown	yes
ME 143		**-7.4**	**40.6**	1	4d	II	Q23			no	no
ME 136		**-8.5**	**38.7**	1	4d	II	Q25			no	no
ME 179		**-7.6**	**37.7**	1	4d	II	T22			brown	yes
ME 25		**-8.3**	**36.0**	1	4d	II	R32	10	15	brown	yes
ME 63	15017	**-8.8**	**44.2**	2	1		Y51	5	10	no	no
ME 64	15019	**-9.5**	**39.1**	2	1		Y46	5	10	no	no
ME 55	15005	**-8.0**	**39.8**	2	1		Y50	0	5	no	no
ME 65	15018	**-8.3**	**40.7**	2	1		Y49	5	10	no	no
ME 60	15013	**-8.2**	**42.6**	2	1		Y46	15	25	no	no
ME 62	15015	**-11.1**	**31.6**	2	1		Y48	5	10	no	no
ME 57	15008	**-7.7**	**34.7**	2	1		Y46	0	5	no	no
ME 54	15004	**-11.1**	**31.7**	2	1		Y52	10	15	no	no
ME 52	15002	**-11.2**	**35.7**	2	1		Y50	10	15	no	no
ME 61	15014	**-8.7**	**42.4**	2	1		Y46	15	25	no	no
ME 58	15009	**-9.2**	**45.1**	2	1		Y47	0	5	no	no
ME 56	15006	**-11.2**	**31.7**	2	1		Y48	0	5	no	no
ME 50	15000	**-9.0**	**39.9**	2	1		Y46	10	15	no	no
ME 51	15001	**-9.5**	**34.7**	2	1		Y51	10	15	no	no
ME 53	15003	**-11.2**	**31.8**	2	1		Y49	10	15	no	no
ME 72	15029	**-8.3**	**40.7**	2	2		X48	5	10	no	no

ME 77	15034	**-10.2**	**36.3**	2	2		X54	10	15	no	no
ME 66	15023	**-9.1**	**38.1**	2	2		W47	0	5	brown	no
ME 70	15027	**-9.3**	**38.1**	2	2		V48	5	10	brown	no
ME 78	15035	**-9.1**	**32.3**	2	2		Y48	15	20	no	no
ME 80	15037	**-9.7**	**38.2**	2	2		Y56	15	20	brown	no
ME 71	15028	**-8.7**	**30.8**	2	2		X47	5	10	brown	yes
ME 79	15036	**-8.6**	**38.9**	2	2		Y56	15	20	black	yes
ME 68	15025	**-9.3**	**36.6**	2	2		W50	0	5	brown	no
ME 76	15033	**-7.4**	**48.4**	2	2		V51	10	15	no	no
ME 67	15024	**-9.0**	**38.0**	2	2		X48	0	5	no	no
ME 74	15031	**-9.7**	**33.4**	2	2		Y56	5	10	brown	no
ME 75	15032	**-8.7**	**39.3**	2	2		Y56	10	15	black	yes
ME 69	15026	**-9.4**	**36.8**	2	2		W50	0	5	brown	no
ME 81	15038	**-8.4**	**35.1**	2	2		W47	15	20	no	no
ME 82	15039	**-8.7**	**31.0**	2	2		X48	15	20	no	no
ME 59	15022	**-8.6**	**39.2**	2	2		V50	0	5	brown	yes
ME73	15030	**-9.0**	**37.3**	2	2		X48	5	10	no	no
ME 86	15047	**-8.7**	**32.6**	2	3		X47	0	5	no	no
ME 87	15048	**-10.6**	**40.0**	2	3		X49	0	5	no	no
ME 98	15060	**-8.2**	**35.8**	2	3		V46	15	20	no	no
ME 89	15051	**-10.6**	**33.3**	2	3		W47	5	10	brown	no
ME 84	15045	**-10.0**	**34.8**	2	3		Y47	0	5	no	no
ME 88	15050	**-10.4**	**40.0**	2	3		Y47	5	10	no	no
ME 97	15059	**-10.7**	**33.3**	2	3		Y49	15	24	no	no
ME 83	15044	**-9.8**	**35.0**	2	3		Y47	0	5	no	no
ME 94	15056	**-11.0**	**33.5**	2	3		W47	10	15	no	no
ME 96	15058	**-10.7**	**33.4**	2	3		X47	10	15	no	no
ME 85	15046	**-10.4**	**39.9**	2	3		X47	0	5	no	no
ME 91	15053	**-10.5**	**33.2**	2	3		X49	5	10	no	no
ME 100	15063	**-8.3**	**35.7**	2	3		V46	20	30	no	no
ME 92	15054	**-8.5**	**35.5**	2	3		V46	10	15	no	no

ME 93	15055	**-10.6**	**33.3**	2	3		Y49	10	15	no	no
ME 101	15064	**-10.7**	**33.4**	2	3		X47	20	25	no	no
ME 95	15057	**-10.7**	**33.4**	2	3		W47	10	15	no	no
ME 102	15020	**-9.4**	**38.7**	2	4		W41	0	30	brown	yes
ME 99	15021	**-10.7**	**33.5**	2	4		W47	0	10	no	no
ME 104	15040	**-9.0**	**40.7**	2	5		V42	0	10	grey	yes
ME 106	15043	**-10.2**	**35.6**	2	5		W42	5	10	black	yes
ME 103	15041	**-5.8**	**33.9**	2	5		W42	5	10	black	yes
ME 105	15042	**-5.6**	**34.4**	2	5		W41+42	0	5	black	yes

5.2 All stable isotope data for faunal enamel samples of Excavation 1 Stratum 1-4d, indicating species, origin and tooth type.

Sample	**Mass (mg)**	**$\delta^{13}C_{VPDB}$ ‰**	**$\delta^{18}O_{VSMOW}$ ‰**	**SPF #**	**Square**	**Stratum**	**Species**	**Tooth**	**Comments**
ME542	2.867	-1.9	29.6	8294	R22	1b	*A. buselaphus*	$P^{3/4}$	very worn
ME525		2.0	32.4	8280	Q23	2bII	*A. buselaphus*	R M_2	
ME474	2.592	1.4	30.5	8258	S27	3aI	*A. buselaphus*	L M_1	mid-wear
ME503	2.811	2.7	33.4	8259	S27	3aI	*A. buselaphus*	L $M^{1/2}$	
ME477		1.6	33.5	8232	S27	3aII	*A. buselaphus*	L M_2	mid-wear
ME495	2.894	3.0	34.9	8264	T25	3aII	*A. buselaphus*	R P_3	
ME518	2.569	1.5	31.9	8267	T27	3aII	*A. buselaphus*	R M^2	
ME505	2.830	2.3	31.9	8233	S27	3aIII	*A. buselaphus*	M_2	mid-wear
ME441	2.787	2.2	35.8	8182	T28	3bI	*A. buselaphus*	R P_3	
ME442	3.014	1.5	36.1	8183	T28	3bI	*A. buselaphus*	R $M^{1/2}$	burnt?
ME 426		2.2	29.2	8214	T25	3bI	*A. buselaphus*	L M^1	
ME421	2.625	2.7	34.9	8199	T27	3bI	*A. buselaphus*	L M^1	late-mid wear
ME447	2.522	1.7	30.6	8212	T25	3bI	*A. buselaphus*	L M_2	one lobe missing
ME434		2.8	30.6	8407	T27	3bII	*A. buselaphus*	L M^x	
ME425	2.564	2.0	34.6	8198	S28	3bII	*A. buselaphus*	R M^1	

ME428	2.967	1.1	33.4	8202	T27	3bII	*A. buselaphus*	L M_3	late wear
ME376	2.926	3.0	31.2	8428	P21	4a	*A. buselaphus*	R M^1	
ME342	2.837	2.6	32.9	8116	P21	4a	*A. buselaphus*	L M_3	
ME326	1.543	2.7	31.1	8119	P20	4a	*A. buselaphus*	L P^3	late mid-wear
ME337	2.840	3.1	35.0	8129	O19	4a	*A. buselaphus*	R M_3	early wear
ME338	2.663	2.4	33.5	8125	O22	4a	*A. buselaphus*	R M^3	early wear; maybe same ind 8124
ME341	1.880	2.5	31.4	8128	P19	4a	*A. buselaphus*	L M_3	late wear
ME344	2.977	1.7	30.8	8124	O22	4a	*A. buselaphus*	R M_2	early wear; maybe same ind 8125
ME381	2.780	1.9	31.8	8123	O22	4a	*A. buselaphus*	P^4	mid-wear
ME371		1.4	32.8	8089	T26	4aI	*A. buselaphus*	L M^1	mid-wear
ME336	2.743	2.4	36.4	8088	T26	4aI	*A. buselaphus*	L M^3	early wear; maybe same ind 8089
ME334	2.666	2.3	34.5	8102	Q23	4aI	*A. buselaphus*	R M_2	
ME388	2.848	1.5	32.8	8155	Q22	4aII	*A. buselaphus*	L M^3	
ME350	2.654	3.1	32.9	8139	S24	4aIV	*A. buselaphus*	M	
ME360	2.942	2.9	30.9	8142	Q22	4aIV	*A. buselaphus*	L M_1	mid-wear
ME301	2.930	-0.0	33.3	8177	R25	4aLF	*A. buselaphus*	R M^1	mid-wear, glued
ME302		2.4	33.1	8172	R23	4aLH	*A. buselaphus*	L M^3	mid-wear
ME308		2.8	36.4	8176	S25	4aLH	*A. buselaphus*	L M_2	mid-wear
ME309		2.0	31.0	8171	Q23	4aLH	*A. buselaphus*	R M_2	mid-wear
ME271	2.620	1.9	34.7	8064	P23	4b	? (med. Alcelaphine)	$M_{2/3}$	
ME269		2.5	33.9	8056	P21	4b	*A. buselaphus*	L M_2	mid-wear
ME275		-2.1	34.6	8037	S25	4bII	*A. buselaphus*	L P_2	mid-wear
ME227	1.3	3.7	34.6	8309	P26	4c UP	*A. buselaphus*	R M_1	mid-wear
ME216		0.8	32.1	8307	N26	4cI	*A. buselaphus*	R M^1	late-mid wear
ME485	2.769	3.0	32.6	8394	R24	3aI	*A. buselaphus* (cf)	M	
ME489	2.800	2.5	33.1	8392	S21	3aI	*A. buselaphus* (cf)	M^x	
ME491	2.774	2.3	35.3	8403	T26	3aII	*A. buselaphus* (cf)	L P^4	
ME400	2.724	2.2	36.7	8122	O20	4a	*A. buselaphus* (cf)	P_2	
ME310	2.809	2.3	36.0	8384	R23	4aLH	*A. buselaphus* (cf)	M^2	

ME554	2.735	0.9	34.0	8435	S21	1a	Alcelaphine	M^x	
ME492	2.672	0.2	31.9	8397	T25	3aI	Alcelaphine	M	
ME496	2.721	2.7	33.3	8391	R22	3aI	Alcelaphine	M	
ME509	3.065	2.5	34.3	8257	T22	3aI	med. Alcelaphine (*A. bus./C. taurinus*)	R M^3	
ME511	2.711	2.3	36.1	8256	T22	3aI	Alcelaphine	M	
ME512	2.637	2.5	34.2	8242	R22	3aI	Alcelaphine	M	burnt?
ME513	2.638	1.7	31.0	8396	S22	3aI	Alcelaphine	M	
ME519	2.764	2.5	34.6	8398	Q21	3aI	Alcelaphine	frag	
ME484	2.662	2.2	36.2	8395	S27	3aII	Alcelaphine	M3	
ME516	0.34	0.7	33.0	8224	T25	3aIII	*Damaliscus* sp.?	$M_{1/2}$	
ME433	2.864	3.5	34.4	8190	T26	3bI	Alcelaphine	M^x	
ME435	2.593	2.1	35.2	8185	T28	3bI	Alcelaphine	M^x	late wear
ME444	2.644	-3.5	30.8	8420	Q23	3bI	Alcelaphine	M	
ME456	2.940	2.3	35.0	8186	T28	3bI	Alcelaphine	M^x	early-mid wear
ME459	2.894	2.8	34.8	8210	R24	3bI	Alcelaphine	M	
ME416	2.641	1.8	30.9	8408	T27	3bII	Alcelaphine	M	
ME424	2.970	2.3	36.5	8413	S27	3bII	Alcelaphine	M	burnt?
ME438	2.690	1.7	32.8	8205	T27	3bII	Alcelaphine	M_x	
ME460	2.992	-1.6	35.6	8406	T28	3bII	Alcelaphine	M	
ME335	2.649	1.6	29.7	8127	O24	4a	Alcelaphine	$M_{2/3}$	
ME370	2.686	2.6	34.1	8112	P23	4a	Alcelaphine	M_x	
ME384	2.897	2.5	32.3	8120	P20	4a	Alcelaphine	M	
ME366	2.678	3.1	36.8	8091	T25	4aI	Alcelaphine	M_x	
ME369	2.790	-1.2	39.2	8078	T28	4aI	Alcelaphine	M_x	
ME383	2.865	2.5	34.6	8101	R24	4aI	Alcelaphine	M	
ME393	2.580	2.5	31.9	8097	S21	4aI	Alcelaphine	M_x	
ME327	2.712	3.0	37.8	8082	T26	4aI	Alcelaphine	M^x	
ME333	2.994	2.2	31.4	8083	T26	4aI	Alcelaphine	M_x	
ME351	3.056	0.6	35.0	8150	T28	4aII	Alcelaphine	L M_3	
ME331	2.615	2.6	31.2	8165	S22	4aIII	Alcelaphine	M_x	

ME347	2.658	1.0	30.8	8160	S23	4aIII	Alcelaphine	M_3	
ME367	2.938	2.9	39.0	8148	S24	4aIV	Alcelaphine	M	
ME391	2.706	2.8	30.7	8146	S23	4aIV	Alcelaphine	R P_4	
ME303	2.849	3.3	33.7	8170	R25	4aLF	Alcelaphine	M_x	
ME307	2.895	2.5	32.9	8181	R24	4aLF	Alcelaphine	M_x	
ME311	2.756	3.0	38.3	8382	S25	4aLH	Alcelaphine	M_x	
ME286	2.525	3.9	32.0	8385	O21	4b	Alcelaphine	P_2	
ME279	3.042	1.1	32.1	8039	S24	4bII	Alcelaphine?	frag	
ME220	2.391	0.8	31.6	8029	O24	4c	Alcelaphine?	M	
ME226	2.465	0.7	33.1	8026	P20	4c	Alcelaphine?	P_x	Burnt, late wear
ME221	2.673	2.2	33.9	8009	O25	4cI	Alcelaphine	M_x	
ME225	2.685	1.9	32.1	8014	S25	4cI	Alcelaphine	P_x	
ME217		2.1	33.0	8349	P26	4cI	*Alcelaphus/Damaliscus*	M	
ME224	2.660	-11.0	36.2	8314	P27	4cMID	Alcelaphine?	M_x	burnt (smell), excluded from analyses
ME206		-1.4	35.3	8318	P25	4dI	Alcelaphine	frag	burnt?
ME202		2.7	34.0	8000	T22	4dI	*Damaliscus* sp.	R $M_{2/3}$	
ME207		-1.4	33.4	8332	S24	4dII	Alcelaphine	frag	burnt?
ME205		0.1	32.6	8319	T22	4dII	Alcelaphine	frag	mid-late wear, burnt?
Antid.	0.08	-2.5	31.4	8346	K27 mix	4c	*A. bondi* (cf)	L M_1 & P_3	M1 late-mid wear
ME527		-8.8	32.2	8274	T25	2bII	*A. marsupialis*	L M_3	
ME537		-10.7	31.2	8439	T24	2bII	*A. marsupialis*	L M_1	same ind as 8289
ME540		-9.9	31.8	8289	T24	2bII	*A. marsupialis*	L P_4	same ind as 8439
ME475		-9.0	33.5	8253	T23	3aI	*A. marsupialis*	R M_2	late wear, same ind as 8254?
ME508		-6.2	32.2	8368	S23	3aI	*A. marsupialis*	R M^3	
ME510		-7.9	32.4	8239	S26	3aI	*A. marsupialis*	L $M_{2/3}$	mid-wear
ME486	2.654	-2.9	34.0	8243	R22	3aI	*A. marsupialis*?	M_x	
ME515	2.601	-6.4	35.2	8399	Q21	3aI	*A. marsupialis*?	frag	
ME517	2.842	-8.4	31.3	8254	T23	3aI	*A. marsupialis*	L M^1	late wear, same ind as 8253?

ME420		-10.8	34.5	8216	T26	3bI	*A. marsupialis*	L M_2	(cf hofmeyri)?
ME432		-8.9	30.9	8218	S27	3bI	*A. marsupialis*	M	
ME396		-3.2	33.2	8131	O23	4a	*A. marsupialis*	L M^3	(cf hofmeyri)?
ME413		-7.1	30.4	8126	O23	4a	*A. marsupialis*?	R P_3	
ME306	2.648	-7.1	30.6	8175	R23	4aLF2	*A. marsupialis*	L M^1	same ind as 8174?, late-mid wear
ME305		-6.9	31.4	8174	R23	4aLH2	*A. marsupialis*	R M_1	same ind as 8175?
ME283		-7.7	35.0	8059	T27	4bI	*A. marsupialis*	L M^3	(cf hofmeyri)?
ME287	2.666	-11.2	32.2	8040	S23	4bII	Bovid	M	was Alcelophine - wrong id?
ME219	2.737	-7.1	29.5	8034	O20	4c	Bovid	frag	was Alcelophine - wrong id?
ME222	2.964	-6.6	34.1	8317	L28	4cMID	Bovid	M	was Alcelophine - wrong id?
ME228	2.895	2.0	31.6	8311	P26	4c MID	*C./M. taurinus*	M^3	mid-wear. burnt?
ME419	2.655	2.9	32.5	8217	S27	3bI	*C. taurinus*	R M_3	
ME230	2.368	1.8	34.4	8360	N27	4c UP	*C. taurinus*	M^x	
ME343	2.952	2.5	34.1	8099	T25	4aI	*Connochaetes* sp.	R M^3	mid-wear. poss. *C. gnou*
ME339	2.623	2.7	35.0	8077	T24	4aI	*C. taurinus*	L M^3	mid-wear, burnt?
ME377	2.922	1.5	32.0	8153	Q22	4aII	*C. taurinus*	L P^3	glued, late mid-wear
ME345		2.8	32.9	8144	Q23	4aII	*C. taurinus* (cf)	M_3	early wear
ME427	2.795	2.2	31.4	8211	T24	3bI	*C. taurinus/gnou*	L M^2	
ME340	2.960	2.3	33.4	8135	Q21	4aV	*C. taurinus/gnou*	R M_3	early wear
ME523		1.5	31.5	8286	Q21	2bII	*C. taurinus*	L M_3	
ME480		1.2	31.6	8251	T28	3aI	*C. taurinus*	M_3	mid-wear, burnt?
ME330	1.385	3.7	34.9	8132	O23	4a	*C. taurinus*	$M^{2/3}$	
ME346		0.7	33.1	8136	T23	4aII	*C. taurinus*	L M^3	mid-wear
ME229		2.0	34.4	8310	P26	4c MID	*C. taurinus*	L $M^{2/3}$	burnt?
Blesbok	0.19	0.3	32.0	8238	T28	3aIII	*D. pygargus*	L M_3	
ME423	2.739	1.2	34.0	8201	S24	3bI	*Damaliscus* sp.	R M_1	late wear
ME547	2.841	-5.4	31.6	8304	Q23	1	*Equus* sp	M^x/P^x	
ME487	3.050	-0.6	33.6	8400	T27	3aI	*Equus* sp	frag	

ME546	3.026	-7.1	30.5	8437	S27	1b	*Equus* sp.	M^x	
ME533	2.769	-1.8	27.7	8372	T21	2b	*Equus* sp.	R M_x	
ME535	2.588	0.2	33.0	8276	S22	2b	*Equus* sp.	P^x?	burnt?
ME538		-0.8	30.4	8275	T25	2bII	*Equus* sp.	M_l	burnt?
ME476	2.623	-0.2	32.0	8247	S25	3aI	*Equus* sp.	M_x/P_x	
ME482	2.781	0.9	29.9	8390	T26	3aI	*Equus* sp.?	P/M	
ME488	2.837	-0.8	31.8	8245	T27	3aI	*Equus* sp.	M^x/P^x	
ME504	2.916	-0.3	30.8	8388	T22	3aI	*Equus* sp.	M^x	
ME520	2.995	-2.1	30.8	8240	S26	3aI	*Equus* sp.	M^x/P^x	burnt?
ME522	2.740	0.3	30.9	8393	R24	3aI	*Equus* sp.	L $M^{1/2}$	burnt?
ME521		0.1	32.4	8235	S27	3aII	*Equus* sp.	L P_2	early wear
ME479	2.861	0.3	33.2	8236	S27	3aIII	*Equus* sp.	M^x/P^x	
ME448	2.850	-1.6	33.7	8369	T26	3bI	*Equus* sp.	M_x	only inner part left, burnt?
ME395	2.906	0.9	31.7	8427	P21	4a	*Equus* sp.	R M1/2	
ME361	2.671	0.7	34.7	8154	Q23	4aII	*Equus* sp.	M_x	
ME382	2.638	-0.9	32.5	8161	Q23	4aIII	*Equus* sp.	P^x/M^x	burnt?
ME304		2.9	37.1	8380	R23	4aLH	*Equus* sp.	M_x	burnt?
ME267		1.1	34.4	8069	P22	4b	*Equus* sp.	R P_2	burnt?
ME270	2.810	-0.2	31.65	8076	O24	4b	*Equus* sp.	P/M	
ME223		0.7	33.0	8021	T25	4cI	*Equus* sp.	P^x/M^x	
ME532	3.024	-4.3	41.4	8374	S22	2b	*P. capensis*	P^x/M^x	
ME550	2.676	-6.1	30.0	8295	R23	1b	*H. africaeaustralis*	L M^1	
ME551	3.034	-7.1	30.4	8302	S22	1b	*H. africaeaustralis*	L M_3	
ME552	2.863	-7.41	31.7	8300	R24	1b	*H. africaeaustralis*	L M^1	
ME549	2.740	-6.0	29.2	8299	P24	2a	*H. africaeaustralis*	L M3	unworn
ME494	2.7443	-10.1	28.3	8249	R23	3aI	*H. africaeaustralis*	L M^1	
ME507	2.902	-13.0	29.1	8227	T27	3aIII	*H. africaeaustralis*	R M^2	
ME449	3.011	-11.3	28.4	8196	R24	3bI	*H. africaeaustralis*	L P_4-M_1	M1 sampled, burnt?
ME430	2.990	-10.3	30.8	8405	T28	3bII	*H. africaeaustralis*	M	

ME437	2.932	-11.7	29.8	8220	T26	3bII	*H. africaeaustralis*	R M_1&$_2$	M2 sampled, in mandible
ME463	2.725	-12.3	25.8	8197	T28	3bII	*H. africaeaustralis*	L M^3	
ME402	0.4	-7.7	28.1	8087	S25	4aI	*H. africaeaustralis*	L M^2	
ME403	2.908	-10.0	31.2	8104	S26	4aI	*H. africaeaustralis*	M2?	
ME406	1.750	-0.2	31.8	8164	S22	4aII	*H. africaeaustralis*	L M^1	
ME409	2.749	-4.7	28.1	8137	Q21	4aIV	*H. africaeaustralis*	L M^3	
ME322	2.830	-9.4	31.5	8173	R23	4aLF	*H. africaeaustralis*	frag	burnt?
ME408	2.780	-11.5	30.6	8133	R23	4aV	*H. africaeaustralis*	R M^2	
ME294	2.905	-0.8	29.1	8055	Q23	4bI	*H. africaeaustralis*	R M^3	
ME215	2.947	-6.1	31.4	8025	P22	4c	*H. africaeaustralis*	P_4	unworn
ME232	2.925	-7.5	29.0	8017	O21	4c	*H. africaeaustralis*	R M_3	worn, burnt
ME233	3.078	-7.6	29.7	8315	O28	4c MID	*H. africaeaustralis*	M^x	Incomplete, burnt
ME234	0.990	-10.8	28.9	8008	P25	4cII	*H. africaeaustralis*	L P^4	mid-wear, incomplete
ME210	2.828	-6.9	29.8	8003	P24	4d	*H. africaeaustralis*	R M_2	
ME211	2.802	-9.1	27.1	8001	O22	4d	*H. africaeaustralis*	R P^4	in maxilla
ME212	2.681	-10.7	29.1	8004	S24	4dI	*H. africaeaustralis*	R M^3	burnt?
ME213	2.751	-10.2	31.4	8005	S24	4dI	*H. africaeaustralis*	R M^3	burnt
ME284	2.808	-2.1	34.0	8042	T24	4bI	large-med bovid	M	burnt?, excluded from analyses
ME536	1.6	-11.7	35.0	8373	R21	2b	*O. oreotragus*	L M_1	
ME440	2.687	-0.9	27.2	8203	T27	3bII	*P. capensis*	M1	
ME364	2.645	-1.2	29.4	8117	P23	4a	*P. capensis*	M_3	
ME353	2.790	-1.1	30.3	8084	T26	4aI	*P. capensis*	M1/2	
ME356	2.670	-0.8	28.8	8093	T27	4aI	*P. capensis*	M2/3	
ME357	2.552	-0.3	29.0	8092	T27	4aI	*P. capensis*	M2/3	
ME365	1.900	-0.3	24.3	8085	T26	4aI	*P. capensis*	M3	
ME354	2.671	-1.0	28.7	8163	T26	4aII	*P. capensis*	R $M^{1/2}$	
ME355	2.942	0.3	30.1	8158	S26	4aII	*P. capensis*	L M^1	
ME363	2.679	0.2	28.6	8159	S26	4aII	*P. capensis*	L M_2	
ME320	2.489	-0.0	31.5	8179	S25	4aLF	*P. capensis*	L M_1	

ME321	2.765	-0.1	29.7	8180	R24	4aLF	*P. capensis*	R P^4-M^2	
ME296	2.968	0.5	27.7	8068	O21	4b	*P. capensis*	R P^4	
ME297	0.939	1.4	30.7	8065	P23	4b	*P. capensis*	R M^1	
ME299	2.887	0.7	30.6	8067	O23	4b	*P. capensis*	L $M^{1/2}$	
ME295		-0.5	29.3	8073	P22	4b	*P. capensis*	M2/1	
ME298		-1.5	27.9	8047	S23	4bI	*P. capensis*	R M_3	
ME241	2.664	0.6	28.2	8018	O19	4c	*P. capensis*	R $M^{1/2}$	mid-late wear, same ind as 8019?
ME242	2.778	-1.7	29.1	8019	O19	4c	*P. capensis*	R $M_{1/2}$?	mid-late wear, same ind as 8018?
ME243	2.788	-2.3	27.5	8020	O19	4c	*P. capensis*	M1/2	late wear
ME244	2.753	-0.2	30.1	8023	P24	4c	*P. capensis*	L $M^{1/2}$	mid-wear
ME245	2.725	-0.5	30.5	8024	O23	4c	*P. capensis*	L $M^{1/2}$	early-mid wear
ME246	1.818	0.1	28.5	8033	O20	4c	*P. capensis*	M1/2	mid-wear, same ind 8032?
ME314	2.608	-11.9	35.2	8169	R25	4aLF	*P. capreolus*	R M_1	
ME325	2.901	-6.2	35.0	8110	P21	4a	*P. capreolus*?	M	
ME389	2.709	-5.9	32.6	8107	O20	4a	*P. capreolus*?	M_x	
ME539	2.956	-0.0	31.5	8285	S27	2b	*Phacocerus sp.*	M_2	no wear
ME362	2.659	0.7	30.5	8121	O20	4a	*Phacocerus sp.*	M3	
ME387	2.762	0.4	31.0	8114	P21	4a	*Phacocerus sp.*	M3	
ME352	2.873	1.0	33.9	8098	S24	4aI	*Phacocerus sp.*	M3	
ME401	2.552	1.9	37.2	8433	S27	4aII	*Phacocerus sp.*	P_4	
ME375	2.825	1.0	32.7	8145	S23	4aIV	*Phacocerus sp.*	M3	burnt?
ME499		-11.4	35.0	8269	S27	3aII	*R. campestris*	R M^1	late-mid wear
ME501		-14.1	35.8	8402	S28	3aII	*R. campestris*	$M_{1/2}$	
ME467		-12.8	36.6	8139	S28	3bI	*R. campestris*	L M_3	
ME443	2.251	-10.2	33.9	8219	S27	3bI	*R. campestris*	$M^{2/3}$	
ME469	2.986	-10.1	28.5	8191	T26	3bI	*R. campestris*	M_3	
ME436		-9.3	36.2	8208	S27	3bII	*R. campestris*	$M_{2/3}$	
ME470		-11.8	36.4	8204	T27	3bII	*R. campestris*	R M^3	
ME472		-11.1	37.8	8412	S27	3bII	*R. campestris*	L M^1	

ME466	2.785	-10.4	36.7	8207	S27	3bII	*R. campestris*	L P^2&^{3}	P3 sampled
ME411	2.798	-8.1	34.2	8113	P23	4a	*R. campestris*	R$M_{2/3}$	
ME412		-9.7	33.5	8106	S26	4aI	*R. campestris*	M	
ME414		-10.7	34.3	8426	S27	4aI	*R. campestris*	L P_3	
ME378	2.527	-7.9	34.0	8100	S28	4aI	*R. campestris*	R P^4-M^1	P4 sampled
ME385	2.703	-8.2	31.1	8096	R21	4aI	*R. campestris*	M^x	
ME404	2.738	-9.3	31.8	8105	S26	4aI	*R. campestris*	M	
ME405	2.672	-9.7	35.0	8095	T27	4aI	*R. campestris*	M_x	
ME410		-9.4	36.7	8149	T24	4aII	*R. campestris*	L P^2	
ME407	2.721	-10.0	36.2	8430	T22	4aII	*R. campestris*	M^1	
ME399	2.745	-10.4	37.0	8141	S24	4aIV	*R. campestris*	L M^3	
ME319		-11.3	33.4	8167	T25	4aLH	*R. campestris*	M_x	
ME317		-11.8	42.3	8168	R25	4aLH	*R. campestris*	R M_{1-3}	Glued, burnt?, M1 sampled
ME318		-11.0	32.9	8166	S24	4aLH2	*R. campestris*	L P_{3-4}	glued
ME291	2.946	-9.1	33.4	8071	P22	4b	*R. campestris*	L M_2	
ME288		-9.6	38.2	8054	T25	4bI	*R. campestris*	$M_{2/3}$	slightly too big?
ME285	2.920	-10.3	32.1	8061	T27	4bI	*R. campestris*	$M^{2/3}$	early wear
ME289	1.520	-8.7	36.7	8052	Q25	4bI	*R. campestris*	L $M_{2/3}$	
ME290	2.613	-10.7	39.5	8060	T27	4bI	*R. campestris*	L M^2	worn
ME293	2.638	-8.3	32.3	8044	R23	4bI	*R. campestris*	L P_{2+3}	in mandible, P3 sampled
ME292		-7.6	31.7	8035	T25	4bII	*R. campestris*	M	late wear
ME300	2.950	-8.7	32.2	8036	T25	4bII	*R. campestris*	M	mid wear
ME247		-8.8	40.2	8015	O21	4c	*R. campestris*	$M^{2/3}$	mid-late wear, burnt?
ME248		-10.7	33.7	8016	O21	4c	*R. campestris*	$M^{2/3}$	mid wear
ME249		-9.1	33.0	8031	O20	4c	*R. campestris*	$M_{2/3}$	
ME529	2.627	2.0	34.6	8282	S23	2b	*R. fulvorufula*	L M^2	
ME534	2.644	1.9	31.2	8281	S20	2b	*R. fulvorufula*	L M^3	
ME528		-0.6	31.9	8288	Q21	2bII	*R. fulvorufula*	R M_3	
ME478	2.770	1.3	34.0	8263	T28	3aII	*R. fulvorufula*	L M^1	late-mid wear

ME500	2.692	2.5	31.1	8225	T25	3aIII	*R. fulvorufula?*	L P^4	very worn
ME422	2.157	1.7	31.6	8215	T25	3bI	*R. fulvorufula*	R M^3	
ME451	2.632	1.1	35.1	8195	S25	3bI	*R. fulvorufula*	M^x	
ME454	3.064	2.4	33.5	8187	T28	3bI	*R. fulvorufula*	L M^3	
ME468	2.603	-9.8	32.9	8370	T25	3bI	*R. fulvorufula*	L M^x	Burnt (smell), excluded from analyses
ME471	2.866	3.1	32.8	8404	T28	3bII	*R. fulvorufula*	P^3	
ME386	2.775	2.7	34.9	8138	T22	4aIV	*R. fulvorufula*	L P_4-M_1	M1 mid-wear, M1 sampled
ME313	2.722	3.5	37.4	8178	R24	4aLF	*R. fulvorufula*	P^4	
ME380	2.986	1.9	31.3	8134	R23	4aV	*R. fulvorufula*	L M^1	late wear
ME398	2.913	2.1	31.6	8115	P21	4a	*R. fulvorufula*	R P^4	
ME390	2.677	-1.6	35.8	8103	T27	4aI	Reduncini indet.	R $M_{2/3}$	
ME374	2.624	2.1	38.0	8143	Q22	4aIV	*R. fulvorufula*	L M_1	mid-wear
ME397	2.887	2.9	35.8	8140	S24	4aIV	*R. fulvorufula*	R $M_{2/3}$	burnt?
ME490	2.551	1.5	35.0	8229	T26	3aIII	small-med bovid	M	excluded from analyses
ME531	2.993	-10.4	33.1	8376	T23	2bII	*T. oryx*?	P_x	
ME473		-9.7	31.1	8365	T24	3aI	*T. oryx*	P_4	
ME455		-8.6	33.0	8423	T27	3bI	*T. oryx*	R M^1	
ME231		-9.5	37.9	8362	M26	4cII	*T. oryx*	R P^2	late wear
ME530		-9.5	30.6	8377	T23	2bII	*T. oryx* (cf)	M_x	
ME273		-7.7	32.7	8386	O21	4b	*T. oryx* (cf)	R P^2	
ME258		-8.9	34.9	8350	Q26	4c MID	*T. oryx* (cf)	M^x	
ME257	2.628	-1.1	33.6	8335	O28	4c MID	*T. oryx* (cf)	cf M_3	burnt? brittle thin enamel, excluded from analyses
ME526	2.738	-8.2	35.0	8375	S24	2bII	Tragelaphini?	frag	
ME498	3.027	-11.4	33.1	8367	T26	3aI	Tragelaphini?	M	
ME502	2.997	-8.6	31.1	8389	R23	3aI	Tragelaphini	M	
ME493	2.777	-9.1	34.8	8366	T28	3aIII	Tragelaphini?	M^x	burnt?
ME481	2.759	-10.3	28.5	8401	T25	3aIII	Tragelaphini?	frag	
ME418	3.018	-9.3	35.9	8419	T26	3bI	Tragelaphini	M	

ME446	2.644	-9.0	33.0	8416	T27	3bI	Tragelaphini	frag	
ME450	2.582	-8.1	33.0	8415	T27	3bI	Tragelaphini	frag	
ME458	2.877	-10.5	35.9	8414	T27	3bI	Tragelaphini	frag	
ME379	1.230	-4.4	34.3	8151	T22	4aII	Tragelaphini	L M_x	
ME328	2.389	-4.9	31.8	8429	T22	4aV	Tragelaphini	M	
ME278	2.663	-8.5	33.9	8063	T27	4bI	Tragelaphini	frag	
ME274		-8.5	33.3	8062	T27	4bI	Tragelaphini	P^x	
ME250	3.062	-8.6	35.3	8358	O28	4c MID	Tragelaphini	frag	
ME251	2.850	-10.9	37.8	8338	M27	4c LR	Tragelaphini	M	
ME252	2.915	-10.1	37.9	8363	L27	4c MID	Tragelaphini	frag	
ME253	2.791	-8.0	34.7	8340	L27	4c MID	Tragelaphini	frag	
ME254	2.678	-9.4	36.1	8361	L27	4c MID	Tragelaphini	M	
ME255	3.013	-7.9	35.5	8359	Q26	4c UP	Tragelaphini	frag	
ME256	2.990	-9.5	36.5	8364	Q26	4c UP	Tragelaphini	frag	
ME201		-10.2	36.7	8331	O23	4d	Tragelaphini	frag	
ME415	2.938	-8.4	34.6	8424	T27	3bI	Tragelaphini	M	
ME429	2.949	-10.7	34.9	8425	T27	3bI	Tragelaphini	M	
ME431	2.920	-8.6	31.4	8422	S28	3bI	Tragelaphini	M	
ME462	2.625	-7.4	34.3	8209	R24	3bI	Tragelaphini	M	
ME465		-9.8	31.3	8409	T27	3bII	Tragelaphini	M	
ME417	2.951	-7.8	32.4	8421	S26	3bII	Tragelaphini	M	
ME445	2.952	-9.3	32.3	8206	T27	3bII	Tragelaphini	frag	
ME452	2.611	-8.3	34.1	8410	T27	3bII	Tragelaphini	M	
ME461	3.050	-10.7	34.8	8411	T27	3bII	Tragelaphini	M	
ME332	2.755	-9.6	38.1	8434	T24	4aIII	Tragelaphini	M^x	
ME358	3.052	-8.2	33.1	8431	S23	4aIV	Tragelaphini	M	
ME316	2.966	-10.0	37.4	8383	Q23	4aLH	Tragelaphini	M	burnt?
ME316	2.798	-9.9	38.1	8383	Q23	4aLH	Tragelaphini?	M	burnt?
ME272	2.996	-9.5	37.8	8387	O21	4b	Tragelaphini	M^x	
ME208		-10.3	36.0	8330	Q24	4dI	Tragelaphini?	frag	
ME209		-10.5	32.8	8333	P25	4dI	Tragelaphini?	frag	

ME524		-7.2	31.6	8277	S22	2bII	*T. strepsiceros*	$M^{1/2}$	
ME497	2.663	-9.6	36.5	8261	S24	3aI	*T. strepsiceros*?	R P^{x}	
ME514		-9.6	31.9	8268	T27	3aII	*T. strepsiceros*	L M^{2}	early mid-wear, same as ind 8266?
ME483	2.581	-11.3	33.9	8221	S28	3aIII	*T. strepsiceros*?	M frag	
ME506	2.94	-8.2	35.9	8237	S27	3aIII	*T. strepsiceros*	M frag	
ME453	2.763	-10.3	38.1	8200	T27	3bI	*T. strepsiceros*	L M^{1}	
ME464	2.597	-8.0	35.2	8213	T25	3bI	*T. strepsiceros*	M^{x}	burnt?
ME439	2.894	-10.1	35.0	8184	T28	3bI	*T. strepsiceros*	L M_3	
ME457	3.034	-8.8	33.1	8194	S26	3bII	*T. strepsiceros*?	M^{x}	
ME392	3.043	-9.4	35.3	8118	P20	4a	*T. strepsiceros*	L P_2	early wear
ME323	2.665	-6.8	33.8	8108	P21	4a	*T. strepsiceros*	M_x	
ME324	2.964	-8.6	33.3	8109	P21	4a	*T. strepsiceros*	M	
ME 348		-8.8	35.3	8086	T23	4aI	*T. strepsiceros*	M^{x}	
ME349	3.031	-8.6	32.8	8090	R23	4aI	*T. strepsiceros*	$M^{2/3}$	
ME372	2.866	-8.2	34.2	8081	T26	4aI	*T. strepsiceros*	M_x	
ME368	2.671	-9.1	33.6	8094	T27	4aI	*T. strepsiceros*?	M	
ME359		-7.2	37.6	8156	S23	4aII	*T. strepsiceros*	M_x	
ME394	2.796	-6.7	32.4	8162	Q21	4aIII	*T. strepsiceros*	M	
ME373	2.670	-4.3	31.6	8432	Q21	4aIV	*T. strepsiceros*	L M_2	
ME268	2.806	-6.5	34.3	8075	O22	4b	*T. strepsiceros*	M^{x}	
ME265	2.978	-8.4	37.1	8341	N27	4c LR	*T. strepsiceros*	frag	
ME266	2.904	-7.8	35.2	8336	P26	4c MID	*T. strepsiceros*	L M^{1}	burnt?
ME541		-7.8	31.9	8378	R23	2bII	*T. strepsiceros* (cf)?	L $M_{2/3}$	late wear
ME312		-9.6	32.6	8381	R25	4aLH	*T. strepsiceros* (cf)	M_x	
ME315		-7.4	33.3	8379	R24	4aLH	*T. strepsiceros* (cf)	M_x	
ME264	2.843	-8.4	34.4	8306	M28	4c	*T. strepsiceros* (cf)	M_x	
ME259	2.839	-8.7	33.4	8334	O28	4c MID	*T. strepsiceros* (cf)	M^{x}	.
ME260	2.797	-10.2	34.5	8337	P26	4c MID	*T. strepsiceros* (cf)	M_x	
ME261	2.608	-8.5	39.6	8342	K28	4c MID	*T. strepsiceros* (cf)	frag	
ME262	2.962	-8.7	33.5	8347	K27	4c MID	*T. strepsiceros* (cf)	M^{x}	

ME263		-10.5	31.6	8352	N27	4cI	*T. strepsiceros* (cf)	M	burnt?
ME203		-9.0	35.3	8328	P25	4dI	*T. strepsiceros* (cf)	M_x	mid-late wear

5.3 All stable isotope data for faunal enamel samples of Excavation 1 Stratum 5-12, indicating specimen number, species, origin and tooth type.

Sample	**Mass (mg)**	**$\delta^{13}C_{VPDB}$ ‰**	**$\delta^{18}O_{VSMOW}$ ‰**	**SPF#**	**Square**	**Stratum**	**height 1**	**height 2**	**Species**	**Tooth**	**Comments**
ME675	2.680	-5.8	33.8	7701	K27	5	5	10	Alcelaphine	M/P	
ME657	2.546	-7.2	29.1	7319	T32	6			Alcelaphine	M^x	Spit 1
ME651	2.874	-0.3	35.8	7001	L29	7	10 basal	15 red	Alcelaphine	M^x	central cavity
ME652	3.054	1.8	31.7	7156	S34	7	0	5	Alcelaphine	frag	
ME654	2.946	2.1	30.6	7192	S33	7	15	20	Alcelaphine	frag	
ME655	3.006	-8.8	31.1	7122	L31	7			Alcelaphine	frag	
ME589	2.954	0.6	30.0	10014	P34	8	5	10	Alcelaphine		
ME632	2.896	-4.5	29.3	10045	Q33	10	15	20	Alcelaphine	M	
ME636	2.984	-6.1	34.2	10048	T32	10	50		Alcelaphine	M_x	
ME579	3.006	-8.2	25.6	964	P29	11	0	5	Alcelaphine	M^x	dentine brittle, some glue
ME598	3.022	-10.3	31.2	425	T30	11	25	30	Alcelaphine	M	
ME602	2.879	-7.9	26.8	1075	R 24	11	5	10	Alcelaphine	frags	
ME603	2.916	-0.7	31.7	608	R 28	11	25	30	Alcelaphine	M	glued
ME564	2.995	-7.4	29.0	1015	R 31	12	0	5	Alcelaphine	M_x	
ME569	3.032	-8.3	28.0	1027	R 30	12	0	5	Alcelaphine	M^x	
ME572	2.786	-9.9	31.5	170	P30	12	0	10	Alcelaphine	M	
ME573	0.55	-7.9	26.1	152	T33	12	5	10	Alcelaphine	frag	
ME641	2.907	-12.9	28.6	10066	Q33	9b	5	10	Large bovid	M	Excluded from analyses
ME647	2.559	-5.3	30.8	7007	L34	7			Alcelaphine	frag	same indiv. 7006?
ME575	2.771	-5.6	31.5	1014	S31	12	10	15	Alcelaphine	frag	

ME596	3.021	-9.8	36.0	48	Q32	12	55	60	Alcelaphine. cf *D. pygrargus*	frag	Chazan Exc07
ME650	2.729	-6.7	32.8	7184	N34	7	20	25	Alcelaphine?	frag	
ME574	2.722	-6.2	33.7	910	Q33	12	45	50	Alcelaphine?	M_x	
ME595	2.903	-2.5	29.4	679	R 26	12	20	25	Alcelaphine?	M^x	
ME646	2.731	0.6	28.0	10056	R26	8a	20	25	Alcelaphine?	M	
ME662	2.833	3.2	36.8	7620	Q29	5	5	10	Alcelaphini cf *Damaliscus*	M/P	
ME664	0.8	-2.2	29.1	7597	R31	5	0	5	*A. bondi*	M^x/P^x	
ME668	3.021	-1.5	28.8	7586	Q26	5	35	40	*A. bondi*	frag	
ME673	2.705	-1.5	29.4	7582	Q26	5	0	5	*A. bondi*	frag	
ME676	2.750	0.1	30.0	7578	R26	5	0	5	*A. bondi*	frag	
ME648	2.896	-3.4	29.3	7070	N33	7			*A. bondi*	M^3	
ME667	2.561	-5.0	33.3	7618	N28	5	10	15	*A. bondi?*	frag	
ME669	2.992	0.6	33.4	7665	O28	5	5	10	*A. bondi?*	frag	
ME593	2.717	-12.4	36.5	7329	R34	6	35	43	*A. bondi?*	frag	
ME685	2.637	-10.4	28.3	10070	Q30	7			*A. marsupialis*	M_3	was no. 88. glued
ME671	2.597	-8.9	32.6	7695	Q29	5	0	5	*A. marsupialis?*	frag	
ME658	2.986	-11.6	35.8	7338	P34	6	35	40	*A. marsupialis?*	M	
ME656	2.3	-7.0	33.6	7003	L29	7	10 basal	15 red	*Antidorcas sp.?*	M^x	
ME633	1.2	-9.3	29.6	4351	S24	10a	35	40	*Antidorcas sp.?*	frag	
ME672	2.952	-0.5	32.0	7589	Q26	5	5	10	Equid	P/M	glued
ME640	2.876	-9.1	31.2	10046	P34	10	25	30	Equid	P/M	heat fractures?
ME581	2.733	-5.3	24.1	316	R 34	11	30	35	Equid	P	
ME560	2.694	-8.6	27.9	1062	R 31	12	5	10	Equid	P^x/M^x	
ME562	2.584	-3.2	27.1	254	Q29	12	5	10	Equid	P^x	
ME563	2.707	-5.8	29.6	199	Q30	12	5	10	Equid	P^x	
ME565	2.792	-8.4	28.2	202	Q30	12	5	10	Equid	P	
ME567	2.866	-7.3	29.2	1019	R 31	12	5	10	Equid	P^x/M^x	
ME568	3.061	-5.1	22.7	974	S33	12	0	5	Equid	frags	

ME570	2.757	-8.8	24.5	1404	R 30	12	10	15	Equid	frag	
ME571	1.99	-5.7	31.5	258	Q29	12	50	55	Equid	P	many small angular fragments
ME584	2.992	-4.4	31.4	10051	Q30	10a	25	30	Equid	I	inner core with two enamel plates
ME642	3.005	-2.6	31.4	10060	R33	9a	0	5	Equid	frag	
ME645	2.971	-3.2	30.4	10064	P29	9d-e	35	40	Equid	frags	
ME605	2.953	-1.8	25.1	936	R 27	11	30	35/40	Equid *(?Hipparion)*	P^x	
ME580	2.884	-8.0	27.0	313	R 34	11	10	15	Equid?	frags	
ME604	2.3	-8.1	28.6	318	R 34	11	10	15	Equid?	frags	
ME561	2.744	-0.9	32.5	733	S29	12	20	25	Equid?	P/M	
ME566	2.877	-2.9	29.4	720	R 31	12	50	55	Equid?	frags	
ME585	2.599	-7.6	27.7	10038	R24	10a	35	40	Equid?	frag	heat fractures?
ME635	2.25	-6.6	27.6	10037	S25	10a	30	35	Equid?	frag	
ME678	2.920	0.2	31.0	10059	T28	8	0	5	*Equus sp.*	M_3	
ME686	2.739	-6.8	31.1	7000	L29	7	10 basal	15 red	*E. quagga*	P_4 - M_3	In mandible, M2 sampled
ME683	2.1	-3.0	32.0	4298	S24	10a	15	20	*E. quagga*	$M_{1/2}$	early wear
ME663	2.679	-2.9	29.9	7625	M29	5	15	20	*Equus sp.*	M/P	brittle enamel
ME660	2.933	-1.6	31.7	7572	Q28	5	0	5	*Equus sp.?*	frag	
ME661	2.728	-11.8	27.0	7662	M28	5	15	20	*H. africaeaustralis*	frag	
ME670	2.921	-3.9	30.3	10071	Q29	5	0	5	*H. africaeaustralis*	frag	
ME653	1.85	-9.8	27.9	7158	R33	7	15	20	*H. africaeaustralis*	I	
ME592	2.733	-7.9	28.7	10028	Q30	8	25	30	*H. africaeaustralis*	M^x/P^x	
ME577	2.941	-10.7	29.3	293	S30	12	50	55	*H. africaeaustralis*	M	
ME578	2.768	-8.2	26.3	1008	R 27	12	60	70	*H. africaeaustralis*	M	
ME594	2.639	-12.0	21.8	150	T33	12	5	10	*H. africaeaustralis*	I	
ME601	2.641	-9.8	26.0	232	Q29	12	15	20	*H. africaeaustralis*	P/M	
ME582	2.813	-10.2	28.7	4339	S24	10a	35	40	*H. africaeaustralis*	P/M	
ME588	2.643	-11.4	25.5	10055	R22	8a	15	20	*H. africaeaustralis*	P/M	
ME590	2.701	-10.5	24.4	10057	T26	8c/d	5	10	*H. africaeaustralis*	P/M	

ME586	2.934	-9.9	25.4	10065	S29	9b	15	20	*H. africaeaustralis*	P/M	
ME587	2.961	-10.9	24.6	10063	S27	9b	0	5	*H. africaeaustralis*	P/M	
ME576	2.819	-1.5	28.3	109	T31	12	5	10	*H. africaeaustralis?*	M	
ME681	2.0	-6.8	29.1	10047	R34	10	25	30	*K. leche*	M_1+M_2	M2 sampled
ME680	1.4	-1.4	31.2	10049	S25	10a	15	20	*K. leche*	$M_{2/3}$	
ME659	2.847	-1.7	27.3	10054	Q30	6	10	15	*P. capensis*	P/M	labelled SPF 24, bag 9, very worn
ME677	1.45	-1.6	26.3	10053	S30	6			*P. capensis*	P/M	Spit 1, labelled SPF 11
ME682	0.1	-8.8	24.5	10050	Q31	10	55	60	*P. capensis*	P/M	Excluded from analyses
ME684	2.600	-2.7	28.4	7152	Q34	7b	0	5	*P. capensis*	P/M	
ME600	2.819	-10.4	29.8	240	Q29	12	45	50	*P. capensis*	M	
ME599	0.5	-4.4	21.7	985	R 29	12	5	10	*Pedetes sp.*	P^x/M^x	
ME630	0.68	-8.5	29.4	4327	S22	10a	35	40	*P. capreolus?*	M^1	buccal plate
ME665	2.630	-10.2	36.4	7574	R32	5	0	5	*R. campestris*	frag	
ME666	1.0	-8.8	30.8	7594	M28	5	10	15	*R. campestris*	frag	
ME674	2.832	-11.1	35.9	7600	K27	5	0	5	*R. campestris (cf)*	frag	
ME679	2.800	-12.6	33.5	10036	Q29	10	30	35	*R. fulvorufula*	M^x	
ME631	3.043	-10.6	29.7	10052	R25	10a	35	40	*T. oryx*	M^x	
ME634	3.044	-9.1	28.9	4361	S24	10a	25	30	*T. oryx*	M_x	
ME649	2.591	-10.0	30.9	7072	R34	7	0	5	Tragelaphini	frag	
ME637	2.871	-11.0	30.6	10044	P29	10	25	30	Tragelaphini	M	
ME597	2.795	-10.6	30.5	1136	T29	11	0	5	Tragelaphini	P^x	Unerupted, adult tooth, pieces glued
ME591	2.861	-10.7	31.9	10058	P29	8a	0	5	Tragelaphini?	P/M	SPF 166, bag47,
ME583	2.714	-7.8	30.9	10042	T33	10	45	50	*T. strepsiceros*	I	
ME638	2.562	-10.0	30.1	10043	R24	10a	40	45	*T. strepsiceros*	M^x	very worn
ME643	2.778	-6.2	27.1	10069	R32	9d-e	5	10	*T. strepsiceros (cf)*	frag	
ME639	2.884	-6.2	30.8	10040	S25	10a	25	30	*T. strepsiceros?*	M^x	

5.4 All stable isotope data for faunal enamel samples of Excavation 2 Stratum 2, indicating specimen number, species, origin and tooth type.

Sample	Mass (mg)	$\delta^{13}C_{VPDB}$ ‰	$\delta^{18}O_{VSMOW}$ ‰	SPF#	Square 1	Square 2	height 1	height 2	Species	Tooth	Comments
ME622	3.026	-1.3	31.9	1279	W	48	0	5	*Damaliscus* sp.?	L M3?	
ME614	3.048	-2.3	35.4	1272	X	49	0	5	*Damaliscus* sp. (cf)	L P3/4	small Alcelaphine
ME612	1.1	2.3	30.3	1266	Y	50	0	5	*Damaliscus* sp.	P_3	
ME617	2.895	-2.7	29.0	1217	Y	54	15	20	*Damaliscus* sp.	R M^1	late wear
ME629	0.83	-0.5	31.1	1253	W	47	0-5	5-10	*A. buselaphus*	R M_3	cf same indiv. as #1186, glued, mid-wear
ME615	1.3	-9.9	28.9	1252	W	47	0	5	*A. marsupialis*	R P_4	mid-wear
ME619	2.991	-8.4	41.1	10072	Y	52	0	5	*A. marupialis*?		
ME687	2.711	-7.8	20.0	1189	X	54	20	25	*C. simum*	R P_3	Glued, burnt?
ME606	2.3	-0.5	30.6	1188	X	48	10	15	*C. taurinus*	L M^3	Glued, early wear
ME610	2.804	-3.5	28.7	1222	Y	52	0	5	*C. taurinus*	R M3	mid-wear
ME616	2.946	-2.6	31.5	1229	Y	52	0	5	*Equus* sp.	M^x	
ME624	3.020	-1.4	33.4	1238	Y	54	5	10	*Equus* sp.	P/M	
ME626	2.878	-0.4	33.4	1175	W	48	0	5	*Equus* sp.	R M_x	partly glued
ME625	2.983	-10.6	30.1	1215	W	48	5	10	*H. africaeaustralis*	M	unworn
ME627	1.2	-8.2	23.6	1292	W	49	spit III		*H. africaeaustralis*	I_1	
ME623	2.669	-11.8	35.4	1153	X	48	0	5	*P. capreolus*	L P4	
ME609	3.006	-11.6	34.9	1233	X	48	15	20	*P. capreolus*	L M^3	mid-wear
ME607	1.1	-2.0	26.8	1312	X	50	spit III		Small-medium bovid	$M^{2/3}$	Was *Pelea* cf – wrong id?
ME620	2.743	-13.0	33.7	1313	X	50	spit III		*R. campestris*	M^x	
ME618	1.2	-13.0	28.8	1271	Y	54	20	25	*R. campestris*	R M^3	Glued, mid wear
ME628	3.054	-0.0	33.4	1396	Y	54	10	15	*K. leche*	L M^1	late wear
ME608	2.769	-7.4	26.6	1393	Y	54	10	15	Reduncini cf.	R P^4	mid-wear, *K. leche* size
ME621	2.982	-11.5	33.6	1180	V	49	5	10	*T. strepciseros*	M	

ME613	2.930	-9.5	32.0	1184	X	47	0	5	*T. strepciseros* (cf)	R M_3	
ME611	1.281	-11.2	34.2	1288	V	47	0	5	*T. strepciseros* (cf)	M_x	

Appendix 6: Results of statistical analyses.

6.1 Results of statistical analysis of OES $\delta^{13}C$ and $\delta^{18}O$ data. Includes data from Lee-Thorp and Ecker (2015).

6.1.1 Levene's test; * significant values.

Test	**Pr(>F)**
Excavation 1 $\delta^{18}O$	0.347
Excavation 1 $\delta^{13}C$	0.003*
Excavation 1 $\delta^{13}C$ without stratum 10	0.664
Excavation 2 $\delta^{18}O$	0.153
Excavation 2 $\delta^{13}C$	0.002*
Excavation 1 and 2 $\delta^{18}O$	0.134
Excavation 1 and 2 $\delta^{13}C$	0.000*

6.1.2 One-way ANOVA with Tukey's HSD post-hoc test of $\delta^{18}O$ results. Only significant p-values are listed; all other strata showed no statistical significant differences.

Strata	**p-value**
5I-3a	0.005
10-3a	0.002
5I-3b	0.016
10-3b	0.016
5I-4bII	0.029
10-4bII	0.026
Exc 2 Str 3 – Exc 1 Str 3a	0.000

Exc 2 Str 3 – Exc 1 Str 3b	0.002
Exc 2 Str 3 – Exc 1 Str 4aI	0.039
Exc 2 Str 3 – Exc 1 Str 4bII	0.003
Exc 2 Str 3 – Exc 1 Str 6	0.025

Excluding spits in the LSA strata:

Strata	**p-value**
10-3a	0.002
10-3b	0.013
Exc 2 Str 3 – Exc 1 Str 3a	0.000
Exc 2 Str 3 – Exc 1 Str 3b	0.002
Exc 2 Str 3 – Exc 1 Str 6	0.025
Exc 2 Str 3 – Exc 1 Str 4a	0.004
Exc 2 Str 3 – Exc 1 Str 4b	0.007
Exc 2 Str 3 – Exc 1 Str 4c	0.022
Exc 2 Str 3 – Exc 1 Str 4d	0.002

6.1.3 Kruskal Wallis test of $\delta^{13}C$.

p-value = 2.43e-05

6.1.4 Mann-Whitney U-test of $\delta^{13}C$ in Excavation 1. Only significant p-values are listed.

Strata	**p-value**
2b-4aII	0.025
4aI-4dII	0.048
4aII-5II	0.002
4bI-5II	0.009
9-5II	0.028
5I-all strata	significant

6.2 Results of statistical analysis of enamel $\delta^{13}C$ and $\delta^{18}O$ data.

6.2.1 Levene's test for differences between the species in each stratum; * significant values.

Stratum	Pr(<F) value $\delta^{13}C$	Pr(<F) value $\delta^{18}O$
12	0.831	0.542
11	0.718	0.036*
10	0.255	$6.842e^{-06}$*
9	2.2e-16*	$2.2e^{-16}$*
6-8	0.125	0.188
5	0.004*	0.889
4d	0.571	0.702
4c	0.575	0.759
4b	0.668	0.540
4aLH	0.899	0.755
4a	0.001*	0.261
3b	0.790	0.914
3a	0.146	0.404
2b	0.873	0.664
Exc. 2 Stratum 2	0.060	0.001*

6.2.2 One-way ANOVA with Tukey's HSD post-hoc test for differences between the species in each stratum. Only significant p-values are listed.

Test	**p-value**
$\delta^{13}C$ – various strata	
Stratum 6-8 *H. africaeaustralis* - Alcelaphini	0.044
Stratum 4d *H. africaeaustralis* - Alcelaphini	<0.000
Stratum 4d Tragelaphini - Alcelaphini	0.002
$\delta^{13}C$ Stratum 4c	
H. africaeaustralis - *A. buselaphus*	<0.000
R. campestris - *A. buselaphus*	<0.000
T. oryx - *A. buselaphus*	<0.000
Tragelaphini - *A. buselaphus*	<0.000
T. strepsiceros - *A. buselaphus*	<0.000

H. africaeaustralis - Alcelaphini	<0.000
R. campestris - Alcelaphini	<0.000
Tragelaphini - Alcelaphini	<0.000
T. strepsiceros - Alcelaphini	<0.000
H. africaeaustralis - *Connochaetes* sp.	<0.000
R. campestris - *Connochaetes*. sp.	<0.000
T. oryx - *Connochaetes* sp.	<0.000
Tragelaphini - *Connochaetes* sp.	<0.000
T. strepsiceros - *Connochaetes* sp.	<0.000
P. capensis - *H. africaeaustralis*	<0.000
R. campestris - *P. capensis*	<0.000

T. oryx - *P. capensis*	<0.000
Tragelaphini – *P. capensis*	<0.000
T. stresiceros – *P. capensis*	<0.000
δ^{13}C Stratum 4b	
A. marsupialis - Alcelaphini	<0.000
R. campestris - Alcelaphini	<0.000
Tragelaphini - Alcelaphini	<0.000
Equus sp. - *A. marsupialis*	0.001
P. capensis - *A. marsupialis*	0.001
R. campestris - *Equus* sp.	<0.000
Tragelaphini - *Equus* sp.	<0.000
R. campestris - *P. capensis*	<0.000
Tragelaphini - *P. capensis*	<0.000
δ^{13}C Stratum 4aLH	
A. marsupialis - Alcelaphini	<0.000
H. africaeaustralis - Alcelaphini	<0.000
P. capreolus - Alcelaphini	<0.000
R. campestris - Alcelaphini	<0.000
Tragelaphini - Alcelaphini	<0.000
Equus sp. - *A. marsupialis*	<0.000
P. capensis - *A. marsupialis*	<0.000
P. capreolus - *A. marsupialis*	0.015
R. campestris - *A. marsupialis*	0.004
R. fulvorufula - *A. marsupialis*	<0.000
H. africaeaustralis - *Equus* sp.	<0.000
P. capreolus - *Equus* sp.	<0.000
R. campestris - *Equus* sp.	<0.000
Tragelaphini - *Equus* sp.	<0.000
P. capensis - *H. africaeaustralis*	<0.000
R. fulvorufula - *H. africaeaustralis*	<0.000
P. capreolus - *P. capensis*	<0.000
R. campestris - P. *capensis*	<0.000
Tragelaphini - *P. capensis*	<0.000
R. fulvorufula - *P. capreolus*	<0.000
R. fulvorufula - *R. campestris*	<0.000
Tragelaphini - *R. fulvorufula*	<0.000
δ^{13}C Stratum 3b	
A. marsupialis - *A. buselaphus*	<0.000
A. marsupialis - Alcelaphini	<0.000
H. africaeaustralis - *A. buselaphus*	<0.000
H. africaeaustralis - Alcelaphini	<0.000
R. campestris - *A. buselaphus*	<0.000
R. campestris - Alcelaphini	<0.000
Tragelaphini - *A. buselaphus*	<0.000
Tragelaphini - Alcelaphini	<0.000
T. strepsiceros - *A. buselaphus*	<0.000
T. strepsiceros - Alcelaphini	<0.000
Connochaetes sp. - *A. marsupialis*	<0.000
Equus sp. - *A. marsupialis*	<0.000
P. capensis - *A. marsupialis*	<0.000
R. fulvorufula - *A. marsupialis*	<0.000
H. africaeaustralis - *Connochaetes* sp.	<0.000
R. campestris - *Connochaetes* sp.	<0.000
Tragelaphini - *Connochaetes* sp.	<0.000
T. strepsiceros - *Connochaetes* sp.	<0.000
H. africaeaustralis - *Equus* sp.	<0.000
R. campestris - *Equus* sp.	<0.000
Tragelaphini - *Equus* sp.	<0.000
T. strepsiceros - *Equus* sp.	<0.000
P. capensis - *H. africaeaustralis*	<0.000
R. fulvorufula - *H. africaeaustralis*	<0.000
R. campestris - *P. capensis*	<0.000
Tragelaphini - *P. capensis*	<0.000
T. strepsiceros - *P. capensis*	<0.000
R. fulvorufula - *R. campestris*	<0.000
Tragelaphini - *R. fulvorufula*	<0.000
T. strepsiceros - *R. fulvorufula*	<0.000
δ^{13}C Stratum 3a	
A. marsupialis - *A. buselaphus*	<0.000
Equus sp. - *A. buselaphus*	0.010
H. africaeaustralis - *A. buselaphus*	<0.000
R. campestris - *A. buselaphus*	<0.000
Tragelaphini - *A. buselaphus*	<0.000
T. strepsiceros - *A. buselaphus*	<0.000

A. marsupialis - Alcelaphini	<0.000
Equus sp. - Alcelaphini	0.042
H. africaeaustralis - Alcelaphini	<0.000
R. campestris - Alcelaphini	<0.000
Tragelaphini - Alcelaphini	<0.000
T. strepsiceros - Alcelaphini	<0.000
Connochaetes sp. - *A. marsupialis*	<0.000
Equus sp. - *A. marsupialis*	<0.000
H. africaeaustralis - *A. marsupialis*	0.002
R. campestris - *A. marsupialis*	<0.000
R. fulvorufula - *A. marsupialis*	<0.000
Tragelaphini - *A. marsupialis*	0.013
T. strepsiceros - *A. marsupialis*	0.040
H. africaeaustralis - *Connochaetes* sp.	<0.000
R. campestris - *Connochaetes* sp.	<0.000
Tragelaphini - *Connochaetes* sp.	<0.000
T. strepsiceros - *Connochaetes* sp.	<0.000
H. africaeaustralis - *Equus* sp.	<0.000
R. campestris - *Equus* sp.	<0.000
Tragelaphini - *Equus* sp.	<0.000
T. strepsiceros - *Equus* sp.	<0.000
R. fulvorufula - H. *africaeaustralis*	<0.000
R. fulvorufula - *R. campestris*	<0.000
Tragelaphini - *R. fulvorufula*	<0.000
T. strepsiceros - *R. fulvorufula*	<0.000
δ^{13}C Stratum 2b	
A. marsupialis - *A. buselaphus*	<0.000
Tragelaphini - *A. buselaphus*	<0.000
Connochaetes sp. - *A. marsupialis*	<0.000
Equus sp. - *A. marsupialis*	<0.000
Phacocerus sp. - *A. marsupialis*	0.001
R. fulvorufula - *A. marsupialis*	<0.000
Tragelaphini - *Connochaetes* sp.	<0.000
Tragelaphini - *Equus* sp.	<0.000
Tragelaphini - *Phacocerus* sp.	0.001
Tragelaphini - *R. fulvorufula*	<0.000
δ^{13}C Excavation 2 Stratum 2	

A. marsupialis - Alcelaphini	0.016
H. africaeaustralis - Alcelaphini	0.013
P. capreolus - Alcelaphini	0.002
R. campestris - Alcelaphini	0.001
T. strepciseros - Alcelaphini	0.001
P. capreolus - *A. buselaphus*	0.020
R. campestris - *A. buselaphus*	0.008
T. strepciseros - *A. buselaphus*	0.024
Equus sp. - *A. marsupialis*	0.034
P. capreolus - *C. taurinus*	0.013
R. campestris - *C. taurinus*	0.005
T. strepciseros - *C. taurinus*	0.014
H. africaeaustralis - *Equus* sp.	0.023
P. capreolus - *Equus* sp.	0.004
R. campestris - *Equus* sp.	0.001
T. strepciseros - *Equus* sp.	0.003
K. leche - *R. campestris*	0.018
δ^{18}O Stratum 4d	
H. africaeaustralis - Alcelaphini	0.015
Tragelaphini - *H. africaeaustralis*	0.012
δ^{18}O Stratum 4c	
P. capensis - *Connochaetes* sp.	0.046
R. campestris - *H. africaeaustralis*	0.007
T. oryx - *H. africaeaustralis*	0.008
Tragelaphini - *H. africaeaustralis*	<0.000
T. strepsiceros - *H. africaeaustralis*	0.002
R. campestris - *P. capensis*	0.001
T. oryx - *P. capensis*	0.001
Tragelaphini - *P. capensis*	<0.000
T. strepsiceros - *P. capensis*	<0.000
δ^{18}O Stratum 4b	
R. campestris - *P. capensis*	0.007
Tragelaphini - *P. capensis*	0.020
δ^{18}O Stratum 4a	
P. capensis - *A. buselaphus*	0.003
P. capensis - Alcelaphini	<0.000
P. capensis - *Connochaetes* sp.	0.004

R. campestris - *H. africaeaustralis*	0.035
R. fulvorufula - *H. africaeaustralis*	0.040
R. campestris - *P. capensis*	<0.000
R. fulvorufula - *P. capensis*	0.001
Tragelaphini - *P. capensis*	0.012
T. strepsiceros - *P. capensis*	<0.000
$\delta^{18}O$ Stratum 3b	
H. africaeaustralis - Alcelaphini	0.008

R. campestris - H. *africaeaustralis*	0.001
Tragelaphini - *H. africaeaustralis*	0.021
T. strepsiceros - *H. africaeaustralis*	0.004
R. campestris - *P. capensis*	0.049
$\delta^{18}O$ Stratum 3a	
H. africaeaustralis - Alcelaphini	0.010
R. campestris - *H. africaeaustralis*	0.009
T. strepsiceros - *H. africaeaustralis*	0.008

6.2.3 Kruskal-Wallis test for differences between the species in each stratum.

$\delta^{13}C$:	$\delta^{18}O$:
Statum 4a: p= 2.607e-10*	Stratum 9: p= 0.165
Stratum 5: p=0.08	Stratum 10: p= 0.698
Stratum 9: p= 0.165	Stratum 11: p=0.322
	Exc. 2 Stratum 2: p= 0.287

6.2.4 Levene's test for differences throughout the sequence by species; * significant values.

Species	Pr(<F) value $\delta^{13}C$	Pr(<F) value $\delta^{18}O$
Alcelaphini	$1.029e^{-08}$*	0.312
Equid	0.1089	0.598
H. africaeaustralis	0.400	0.362
P. capensis	0.001*	0.031*
Antidorcas sp.	0.735	0.002*
R. campestris	0.5341	0.950
Tragelaphini	0.3863	0.290

6.2.5 One-way ANOVA with Tukey's HSD post-hoc test for differences throughout the sequence by species. Only significant p-values are listed.

Strata	p-value
Alcelaphini $\delta^{18}O$	
3a – 11	0.027
3b – 11	0.016

4a – 11	0.009
4aLH - 11	0.006
Equid $\delta^{18}O$	
3a – 11	0.007
4a – 11	0.010
4aLH – 11	0.003
4b – 11	0.035
Exc. 2 Stratum 2 - 11	0.016
4aLH - 12	0.019
Equid $\delta^{13}C$	
2b – 10	0.045
3a – 10	0.001
4a - 10	0.007
4aLH - 10	0.013
4b - 10	0.020
3a - 11	0.003
4a - 11	0.021
4aLH - 11	0.024
4b - 11	0.047
2b - 12	0.043
3a - 12	<0.000
4a - 12	0.005
4aLH – 12	0.015
4b – 12	0.020
Antidorcas sp. $\delta^{13}C$	
5 – 2b	0.020

6 - 5	0.007
R. campestris Carbon	
4a – 3a	0.005
4b – 3a	0.003
4c – 3a	0.036
Exc. 2 Stratum 2 – 4a	0.002
Exc. 2 Stratum 2 – 4b	0.001
Exc. 2 Stratum 2 – 4c	0.020
Tragelaphini $\delta^{13}C$	
4a – 3a	0.006
4a – 3b	0.041
4d – 4a	0.047
Exc. 2 Stratum 2 – 4a	0.010
Tragelaphini $\delta^{18}O$	
3b – 10	0.005
4a – 10	0.006
4aLH – 10	0.006
4b - 10	0.031
4c - 10	<0.000
4d - 10	0.009
9 – 3b	0.048
9 – 4a	0.047
9 – 4aLH	0.018
9 – 4c	0.004
9 – 4d	0.022

6.2.6 Additional statistical tests.

A. marsupialis vs *A. bondi*:
Levene's test $\delta^{13}C$: 0.480.
ANOVA with Tukey-HD post-hoc testing $\delta^{13}C$: *A. marsupialis - A. bondi* p-value = $5.78e^{-05}$.

Levene's test $\delta^{18}O$: 0.044.
Kruskal-Wallis test: p-value $\delta^{18}O$ = 0.371.
Kruskal-Wallis test for Alcelaphini $\delta^{13}C$: p-value = $4.017e^{-08}$ (by strata) / p-value = 0.004 (by species).